CLAY MINERALOGY, PETROGRAPHY, CHEMICAL COMPOSITION AND STRATIGRAPHIC CORRELATION OF SOME MIDDLE ORDOVICIAN K-BENTONITES IN THE EASTERN MID-CONTINENT

A thesis submitted to the

Division of Graduate Education and Research
of the University of Cincinnati

in partial fulfillment of the
requirements for the degree of

DOCTOR OF PHILOSOPHY

in the Department of Geology
of the College of Arts and Sciences

1979

by

Asuman Günal

B.S. Middle East Technical University, 1970

M.S. Middle East Technical University, 1974

UNIVERSITY OF CINCINNATI

May 3, 1979

I hereby recommend that the thesis prepared under my supervision by Asuman Günal

entitled Clay Mineralogy, Petrography, Chemical Composition and Stratigraphic Correlation of Some Middle Ordovician K-bentonites in the Eastern Mid-continent.

be accepted as fulfilling this part of the requirements for the degree of Doctor of Philosophy

Approved by:

ACKNOWLEDGMENTS

I gratefully acknowledge Dr. Warren D. Huff, my supervisor, for his continued support, guidance and constant interest in this study. I have greatly benefitted from his knowledge and experience in clays, especially in bentonites. I also express my gratitudes to Dr. J. Barry Maynard and Dr. Leonard H. Larsen, members of my doctoral committee, for their constructive criticism and valuable advice which were essential to the completion of the study. I am indebted to members of the Geology Faculty of the University of Cincinnati, particularly to Dr. I. A. Kilinc, whose stimulating discussions and suggestions helped further to improve my thesis. A clarifying discussion on Ordovician K-bentonites with Mr. E. R. Cressman of U. S. Geological Survey should be mentioned with appreciation. My special thanks are due to Mr. J. A. Harrell for his valuable help during the statistical data analyses.

I wish to extend my thanks to various organizations and friends who courteously provided assistance in many forms. I deeply appreciate the access to the core libraries and the information in the files of the Indiana Geological Survey, Kentucky Geological Survey, Cominco American Company and Cincinnati Gas and Electric Company. Mr. Grover Reinbold of the Exxon Corporation and Mr. H. W. Robinson of the Geological Services Branch of the Tennessee Valley Authority in Knoxville, kindly provided me some K-bentonite

samples and stratigraphic information on them. Dr. Warren D. Huff courteously gave me valuable samples from his own collection. Here, it is a pleasant duty to thank Mr. D. E. Joyce who provided technical assistance during laboratory work and to Per-Erik Litz, for the preparation of thin-sections. My thanks are also due to Mr. J. D. Williams for drawing the illustrations and to Mrs. D. Moorman who patiently typed the entire manuscript.

Finally, I would like to thank my family whose warm support and continued encouragement enabled me to complete this study.

ABSTRACT

The clay mineralogy, petrography and major and trace element composition of some widespread K-bentonite horizons occurring in the upper Black River Group of Middle Ordovician strata in Indiana, Kentucky, Tennessee and Alabama were investigated. Long-distance stratigraphic correlation of the horizons was accomplished on the basis of selected chemical parameters of bulk samples. Several methods of investigation were employed during the study and analyses were performed on both bulk samples and < 2 μm clay fractions by polarizing microscope, x-ray powder diffractometer, x-ray fluorescence and atomic absorption spectrometers. During the chemical analyses Si, Al, total Fe, Mg, Ca, Na, K, Ti, Mn, Rb, Sr, Y, Zr, Zn, Nb, Ga and Ge contents of samples were determined. Parts of the chemical data were subjected to cluster analyses for statistical data processing. The data obtained were used to study the clay composition and structure, to determine the original composition of volcanic ash, to interpret the effects of post-depositional alteration and for stratigraphic studies.

K-bentonites are the alteration products of volcanic tuffs or ashes, mostly trachyandesitic in composition and belonging to an alkaline magma series, which have undergone post-depositional alteration at low temperatures and pressures over a long period of time. They are composed mainly of a clay mineral fraction consisting of a regularly interstratified, dioctahedral, allevardite-

type (IM) mineral with an illite/smectite ratio between 3:1 and 4:1, and non-clay components, chiefly biotite, alkali-feldspars (sanidine and orthoclase), zircon, apatite and Fe-Ti oxides. The interstratified clay originated during the devitrification of volcanic glass in a shallow marine environment with subsequent adsorption and fixation of K in the interlayer positions. The calculated structural formulae reveal that the clay has a structure and composition between those of illite and smectite and seems to merit consideration as a geologic environmental indicator.

Post-depositional chemical changes altered the composition of the original volcaniclastic rocks in the form of a net loss of Na, Ca and Si and accompanying gain of K and Mg. This conclusion was drawn based on the assumption that the original Al content was not affected by alteration. Si shows a minimum amount of loss and K shows maximum amount of gain. Fe and Ti are empirically found to have remained immobile through geologic time. Altogether, these chemical changes illuminate the nature and mechanism of mineralogic changes, as clearly exemplified by genesis of the interstratified illite/smectite clay.

Geochemical characteristics of bulk samples were used to interpret within- and between-bed compositional variability with the purpose of distinguishing the discrete K-bentonite horizons under investigation. The abundances of Fe, Ti, Zr, Ge and Al as

shown in binary and ternary diagrams prove to be good between-bed discriminants. Long-distance stratigraphic correlation of the same horizons in a north-south line is also accomplished on the basis of these data.

The present study suggests that Middle Ordovician K-bentonites stratigraphically correspond to a developing stage of an Early Paleozoic island arc located, in part, along the present Carolina slate belt, between stages characterized by calc-alkaline and alkaline magma series.

Key words: K-bentonite, clay mineralogy, petrography, chemical composition, post-depositional alteration, tephrochronology, stratigraphic correlation.

TABLE OF CONTENTS

	Page
ACKNOWLEDGMENTS	ii
ABSTRACT	iv
LIST OF TABLES	x
LIST OF FIGURES	xi
INTRODUCTION	1
General Statement of the Problem	1
Origin and Significance of the Study	4
Previous Studies	6
Previous Work on Ordovician K-bentonites	6
Previous Work on the Geochemistry of Younger Ash-Fall Deposits	12
Scope and Limitations of the Problem	17
GEOLOGY	20
Location of Study Area	20
Geologic Setting	20
Stratigraphy of the Study Area	26
Paleogeography of the Study Area During Middle Ordovician	38
METHODS OF INVESTIGATION	42
Sampling	42
Sample Preparation	44
Description of the Analytical Techniques	47
X-ray Fluorescence Spectrometry	47
Atomic Absorption Spectrophotometer	50
X-ray Powder Diffraction	51
RESULTS OF INVESTIGATION. PART I: MINERALOGY AND PETROGRAPHY	52
Introduction	52
Mineralogy	57

TABLE OF CONTENTS (Cont'd.)

	Page
Description of Non-Clay Minerals	57
Description of Clay Minerals	65
Alteration of Volcanic Glass	65
X-Ray Analysis	68
Chemistry and Structural Formulae of Clay Minerals	74
Petrography	88
The Relationship Between K-bentonites and Adjacent Limestones	99
RESULTS OF INVESTIGATION. PART II: CHEMICAL COMPOSITION AND CORRELATION	103
Introduction	103
Effects of Post-Depositional Alteration	105
Chemical Variation Within Individual K-bentonite Beds	115
Chemical Differentiation of Individual K-bentonite Horizons	126
Data Processing	127
Binary Discrimination Diagrams	132
Fe_2O_3T - Al_2O_3 Plot	132
Fe_2O_3T - TiO_2 Plot	134
Ge - Fe_2O_3T Plot	134
Ge - Zr Plot	134
Ternary Discrimination Diagrams	138
Fe - Zr - Ti Plot	138
Fe - Zr - Ge Plot	139
Correlation of K-Bentonite Beds	142
DISCUSSION	148
Discussion of Methods	148
Discussion of the Results	149
Origin of K-Bentonites	149
Structure and Composition of Interstratified Clays	152

TABLE OF CONTENTS (Cont'd.)

	Page
Composition of Original Ash and K-Bentonite Bulk Sample	154
Geochronology and Correlation of K-Bentonite Horizons	161
CONCLUSIONS AND SUGGESTIONS	164
Conclusions	164
Suggestions for Further Study	168
REFERENCES	171
APPENDICES	188
A. SUMMARY OF DATA ON MIDDLE ORDOVICIAN K-BENTONITE AND ADJACENT LIMESTONE SAMPLES	189
B. SAMPLE PREPARATION FOR THE STUDY TECHNIQUES	200
C. OPERATING CONDITIONS FOR X-RAY FLUORESENCE SPECTROMETRY	203
D. PRECISION, ACCURACY AND WITHIN SAMPLE HOMOGENEITY OF X-RAY FLUORESCENCE TECHNIQUE	205
E. CALIBRATION CURVE FOR MASS-ABSORPTION COEFFICIENT DETERMINATIONS	209
F. PARTIAL CHEMICAL ANALYSES OF K-BENTONITE BULK SAMPLES AND LESS THAN 2 μm CLAY FRACTIONS	213
G. PRECISION, ACCURACY AND WITHIN SAMPLE HOMOGENEITY OF ATOMIC ABSORPTION TECHNIQUE	232
H. OPERATING CONDITIONS FOR X-RAY POWDER DIFFRACTION EQUIPMENT	236

LIST OF TABLES

Table		Page
1	X-ray powder diffraction data for less than 2 μm clay fractions of K-bentonite samples	69
2	Structural formulae of 29 interstratified illite-smectite clays in K-bentonites	76
3	Calculation of gains and losses during post-depositional alteration processes based on the average of partial chemical analyses of 45 K-bentonite bulk samples	107
4	Comparison of average oxide contents of 21 K-bentonite bulk samples and their clay fractions	109
5	Percent MgO in illites formed in different environments	113
6	Partial chemical analyses of some volcanogenic rocks from the Ordovician island arc sequence of North America	160

LIST OF FIGURES

Figure		Page
1	Map of study area showing the location of samples	21
2	Tectonic map of southeastern United States, showing Appalachian and Ouachita mountain systems, and adjacent regions to the northwest and southeast	22
3	View from the high railroad bridge at the junction of Kentucky and Dix Rivers	25
4	Selected examples of stratigraphic nomenculature of rock units within the Mohawkian Series as defined in Indiana, Kentucky, Tennessee and Alabama	27
5	"Mud cave" bentonite at the contact of Curdsville Limestone Member of Lexington Limestone and Tyrone Limestone in the railroad cut, High Bridge, Kentucky	32
6	Distribution of "mud cave" bentonite of drillers and approximate thickness of interval between base of "pencil cave" bentonite of drillers and base of Lexington Limestone	33
7	Diagrammatic section showing the generalized stratigraphic relationships of the Middle Ordovician K-bentonites and the rocks belonging to the Stones River and Nashville Groups in different parts of central Tennessee	35
8	Distribution of Middle Ordovician K-bentonites throughout the eastern North America	40

LIST OF FIGURES (Cont'd.)

Figure		Page
9	Abundant biotite flakes in core samples KB-6	58
10	Photomicrograph of bended biotite flakes	59
11	Photomicrograph of a biotite crystal with inclusions of secondary Fe-Ti oxides along 001 cleavage planes	59
12	Photomicrograph showing the replacement of alkali-feldspar crystal by microcrystalline calcite	61
13	Photomicrograph of sample KB-6B showing quartz, biotite, alkali-feldspar crystals and micaceous and clayey matrix	62
14	Photomicrograph of a broken apatite inclusion in biotite	63
15	Photomicrograph of an apatite inclusion in biotite crystal	63
16	Photomicrograph of sample KB-35 with a zircon crystal in the middle	64
17	Photomicrograph of opaque minerals as inclusions in alkali-feldspar or as disseminated grains within the matrix	64
18	Photomicrograph of sample KB-35 showing devitrified volcanic glass	66
19	Photomicrograph of relict volcanic glass textures	66
20	Photomicrograph of relict volcanic glass textures forming the matrix	67

LIST OF FIGURES (Cont'd.)

Figure		Page
21	Photomicrograph of a green chloritic material in the 60 to 80 mesh mineral separate	67
22	X-ray powder diffraction patterns for sample KB-5B	71
23	X-ray powder diffraction patterns for sample KB-6E	72
24	X-ray powder diffraction patterns for sample KB-35	73
25	Histograms showing the distribution of octahedral and tetrahedral cations of twenty-nine interstratified illite-smectite structural formulae	81
26	Histograms showing the distribution of interlayer cations and Σ oct cations of twenty-nine interstratified illite-smectite structural formulae	84
27	Histograms showing the distribution of layer charges of twenty-nine interstratified illite-smectite structural formulae	87
28	Photomicrograph of a crystal-tuff	90
29	Photomicrograph of a vitric-crystal tuff	90
30	Photomicrograph of a vitric-crystal tuff	91
31	Photomicrograph of a vitric-crystal tuff	91
32	Photomicrograph of a vitric-crystal tuff	92
33	Photomicrograph of a reworked vitric tuff	92
34	Zr/TiO_2 against Nb/Y diagram	95
35	Zr/TiO_2 against Nb/Y diagram	96

LIST OF FIGURES (Cont'd.)

Figure		Page
36	Zr/TiO_2 against Ga diagram	97
37	Distribution of Al_2O_3, Fe_2O_3T, K_2O, TiO_2 and MgO contents in 29 bulk samples and their clay fractions	117
38	Distribution of Ga, Y, Nb, Rb, Zn, Zr contents in the bulk samples and clay fractions	120
39	Dendogram resulting from Q-mode cluster analysis of chemical data from K-bentonite bulk samples	129
40	Linkage tree resulting from R-mode cluster analysis of chemical data from K-bentonite bulk samples	131
41	Fe_2O_3T - Al_2O_3 plot	133
42	Fe_2O_3T - TiO_2 plot	135
43	Ge - Fe_2O_3T plot	136
44	Ge - Zr plot	137
45	Fe - Zr - Ti plot	140
46	Fe - Zr - Ge plot	141
47	Correlation diagram of K-bentonite horizons in the columnar sections of Tyrone Limestone between Smith County, Tennessee and Lawrence County, Indiana	143

INTRODUCTION

General Statement of the Problem

Ordovician rocks of the eastern United States contain numerous potassium-rich, altered volcanic ash or K-bentonite layers which, collectively, encompass a considerable time span of volcanic activity. It is believed that the original deposits were derived from a number of explosive volcanoes to the east, belonging to an active Paleozoic island arc system. In general, these ash layers were deposited instantaneously into shallow marine environments of the miogeoclinal belt and are preserved in altered form within thick sequences of limestones and shales.

Extensive studies of K-bentonite occurrences include reports from at least eighteen States and southern Ontario. Earlier studies have also demonstrated that the most persistent horizons of K-bentonites are found in the standard upper Black River and the basal Trenton Groups of the New York type section of Middle Ordovician age. The thickness of these beds is highly variable ranging from less than an inch to nine feet. As indicated by Bowen (1967) at least two of the numerous K-bentonites recognized in Middle Ordovician strata of eastern United States apparently represent major eruptions. What was called by Wilson (1949) the T-3 event records a minimum ejection of 10 cubic miles (42 km^3) of tephra, and the Old Rosedale event, best known from the lower Martinsburg Shale of Virginia, records a minimum ejection of 24 cubic miles (98 km^3) as reported by Bowen (1967).

These figures reveal the production and dispersal of great quantities of tephra on the basis of comparison with the similar information obtained from studies of violent volcanic eruptions of recent times. For example, during an eruption about 7000 years ago of ancient Mount Mazama, the precursor of Crater Lake Caldera, Oregon, about 7 to 9 cubic miles (29 to 38 km^3) of material were blown into the atmosphere (Westgate, et al., 1970) and a pumiceous pyroclastic deposit dispersed over almost a 0.38 x 10^6 square miles (10^6 km^2) in the western North America (Kittleman, 1973). It appears that these greatest of the Ordovician ash-falls blanketed large areas, and are of great geologic interest because they form isochronous surfaces within a rock succession characterized by complex facies and structural relationships (Cressman and Noger, 1976).

Earlier studies reveal that Middle Ordovician K-bentonites are of both theoretical and practical interest. Much effort has been given by earlier workers to studying their mineralogic and petrographic properties (Weaver, 1953a; Huff, 1963a) as well as to their stratigraphic and paleontologic significance (Whitecomb, 1932; Fox and Grant, 1944; Fetzer, 1973). In spite of a long period of post-depositional alteration, the non-clay mineral assemblage of K-bentonites mainly of biotite, alkali-feldspars, zircon, apatite and Fe-Ti oxides plus a few relict shard textures (Allen, 1929) are strong evidence of their volcanic origin, and an acid-to-intermediate composition of the original ashes. The clay mineralogy of Ordovician

K-bentonites consists of regularly interstratified illite/smectite clay with a ratio between 3:1 and 4:1 (Weaver, 1953a; Huff, 1963a; Reynolds and Hower, 1970) and is significantly different from that of younger bentonites which are composed mainly of smectite (Slaughter and Early, 1965). These mineralogic characteristics of K-bentonites and their high potassium content, on the order of 6-8 percent, show that more attention to their petrology and geochemistry is needed.

Middle Ordovician K-bentonite horizons are widely used for correlation purposes during stratigraphic investigations of enclosing rocks (Wilson, 1949; Wolcott, et al., 1972). Thicker beds have also been used extensively by miners as marker horizons. However, such applications have been limited and serve only local purposes because none of the mineralogic, petrologic, lithologic or stratigraphic characteristics of K-bentonite horizons have remained unchanged over long distances. On the other hand, the precise long-range subsurface correlation of the Middle Ordovician Black River and Trenton Groups, based on faunal criteria and lithologic characteristics, is not definite (Twehhofel, et al., 1954; Gutstadt, 1958). Under these circumstances it is apparent that widespread K-bentonite beds may permit more precise long-distance correlation of sections and interpretation of facies relationships than are normally possible by conventional bio- and lithostratigraphic approaches if new characterization techniques which remain constant over wide areas can be established for the recognition of individual K-bentonite beds.

This study is a detailed investigation of the distribution and abundances of major and trace element contents of Middle Ordovician K-bentonites, combined with mineralogic and petrologic aspects. It seeks answers to some questions relating the origin, mineralogic composition, effects of post-depositional alteration and the long-distance correlation of widespread K-bentonite horizons in Indiana, Kentucky, Tennessee and Alabama on the basis of geochemical finger printing.

Origin and Significance of the Study

Studies as early as the 1920's demonstrated the usefulness of Ordovician K-bentonites for correlation purposes (Nelson, 1921, 1922a, 1922b, 1925; Sardeson, 1924). Later on, in 1932, Whitecomb listed the methods that could be employed to establish the identity of K-bentonite beds. Among these he underlined the use of the relationship of bentonite beds to certain well-established faunal zones; the use of a zone with a different lithology in the rock immediately adjacent to the K-bentonite, such as a chert layer underlying it; and also the use of possible physical or chemical identification of individual beds. Indeed, most of these methods have been successfully applied during many investigations. However, it has also been observed that due to certain drawbacks of the methods used, their usefulness is limited to local correlations. When Ordovician rock units and the individual K-bentonite beds are correlated over most of the eastern United States, their accuracy

cannot be checked by paleontologic evidence, since Ordovician faunas are typically endemic (Bergström and Sweet, 1966; Berry, 1976; Neuman, 1976; Sweet and Bergström, 1976) and since the biostratigraphic resolution of representatives of no fossil group is precise enough to permit correlation of thin rock units between various K-bentonite horizons (Twehhofel, et al., 1954; Fetzer, 1973). Miller and Fuller (1954, p. 128) discuss the origin of silicified beds which are closely associated with K-bentonites. They suggest that only beds greater than a foot in thickness can build up enough silica in their pore waters to permit replacement of the surrounding rock. If this is true, varying thicknesses of K-bentonite horizons become a major drawback to using chert bands for regional correlation purposes especially when the bentonites become very thin far away from the volcanic sources. Many investigators have considered physical characteristics, mineralogy and petrography of Ordovician K-bentonites for regional correlation purposes. However, they observed that these characteristics of various beds vary region to region, and lack suitable distinguishing characteristics. The possibility of chemical identification of discrete K-bentonite horizons as another approach for their long-range correlation has not been tested, although chemical fingerprinting of Cenozoic tephra layers, commonly recognized throughout the western United States and Canada, has proven to be extremely useful for the recognition of individual beds (Borchardt, et al., 1971b; Randle, et al., 1971; Borchardt,

et al., 1973; Westgate and Fulton, 1975; Westgate, 1977; Westgate, et al., 1977). In most cases widespread tephra layers can be traced back to their source volcanoes. Paleozoic bentonites are much older than these tephras mentioned, thus they have undergone longer periods of post-depositional alteration.

In spite of the rather substantial body of literature dealing with the mineralogy and petrography of Middle Ordovician K-bentonites and their stratigraphic significance there are only a few papers which include some information on their chemical composition (Nelson, 1922b; Allen, 1931, 1932; Fox and Grant, 1944; Huff, 1963a; Smith, et al., 1971). Detailed studies of major and trace elemental composition of Ordovician K-bentonites have not been previously undertaken. The importance of such investigations for long-distance correlation purposes is mentioned above. They are also very important for a better understanding of certain other aspects peculiar to these rocks. For example, knowledge of chemical composition of K-bentonite bulk samples and clay mineral fractions is promising in providing a new perspective on the effects and mechanism of post-depositional alteration processes, hence can answer questions about the original ash composition, the origin of their high potassium content, and the nature of the present mineralogy of K-bentonites.

Previous Studies

Previous Work on Ordovician K-bentonites:

Previous work on Ordovician K-bentonites can be classified into two main groups: one dealing with the mineralogic and petrographic

properties of these rocks and the other studying their stratigraphic and paleontologic significance. Altogether, previous investigations on both North American and Europan Ordovician K-bentonites comprise such a large body of work that only the most critical ones will be mentioned in this section. However, a more interested reader should refer to a recent study by Fetzer (1973) for a detailed discussion and historical review of related studies.

The term "bentonite" was first used by Knight (1898) to describe a highly colloidal plastic clay in the Cretaceous Benton Formation in Wyoming. In the geological sense bentonite carries definite mineralogical, textural and genetic connotations as defined by Ross and Shannon (1926). It is,

> ....a rock composed essentially of a crystalline clay-like mineral formed by devitrification and accompanying chemical alteration of a glassy igneous material, usually a tuff or volcanic ash in situ.

These authors further stated that,

> ....the characteristic clay mineral has a micaceous habit and facile cleavage, higher birefringence, and a texture inherited from the volcanic tuff or ash, and it is usually the mineral montmorillonite, but less often beidellite.

However, the use of the term bentonite varies among some workers. According to Grim (1968) and Grim and Güven (1978) the term is now well-established for any clay which is composed mainly of a smectite clay and may not have originated by the alteration of volcanic ash

or tuff. In other words their definition of bentonite does not include mode of origin. This usage of the term is also exemplified by Kraus (1978) who defines bentonite as a rock of specific mineral composition resulting from the alteration or "bentonitization" of any original material including tuff or volcanic ash. In the present study the term bentonite is used in the sense defined by Ross and Shannon.

The earliest reference to Ordovician K-bentonite was made by Safford in 1869 as a,

....layer of clay, a foot or more thick....

at the very top of Carters Limestone in central Tennessee (in Wilson, 1949, p. 44). Later, in 1888, Ulrich described a five-foot bed of plastic clay in the Ordovician section at High Bridge, Kentucky. However, these two authors did not recognize the original volcanic nature of the clay. Nelson (1921) identified the Ordovician clay beds of Kentucky and Tennessee as being of volcanic origin and suggested for the first time the possibility of regional correlation by these bentonites across Kentucky, Tennessee, Alabama and neighbouring States. In his next paper (Nelson, 1922b) he postulated the location of an ancient volcano as the source of this widespread bentonite layer no farther east than the Kentucky-West Virginia border. Nelson's findings generated a great deal of interest in bentonite studies and numerous workers have since described Ordovician K-bentonites from many places at North America. A number

of investigators suggested different source areas for these beds. Whitecomb (1932, 1934) was the first to postulate that the Ordovician K-bentonites of eastern North America were derived from numerous local, rather than one centrally located volcano as thought by previous investigators. He suggested that the zone of volcanoes extended along the western edge of Appalachia. Later, Fox and Grant (1944) suggested that a belt of volcanics extending from Virginia across central North Carolina and into South Carolina was the source of these altered volcanic ash layers. Sardeson (1924) reported the presence of a bentonite bed in the Ordovician Decorah Formation of Minnesota and Wisconsin. Butts (1926) and Stose and Jonas (1927) described the occurrences of new Ordovician K-bentonite horizons from Virginia and Pennsylvania, respectively. Later investigations by Bonnie and Honess (1929), Muddox (1930), Allen (1931, 1932), Kay (1931a, 1931b, 1935), Smith (1931), Sardeson (1933), Adams and Lester (1957) and Shearrow (1959) extended the known areal distribution of different K-bentonite horizons within the same stratigraphic interval in Pennsylvania, southern Ontario, Missouri, New York, Iowa, Vermont, Michigan, Georgia and West Virginia. The works of Fettke (1948), Gutstadt (1958) and Mossler and Hayes (1966) further showed that the similar beds were also present in Ohio, Indiana and Illinois.

Subsequent investigations revealed the number of K-bentonite horizons within a relatively narrow sequence of Ordovician rocks

was greater than previously reported (Mossler and Hayes, 1966). This fact coupled with the lack of distinct petrographic characteristics and uniform clay mineralogy and similar non-clay mineral concentration of K-bentonite layers (Huff, 1963a) prevented any long-range correlation based on stratigraphic, mineralogic and petrographic criteria. Recently, Fetzer (1973) attempted to evaluate the reliability of Middle and Upper Ordovician K-bentonite correlations from Pennsylvania, Virginia and Tennessee in terms of conodont zonation. He was not successful in correlating individual beds but only K-bentonite groups or complexes, because of the lack of good paleontologic resolution. Thus, it seems that none of the methods that have been used for regional correlation purposes are completely reliable.

The evidence for a volcanic origin of K-bentonite is based on detailed petrographic microscopic examination. Ross (1928) listed criteria for their recognition and presented evidence that they were in fact derived from volcanic ashes. He summarized that the,

> ....presence of glass relict structure, presence of minerals and crystal forms characteristic of volcanic rocks, absence of minerals that do not have a volcanic origin, waxy luster, reaction with water, optical properties and chemical properties....

were useful features in recognizing bentonites. Ross proposed the term "metabentonite" because he thought that the ashes in Virginia had been subjected to low grade metamorphism subsequent to deposition.

Allen (1929) reported the clay beds in the Ordovician of Minnesota were of volcanic origin as evidenced by their textural, mineralogic and chemical characteristics. Ross and Kerr (1931, 1934) found the clays of Ordovician bentonites were composed of a clay mineral constituent other than montmorillonite and beidellite which were the major constituents of Tertiary and Cretaceous bentonites. They observed that in this clay sericite was dominant. Ross and Kerr did not approve the term "metabentonite" because according to them the alteration process of the original volcanic ash did not include the metamorphic processes. According to Bradley (1945) the diagenetic fixation of potassium in the interlayer position of expandable montmorillonite structure resulted in the formation of a mixed-layer clay mineral composed of illite and montmorillonite. Weaver (1953a), Huff (1963a) and Reynolds and Hower (1970) determined that the clay mineralogy of Ordovician K-bentonites consists mainly of regularly interstratified, dioctahedral, 2:1 clays with parameters similar to illite and montmorillonite ranging between the ratios of 4:1, 3:1 and 3:2. Weaver detected chlorite in some samples. According to him the term "metabentonite" should be abandoned in favor of "K-bentonite" or "potassium bentonite". Huff (1963 a, b) studied in detail the Middle Ordovician K-bentonites from Kentucky and southern Ohio. Based on differential thermal analysis he concluded that mixed-layer clays of K-bentonites were derived from montmorillonite after the devitrification of volcanic glass, and could be

distinguished from "mixed-layer" degraded mica, thus proving the volcanic origin of Ordovician K-bentonites. His cation exchange data suggested a fairly stable structure and narrow compositional range for these clays. Huff did not observe any chlorite. Lounsbury and Melhorn (1964) described the clay mineralogy of Paleozoic K-bentonites and found mixed-layer illite-montmorillonite in the majority of samples. Mossler and Hayes (1966) studied Ordovician K-bentonites from Iowa, Wisconsin, Illinois and Minnesota and determined that the clay minerals show characteristic reflections of mica polytype intermediate between 1M and 1Md of Yoder and Eugster (1955) which indicates a low temperature origin for K-bentonites.

Occurrences of Ordovician K-bentonites in Europe reported from Sweden (Byström, 1954, 1956; Byström, et al., 1961), Denmark (Bergström and Nilsson, 1974), Norway (Hagemann and Spjeldnoes, 1955), Poland and northern Germany (Ross, 1955). These studies were largely concerned with the petrographic and mineralogic nature, stratigraphy, age and correlation of these bentonites. Recently, interest in various aspects of Ordovician K-bentonites has increased as indicated by current research (Snäll, 1977; Velde and Brusewitz, 1978).

Previous Work on the Geochemistry of Younger Ash-Fall Deposits:

The great value of chemical fingerprinting in solving tephrochronologic problems of widespread Cenozoic ash layers has recently been emphasized by various investigators. Several

characterization methods and laboratory techniques for identification of individual layers have been suggested and applied with varying degrees of success. Czamanske and Porter (1965) determined the bulk chemical composition of some Cascade pyroclastic horizons by using x-ray fluorescence techniques, and were able to distinguish between them on the basis of TiO_2 content. Trace element concentrations determined by an x-ray fluorescence method had been successfully used by Jack, et al., (1967) to distinguish acid volcanics in California and adjacent areas. Although, tephrochronological studies based on bulk chemical composition are believed to be unreliable by some investigators (Westgate and Dreimanis, 1967; Lerbekmo and Campbell, 1969; Westgate, et al., 1970) more encouraging progress has been made by several investigations of major and trace element distribution within Pleistocene ash-falls. Kittleman (1973) found that within about 186 miles (300 km) of Crater Lake, mineral abundances and refractive index of glass of Mazama tephra were homogenous. The abundance of discrete mineral grains decreased, but the proportion of heavy minerals did not change with increasing distance. Borchardt, et al., (1971b) determined major and minor elements in the glass separates of Mazama ash by instrumental neutron activation analysis. They found that the abundances of the elements were independent of distance from the source. These data strongly suggest elemental distribution, whether related to heavy mineral content or the shard

composition, might be laterally persistent within individual ash beds. Several other characterization techniques which require the use of sophisticated equipment have been successfully applied. They involve determination of compositions of glass, magnetite and ilmenite by use of electron microprobe (Smith and Westgate, 1969; Westgate and Fulton, 1975; Westgate, 1977; Westgate, et al., 1977), determination of the volcanic glass composition by neutron activation analysis (Theisen, et al., 1968) and study of paleomagnetic characteristics of ash layer further to support correlation efforts (Westgate, et al., 1977).

The choice of particular elements and elemental ratios to be used as potential discriminators between individual ash layers depends on the geochemical characteristics of the element, geologic history of ash layers and the analytical methods used. Various workers studied numerous elements which might permit correlation of ashes. Smith and Westgate (1969) separated the Mazama, St. Helens "Y" and Bridge River ashes on the basis of as few as three key elements, Ca, K and Fe or Ca, K and Na. Jack and Carmichael (1969) calculated expressions of variation for nineteen major and minor elements in Quaternary acid volcanics in California and found sufficient variation for Rb, Sr, Zr, Mn, Ba, Ti, Pb, Y, Nb and also for K/Rb to permit fingerprinting of individual ash beds. Randle, et al., (1971) reported that the contents of La, Th and Co, and La/Yb ratio could discriminate between ash samples from

Cascade range volcanoes. Borchardt and Harward (1971) found that only five elemental ratios were needed to distinguish between Mazama ash and five reference ash layers. Specifically, these were Ce/Sc, La/Hf, Sc/Fe, Cs/Yb and Sc/Yb. Wood (1977) correlated two pumiceous Holocene tephra layers with two eruptive centers in eastern California, based on their Sr, Rb and Zr contents. These previous works on the geochemistry of Quaternary pyroclastics from the western North America mainly deal with terrestrial deposits. However, similar tephrochronological studies were also successfully applied to widespread deep-sea volcanic ash layers. Bowles, et al., (1973) studied fifteen chemical parameters for the purpose of identification and correlation of individual volcanic ash layers of Quaternary age from the eastern equatorial and southeastern Pacific Ocean. They concluded that among these parameters only nine, Ba, Zr, Sr, Rb, Mn, Ti, Fe, Ca and K had sufficiently high statistical variability to enable them to establish correlation. Keller, et al., (1978) studied as many as 20 air-borne tephra layers in the upper Quaternary sequence of deep-sea cores from the eastern Mediterranean. They were able to correlate tephra layers with their source volcanoes on the basis of major element contents. The distribution for single layers had been traced over more than 1240 miles (2000 km). In the case of Ordovician ash-falls the problem is more complicated because these ashes have undergone longer period of post-depositional alteration and the original composition has changed due to the loss

and/or gain of mobile elements. However, comparative data are available as exemplified by Borchardt and Harward (1971) and Borchardt, et al., (1971a) who studied the major and trace element contents of soils developed on Mazama ash. They found that the rare earth element and transition metal concentration in the clay fraction showed an enrichment relative to that in the glass. But the abundances of Hf, Th and rare earth elements as well as Sc/Fe ratio were relatively constant with soil depth and stable elemental ratios unique to Mazama ash aided long-distance correlation of weathered soil horizons. Weathering processes are not analagous to submarine devitrification and post-depositional alteration of volcanic ash but it raises the question of the extent of compositional change during alteration of K-bentonites.

Recently, a classification scheme has emerged which relates basic volcanics to magma type and tectonic setting based on the studies of Cann (1970), Pearce and Cann (1971), Floyd and Winchester (1975) and Smith and Smith (1976). Their method designates certain minor and trace elements such as Ti, P, Zr, Y and Nb which are considered to be immobile during the alteration process, consequently they should retain the essential characteristics of certain magma types of ancient basic volcanics that had been subjected to submarine weathering, spilitization and low-grade metamorphism. This principle of chemical uniformitarianism had been successfully applied to

dacitic and rhyolitic pyroclastics and lavas from Canada (Whitehead and Goodfellow, 1978) on the basis of their Ti, Y, Zr, Nb, Ni and Cr contents. Similarly, Winchester and Floyd (1977) and Floyd and Winchester (1978) identify and discriminate altered and metamorphosed volcanic rocks such as spilites, keratophyres, tuffs and greenstones in terms of magma series and degree of differentiation using their immobile element (Ti, Zr, Y, Nb, Ce, Ga, Sc) contents. These studies suggest the possibility that immobile elements in Ordovician K-bentonites can be used for similar correlations and the determination of original ash composition.

Scope and Limitations of the Problem

The present study was carried out to investigate the chemical, petrographic and mineralogic characteristics of Middle Ordovician K-bentonites in Indiana, Kentucky, Tennessee and Alabama. During this investigation core, outcrop and quarry samples were limited to widespread K-bentonite horizons in the upper Black River Group. In general, they were collected from cores and new quarries for the purpose of obtaining those affected the least by surface weathering. Such samples were especially needed for the correlation purposes of the study. The number of samples were also determined by several other factors such as K-bentonite recovery in the cores depending upon the thickness of horizons, degree of their stratigraphic control and time limitations.

Experiments were carried out for both K-bentonite bulk samples and their less than 2 μm clay fractions. Chemical analyses were made by wavelength dispersive x-ray fluorescence spectrometer and atomic absorption spectrometer. Polarizing microscope and x-ray powder diffraction analysis were used to study the petrography and both non-clay and clay mineralogy of the K-bentonites. Their results were complementary to the studies based on the chemical composition of the samples. The results of the chemical analyses were processed by an IBM System 370 computer available in the University of Cincinnati for the statistical analysis.

The objectives of the present study are as follows:

1. The first objective of this study is to describe the mineralogic and petrographic characteristics of K-bentonite bulk samples and their less than 2 μm clay fractions. It is hoped that the information gathered during this phase of the study will contribute to our knowledge of mineralogy and petrography of K-bentonites within the study area and will be very useful during the interpretation of the results of chemical analyses.
2. The second objective of the study is to determine the effects of post-depositional alteration processes on the original ash composition. An understanding of the gains and losses which occurred during alteration can provide a better understanding of the mechanism and nature of mineralogical

changes in the course of time. If the original bulk composition of the volcanic ash can be determined questions relating the origin of high potassium content of Ordovician K-bentonites can be logically considered.

3. The third objective is, based on the detailed chemical examination of K-bentonites, to initiate a study relating widespread horizons to the early Paleozoic Taconic Orogeny of North America. It is anticipated that a comparison of compositions of the original ash and igneous rocks found along the ancient volcanic belt in eastern United States will reveal some information on location of eruptive centers and/or stage of orogenic development.
4. The fourth objective is to determine chemical parameters, that is, the elements or elemental ratios that can be used for geochronologic studies of K-bentonite horizons. For this purpose within- and between-bed variability of immobile elements will be tested and relative discrimination power of the chemical parameters be determined.
5. The fifth and last objective of this study is to carry out a long-distance stratigraphic correlation of K-bentonite horizons. The correlation can be possible when local within-bed compositional variations, if determined during the geochronologic studies, can be smoothed off by regional data so that they will not mask between-bed compositional variability.

GEOLOGY

Location of Study Area

Figure 1 is a location map of the study area covering portions of southeastern Indiana, central Kentucky, north central Tennessee and northeastern Alabama. Approximate lateral distribution of core and outcrop samples used in this study is shown in the Figure, and sample identity and details on location for each sample are given in Appendix A. As shown in Figure 1, some localities are separated by as much as 316 miles (510 km) in a north to south direction and 124 miles (200 km) in an east to west direction. The regional trend of sample localities lies parallel to the axis of the Cincinnati arch (Fig. 2). Vertical distribution of the samples is restricted to the equivalents of the upper Black River group of the New York type section.

Geologic Setting

A brief description of the regional geology of the study area is felt to be appropriate here for a better understanding of K-bentonites under investigation. Figure 2 is a generalized tectonic map of the southeastern United States after King (1964), showing the physiographic divisions of the Appalachian mountain system and adjacent regions to the northwest and southeast. As outlined on the map, the study area embraces parts of the Appalachian plateau and the interior low plateau of Fenneman (1938). The area is a carbonate platform to the northwest of the Valley and Ridge province, formerly

FIGURE 1. Map of study area showing the location of samples (● core; ▬ outcrop).

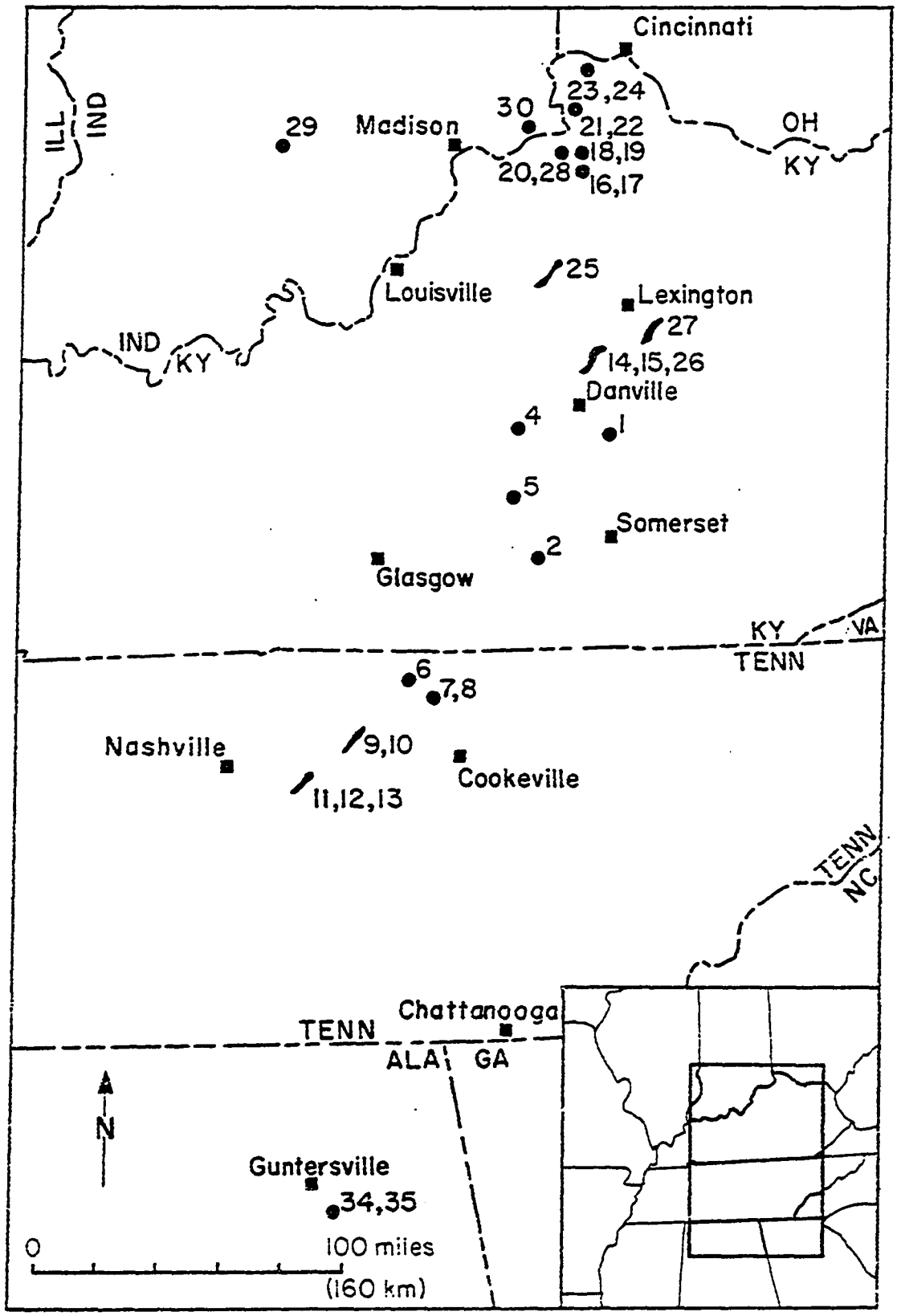

FIGURE 2. Tectonic map of southeastern United States, showing Appalachian and Ouachita mountain systems, and adjacent regions to the northwest and southeast.

(After King, 1964)

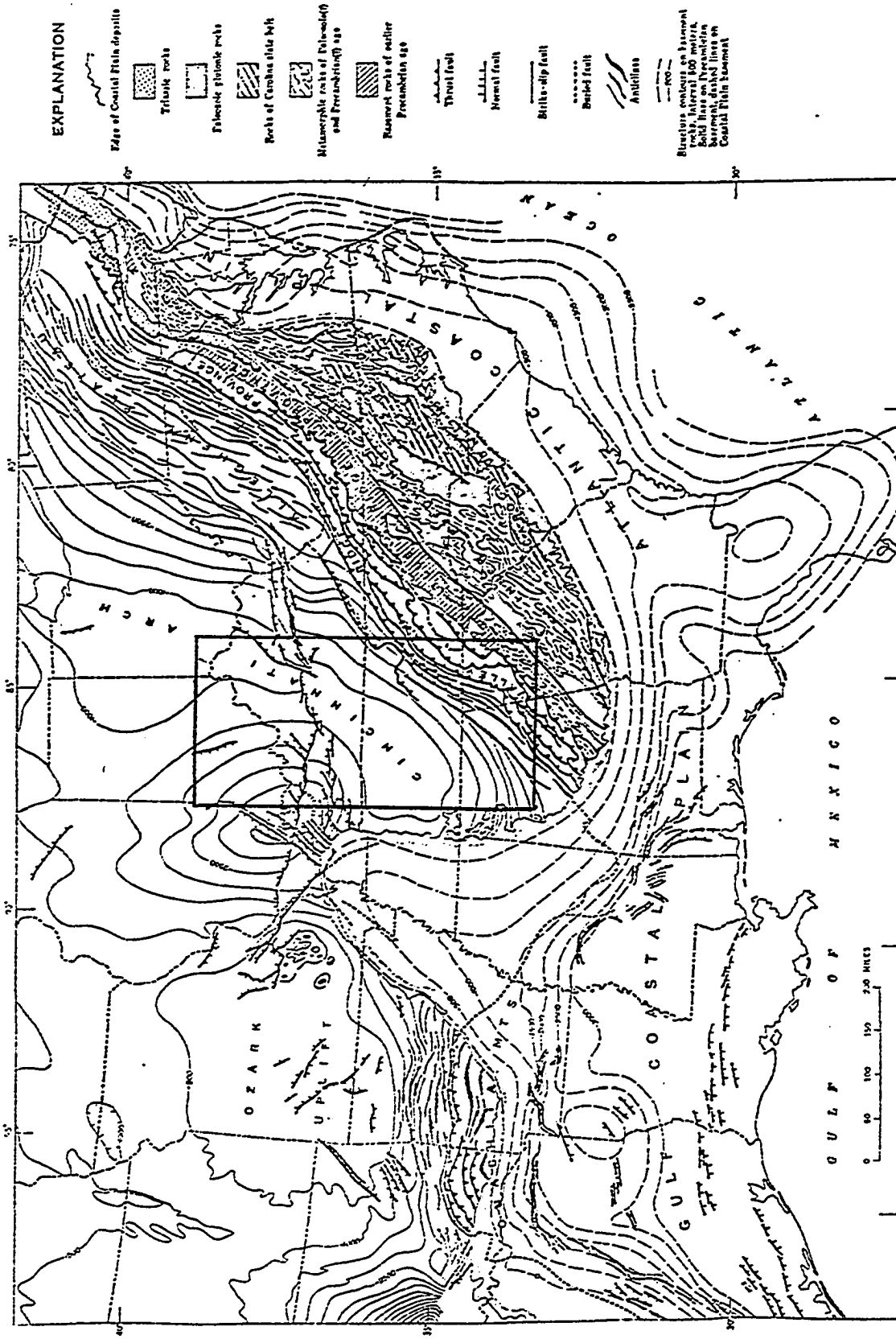

a miogeosynclinal area (King, 1964). During the Lower Paleozoic, the Valley and Ridge province and Appalachian plateau received a considerable thickness of carbonate and clastic sediments, most of it derived from areas outside the Valley and Ridge from the east or southeast (King, 1964, p. 24; Harris and Milici, 1977, p. 3). Miogeosynclinal strata are extensively folded and thrust faulted (King, 1964, p. 21), while the Appalachian plateau toward the northwest has suffered only minor deformation and the rocks are for the most part nearly horizontal (Adams, 1926, p. 25).

One of the most important structural features of the study area is the Cincinnati arch, the axis of which passes through central Tennessee and Kentucky in a southwest by northeast direction (Fig. 2). The arch is one of the several features which determine the distribution of exposed Ordovician strata in the central interior of the United States (Miller, 1919; McFarlan, 1943). Rocks of the Middle and early Late Ordovician age are brought to the surface by two domes along the Cincinnati arch -- the Nashville (Rutherford) dome of central Tennessee (Wilson, 1949), and Lexington (Jessamine) dome of central Kentucky (Cressman, 1973). The oldest Ordovician rocks exposed on the Nashville dome belong to the Murfreesboro Limestone of the Stones River Group (Wilson, 1949, p. 24-32) of Black Riverian age (Van Eysinga, 1975). Its outcrop occupies an approximately circular area around Murfreesboro, in Rutherford County. The Lexington dome occupies the Inner Blue Grass region of Kentucky

and forms an inlier which brings to the surface the limestones of the High Bridge Group of the same age (Cressman, 1973). The two are separated by a saddle in the structure centering over Cumberland County, Kentucky (McFarlan, 1943; Borella and Osborn, 1978). McFarlan (1943, p. 132) recognized two main periods in the development of the Lexington dome, one in the pre-mid-Devonian, and one in the Permian. Further studies by Woodward (1961, p. 1650), Cressman (1973, p. 55) and Wolcott, et al., (1972, p. 1327) agreed that the Cincinnati arch did not exist during the late Middle or early Late Ordovician time. Borella and Osborn (1978) by examining the depositional environments and associated paleobathymetry in the Cincinnati arch province, suggested the presence of the Lexington and Nashville domes or precursors to these domes and the absence of an active, continuous Cincinnati arch during the same time.

The other dominant structural feature within the study area is the fault belt that extends westward from the Appalachians across Kentucky (Fig. 2). In central Kentucky, the Lexington dome is cut by two major normal fault systems (Cressman, 1973, p. 3) -- the Kentucky River fault zone and the West Hickman = Bryan Station fault zone, both oriented in a northeast to southwest direction, and intersecting near the apex of the dome. In this area the Kentucky River crosses the Kentucky River fault nine times before it finally leaves it at Camp Nelson (Miller, 1919, p. 17). Throughout this serpentine divergence the river is bedded in hard, High Bridge rocks forming

300 to 400 feet (90 to 120 m) deep canyons (Fig. 3) wherever its course is in the upthrown or northeast side of the fault. Where the course is on the southeast or downthrown side of the fault the river is bedded in the softer limestones and shales of the younger Middle Ordovician formations (Lexington and Cincinnati) forming wider valley and sloping sides (Miller, 1919, p. 17). The Kentucky River fault zone is thought to extend to basement (Bayley and Muehlberger, 1968) and is an ancient feature. It apparently was active in Cambrian time (McGuire and Howell, 1963; Webb, 1969).

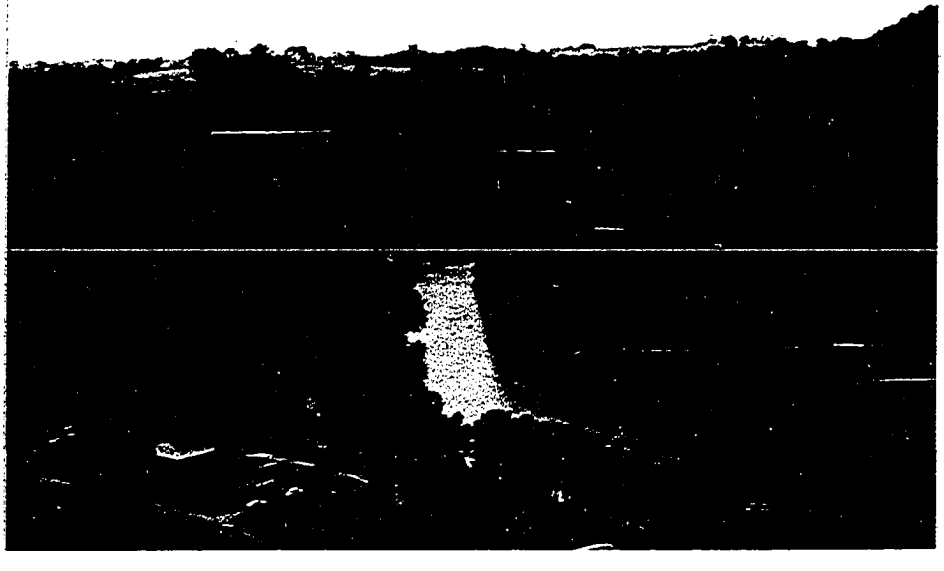

FIGURE 3. View from the high railroad bridge at the junction of Kentucky and Dix Rivers. Rocks of High Bridge Group occurs on the walls of the canyons and at the top of the plateau.

Stratigraphy of the Study Area

Figure 4 shows the approximate correlation of Middle Ordovician rock units within the Mohawkian Series by means of selected examples of stratigraphic nomenculature as applied in Indiana, Kentucky, Tennessee and Alabama. It also relates this nomenculature to the North American Middle Ordovician standard (Van Eysinga, 1975). Thus, the High Bridge Group of Kentucky can be traced into Indiana, where it is known as the Black River Limestone (Gutstadt, 1958), into Tennessee or Alabama where it is known as the Stones River Group or Stones River Formation, respectively (Wilson, 1949; Milici and Smith, 1969; Drahovzal and Neathery, 1971; Kidd and Copeland, 1971). Similarly, the Lexington Limestone of Kentucky can be shown to be the continuation of the Trenton Limestone of north Indiana and Nashville Group or Nashville Formation of Tennessee or Alabama, respectively. However, as pointed out by Moore (1977) much of the Middle Ordovician sequence of the southern Appalachians consist of carbonate and mixed carbonate and clastic rocks deposited in a variety of sedimentary environments. Walker (1974) reconstructed the aerial distribution of the shelf environments in the eastern Tennessee and showed that there were at least six major depositional settings, each characterized by particular lithologies and faunal/floral assemblages at the time of greatest environmental complexity (Late Black Riverian). Read and Tillman (1977) described gross lithofacies distribution in stratigraphic cross sections across

FIGURE 4. Selected examples of stratigraphic nomenculature of rock units within the Mohawkian Series as defined in Indiana, Kentucky, Tennessee and Alabama.

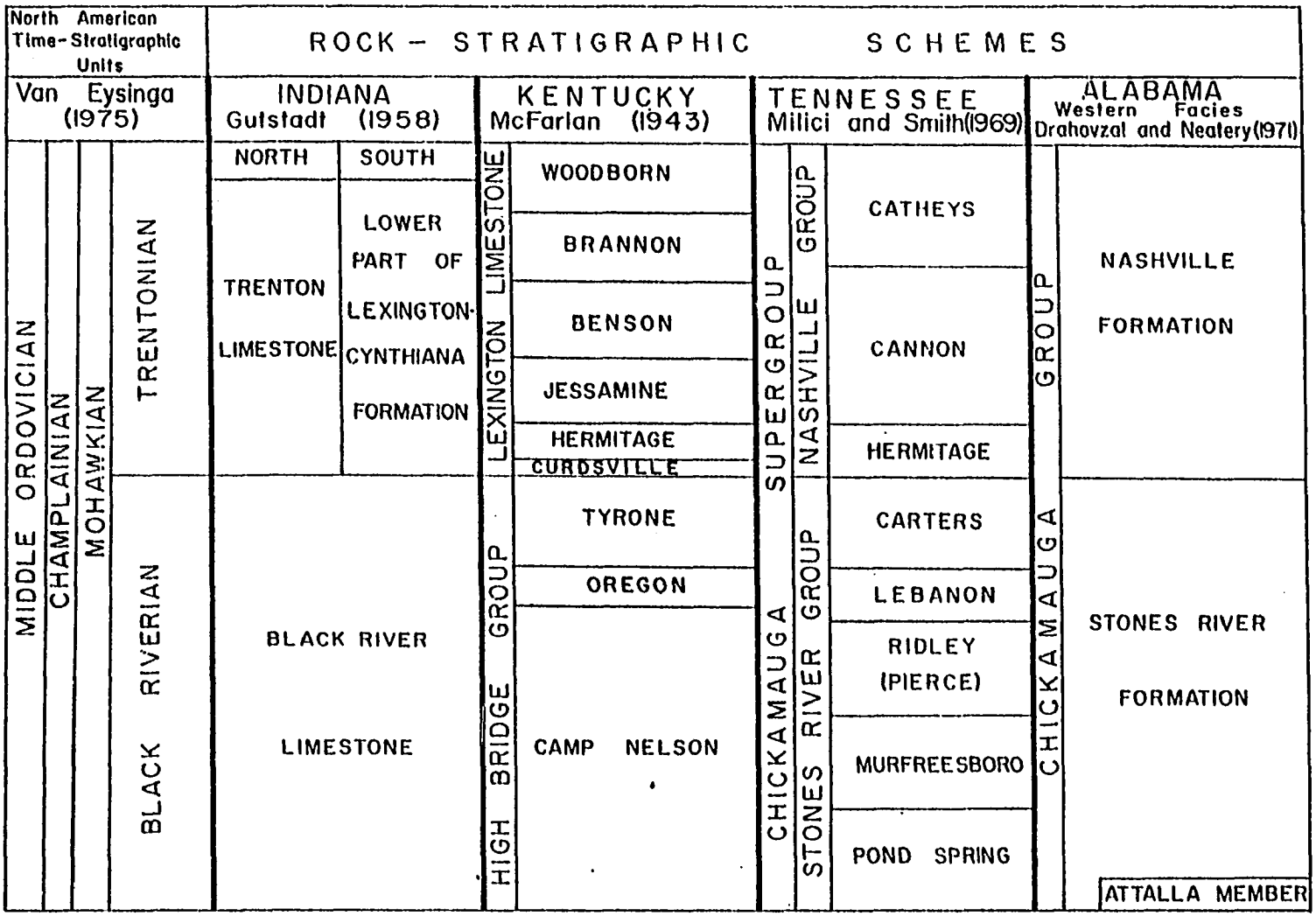

the Middle Ordovician platform to basin environments of southwestern Virginia. These studies reveal the intricate facies relationships which result from deposition in a complex environmental framework. Some workers have attempted to define and correlate these rocks chiefly on lithologic grounds (Rodgers, 1953), and others mainly on paleontological grounds (Cooper, 1956). However, as pointed out by Ruppel (1977), little agreement has been reached regarding the stratigraphy of these rocks. Although the Middle Ordovician sequence is relatively well exposed in Tennessee and Kentucky some lithostratigraphic and biostratigraphic problems still exist. Thus, some workers (Ruppel, 1977) prefer simply undifferentiated group names (e.g. Chickamauga Limestone, Fig. 4) when they refer to Middle Ordovician rocks at certain locations.

Lithologic characteristics and stratigraphic relationships of Middle Ordovician rocks within the study area have been described by various authors. Gutstadt (1958, p. 61-73) discussed the lithology, thickness and correlation of formations belonging to the Mohawkian Series of Indiana, Illinois, Michigan, Ohio, and Kentucky. Similarly, the Lexington Limestone and High Bridge Group of Kentucky were described in detail by Miller (1919), McFarlan (1943), Bergström and Sweet (1966), Wolcott, et al., (1972), Cressman (1973), Cressman and Noger (1976), Ruppel and Walker (1977) and Borella and Osborne (1978). Wilson (1949, 1962) studied the Middle and Upper Ordovician of central Tennessee, and provided comprehensive

information on the lithology, distribution, thickness and stratigraphic relations of different formations. Later, Milici (1969) and Milici and Smith (1969) correlated Middle Ordovician strata at Chickamauga, Georgia with those in the Sequatchie Valley and central Tennessee. Ruppel and Walker (1977) reviewed the record of Middle Ordovician sedimentary environments and their relations to biostratigraphy, paleoecology, and biogeography along a section from the epicontinental platform in central Kentucky across the shelf, shelf margin and into the basin in eastern Tennessee and Virginia. Recently, the various aspects of the Middle and Upper Ordovician of Alabama Appalachians have been summarized by Drahovzal and Neathery (1971).

One of the most important characteristics of Middle Ordovician rocks in the study area is the presence of K-bentonite layers at several stratigraphic horizons. These isochronous deposits have been discussed and employed during the description of various formations (McFarlan, 1943; Wilson, 1949; Drahovzal and Neathery, 1971; Cressman, 1973), and for the correlation of columnar sections in different areas (Wilson, 1949; Milici, 1969; Milici and Smith, 1969; Wolcott, et al., 1972). The number of K-bentonite horizons varies in different columnar sections especially when these sections are separated from each other by long distances. The occurrence of several different K-bentonite horizons within the great thicknesses of Ordovician strata indicates the long duration of repeated volcanic activity during the Ordovician time. As reported by Fox and Grant

(1944), a dam-site exploration and deep excavation by the Tennessee Valley Authority for the construction of the Chickamauga Dam on the Tennessee River, 7 miles (11 km) upstream from Chattanooga, Tennessee, revealed a total of fourteen K-bentonite beds in the Ordovician, the oldest being in the lowermost part of the Murfreesboro Formation, and the youngest in the Sequatchie Formation (Upper Ordovician). Their study also indicated that at this locality seven of these K-bentonite horizons were found within the Middle Ordovician rocks of Late Black Riverian age (Tyrone Limestone of Fox and Grant). Among these there are the two most prominent K-bentonite beds which can be recognized in outcrop and in the subsurface throughout most of the eastern mid-continent. Their use in stratigraphic correlations is exemplified by the work of Wilson (1949, p. 62-65), Gutstadt (1958, p. 62), Drahovzal and Neathery (1971, p. 13) and Wolcott, et al., (1972, p. B33) in central Tennessee, Indiana, Alabama and Kentucky, respectively. The present study also deals with K-bentonites of the same stratigraphic interval near the contact between Middle Ordovician rocks of Trentonian and Black Riverian age. Thus, a more detailed description of these rocks and their K-bentonite horizons will be discussed in the following paragraphs.

In Kentucky, the Tyrone Limestone, the youngest formation of the High Bridge Group (Fig. 4) is 60 to 120 feet (18 to 36 m) thick (Wolcott, et al., 1972), and is a sublithographic, dense, dove or cream colored limestone, breaking with conchoidal fracture and with

small facets of coarsely crystalline calcite. On weathering the surface becomes white, in which the darker facets are conspicuous, giving rise to the name bird's eye (McFarlan, 1943, p. 12). Several K-bentonites occur in the Tyrone Limestone: the "pencil cave" bentonite of drillers (southern and western Kentucky), occurs 15 to 25 feet (4.5 to 7.5 m) below the top of the Tyrone, and is the principal and the most consistently developed bed. It ranges in thickness from a few inches to five feet (McFarlan, 1943, p. 12). The second most persistent and wide spread K-bentonite horizon occurs at about 80 feet (24 m) below the top of Tyrone, and is generally one inch or less thick (Cressman, 1973). A third, "mud cave" bentonite of drillers (Fig. 5), has been observed in several localities at the Tyrone-Curdsville contact, and is present only locally (Cressman, 1973). The mud cave is about two feet thick and more coarsely textured than the pencil cave. It contains abundant flakes of biotite. When both K-bentonites are present, the interval between the mud cave and pencil cave is constant and generally equal to 25 feet (7.5 m) as reported by Cressman (1973).

As noted by Miller (1919) the contact between the Curdsville Limestone and the Tyrone Limestone is disconformable, at least where the mud cave bentonite is missing. Cressman (1973) suggested, as shown in Figure 6, that south and southwest of Lexington, the Curdsville rests directly on the mud cave bentonite, elsewhere the bentonite is missing. He also concluded that the Tyrone-Lexington

FIGURE 5. "Mud cave" bentonite (b) at the contact of Curdsville Limestone Member of Lexington Limestone (above) and Tyrone Limestone (below) in the railroad cut, Highbridge, Kentucky.

disconformity probably does not indicate any great interval of time, and although his data are sparse north of Lexington and east of Winchester (Fig. 6) he found that not more than 10 feet (3 m) of the upper Tyrone was removed before Curdsville deposition.

In central Tennessee the Carters is the uppermost limestone of Stones River Group (Fig. 4), and is divided into upper thin-bedded and lower massive-bedded units separated by T-3 (pencil cave

FIGURE 6. Distribution of "mud cave" bentonite of drillers (patterned areas) and approximate thickness of interval between base of "pencil cave" bentonite of drillers and base of Lexington Limestone. Line representing edge of mud cave bentonite is solid where based on mapping and dashed where edge is inferred.

(After Cressman, 1973)

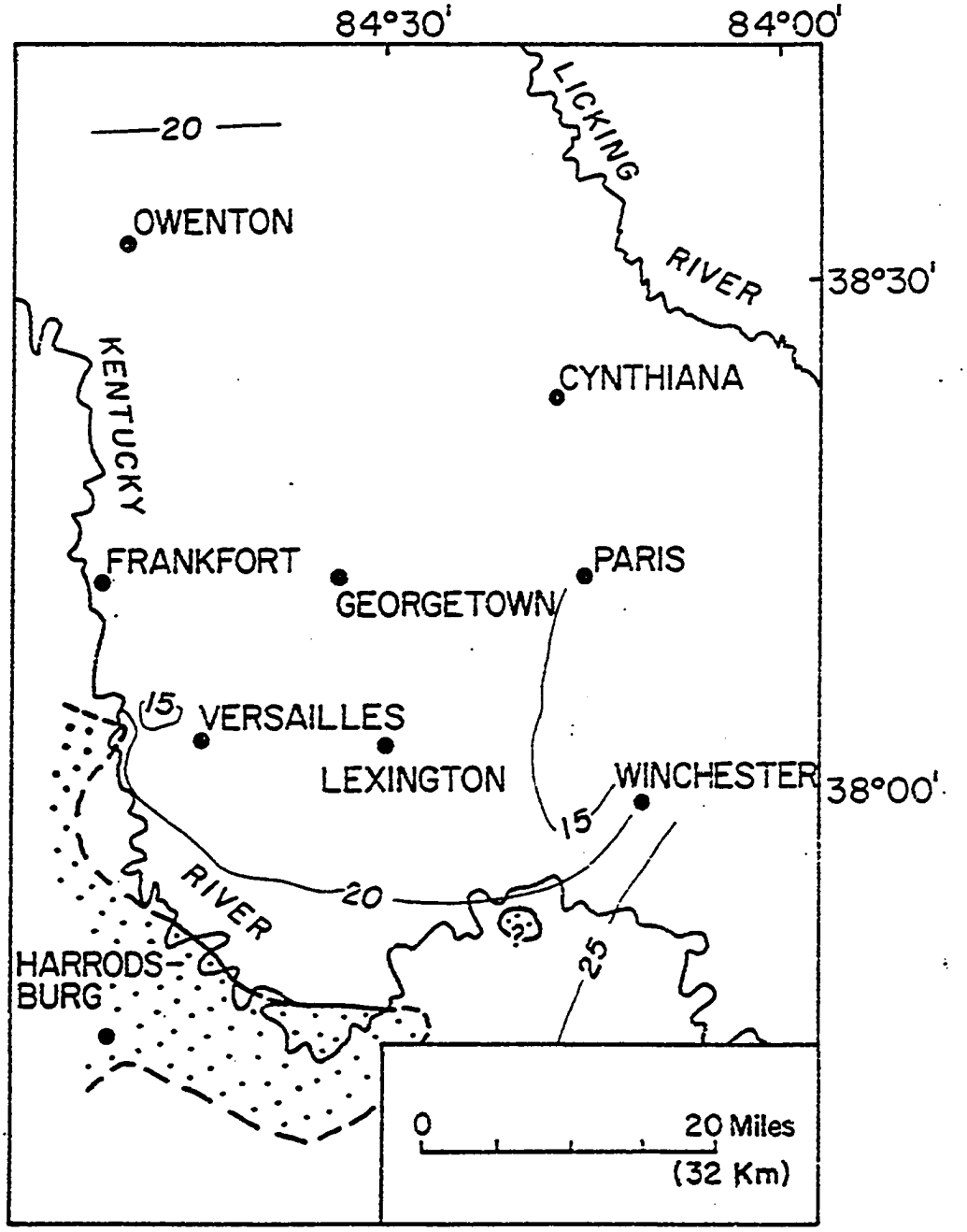

bentonite of Kentucky), as shown in Figure 7. The lower member is a fine to medium or coarse crystalline, light gray to dove, and massively bedded limestone with specks of clear calcite. It mainly consists of pure limestone with very little silt and clay (Wilson, 1949). It contains K-bentonite beds T-2 and T-1 (Fig. 7). T-2 averages 19 feet (6 m) below T-3, and this interval is constant throughout central Tennessee. Wilson recorded a maximum thickness of 12 inches for this bed, but commonly it is no more than 3 inches. He also observed that T-2 is locally absent within the central Tennessee. T-1 averages 16 feet (5 m) below T-2, and is usually less than 2 inches in thickness. Due to its thin character, T-1 is often locally absent. The lower Carters Member is believed to overlie the Lebanon Limestone unconformably (Fig. 7), and its average thickness is 50 feet (15 m) in central Tennessee (Wilson, 1949, p. 54).

The upper Member of the Carters Limestone occurs between the K-bentonite bed T-3 and the overlying Curdsville Member (Fig. 7). It is characterized by dense, fine-grained, dove-colored lithology and thin-bedding which contains partings of silt and clay. Throughout a large part of the central Basin its average thickness is 10 feet (3 m). At few localities within the eastern part of the central Basin K-bentonite bed T-4 (mud cave of Kentucky) occurs near the top of this member (Wilson, 1949, p. 59). Wilson pointed out the presence of an erosional unconformity immediately overlying

FIGURE 7. Diagrammatic section showing the generalized stratigraphic relationships of the Middle Ordovician K-bentonites (T-1 through T-5) and the rocks belonging to the Stones River (Carters and Lebanon Limestones) and Nashville (Hermitage Formation) Groups in different parts of central Tennessee. (After Wilson, 1949)

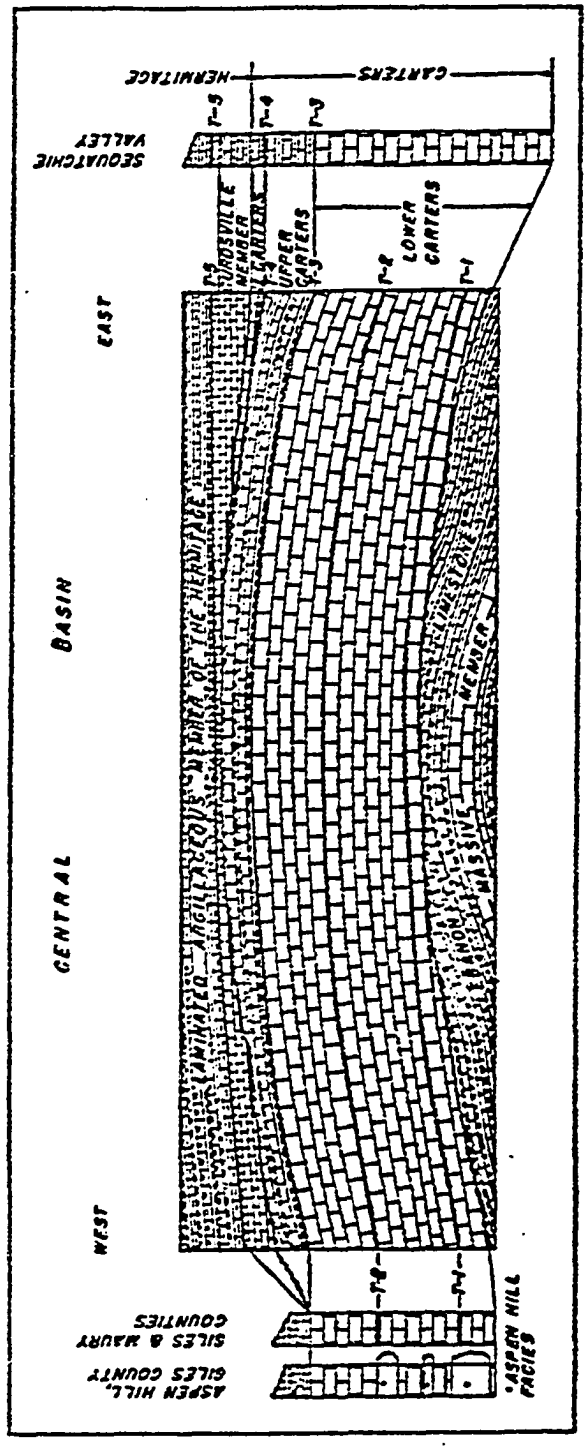

this bed, and separating the Nashville and Stones River Groups. Its absence over the central and western parts of the central Basin is believed to be the result of this post-Carters erosion.

The correlation of T-3 K-bentonite is fixed by its relationship to the upper and lower Members of the Carters Limestone (Fig. 7). In central Tennessee this bed is the thickest and the most persistent of the four (Wilson, 1949, p. 64). Its recorded thickness varies from 1 to 21 inches, thickening eastward. In an exposure at south Carthage, Smith County, it is an extremely sticky, green to olive-yellow clay. T-3, while not actually seen in the outcrop, may be predicted by a dark-brown chert layer forming a more resistant layer on the underlying massive lower Member of the Carters Limestone.

In Alabama, the western facies of the Middle and Upper Ordovician (Fig. 4) lies west and north of the Helena thrust fault (Drahovzal and Neathery, 1971). The undifferentiated Stones River Formation and the Nashville Formation constitute the Chickamauga Group of the Middle Ordovician. It is largely composed of limestone and several K-bentonite horizons have been reported (Drahovzal and Neathery, 1971, p. 12-13) and they can be correlated with the Tennessee K-bentonites. The T-1 of Wilson (1949) may be represented in the Stones River Formation of Alabama by green shales that occur locally at the top of the Attalla Chert Conglomerate Member (Fig. 4). A 1- to 5-foot thick interval of green shale at the Red Mountain cut in Birmingham may be bentonitic (Drahovzal and Neathery, 1971).

North of the latitude of Gadsden, Etowah County, the K-bentonites occur in a 30 or 40 feet (9 to 12 m) thick interval and lie approximately 20 feet (6 m) below the top of the Stones River Formation. In this area, T-3 and T-4 K-bentonites of Wilson (1949) have been traced from Tennessee. The T-3 K-bentonite is often 3 to 4 feet (1 to 1.2 m) thick in Alabama (Drahovzal and Neathery, 1971) and its color is yellow-gray to light yellow-green. It is characteristically underlain by a chert layer. The upper T-4 K-bentonite may be as much as 2 feet thick, and is characterized by abundant biotite flakes. T-4 is also underlain by a chert layer.

As defined in Indiana, the Black River Limestone (Fig. 4) is in most places a light to dark tan, mostly lithographic, and in part argillaceous and dolomitic limestone. It thickens regularly in a southerly direction from about 200 feet (60 m) in north-central Indiana to more than 500 feet (150 m) in the southern part of the State (Gutstadt, 1958). Soft green shales occur within the upper 50 feet (15 m) throughout most of the State and probably represent the pencil cave and mud cave of Kentucky as indicated by Gutstadt.

In the study area rocks of the Black Riverian age are overlain disconformably by coasely crystalline, bioclastic and fossiliferous limestone of Trentonian age (Fig. 4). In Kentucky and Tennessee their complex facies relationships have been studied for many years (Wilson, 1949; Black, et al., 1965; Milici, 1969; Cressman, 1973) and their nomenculature has undergone many changes. Several

K-bentonite horizons have been reported from Trentonian rocks in Tennessee (Fox and Grant, 1944; Wilson, 1949, 1962) and within the Curdsville Member in Kentucky (Young, 1940; MacQuown, 1967). T-5 K-bentonite (Fig. 7) which is probably the equivalent of B-10 of Fox and Grant (1944) is found at the base of the Laminated Argillaceous Member of the Hermitage Formation and it is moderately persistant within the central Basin of Tennessee (Wilson, 1949). Locally it is absent or not recognizable probably because during deposition, the ash was disseminated through a zone of silt rather than concentrated as a pure ash layer like T-1, T-2, T-3 and T-4 K-bentonites. These four are interbedded with pure limestone of the Carters Formation (Wilson, 1949, p. 91).

Paleogeography of the Study Area During Middle Ordovician

During Middle Ordovician time most of eastern North America, including the study area, was covered by shallow waters of the pre-Trentonian inland sea (Kay, 1935). For a period this sea was the scene of calcereous ooze deposition of Late Black Riverian age that later became the Carters Limestone (Wilson, 1962). The fine clastics and K-bentonites within the limestone sequences indicate volcanism of varying intensity and uplift at some distance to the east, corresponding to the Blountian Phase of the Taconic Orogeny (Rodgers, 1953).

At the beginning of Trentonian time crustal movement resulted in a relative uplift in three parts of the region (Kay, 1935;

Wilson, 1962) so that the Appalachian and Ozark domes became capable of supplying fine grained sediments to the surrounding basins while the land corresponding to the Cincinnati arch was too low to yield any clastic material. Periodic exposure of these uplifted areas to subaerial erosion resulted in the pre-Trentonian disconformity. Coarser-grained, bioclastic carbonate sediment of the Curdsville Limestone of central Kentucky was deposited in an agitated water environment (Cressman, 1973, p. 13). Repeated regression and transgression of the sea during Trentonian time developed in each formation complex lithic and faunal facies patterns that intertongue laterally and intergrade vertically with one another (Bergström and Sweet, 1966). Meanwhile, repeated volcanic activity as a continuing phase of the Taconic orogeny caused the deposition of tephra layers in shallow seas.

As illustrated in Figure 8, the Middle Ordovician K-bentonites are distributed over large areas in the eastern North America. K-bentonites of Late Black Riverian age are among the most distantly distributed of all Mohawkian K-bentonites, while those of Trentonian age are limited to thin layers, especially in the study area. As suggested by Kay (1935) the latter K-bentonites are the most abundant and the thickest in Vermont, New York and northern Michigan but they are not as widespread as the earlier ones. Kay also pointed out the increased thickness of K-bentonites in a southeastward direction and suggested a center of active volcanism possibly in

FIGURE 8. Distribution of Middle Ordovician K-bentonites throughout the eastern North America.

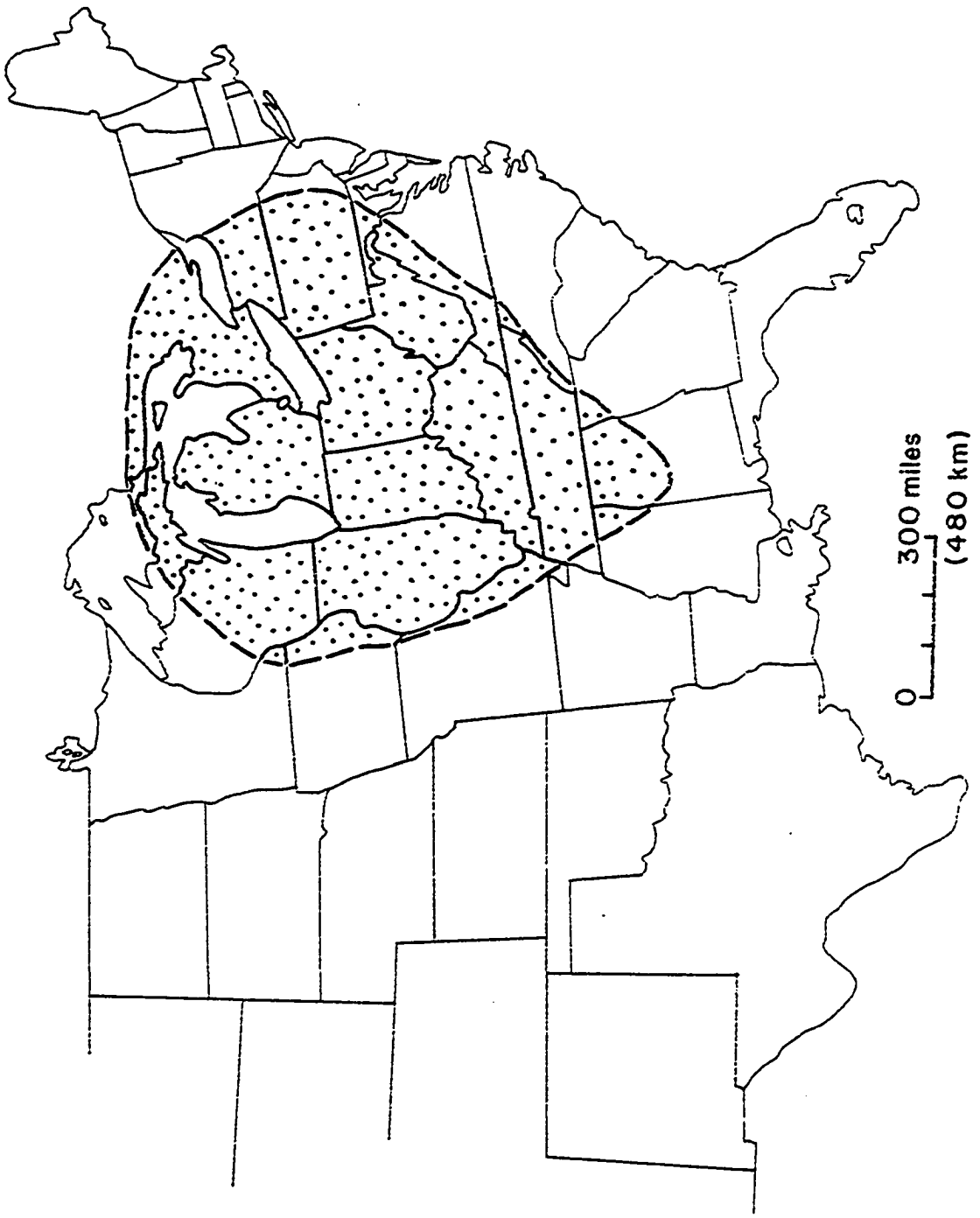

northwestern North Carolina. His suggestion is in accordance with the recent findings of Whitney, et al., (1978) who studied the felsic volcanic rocks of the southwestern extension of the Carolina slate belt in Georgia and South Carolina as a portion of the primary volcanic arc system during early Paleozoic time. Two of their major conclusions are that the area served as a source of pyroclastic sediments for hundreds and possibly thousands of square miles and that further north in central North Carolina later volcanism acquired more calc-alkaline affinities, as is to be expected in an island arc undergoing continued development.

Today, the widespread distribution pattern of Middle Ordovician K-bentonites to the west of the Appalachian volcanic belt (Fig. 8) may seem to be contradictory to the prevailing westerly winds. However, paleolatitudes in the eastern United States based on the geomagnetic pole for the Ordovician time as determined by Collinson and Runcorn (1960) indicate that the eastern United States was in the Southern Hemisphere in the zone of prevailing easterly trade winds (Cressman, 1973, p. 55).

METHODS OF INVESTIGATION

Sampling

The selection of sample localities as shown in Figure 1 (p. 21) was determined by outcrop distribution and availability of core material. An effort was made to collect primarily from the two thick, widespread and persistent K-bentonite beds, namely T-4 and T-3 of Wilson (1949), within the upper Tyrone Limestone in Kentucky and equivalents in Indiana, Tennessee and Alabama. A third K-bentonite bed, possibly B-8 of Fox and Grant (1944) was sampled in south-central Kentucky and north-central Tennessee. According to these authors B-8 occurs near the top of the Tyrone, and is thus the youngest of all three horizons studied.

It is essential for the geochronologic and correlation purposes of this study that samples have good stratigraphic control. Therefore, special attention was paid to obtaining outcrop, quarry and core samples from well-known horizons as defined by earlier workers. However, a smaller group of samples have doubtful stratigraphic settings and only their approximate positions are known. These samples illustrate the difficulties that arise in trying to maintain stratigraphic control of K-bentonite horizons in rocks with complex facies relationship. During the evaluation of the data, samples from the known horizons are used as control samples. Those from the suspicious horizons then are compared with the control samples in order to determine their exact stratigraphic settings.

In a regional study such as this the occurrence of distinct and widely separated K-bentonite horizons in the subsurface and outcrop provides a reasonable control in sampling the individual layers. This is the main reason the present study deals only with the three major horizons in upper Tyrone Limestone. Besides, these beds are the most widespread marker horizons within the Middle Ordovician because they represent major volcanic ash deposits which blanketed large areas and are, therefore, very suitable for long-distance correlation studies.

As shown in Figure 1, with the exception of five sample location sites, all specimens were obtained from cores provided by Cominco American Co., Cincinnati Gas and Electric Co., Indiana and Kentucky Geological Surveys. The smectite component of the clay minerals in K-bentonites appears to be susceptible to weathering making reliable outcrop samples difficult to obtain. Indeed, the chemical analysis of some outcrop samples revealed that those most severly altered had to be excluded for correlation purposes. Exposures in recent road cuts and new quarries, however, proved to be adequate.

A total of 100 samples were collected for this study (see Appendix A). In addition to 78 K-bentonite specimens, 22 limestone samples just below and above the K-bentonite beds were obtained in order to observe the environment of deposition of the original volcanic ashes and the contact relationships between these beds and their carbonate host rocks. Due to the possible compositional

variations within beds, the results of analysis of one K-bentonite sample from a thick horizon is not necessarily representative of the entire K-bentonite bed. For this reason, wherever the thicknesses of the horizons permitted, samples were collected at 2 inch intervals. An average of the chemical analyses of such samples should be more representative of the chemistry of K-bentonite horizons if a variation in composition within a bed exists, and serve more accurately for the geochronologic and regional correlation purposes of the study.

Sample Preparation

This section summarized the preparation of 72 K-bentonite bulk samples and 47 selected clay fractions (less than 2 μm). A more detailed discussion on sample preparation is included in Appendix B.

Hand specimens of K-bentonites were broken up into smaller chips with a hammer and then pulverized for two minutes by means of a shatter box equipped with a tungsten carbide grinder. From this stage on, the preparation of samples varied according to the analytical methods to be used.

Pulverized bulk samples were sieved and minus 200 mesh (U.S.A. Standard Testing Sieve) powder used for chemical analyses. Methods of sample preparation for major and trace element x-ray fluorescence analysis of silicate rocks vary from author to author, although in principle they are similar. During this study Al_2O_3, total

iron as Fe_2O_3 (Fe_2O_3T), K_2O, and TiO_2 values were determined from fused borate glass pellets following the technique described by Elsheimer and Fabbi (1977) and summarized in Appendix B. Determination of Rb, Sr, Y, Zr, Zn, Nb, Ga and Ge was carried out using pressed powder pellets made of undiluted rock powder as described by Fabbi (1970). Such pellets give high x-ray fluorescence intensity, and consequently the detection limits are generally low. SiO_2, MgO, CaO, Na_2O and MnO were analyzed by means of atomic absorption spectrophotometry. Their contents in K-bentonite bulk samples and the less than 2 μm clay fraction were determined using solutions prepared according to a procedure developed by Medlin, et al., (1969). The samples were fused with $LiBO_2$ and dissolved in a dilute nitric acid solution followed by dilution with a lanthanum nitrate solution and water. The method requires only routine fusion and dilution techniques and allows a maximum number of elements to be determined in one solution.

The less than 2 μm clay fraction was separated from the rest of the bulk samples by suspension in a solution prepared by dissolving 1 gram of sodium pyrophosphate hydrate ($Na_4P_2O_7$ $10H_2O$) in 1 liter of distilled water in order to prevent the flocculation of clay minerals. A satisfactory suspension was achieved by first mixing with a blender and then waiting overnight to settle the particles larger than 2 μm in size. The sample preparation for chemical analyses of less than 2 μm clay fractions was carried out the same way as described for the bulk samples.

In order to study the mineralogy of the less than 2 μm clay fraction using x-ray powder diffraction, three oriented clay slides for each sample were prepared using a smear technique. A thick clay paste is placed on the petrographic glass slide and spread across the slide in a thin, even layer with the help of a spatula. These samples were air-dried before any further processing, then one of them glycolated at 60°C overnight and the other heated at 600°C for an hour.

A number of thin-sections were prepared from K-bentonite hand specimens and adjacent limestone samples for petrographic study with a polarizing microscope. The swelling property of smectite imposed difficulties during the preparation of thin-sections. In order to overcome this difficulty a different method was applied by impregnating the rock as described in Appendix B. The thin-sections obtained by this method are of excellent quality: they are free from any scratches and show primary textures without any artificial disturbance.

Standard rock samples obtained from the U.S. Geological Survey and the Geological Survey of Canada were used during the chemical analyses. Their sample preparation was the same as those of unknown samples as described in this section.

Description of the Analytical Techniques

X-Ray Fluorescence Spectrometry:

The theory and practice of element analysis by means of x-ray fluorescence spectrometry have been well-developed and described by various authors (Jenkins and De Vries, 1967; Norrish and Chappel, 1967; Norrish and Hutton, 1969; Hutchison, 1974). For a more complete description of the x-ray fluorescence methods the reader should refer to these authors.

Al_2O_3, Fe_2O_3T, K_2O, TiO_2, Rb, Sr, Y, Zr, Zn, Nb, Ga and Ge were determined by wavelength dispersive x-ray fluorescence on a single channel vacuum spectrograph (General Electric XRD-6) with a dual target (Cr and W) tube and a pulse height analyzer. Operating conditions for the instrument are given in Appendix C.

Matrix effects were avoided in the major oxide determinations (e.i. Al_2O_3, Fe_2O_3T, K_2O, TiO_2) by the application of a fusion technique as explained in Appendix B and preparing diluted glass pellets from both standards and the samples. The percentage of each major element analyzed was determined from the following relationship:

$$P_x = \frac{C_x}{C_{std}} \times P_{std} \qquad (1)$$

where C_x and C_{std} are, respectively, the background corrected counts in a fixed time for the sample and the standard, P_{std} is the reported value of oxide for the standard, and P_x is the percentage of the oxide sought. A more detailed discussion of this procedure is given by Hutchison (1974).

The U.S. Geological Survey rock standard GSP-1 (Flanagan, 1969) was used as a standard sample during the chemical analyses. Four U.S. Geological Survey rock standards: G-2, AGV-1, PCC-1 and BCR-1 (Flanagan, 1969) and one Geological Survey of Canada standard rock sample; SY-2 (Abbey, 1976) were analyzed similarly as the unknown samples in order to measure the precision and accuracy of the technique. Within-sample homogeneity was measured for two of the K-bentonite bulk samples. The result of these studies are listed in the Tables I through III in Appendix D.

The concentrations of trace elements Rb, Sr, Y, Zr, Zn, Nb, Ga and Ge in each sample were determined by the following equation:

$$\text{ppm } Z_x = \frac{I\ Z\ K_{\alpha,x}}{I\ Z\ K_{\alpha,std}} \times \frac{\mu_{\lambda,x}}{\mu_{\lambda,std}} \times \text{ppm } Z_{std} \qquad (2)$$

where $I\ Z\ K_{\alpha,x}$ and $I\ Z\ K_{\alpha,std}$ refer, respectively, to the intensities in a fixed time of the background-corrected $Z\ K_{\alpha}$ peaks from the unknown and the standard, $\mu_{\lambda,x}/\mu_{\lambda,std}$ refers to the mass absorbtion coefficients at wavelength λ of both the unknown and standard sample, and ppmZ refers to the reported concentration of element Z in the standard (Reynolds, 1963). This equation is only valid if the K_{α} radiation of the element sought is of shorter wavelength than the absorbtion edge of the heaviest matrix element, namely iron (Hower, 1959; Reynolds, 1963).

The intensities of the fluorescent x-rays of the unknown sample and standard could be directly read on the scaler-timer unit of the

x-ray fluorescence equipment. During this study they were obtained by selecting a preset time which was used to make the scaler give the intensity readings in counts per the fixed time. The only unknown factor for determining ppm Z_x was $\mu_{\lambda,x}$ / $\mu_{\lambda,std}$: $\mu_{\lambda,std}$ could be calculated from the following relationship for any compound or composite material as explained by Jenkins and De Vries (1967, p. 16-17),

$$\mu \text{ (compound)} = \sum(\mu_i \times W_i) \qquad (3)$$

where, μ_i and W_i are individual mass-absorption coefficients and weight fractions, respectively. For 17 samples $\mu_{\lambda,std}$ values were calculated at 1.5 Å by using the tabulated data of Jenkins and De Vries (1967, Appendix 2c). The mass-absorption coefficients, $\mu_{\lambda,x}$, then, were estimated by using the intensity of Compton-scattered x-rays (I W $L\alpha_c$) following the method developed by Reynolds (1963) and refined by DeLong and McCullough (1973). Table I in Appendix E lists the calculated values of $\mu_{\lambda,std}$ for 17 standards and their x-ray fluorescent intensities. Using this information, a calibration curve was obtained as shown in Figure E.1 (Appendix E), and used to calculate $\mu_{\lambda,x}$ value for each unknown sample.

The U.S. Geological Survey rock standard GSP-1 (Flanagan, 1969) was used during the calculation of ppm Z_x in equation (2). Background intensity corrections were made by using a blank pressed powder pellet made of a composite material having a mass-absorption

coefficient similar to the unknown samples. In addition to GSP-1, U.S. Geological Survey rock standards G-2, AGV-1, PCC-1 and BCR-1 (Flanagan, 1969), and Geological Survey of Canada rock standard, SY-2 (Abbey, 1976) were used for the determination of the trace elements to measure the accuracy of the technique. The estimated means and conclusions resulting from the precision, accuracy and within bed sample homogeneity calculations are given in Tables I through III in Appendix D.

Results of the chemical analysis of K-bentonite bulk samples and less than 2 μm clay fraction as carried out by means of x-ray fluorescence are tabulated, respectively, as Table I and Table II in Appendix F.

Atomic Absorption Spectrophotometer:

SiO_2, MgO, CaO, Na_2O and MnO were analyzed by means of a Perkin-Elmer 403 model atomic absorption spectrophotometer. The theory of the method has been discussed by many authors including McLaughlin (1967) and Hutchison (1974).

Solutions of the rock standards GSP-1, G-2, PCC-1, BCR-1 and SY-2 were used for calibration in order to permit direct read-out of the oxide concentrations at each particular setting of the instrument. The results of the analyses of K-bentonite bulk samples and the less than 2 μm clay fraction are tabulated respectively, in Table I and Table II of Appendix F. The estimated means and conclusions of precision, accuracy and within-sample homogeneity calculations for this technique are listed in Tables I through III

in the Appendix G.

X-Ray Powder Diffraction:

Qualitative estimation of the minerals in the less than 2 μm clay fraction was carried out on a General Electric XRD-5 x-ray powder diffractometer with a copper target. For each sample three different smear slides were tested after air-drying, glycolation and heating. Instrumental setting during these scans are listed in Appendix H. Information gathered during the x-ray diffraction analysis is also used for the quantitative estimation of illite/ smectite ratio in the interstratified clays of K-bentonites and for the determination of the type of interlayering by employing the method of Reynolds and Hower (1970).

RESULTS OF INVESTIGATION

PART I: MINERALOGY AND PETROGRAPHY

Introduction

The mineralogy and petrography of Middle Ordovician K-bentonites have received considerable attention from the standpoint of both their relationships to Appalachian history and their uniqueness as indicators of a process of clay mineral formation and diagenesis. Ross (1928) studied the gross physical properties and general mineralogy of K-bentonites, and presented evidence that these beds were in fact of volcanic origin. The assumption of an acid-to-intermediate composition of the original ash has been reported by previous investigators such as Weaver (1953a). Allen (1929, 1932) gave a mineralogic description of K-bentonites from the northeastern States based upon observations with the polarizing microscope. He noticed in thin-section a texture similar to pumice fragments with minute vesicular cavities and suggested that montmorillonite had formed from volcanic glass with the retention of its texture (1929, p. 242). Fox and Grant (1944) studied K-bentonite horizons in Tennessee and reported their physical and mineralogic characteristics in detail. Later studies on the clay mineralogy of K-bentonites from Pennsylvania, Michigan and Illinois (Launsbury and Melhorn, 1964) and Iowa (Mossler and Hayes, 1966) further proved that they are altered products derived from volcanic ash.

X-ray powder diffraction, differential thermal analysis and cation exchange data on Ordovician K-bentonites have been provided in more recent studies. The investigations by Weaver (1953a) and Huff (1963a, b) concluded that the clay fraction consists primarily of dioctahedral illite-montmorillonite with a component ratio between 4:1 and 3:1. A detailed description of heavy and light mineral separates from K-bentonites and adjacent limestones is also given in these studies. Coker (1962) described a 50-inch thick K-bentonite outcrop in Tennessee, and concluded that although the percentage of heavy minerals in general decreases upward, the relative amounts of each species remains essentially constant. Both Weaver and Coker detected illite-montmorillonite and chlorite packets in x-ray patterns, although Coker (p. 42) inferred the presence of an interstratified illite-montmorillonite-chlorite phase rather than two separate phases. Cation exchange data (Huff, 1963a, b) suggest that K-bentonites were essentially Ca-montmorillonites partially transformed to 10Å-illites through the absorption and fixation of interlayer potassium. Huff (1963a) observed that although an additional, less than 10 percent absorbtion of interlayer cations such as K^+, Na^+ and NH_4^+ was possible in the lattice, essentially all vacancies for fixed potassium had been filled and the clay appeared to be a fairly stable structure. According to the structural considerations, absorption of K^+ in the lattice must be controlled by octahedral substitution rather than the low tetrahedral substitution (p. 88).

The nature of mixed-layering in interstratified illite-montmorillonites has been investigated by Reynolds and Hower (1970). On the basis of detailed comparison of diffraction patterns of illite-montmorillonites with calculated profiles, they concluded that the type of mixed-layering in Ordovician K-bentonites is regularly interstratified allevardite-type (IM superlattice) ordering, which is composed of high-charge layers with fixed interlayer cations alternating with low-charge layers that have exchangable cations and are capable of hydration (Weaver and Pollard, 1973, p. 107).

Observations made in the studies of clay mineralogy and clay petrology of rocks are found to be useful in investigations involving various geologic environments. Suchecki, et al., (1977) reported three stratigraphically restricted suites of clay minerals of Paleozoic rocks in the Cow Head klippe in western Newfoundland. They inferred that the youngest clay mineral assemblage composed of corrensite (expandable chlorite) and illite-smectite, formed as the alteration products of Mg^{+2}-rich volcanic detritus during burial metamorphism. Bodine and Standaert (1977) examined the geochemistry and mineralogy of chlorite and illite in silicate assemblages from a rock salt bed in the Upper Silurian Vernon Formation, New York. According to them the illite had an origin from several detrital micaceous minerals, but the chlorite appeared to be compositionally compatible with marine evaporite brines suggesting a metasomatic hyperhalmyrolitic origin, probably followed by isochemical recrystallization during diagenesis. Velde (1977) proposed a phase

diagram for illite, expanding chlorite, corrensite and illite-montmorillonite mixed-layer minerals through the use of experiments made with natural minerals and mineral assemblages. He suggested that the phase relations as determined under various temperatures (300°-400°C) at 2-kbar water pressure should correspond to those encountered in the nature and could be used to determine relative grades of diagenesis or epimetamorphism. Clay mineralogy and petrology of K-bentonites can be used for similar purposes. Weaver (1956) and Huff (1963a) draw attention to the petrologic importance of K-bentonites in studying geologic environments. As shown by previous studies, their clay mineralogy is confined to a narrow structural and compositional range throughout several hundred meters. The characteristic of K-bentonites can be used to obtain a better understanding of the physicochemical conditions and alteration processes which produced their final mineral assemblages.

Ordovician K-bentonites differ from younger Cenozoic bentonites of similar origin in having higher potassium contents. Younger bentonites are also largely montmorillonitic (Slaughter and Early, 1965). This difference between the two bentonite compositions may be due to the effects of continuing burrial diagenesis. The alteration of volcanic ash and subsequent diagenesis of illite from montmorillonite have been studied by Dunoyer de Segonzac (1965), Perry and Hower (1970), Weaver and Beck (1971), Eberl and Hower (1976), Eberl (1978), Hein and Scholl (1978) and Heling (1978). The effects of burial diagenesis on montmorillonite and gradual

fixation of potassium and magnesium to form illite and chlorite have also been discussed by Burst (1969), Powers (1959) and Weaver (1960) based on changes in diffraction characteristics and chemical composition as a function of depth. These changes are accompanied by the increasing ordering of the illite structure (Dunoyer de Segonzac, et al., 1968). In K-bentonites, it appears that ordering is more a compositional phenomenon rather than one influenced by changing environmental conditions, that is, by P-T conditions (J. Hower, personal communication, Velde, 1977, p. 269). A detailed examination of the clay structure and chemistry of K-bentonites will provide a better understanding of their genesis and of alteration processes involved during the transformation of original ash into bentonites.

In this chapter data concerning the mineralogic and petrographic features of K-bentonite bulk samples and their less than 2 μm clay fractions are presented. In this phase of the study, it is anticipated that observations of mineralogic and petrographic properties of the bulk samples under the microscope and investigation of clay fractions by diffraction will be useful tools and complementary to the chemical analyses in ultimately attempting to relate the present composition of the ash to its original composition, and in delineating the factors controlling the post-depositional alteration processes.

Mineralogy

Description of Non-Clay Minerals:

Non-clay minerals include biotite, alkali-feldspar, quartz, apatite, zircon and Fe-Ti oxides (ilmenite and magnetite) which are generally characteristic for acid-to-intermediate volcanic rocks. Among these, biotite, quartz, apatite and zircon appear to be well preserved while the others show varying degrees of alteration or replacement. Calcite, leucoxene and pyrite are among the major authigenic minerals in K-bentonites with occasional cryptocrystalline quartz and apatite. Zeolites were observed only in one of the thin-sections. Clay minerals, formed mainly as a result of the post-depositional alteration of volcanic glass constitute the major percentage of the authigenic minerals and they will be discussed in the following section.

Biotite flakes are very abundant in some of the K-bentonite samples (Fig. 9) whereas they are few or absent in others. In general, T-4 is characterized by an abundance of fresh biotite crystals which tend to be concentrated along certain horizons within the bentonite layer. Biotite occurs mostly as subhedral crystals which vary between 0.2 to 1 mm in diameter (Huff, 1963a). It is strongly pleochroic and usually brown. Partial chloritization of some biotite is indicated by color changes to 2nd order greens. They have typically perfect basal cleavage and form soft and flexible flakes as indicated by the degree of bending during compaction (Fig. 10). Zircon, alkali-feldspar and apatite crystals are found

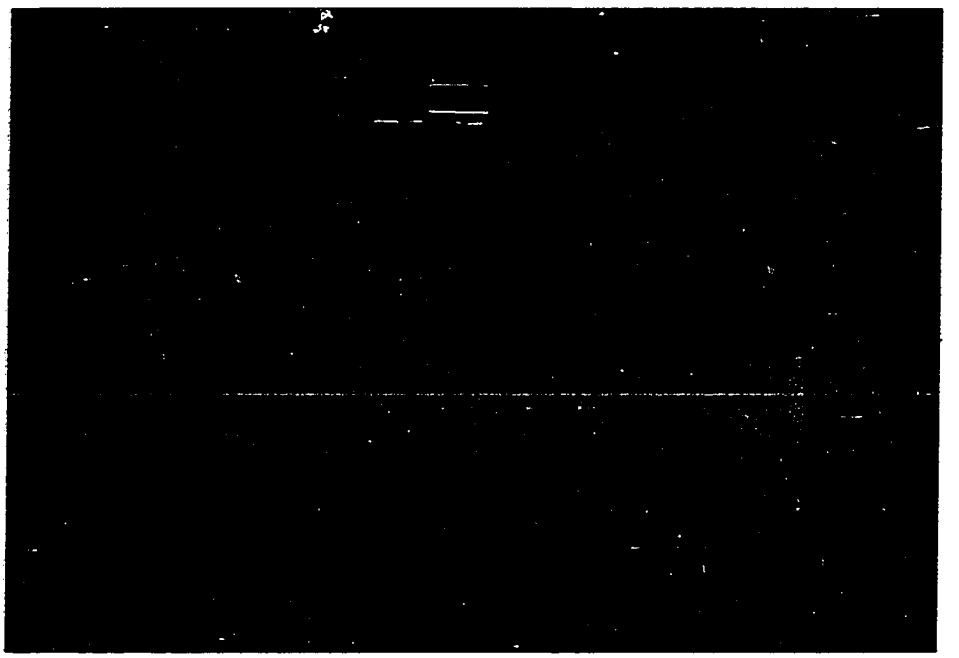

FIGURE 9. Abundant biotite flakes in core samples KB-6. Due to dark green color of the samples KB-8, biotites cannot be distinguished in the photograph.

both as discrete, euhedral crystals and as inclusions in the mica. In some biotite crystals inclusions of opaque minerals are observed (Fig. 11). Rimsaite (1975) examined the effects of alteration processes on biotites of different origins. She observed that secondary Fe-Ti oxides are fixed in the interlayer of partly chloritized mica as the chemical changes during the alteration of mica started along the 001 cleavage planes and fractures. The mica in Figure 11 may be similarly altered because opaque minerals are situated along the cleavage planes. However, a further study which

FIGURE 10. Photomicrograph of bended biotite flakes (sample no. KB-34, x nicols, x10).

FIGURE 11. Photomicrograph of a biotite crystal with inclusions of secondary Fe-Ti oxides along 001 clevage planes. Phengitic muscovite is also replacing the crystal (sample no. KB-34, x nicols, x10).

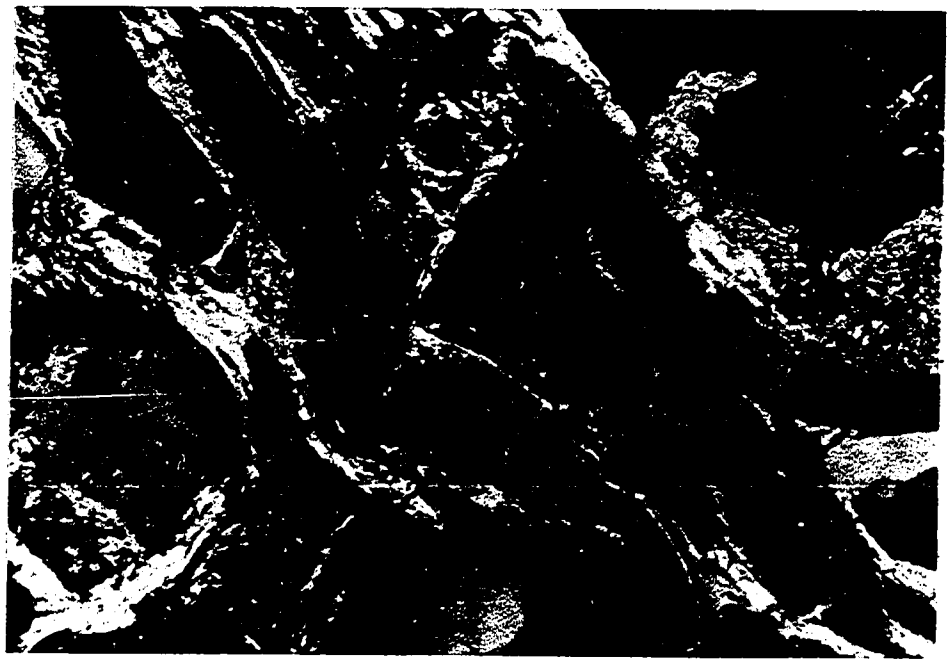

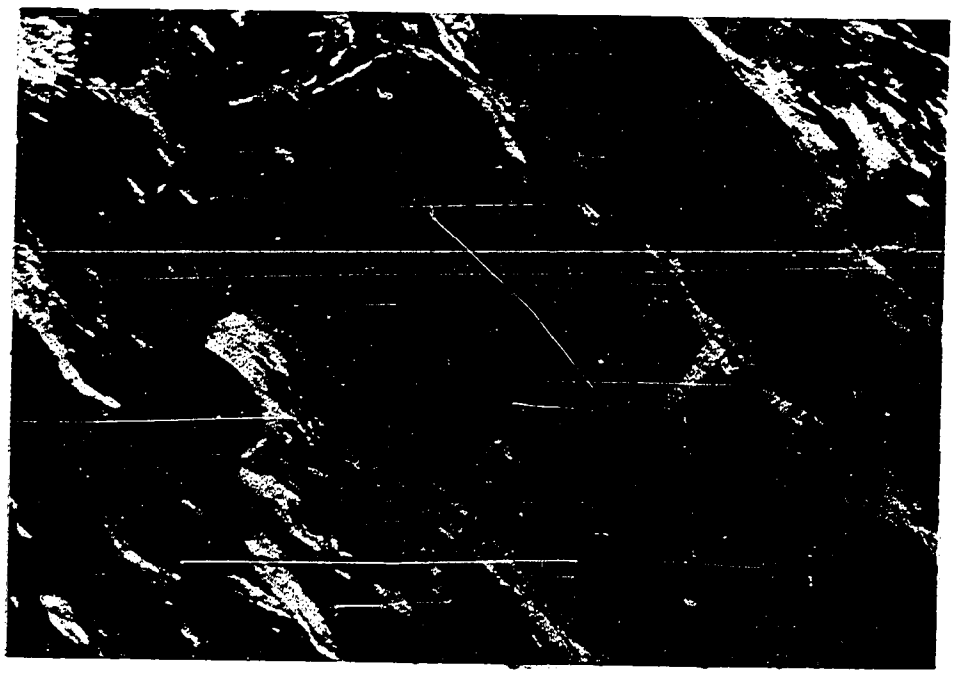

is beyond the scope of the present one, is needed to evaluate the primary or secondary origin of these inclusions. As seen in Figure 11 phengitic muscovite replaces biotite along the 001 cleavage planes. Otherwise the mineral is fresh, especially when compared to alkali-feldspars in the same sample.

The second most common non-clay mineral is alkali-feldspar, primarily sanidine and/or orthoclase. It occurs as subhedral tabular to anhedral grains, sometimes with angular or embayed edges. In few cases Carlsbad twinning is observed. Small inclusions of opaque minerals with subhedral or euhedral cubic forms and also of biotite crystals are enclosed within the crystals. As shown in Figure 12 alkali-feldspars are frequently replaced by microcrystalline calcite. Another alteration product is sericite. Zeolite was seen only in one case associated with a feldspar grain. For some K-bentonite samples extensive alteration is one of the most important characteristics of alkali-feldspars. In such cases the determination of feldspar type using optical methods becomes almost impossible.

Quartz as shown in Figure 13, although not as common as biotite and alkali-feldspars, is another non-clay mineral in K-bentonites. Crystals occur in euhedral or subhedral angular shapes and may be fractured or corroded. They are colorless, easily distinguished from the alkali-feldspars by their straight extinction and resistance to the post-depositional alteration processes. Cryptocrystalline quartz is observed in thin sections of associated carbonate rocks

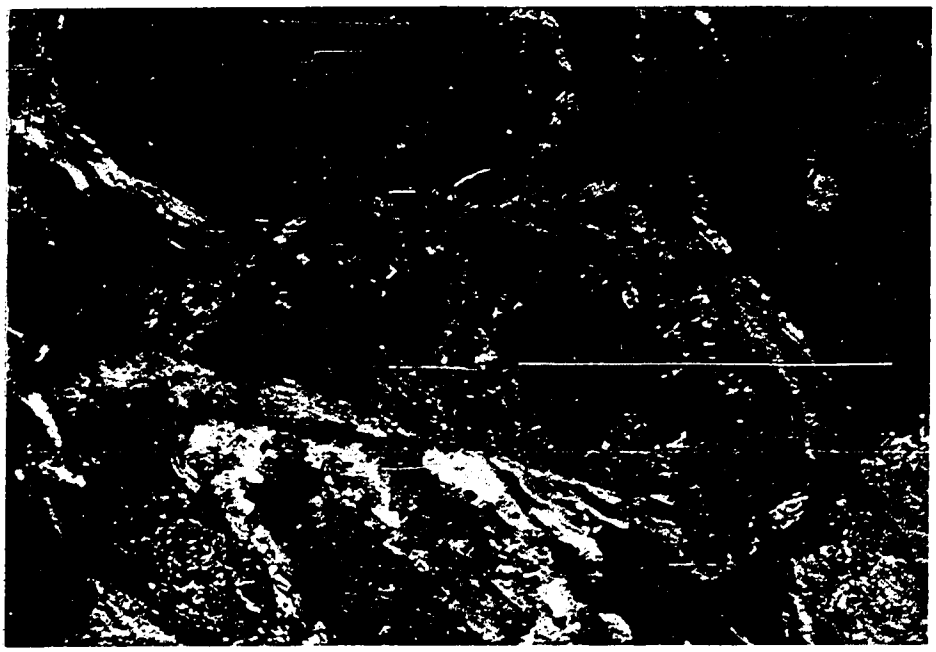

FIGURE 12. Photomicrograph showing the replacement of alkali-feldspar crystal by microcrystalline calcite (sample no. KB-35, x nicols, x10).

as a secondary mineral replacing fossil fragments.

Apatite occurs either as separate crystals in the rock or as inclusions in biotite (Fig. 14). It usually forms euhedral prismatic or hexagonal grains, however anhedral apatite crystals are also present and may be authigenic rather than volcanic in origin. Some apatite crystals contain fluid inclusions as observed in Figure 15.

Zircon with its characteristic high index of refraction and high birefrengence is another common accessory mineral in K-bentonites (Fig. 16). Crystals are mostly in euhedral or subhedral prismatic forms with pyramidal terminations. Rounded zircon grains are also

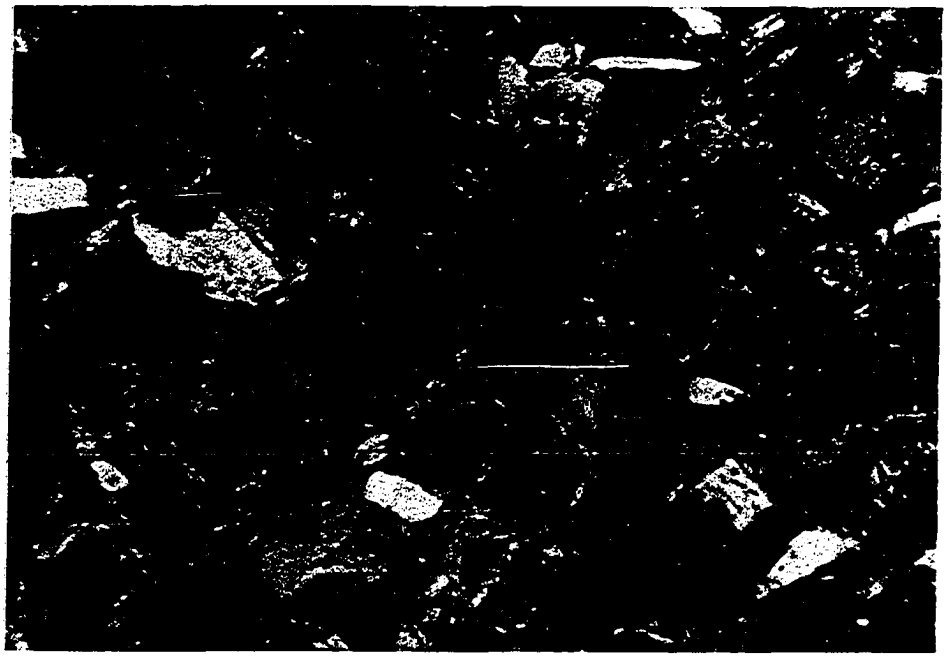

FIGURE 13. Photomicrograph of sample KB-6B with an angular and fresh quartz grain (grayish-brown) at lower left. Sample consists mainly of abundant biotite flakes (brown) and alkali-feldspar crystals (gray) in an altered, micaceous and clayey matrix (x nicols, x 2.5).

observed. Larsen and Poldervaardt (1957) have shown that rounded and irregular zircon crystals from granodiorites and tonalites of Bald Rock Batholith, California, are products of incomplete crystallization. Thus, similar crystals in K-bentonites can form as a result of incomplete crystallization during magmatic differentiation and do not necessarily indicate a detrital origin. Zircon is frequently observed in close association with biotite crystals and produces pleochroic haloes in biotite. Minute opaque mineral inclusions are also present in some zircon grains.

FIGURE 14. Photomicrograph of a broken apatite inclusion in biotite (sample no. KB-5, x 40).

FIGURE 15. Photomicrograph of an apatite inclusion in biotite crystal. Apatite contains fluid inclusions (sample no. KB-35, x 10).

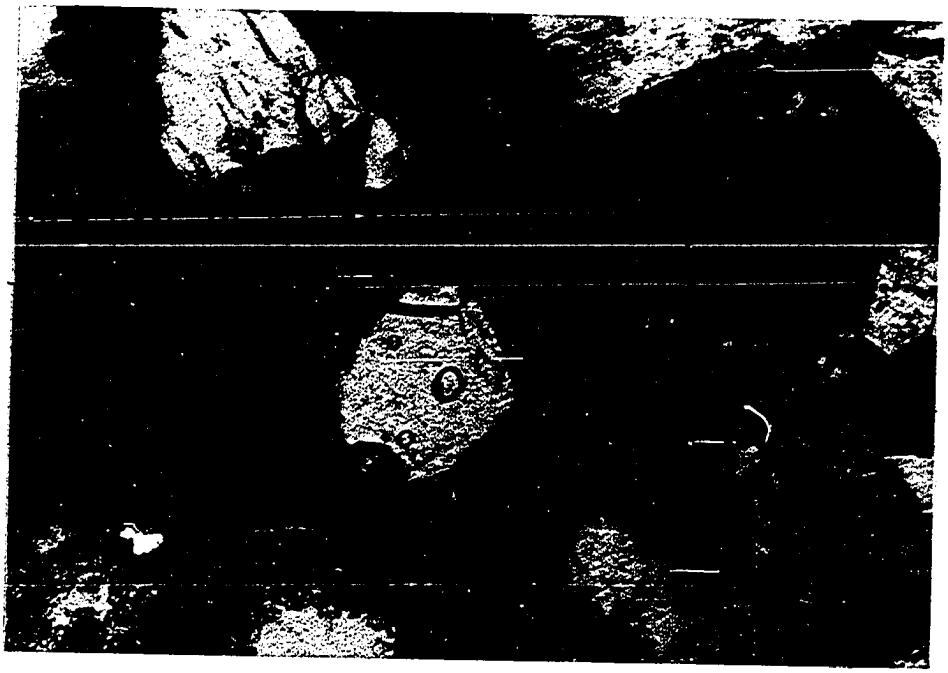

FIGURE 16. Photomicrograph of sample KB-35 with a zircon crystal (blue) in the middle. Alkali-feldspar crystals are extensively replaced by calcite (x nicols, x 10).

FIGURE 17. Photomicrograph of opaque minerals (black) as inclusions in alkali-feldspar (upper right) or as disseminated grains within the matrix (left). Alkali-feldspars are replaced by calcite. Matrix is composed of altered volcanic glass and volcanic dust (sample no. KB-35, x nicols, x 10).

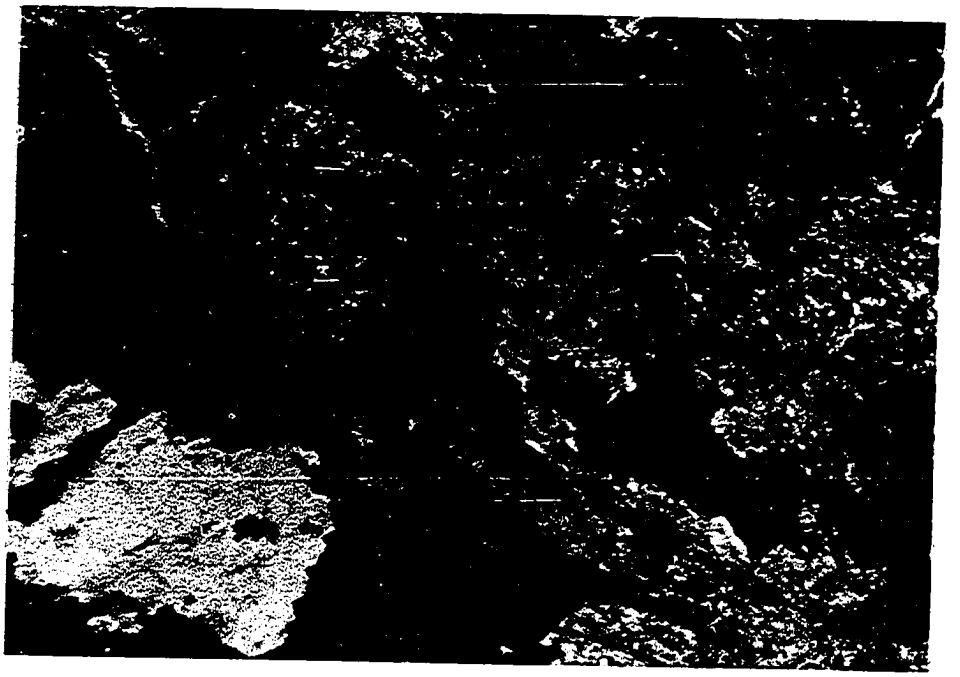

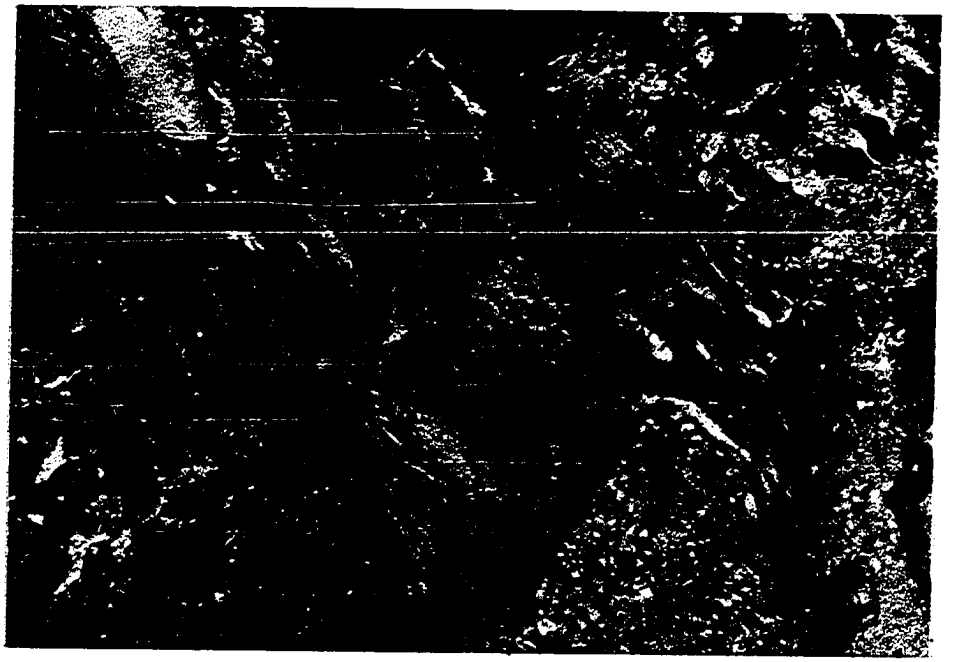

Fe-Ti oxides are frequently observed in thin-section. They are opaque and are found as inclusions the other non-clay minerals or may be disseminated within the matrix (Fig. 17). Euhedral crystals are square-shaped crystals of magnetite and hexagonal plates of ilmenite. Ilmenite is also distinguished by its whiteness in reflected light. Their shape and association with other minerals suggest that Fe-Ti oxides are both of primary and secondary origin.

Pyrite is a diagenetic mineral occurring in K-bentonites. It is rare and observed only in one of the hand specimens.

Description of Clay Minerals:

Alteration of Volcanic Glass: The original volcanic glass has been completely devitrified and altered to argillageous material (Figs. 17 and 18) so that its former presence can only be detected by relict textures such as those shown in Figures 19 and 20. The color of the devitrified glass (Figs. 19 and 20) is usually reddish brown but sometimes colorless or green. They form crescent and Y-shaped particles, suggesting broken vesicle walls, and may have been wrapped around the non-clay minerals.

Interstratified illite-smectite clay is the major alteration product of glass in K-bentonites. However, in one of the samples (KB-35), green chloritic (?) aggregates are observed extensively replacing it (Fig. 19). Chlorite is a rare mineral in the clay fraction of K-bentonites so that generally it is not detected in the x-ray powder patterns of less than 2 μm clay. The only exception in this study is KB-35, as will be discussed in the following section.

FIGURE 18. Photomicrograph of sample KB-35 showing devitrified volcanic glass. Notice the crescent shaped particle in the middle (x nicols, x 25).

FIGURE 19. Photomicrograph of relict volcanic glass textures. Same as Figure 18 but without analyzer. Notice the brown colored, crescent or Y-shaped particles (sample no. KB-35, x 25).

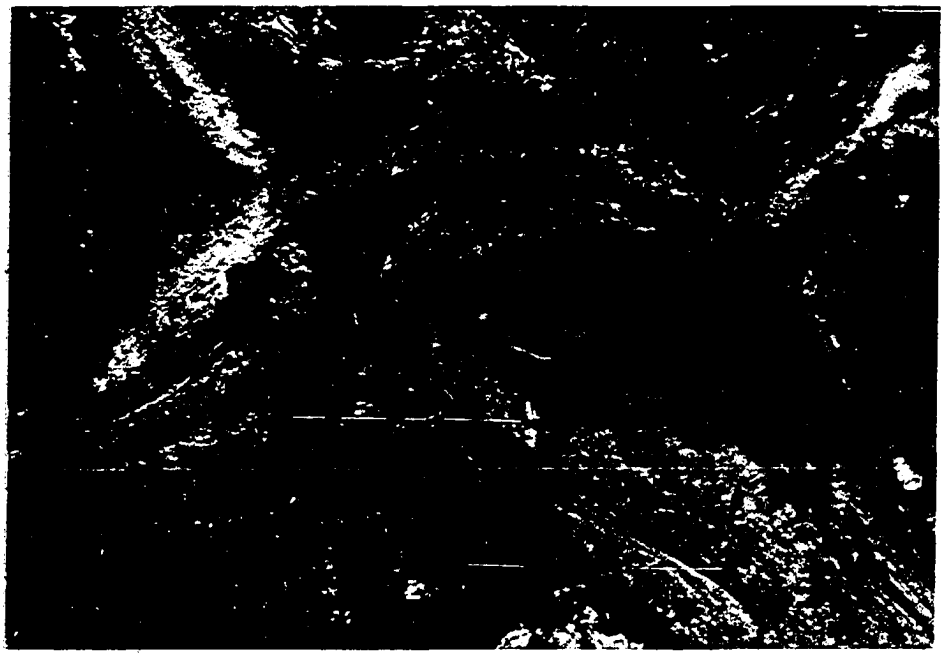

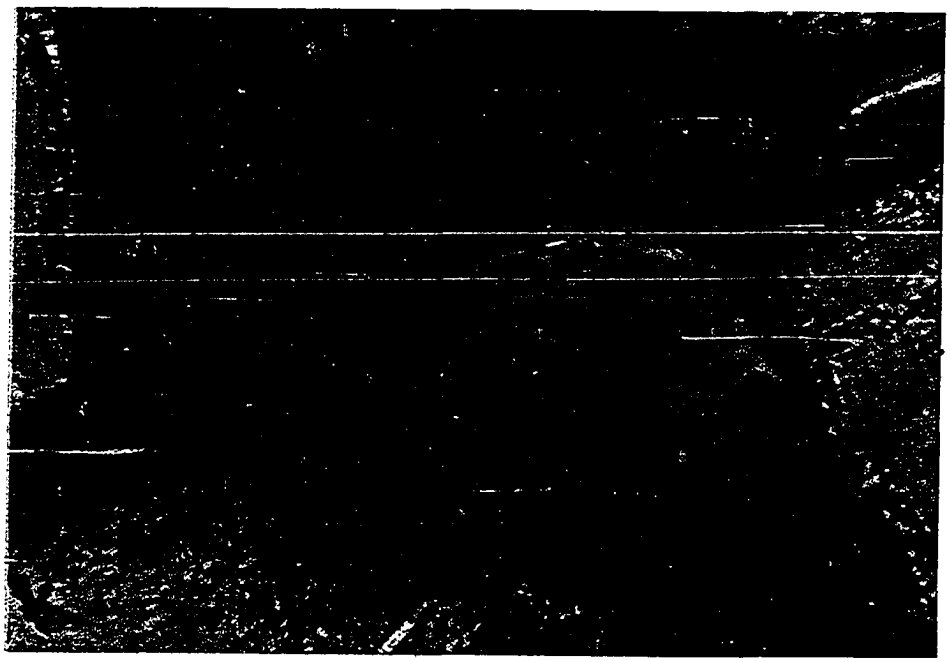

FIGURE 20. Photomicrograph of relict volcanic glass (brown) textures forming the matrix. Original glass shards had curved shapes and surrounded the alkali-feldspar grain (sample no. KB-35, x 25).

FIGURE 21. Photomicrograph of a green chloritic material in the 60 to 80 mesh mineral separate (sample no. KB-18A, x nicols, x 10).

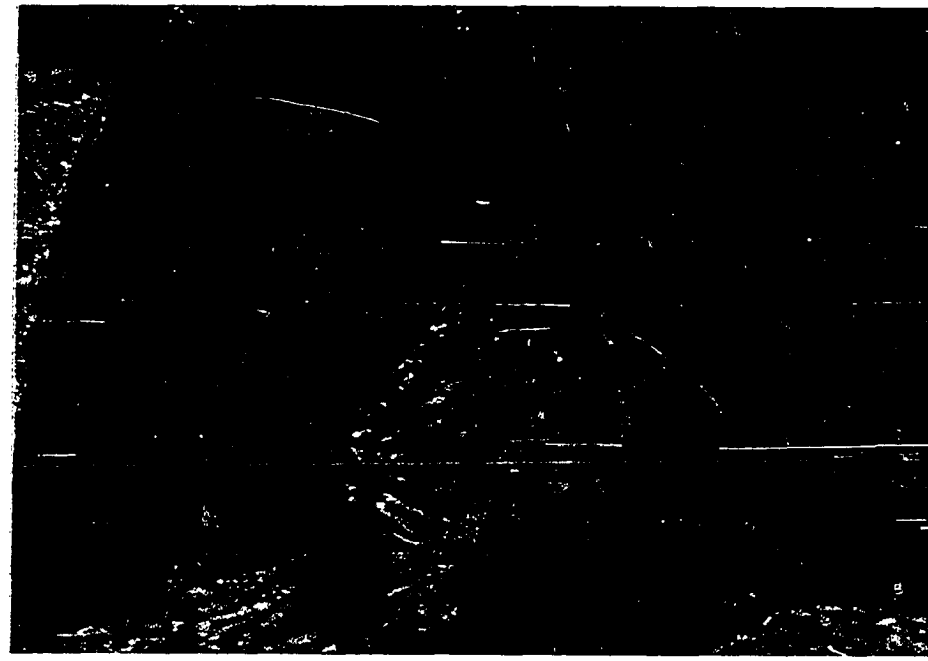

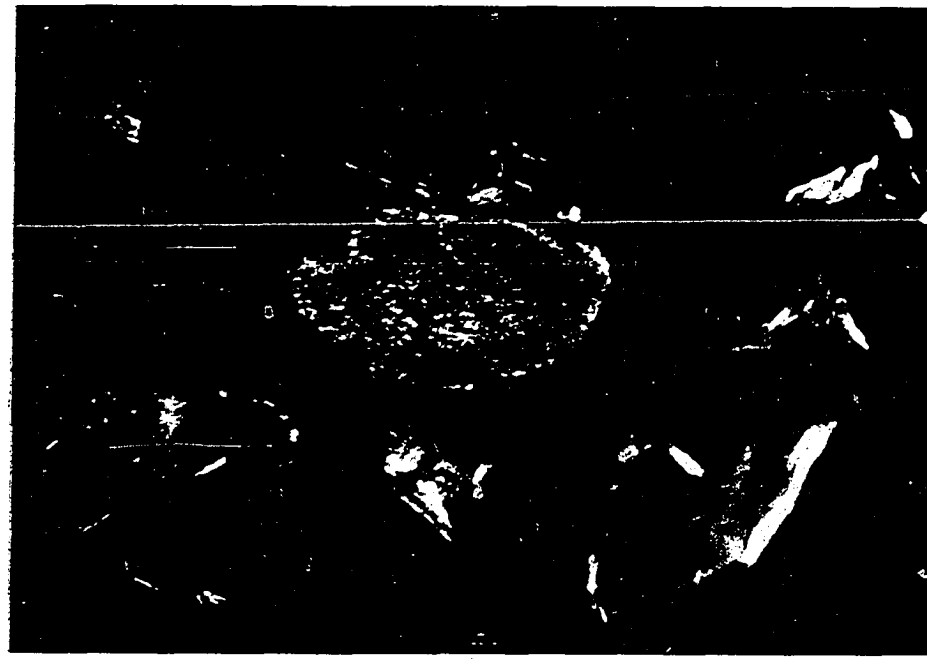

In thin section, however, chlorite is observed as an alteration product of some biotite flakes. The heavy mineral fraction of sample KB-18A, isolated by magnetic separation, contains a small chlorite grain as shown in Figure 21.

X-Ray Analysis: Table 1 presents data obtained from the x-ray studies of less than 2 μm clay fractions. Figures 22, 23 and 24 show diffractometer tracings which illustrate reflections from the interstratified clay minerals in three of these samples.

An examination of the data in Table 1 reveals that for untreated samples, combined reflection of $(001)_{10}/(001)_{17}$ from illite-smectite range between 11.326Å and 10.517Å. When the specimens are glycolated, the presence of interstratified clay becomes evident because the combined reflection peak in untreated samples forms two observable reflections (Fig. 22 and 23). A broad peak occurs at about 12Å, with values varying from 12.009 to 12.800, and the other shifts to about 9.7 Å, its values ranging between 9.604 and 10.900.

Heating the specimen to 600°C causes the expanded layers to collapse to positions between 10.155 and 10.394Å. Figures 22, 23 and 24 also illustrate a marked increase in the intensity of the $(003)_{10}/(004)_{17}$ reflection at 3.3Å as a result of heating. Figures 22 and 23 show the typical diffraction patterns of clay fractions of K-bentonites. Using the above data and information by Reynolds and Hower (1970) and Weaver (1956) on the nature of interlayering in mixed layer illite-smectite clays and on their identification, it is possible to interpret the proportions of illite and smectite

TABLE 1. X-ray powder diffraction data for less than 2 μm clay fractions of K-bentonite samples.

Sample No.	hkl*	Untreated dÅ	Glycolated dÅ	Heated dÅ
5B	$(001)_{10}/(001)_{17}$	10.773	12.267 10.040	10.155
	$(002)_{10}/(002)_{17}$	5.034	5.180	5.034
	$(003)_{10}/(004)_{17}$	3.275	3.335	3.323
6E	$(001)_{10}/(001)_{17}$	10.906	12.617 9.709	10.155
	$(002)_{10}/(002)_{17}$	5.034	5.180	5.034
	$(003)_{10}/(004)_{17}$	3.299	3.348	3.335
7C	$(001)_{10}/(001)_{17}$	10.773	12.267 10.040	10.155
	$(002)_{10}/(002)_{17}$	5.034	5.180	5.034
	$(003)_{10}/(004)_{17}$	3.275	3.335	3.323
20B	$(001)_{10}/(001)_{17}$	10.773	12.267 10.040	10.394
	$(002)_{10}/(002)_{17}$	5.063	5.180	5.034
	$(003)_{10}/(004)_{17}$	3.285	3.348	3.348
21	$(001)_{10}/(001)_{17}$	11.325	12.800 9.604	10.155
	$(002)_{10}/(002)_{17}$	5.006	5.211	5.034
	$(003)_{10}/(004)_{17}$	3.323	3.335	3.335

TABLE 1. X-ray powder diffraction data for less than 2 μm clay fractions of K-bentonite samples - Continued

Sample No.	hkl*	Untreated dÅ	Glycolated dÅ	Heated dÅ
22A	$(001)_{10}/(001)_{17}$	10.900	12.800 10.900	10.273
	$(002)_{10}/(002)_{17}$	5.034	5.211	5.006
	$(003)_{10}/(004)_{17}$	3.299	3.335	3.323
34	$(001)_{10}/(001)_{17}$	10.517	12.009 9.709	10.273
	$(002)_{10}/(002)_{17}$	5.006	5.151	5.063
	$(003)_{10}/(004)_{17}$	3.287	3.335	3.348
35	$(001)_{14}$	14.476	?	14.476
	$(001)_{10}/(001)_{17}$	11.182	10.273	10.394
	$(002)_{14}$	7.189	7.248	destroyed
	$(002)_{10}/(002)_{17}$	5.006	5.034	5.063
	$\begin{Bmatrix}020\\110\end{Bmatrix}_{10} / \begin{Bmatrix}110\\020\end{Bmatrix}_{17}$	4.502	4.525	4.502
	$(004)_{14}$	3.558	3.572	destroyed
	$(003)_{10}/(004)_{17}$	3.332	3.335	3.360

* values for peaks of regularly interstratified 10Å (mica) and 17Å (smectite) phases.

FIGURE 22. X-ray powder diffraction patterns for sample KB-5B.

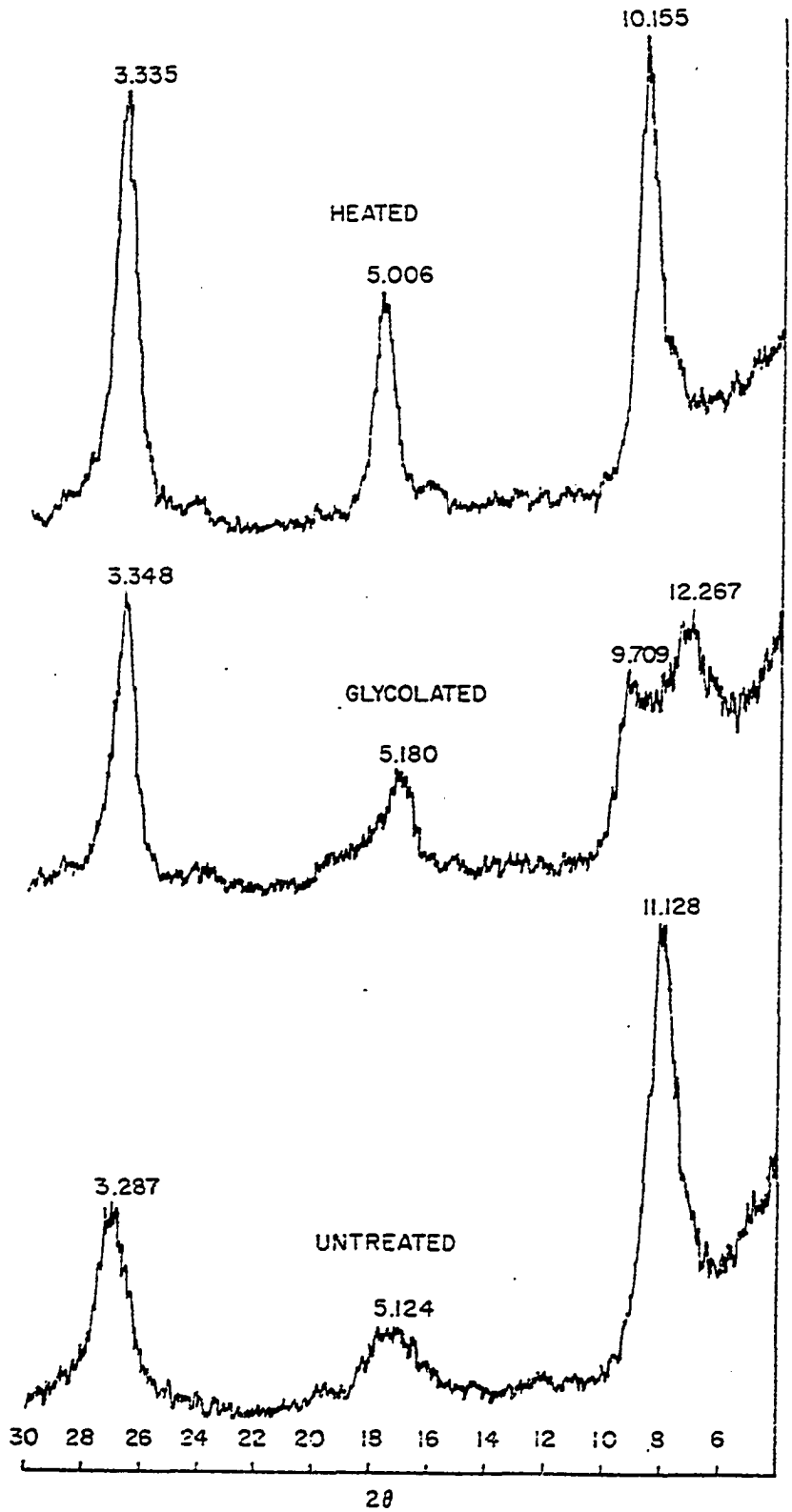

FIGURE 23. X-ray powder diffraction patterns for sample KB-6E.

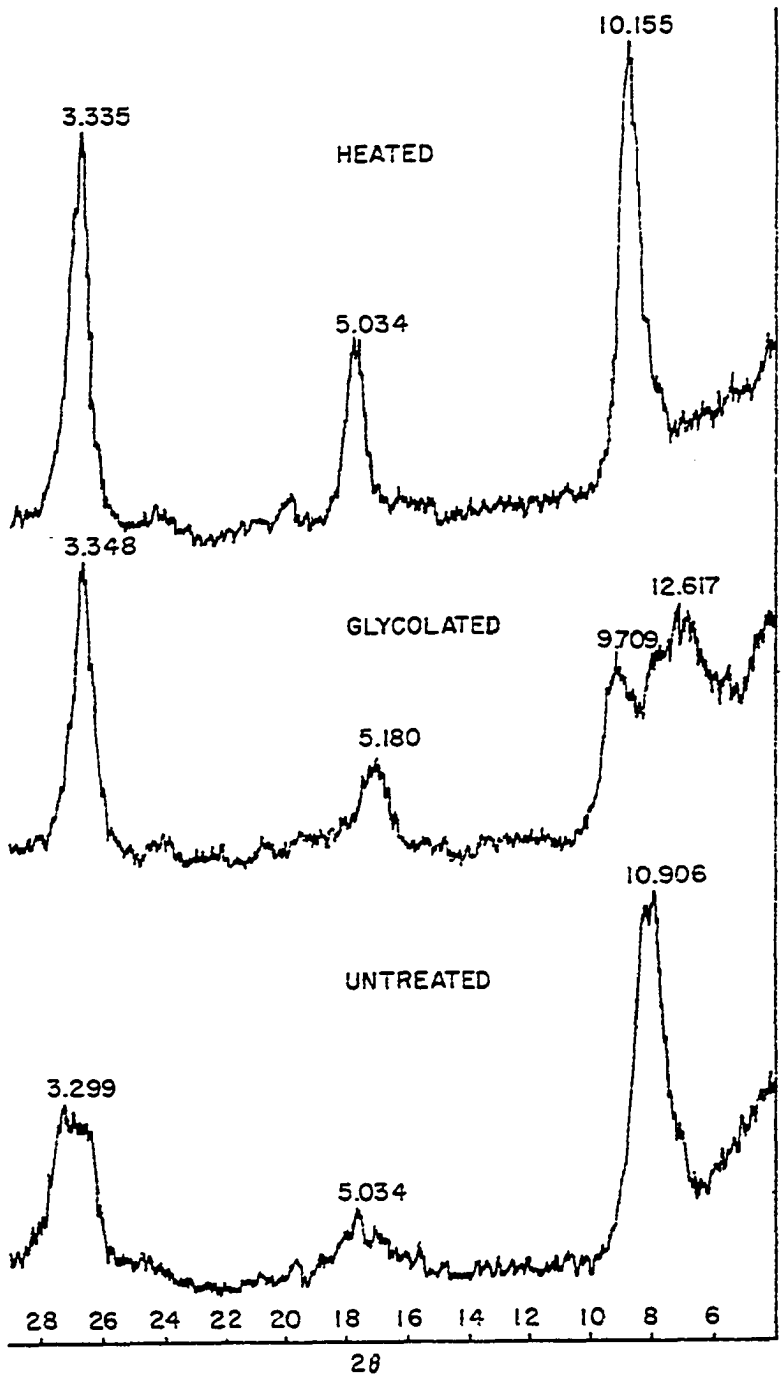

FIGURE 24. X-ray powder diffraction patterns for sample KB-35.

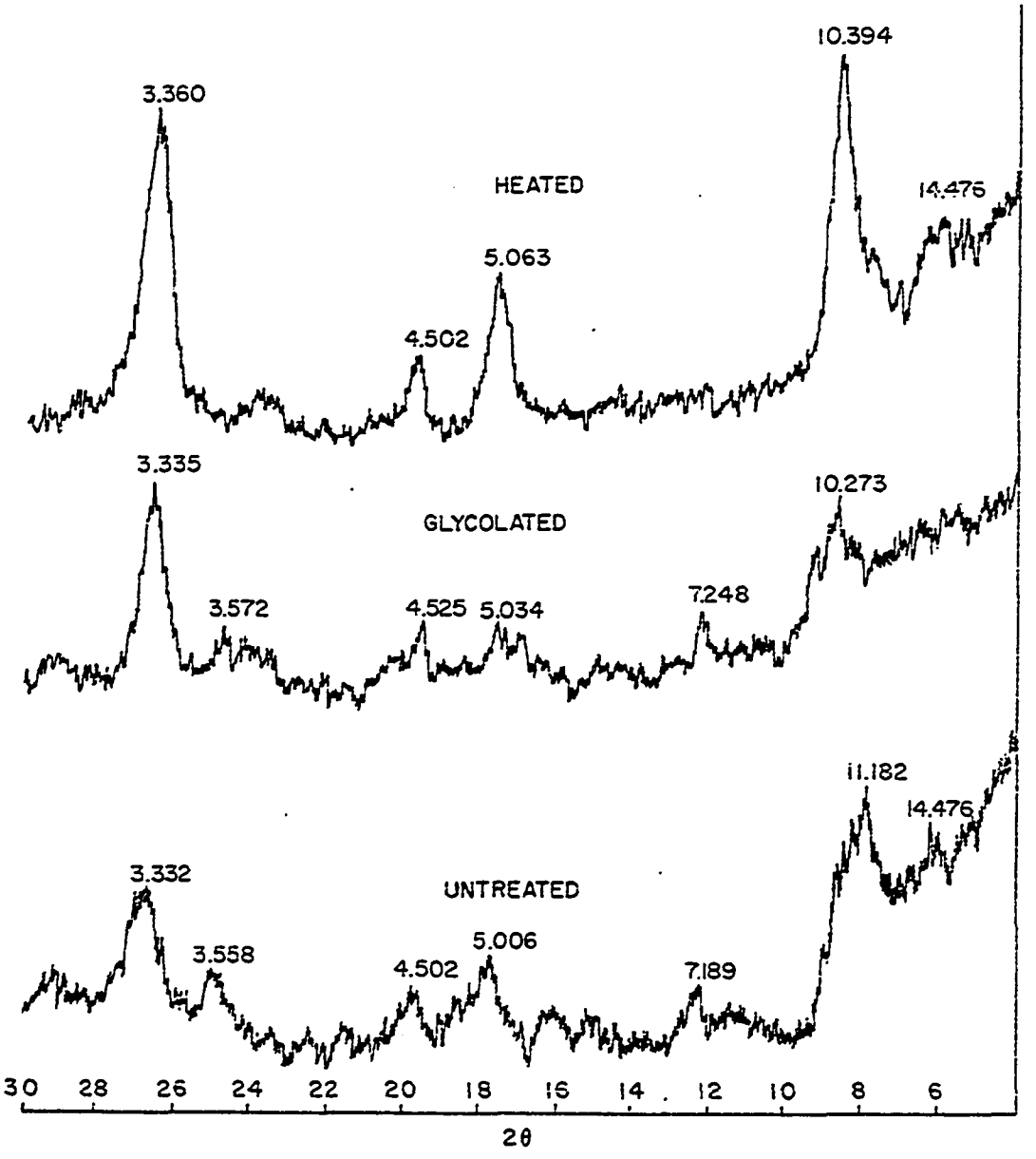

and type of interlayering. Thus, these clays are composed of 20 percent expandable and 80 percent non-expandable, regularly interstratified, allevardite-type layers.

Figure 24 is the diffraction pattern of a chlorite rich sample, KB-35. In the untreated sample chlorite has slightly stronger second order (7.189 Å) and fourth order (3.558 Å) reflections compared with the first order (14.47 Å) and third order (4.79 Å) indicating a slight excess in octahedral iron over magnesium (Brindley, 1961). Upon glycolation the 14 Å peak is diminished almost to background level, probably due to a combination of interference from the expanding smectite phase and some swelling behavior of the chlorite itself. Second order and forth order reflections are slightly shifted to the higher 2θ values suggesting further the swelling character of chloritic material.

The nature of the chloritic material was investigated by separating the clay into 2-0.2 and 0.2-0.08 μm size fractions and obtaining their powder diffraction patterns. The patterns show that chlorite is concentrated in the coarse fraction and is absent in the fine fraction. Consequently, the chloritic material in KB-35 is suggested to be an alteration by-product of biotite rather than a neoformed clay such as illite-smectite.

Chemistry and Structural Formulae of Clay Minerals: Although Ordovician K-bentonites have been well-described by x-ray diffraction investigations, there are relatively few studies which have focused

on their clay chemistry (Weaver, 1953b; Bystrom, 1956; Weaver, 1965). As part of this study 29 analyses were made of the less than 2 μm clay fractions and the results are presented in Table II of Appendix F. These data are used to calculate structural formulae of the interstratified illite-smectite clay because a knowledge of the structural distribution of elements is necessary to interpret the origin of the clay.

Structural formulae are derived by using the conventional method of fixed anionic charges (Foster, 1960). The formula calculation is based on the assumption that 44 anionic charges exist for each $O_{20}(OH)_4$ grouping in each unit cell. In this method, the gram equivalents of cationic constituents are first obtained by dividing the percent oxide of each constituent by its molecular weight, and then multiplying by the cationic charge, that is, converting the cations to equivalents/gram of constituent. Next, the numbers of cations are calculated by setting the sum of gram-equivalents of cationic constituents equal to 44 anionic charges. The chemical formulae obtained for 29 samples by this method are given in Table 2. The calculated values for the cations and charges per unit cell are halved according to conventional usage of reporting structural calculations as half-cell formulae. A formula obtained from averaging 29 tabulated structural formulae in addition to the formulae of an illite and smectite are listed in the last three columns of the Table for the purpose of comparison.

TABLE 2. Structural formulae of 29 interstratified illite-smectite clays in K-bentonites.

Sample No.	1	5Bu	6B	6C	7A	7B	7D	8A	8B	8C	16	18A	18B	19A
Octahedral														
Al	1.430	1.393	1.387	1.399	1.125	1.344	1.360	1.396	1.349	1.395	1.470	1.376	1.464	1.040
Ti	0.027	0.007	0.009	0.010	0.014	0.027	0.008	0.015	0.010	0.010	0.010	0.014	0.004	0.023
Fe^{+3}	0.058	0.092	0.102	0.129	0.091	0.092	0.100	0.089	0.082	0.084	0.036	0.078	0.059	0.067
Mg	0.457	0.426	0.440	0.591	0.395	0.451	0.459	0.374	0.434	0.481	0.386	0.479	0.456	0.482
Mn^{+2}	0.001	0.001	0.006	....	0.001	....	0.001	....	....	0.001	0.001	....	....	0.002
oct	1.973	1.919	1.944	2.129	1.626	1.914	1.928	1.874	1.875	1.971	1.903	1.947	1.983	1.614
Tetrahedral														
Si	3.564	3.747	3.853	3.228	3.732	3.829	3.816	3.947	3.938	3.750	3.867	3.731	3.704	3.601
Al	0.436	0.253	0.147	0.772	0.267	0.171	0.184	0.052	0.062	0.250	0.133	0.268	0.296	0.398
Interlayer														
K	0.654	0.623	0.601	0.831	0.581	0.577	0.601	0.530	0.563	0.610	0.561	0.702	0.628	0.614
Na	0.236	0.202	0.151	0.234	0.161	0.168	0.164	0.170	0.210	0.172	0.143	0.124	0.161	0.229
Ca	0.028	0.014	0.006	0.035	0.516	0.056	0.042	0.042	0.041	0.014	0.046	0.029	0.006	0.566
Charge														
Octahedral	0.507	0.654	0.609	0.190	0.997	0.677	0.665	0.733	0.794	0.552	0.663	0.615	0.501	1.613
Tetrahedral	0.436	0.253	0.147	0.772	0.267	0.171	0.184	0.052	0.062	0.250	0.133	0.268	0.296	0.398
Total	0.943	0.907	0.756	0.962	1.264	0.848	0.849	0.785	0.856	0.802	0.796	0.883	0.797	2.011

TABLE 2. Structural formulae of 29 interstratified illite-smectite clays in K-bentonites - Continued

Sample No.	19B	19C	19D	20A	21	22A	23C	24A	24B	28A	28D	28G	28H	29
Octahedral														
Al	1.280	1.315	1.400	1.377	1.517	1.425	1.084	1.220	1.255	1.451	1.421	1.451	1.448	1.578
Ti	0.023	0.022	0.014	0.014	0.008	0.008	0.004	0.014	0.014	0.007	0.007	0.005	0.009	0.014
Fe+3	0.071	0.089	0.072	0.084	0.037	0.064	0.066	0.051	0.025	0.065	0.066	0.059	0.054	0.032
Mg	0.569	0.561	0.510	0.487	0.382	0.485	0.548	0.554	0.507	0.451	0.473	0.429	0.463	0.380
Mn+2	0.001	0.024	....	0.002	....	0.018	....	0.001	0.001	....	0.002	0.002	0.001	0.001
oct	1.944	2.011	1.996	1.964	1.944	2.000	1.702	1.840	1.802	1.974	1.969	1.946	1.975	1.977
Tetrahedral														
Si	3.455	3.582	3.744	3.762	3.736	3.693	3.704	3.625	3.751	3.735	3.687	3.818	3.752	3.561
Al	0.544	0.418	0.255	0.238	0.264	0.307	0.296	0.375	0.249	0.265	0.313	0.181	0.248	0.438
Interlayer														
K	0.664	0.720	0.616	0.607	0.582	0.612	0.584	0.596	0.595	0.597	0.588	0.551	0.563	0.647
Na	0.251	0.167	0.138	0.224	0.163	0.162	0.144	0.173	0.171	0.192	0.204	0.137	0.162	0.142
Ca	0.168	0.031	0.006	....	0.032	0.036	0.080	0.309	0.230	....	0.036	0.040	0.028	0.001
Charge														
Octahedral	0.710	0.525	0.515	0.581	0.535	0.490	1.435	1.015	0.983	0.518	0.554	0.586	0.528	0.348
Tetrahedral	0.544	0.418	0.255	0.238	0.264	0.307	0.296	0.375	0.249	0.265	0.313	0.181	0.248	0.438
Total	1.254	0.943	0.770	0.819	0.799	0.797	1.731	1.390	1.232	0.783	0.867	0.767	0.776	0.786

TABLE 2. Structural formulae of 29 interstratified illite-smectite clays in K-bentonites - Continued

Sample No.	34A	Average	Illite*	Smectite**
Octahedral				
Al	1.210	1.357	1.51	1.53
Ti	0.028	0.013	....	....
Fe^{+3}	0.200	0.075	0.04	0.15
Mg	0.569	0.471	0.36	0.33
Mn^{+2}	....	0.002	....	....
oct	2.007	1.919	1.98	2.01
Tetrahedral				
Si	3.665	3.709	3.54	4.05
Al	0.334	0.290	0.46	0.00
Interlayer				
K	0.674	0.616	0.70	0.05
Na	0.063	0.173	0.03	0.18
Ca	0.063	0.086	0.10	0.06
Charge				
Octahedral	0.514	0.588	0.49	0.30
Tetrahedral	0.334	0.290	0.46	0.00
Total	0.848	0.878	0.95	0.30

* Weaver and Pollard (1973), p. 11, no. 25: in Silurian dolomites, Marblehead, Wisc., U.S.A.

** Weaver and Pollard (1973), p. 59, no. 11: montmorillonite in sea water, Upton, Wyo., U.S.A.

In all samples except 6C, 19A, 19B, 23C and 24B the calculated total layer charge and the sum of the interlayer cationic charges agree closely, resulting in a plus or minus variation of 0.2 in the unit cell, although this does not mean that off range values are incorrect. It is possible that some interlayer cations such as H^{+} or less probably Mg^{+2} were not detected. During this study all of Mg was allocated to the octahedral sheet so that the neutrality of the clay structure was provided. Histograms showing the distribution of ions in their various structural positions, distribution of Σoct ions, and octahedral, tetrahedral and total layer charges are presented in Figures 25, 26 and 27 in order to discuss more clearly the chemical data in Table 2.

Octahedral Al histogram shows a normal type distribution. The values range from 1.040 to 1.578 and averages 1.357, coinciding the mode (1.3 - 1.4) well. In 93 percent of the samples Al occupancy is less than 1.5 of the octahedral positions. This type of distribution indicates that the amount of Al in the octahedral position is relatively fixed.

Octahedral Ti values vary between 0.004 and 0.028, averaging 0.013. The histogram suggests a bimodal distribution although it may not be real. The exact amount of TiO_2 in clay analysis is difficult to obtain because it is difficult to determine whether it occurs in the clay structure or as a separate phase in the sample. Thus, the inclusion of free TiO_2 in the formula calculations may

introduce errors. Therefore, some investigators (Grim and Güven, 1978) do not include TiO_2 content in the calculations of structural formulae. In this study Ti is included in the formulae based on the findings (Foster, 1960) that a small amount of Ti has only a slight effect on the number of positions occupied by other octahedral cations. In almost 76 percent of the samples Ti fills 0.015 of the octahedral positions and the left portion of the histogram has a negatively skewed distribution. The shape of the histogram suggests that the amount of Ti in the octahedral sheet is not fixed and, further, that this ion is not significant in defining a specific mineral species because of its somewhat bimodal character.

The histogram of octahedral Fe^{+3} indicates a slightly negatively skewed normal distribution with a wide mode at 0.06-0.10. The values range from 0.032 to 0.200, averaging at 0.075. 86 percent of the samples have octahedral Fe^{+3} occupying less than 1.00 of octahedral position. The extereme values to the right of the Figure may reflect contamination by iron.

Octahedral Mg shows a normal distribution and 41 percent of the samples have high kurtosis value in the 0.45-0.50 range indicating a relatively constant Mg population in the octahedral sheet. Minimum and maximum occupancies correspond to 0.374 and 0.591, respectively, and the average is at 0.471. This value of octahedral Mg occupancy for the interstratified illite-smectite clay lies between those of illite (0.283) and Cheto type dioctahedral montmorillonite (0.55) as reported by Weaver and Pollard (1973).

FIGURE 25. Histograms showing the distribution of octahedral and tetrahedral cations of twenty-nine interstratified illite-smectite structural formulae.

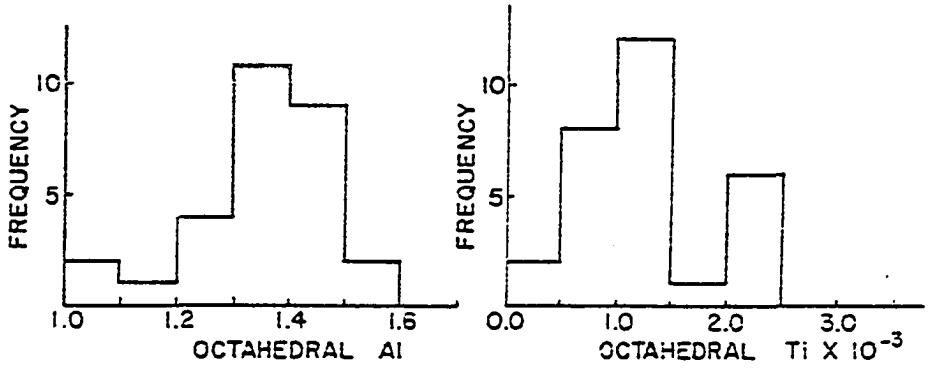

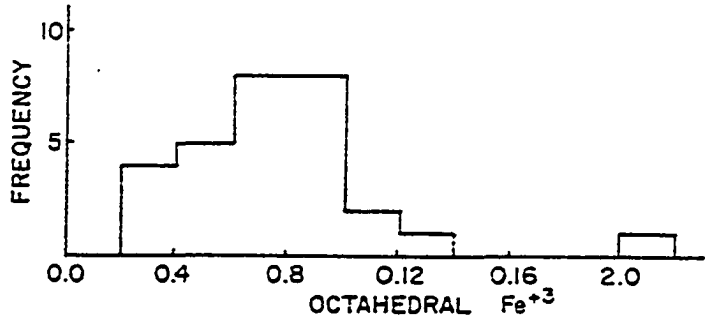

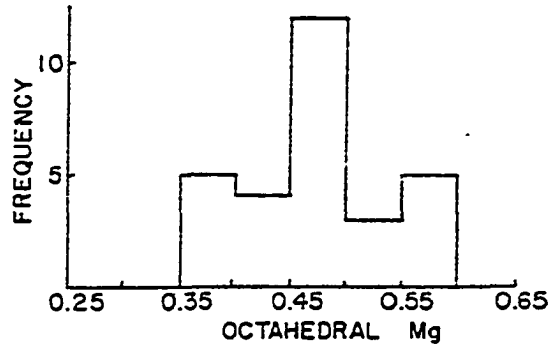

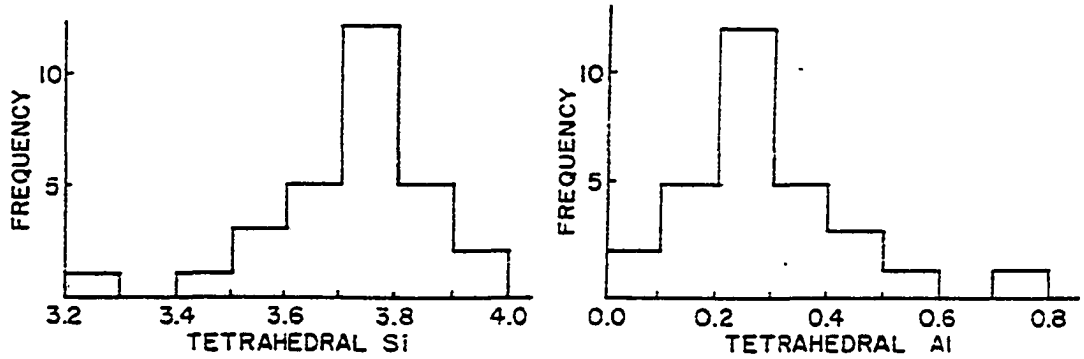

The histograms of tetrahedral Si and Al show normal type distribution. 41 percent of the samples have high kurtosis values in the range of 3.7-3.8 and 0.2-0.3, for tetrahedral Si and Al, respectively. Si occupancy varies from 3.228 to 3.947, averaging at 3.735. Although its mode coincides with the average value very closely, the Si histogram has a slight negative skewness. In the case of tetrahedral Al, occupancy ranges between 0.062 and 0.772 with an average at 0.265. Like tetrahedral Si, the mode and average value of tetrahedral Al coincide closely, but in the latter, the histogram is very slightly positively skewed. Both Si and Al ions have relatively fixed tetrahedral occupancies which can be used in defining the clay structure.

Figure 26 illustrates that among the interlayer cations K^+ and Na^+ have normal type distributions while Ca^{+2} shows a log-normal distribution. K^+ ions per $O_{10}(OH)_2$ vary between 0.530 and 0.831, with an average of 0.616. This average value is lower than those of micas (0.8) when there are no expanded layers (Hower and Mowatt, 1966). In dioctahedral smectites the amount of interlayer K ranges between 0.00-0.16 (Weaver and Pollard, 1973), and is much lower than the value for interstratified illite- smectite clay. That is, an interstratified clay with 20 percent expandable layers would be expected to have an average of 0.7 K^+ ion compared with the 0.616 observed according to the study by Hower and Mowatt (1966). The K distribution is positively skewed with a mode at a value of 0.55-0.6. In 80 percent of the samples K^+ ion occupies less than 0.65

of the interlayer positions. Normal distribution of K^+ ion in the interlayer positions indicate that the fixation of K in the clay structure is well-defined. Positive skewness may be due to the presence of analyses of some samples with less regular structure (i.e. higher percent of expandable layers), and it should be pointed out here that total K analysis of clay fraction does not tell whether or not the K is uniformly distributed among all layers, or concentrated in some more than others.

Interlayer Na values vary between 0.063 and 0.251, averaging at 0.173. 45 percent of the analyzed samples have a high kurtosis at 0.16-0.20 range. Distribution of Ca^{+2} ion in interlayer positions reflects the percentage of low values with an average of 0.086, while the occupancy ranges between 0.00 and 0.586. Among the interlayer cations Ca^{+2} has the lowest average occupancy values and its distribution indicates that the variation in the interlayer occupancy is mainly due to Ca^{+2} ion. It seems that during halmyrolisis and with increasing compaction smectite prefers K^+, Mg^{+2} and Na^+ ions obtained from sea water and pore waters rather than Ca^{+2} in the exchange positions, an observation also supported by the studies of Weaver and Beck (1971) and Weaver and Pollard (1973). Exotic variation of the Ca^{+2} ion distribution within the interlayer positions may also indicate some carbonate mineral (e.g. calcite) contamination during the chemical analysis of the clay.

In Figure 26, the Σoct histogram demonstrates that the distribution of ions in the octahedral coordination is normal with values

FIGURE 26. Histograms showing the distribution of interlayer cations and $\sum$oct cations of twenty-nine interstratified illite-smectite structural formulae.

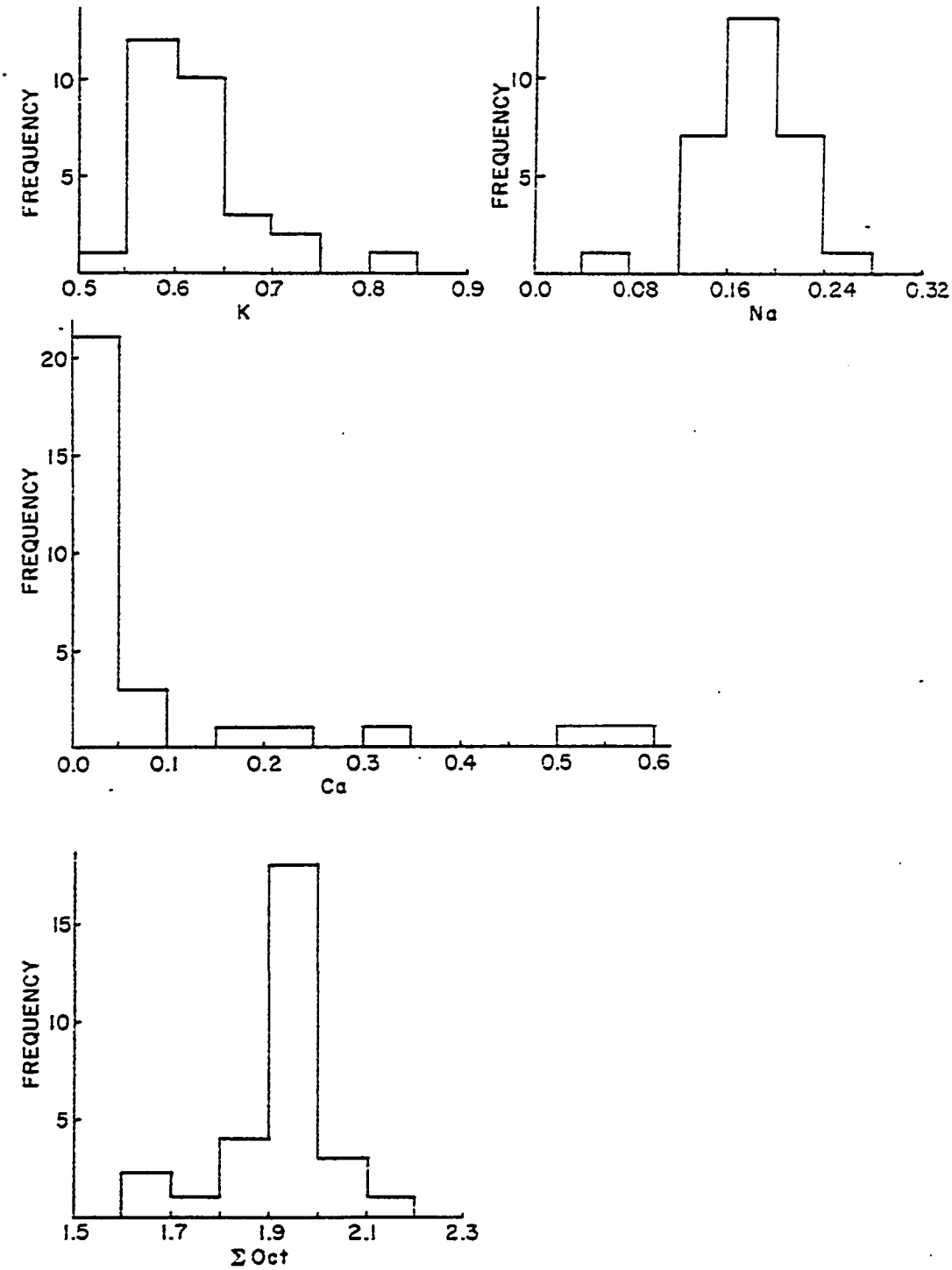

ranging from 1.614 to 2.129, and averaging 1.919. This distribution is quite reasonable when compared with data published for similar dioctahedral structures (Weaver and Pollard, 1973). The values higher than 2.00, the theoretical cation population of the dioctahedral sheet, may be due to the assignment of a portion of interlayer cations to the octahedral sheet. On the other hand, the values less than 2.00 shows the presence of excess negative charge in the octahedral sheet to be satisfied. In the dioctahedral micas, divalent cations occupy some of the octahedral positions ideally presumed to be occupied by Al. Replacement of a trivalent cation in this mica structure by a divalent cation apparently induces a negative charge on the octahedral sheet (Foster, 1960). The structural formulae tabulated in Table 2 are characterized by high octahedral Mg occupancies. Thus, it can be concluded that high octahedral charge resulting from the replacement of Al by Mg is the reason for K-adsorption and fixation in the interlayer position and accounts for the high concentration of K in the clay fraction.

Both octahedral and tetrahedral charges have normal type distribution (Fig. 27). Their values range from 0.190 to 1.612, averaging at 0.588, and from 0.052 to 0.772, with an average at 0.290, respectively. The octahedral charge distribution has a kurtosis in the range of 0.4-0.6, and in almost 83 percent of the samples the octahedral charge has a value less than 0.8. The tetrahedral charge distribution has a better defined kurtosis in

the range of 0.2-0.3, and in almost 83 percent of the samples analyzed the tetrahedral charge has a value less than 0.4. In all structural formulae calculated the tetrahedral charge has a lower value than octahedral charge. Thus, as illustrated in Figure 27, octahedral charge values dominate and form the major portion of the total layer charge in the interstratified clay of K-bentonites. Weaver and Pollard (1973, p. 182) point out that the charge on the tetrahedral sheet is produced by the substitution of Al for Si, and is compensated for by the introduction of Mg in the octahedral sheet and by interlayer cation adsorption. In other words, octahedral charge and overall layer charge originates predominantly from tetrahedral substitution.

Values for the layer charge vary from 0.756 to 2.011, averaging at 0.878 per $O_{10}(OH)_2$. In almost 80 percent of the samples the layer charge is less than 1.00. The distribution pattern is positively skewed due to the effect of lower values of tetrahedral charges on the total layer charge distribution. Weaver and Pollard (1973, p. 7) calculated an average total layer charge for illite of near 0.9. They also calculated the maximum layer charge value for montmorillonites approximately at 0.6 (p. 73) and concluded that if K is available, layers with a charge higher than this would fix the K and contract to 10Å. Hower and Mowatt (1966) have also shown that as total charge increases, K (+Na) and the proportion of 10Å layers increases. The total layer charges calculated for the interstratified illite-smectite clays in K-bentonites during this study

FIGURE 27. Histograms showing the distribution of layer charges of twenty-nine interstratified illite-smectite structural formulae.

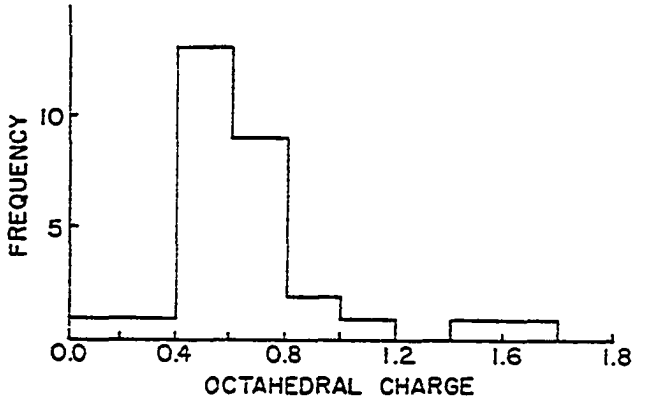

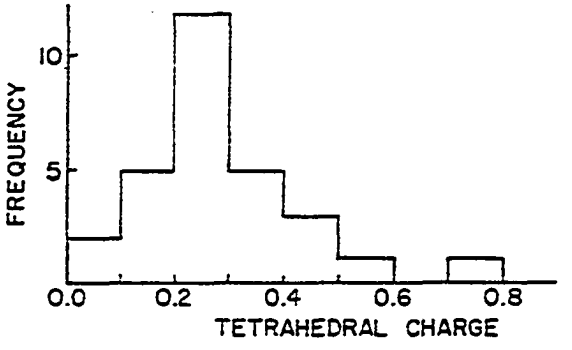

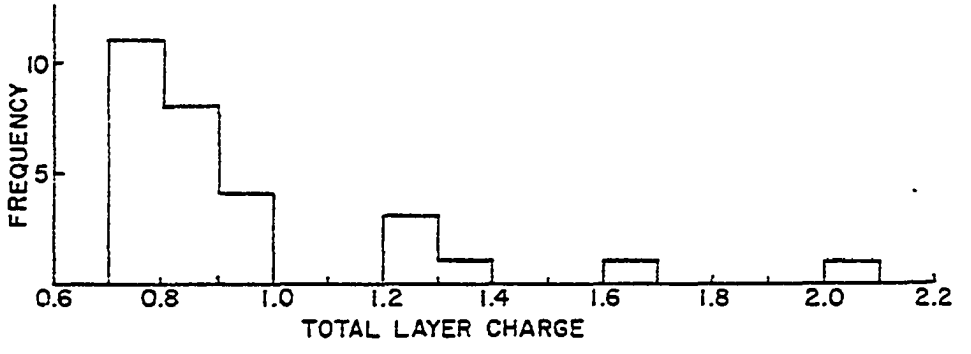

are higher than the maximum layer charge of montmorillonite, meaning that high charges are responsible for the high K content in these rocks. The values obtained are also in accordance with those calculated for similar clays in the literature (Weaver and Pollard, 1973).

Petrography

The petrography of K-bentonites and their chemical classification as igneous rocks form the main content of this section. Optical studies and chemical analyses are used as tools for petrographic definition of the altered rock and form the basis for the calculation of original ash composition.

Detailed lithologic descriptions of samples are given in Appendix A. Generally, K-bentonites consist of dark or light greenish-gray clay and of varying quantities of non-clay minerals, as described in the mineralogy section. The latter averages 0.33 mm in size, but in some specimens reach a maximum of 2 mm and can be distinguished by naked eye (Fig. 9). Abundant platy minerals cause fissility after settling, and in a few samples, grading of crystals indicates that their original distribution in the ash has not changed and the ash was not reworked after deposition. K-bentonites are hard when fresh and break with conchoidal fracture. When weathered they form loose and white material in varying shades of yellow to brown.

All the samples studied are altered crystal to vitric tuffs following the classification of Cook (1965). Figure 28 is a photomicrograph of an altered crystal tuff with acid to intermediate

composition. The rock consists mainly of alkali-feldspars and biotite crystals in addition to less than 50 percent of altered clayey and quartzofeldsphatic material. In the Figure, biotites are distorted, oriented horizontally and the clayey material, in general, is forced into a curved form around the non-clay minerals, suggesting sedimentary compaction. The non-clay minerals in this sample are well-sorted.

Figures 29, 30 and 31 represent microtextures of altered vitric-crystal tuffs consisting of alkali-feldspars, biotite, opaque minerals, clay and quartzofeldsphatic material in addition to very rare quartz crystals. Biotites in Figure 31 well illustrate their horizontal alignment during deposition. More intensive alteration of sample KB-20B (Fig. 29) is indicated by the secondary green and brown pigmentations as observed in the form of horizontal laminations in the Figure. The contact relationships of the non-clay minerals with the surrounding clayey material and their morphology is illustrated by Figure 32. The contacts are distinct and the non-clay crystals have angular shapes. Crystals are moderately well-sorted.

Figure 33 is a photomicrograph of an altered, reworked vitric-tuff which contains fossil ostracodes. There are a few euhedral quartzofeldsphatic grains and the rest is composed of altered volcanic material with carbonate, silica and clay minerals as the replacement or alteration products. Opaque minerals of secondary

FIGURE 28. Photomicrograph of a crystal-tuff. Non-clay minerals are composed of alkali-feldspars (gray), biotite (brown) and quartz (colorless). Matrix is composed of clayey and quartzofeldsphatic material (sample no. KB-34, x nicols, x 2.5).

FIGURE 29. Photomicrograph of a vitric-crystal tuff. Alkali-feldspars (gray) are the major non-clay mineral. Biotite and opaque minerals (black) are also observed. Dark brown lamina and greenish tint within the matrix indicate secondary alteration (sample no. KB-20B, x nicols, x 2.5).

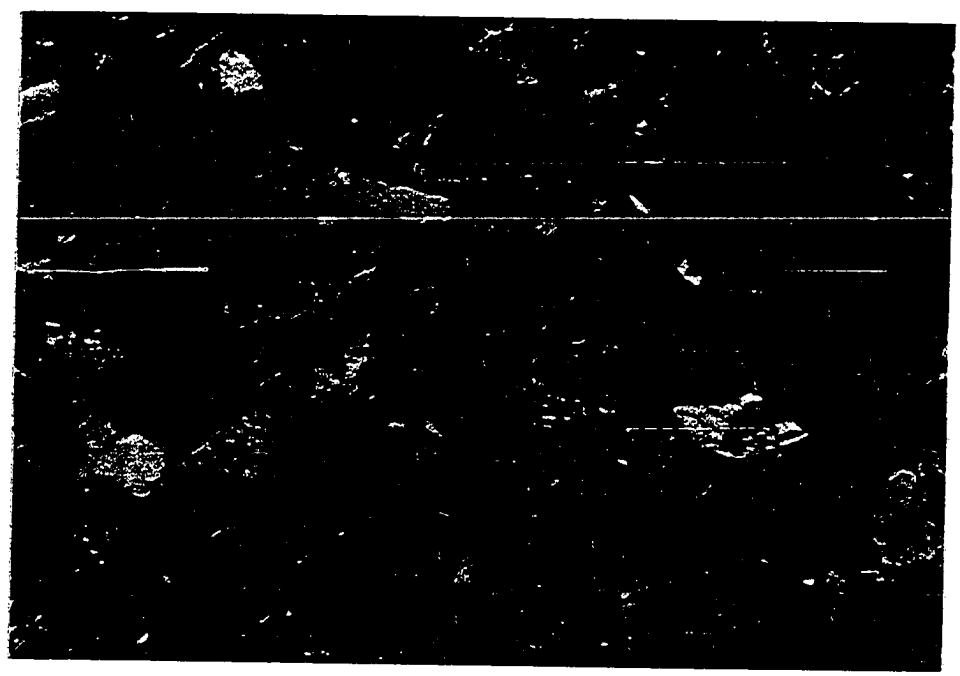

FIGURE 30. Photomicrograph of a vitric-crystal tuff. Non-clay minerals are composed of alkali-feldspars (gray) and biotite (brown). Clay and quartzofeldsphatic minerals form the matrix (sample no. KB-18A, x nicols, x 2.5).

FIGURE 31. Photomicrograph of a vitric-crystal tuff. Biotite flakes (brown) are oriented horizontally (sample no. KB-7D, x nicols, x 2.5).

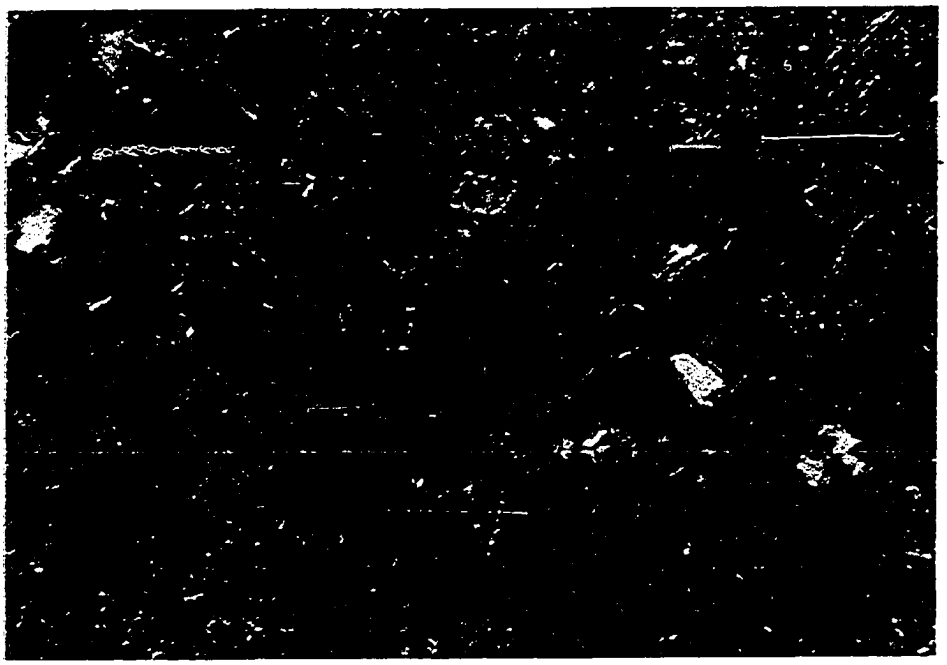

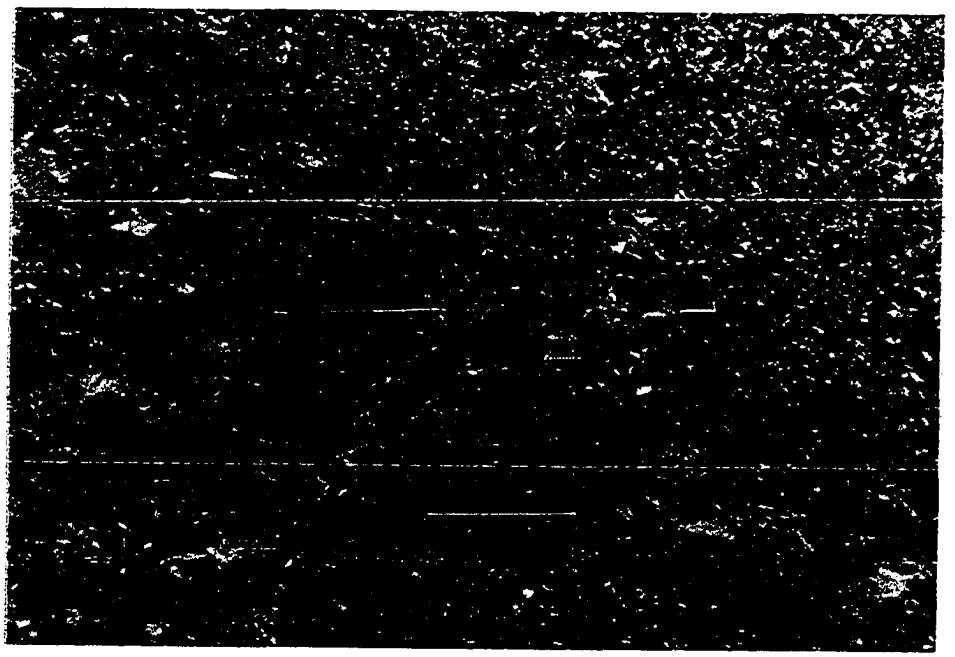

FIGURE 32. Photomicrograph of a vitric-crystal tuff showing the angular shapes of alkali-feldspars (gray), sharp contacts between the non-clay minerals and the matrix, and parallel orientation of minerals (sample no. KB-7D, xnicols, x 10).

FIGURE 33. Photomicrograph of a reworked vitric tuff including ostracode fossils. Tuff is composed of altered volcanic dust (sample no. KB-21, x 10).

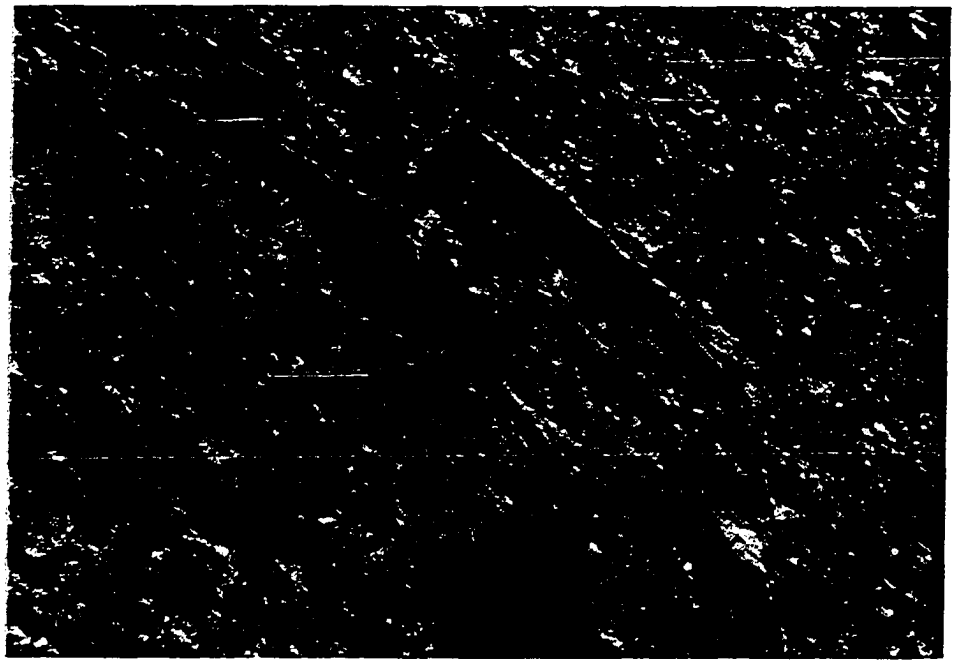

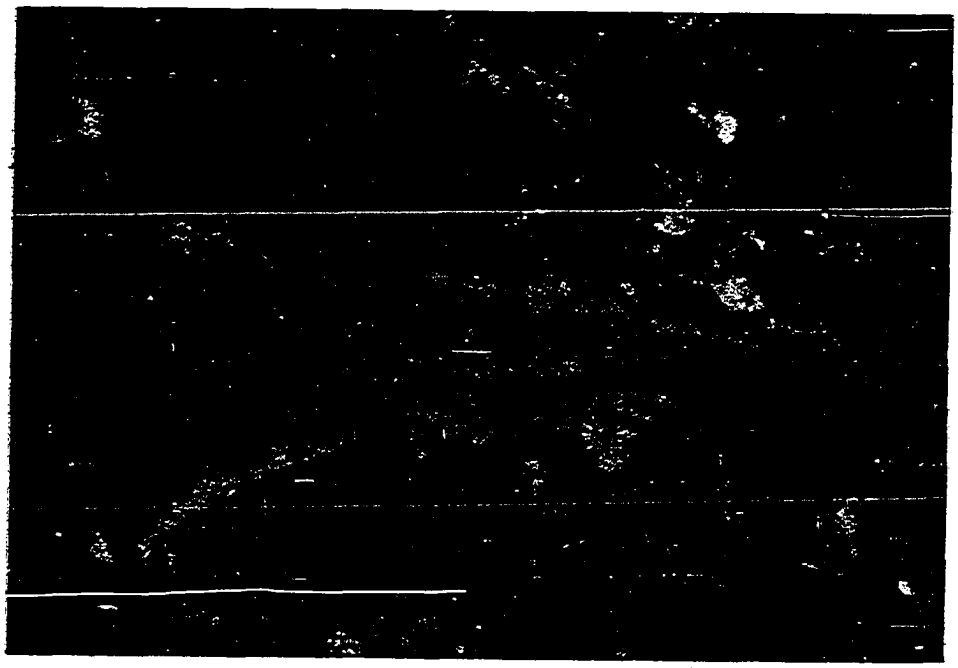

origin are also observed. They form horizontally oriented thin layers in the thin-section.

Microscopic studies of K-bentonites have shown that, although altered, they still preserve some microtextures characteristic of volcanogenic sedimentary rocks. The morphology and composition of the non-clay minerals, presence of relict glass shards, fabric and other microtextural features of rocks as observed under the microscope altogether, are evidences of their volcanic origin. However, earlier studies showed that the petrographic characteristics of K-bentonites may vary within a bed and are generally useless in distinguishing the K-bentonite horizons from one another.

The non-clay mineral assemblage in K-bentonite samples is constant and is characteristic of acid-to-intermediate volcanic rocks. Earlier workers including Weaver (1953a) and Smith, et al. (1971) concluded that the mineralogy of Ordovician K-bentonites compares reasonably with volcanic rocks such as trachyte, latite, phonolite, trachyandesite or andesite. Their conclusions are based on heavy and light mineral studies, and also on comparison of selected major oxides with those of intermediate volcanic rocks in the literature. However, on close inspection it appears these criteria cannot be reliably used to classify K-bentonites. First, even in fresh volcanic rocks petrographic classifications using careful point counting techniques face difficulties due to the porphyritic nature of the rock. Secondly, a chemical classification of K-bentonites based on certain

major element oxide contents may give erroneous results because of the fact that these rocks are a part of an open chemical system during the long period of post-depositional alteration.

Recently, a chemical means of discriminating different volcanic rock types and magma series and which can be applied to extensively altered rocks was proposed (Floyd and Winchester, 1975, 1978; Winchester and Floyd, 1977). The method utilizes seven minor and trace elements, Ti, Zr, Nb, Y, Ga, Ge and Sc which are considered to remain inert during the alteration processes (Cann, 1970; Field and Elliott, 1974). Using these immobile elements and their ratios, geochemical discrimination diagrams can be prepared for fresh volcanic rocks. They subsequently can be used for the determination of original rock types and magma series of the altered volcanic rocks (Floyd and Winchester, 1978). Thus, it is worth testing the usefulness of this technique in determining the original composition of K-bentonites. Contents of immobile elements as tabulated in Table I (App. F) are plotted on the discrimination diagrams of Winchester and Floyd (1977). In some cases when there is more than one sample analysis from a single section of a thick bentonite bed, their average values are plotted so that a better chemical description of rock is achieved. The results of this phase of the study are shown in Figures 34, 35 and 36. Figure 34 is a plot of Nb/Y against Zr/TiO_2. Both ratios are indices of alkalinity, but only

FIGURE 34. Zr/TiO_2 against Nb/Y diagram showing the magma series and rock type of the original volcanic ash formed the K-bentonites (Based on data by Winchester and Floyd, 1977). Symbols are as follows: ● , K-bentonite; ▼, rhyolite; x , trachyte; □ , phonolite; △ , dacite, rhyodacite; ▲ , andesite; ◆ , comendite; + , trachyandesite, benmoreite; 0, tholeiitic, high alumina basalt; ■ , basanite, trachybasanite.

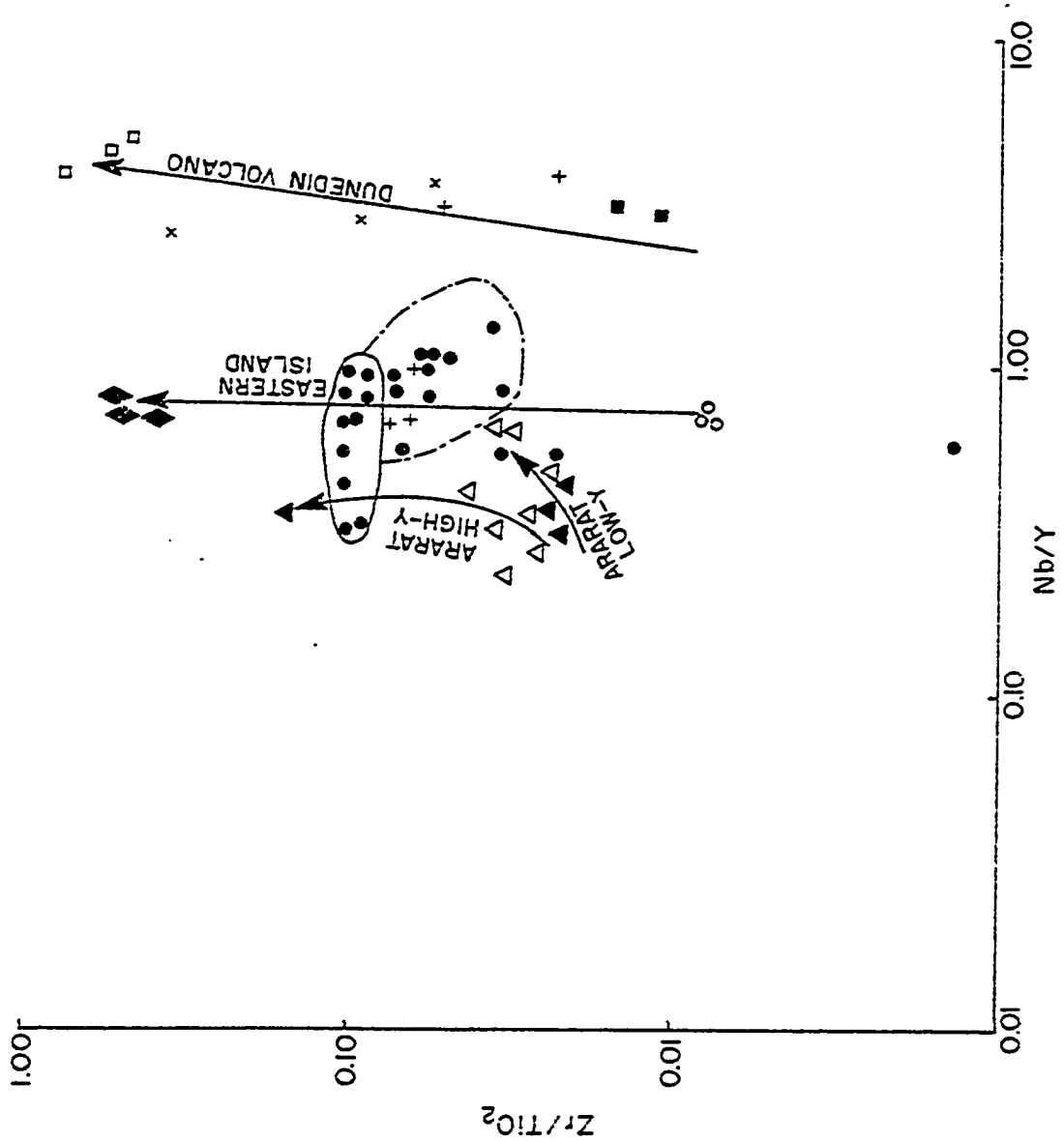

FIGURE 35. Zr/TiO_2 against Nb/Y diagram showing the limited fields of volcanic rocks and original rock types of K-bentonites (Based on data by Winchester and Floyd, 1977).

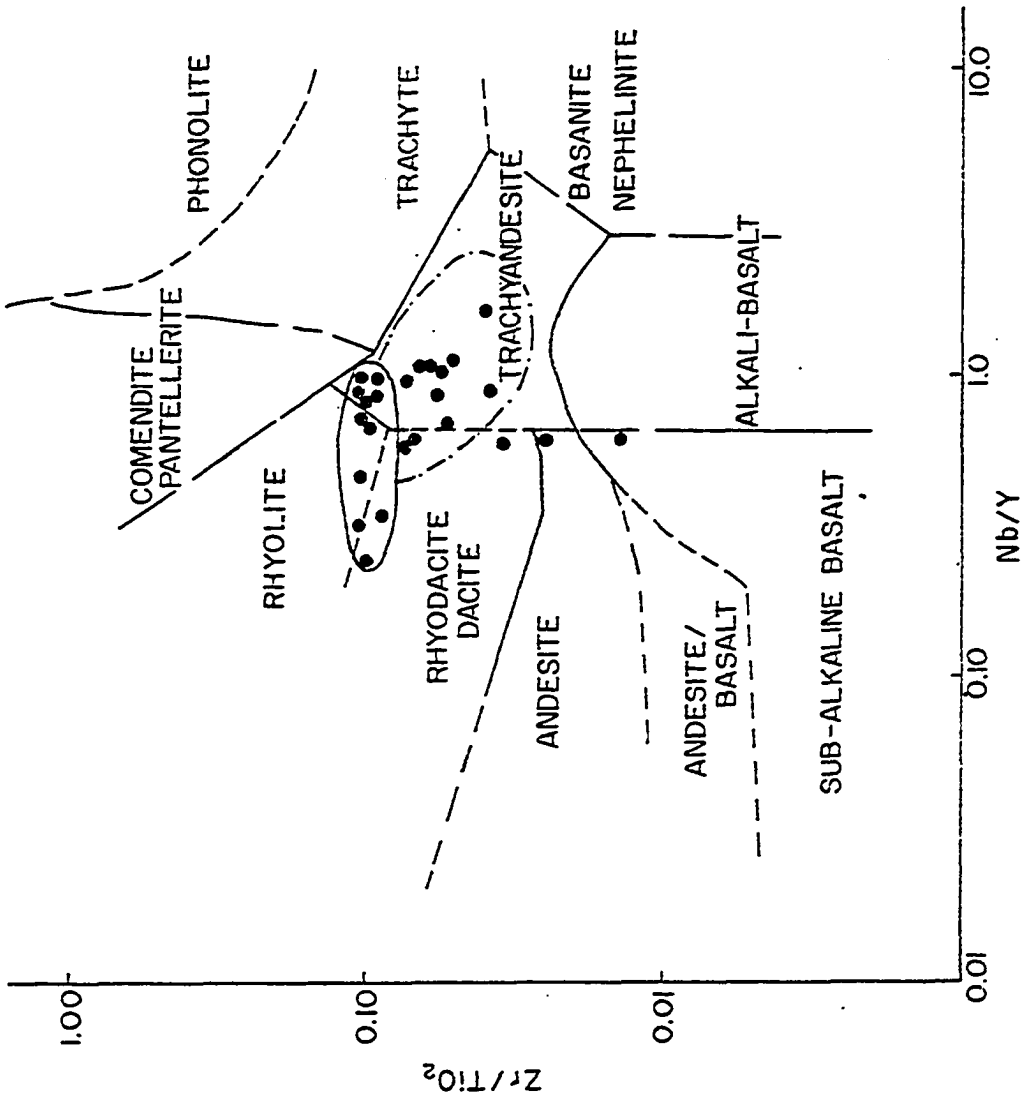

FIGURE 36. Zr/TiO_2 against Ga diagram showing the fields of common volcanic rock types and the original composition of K-bentonites (Based on data by Winchester and Floyd, 1977).

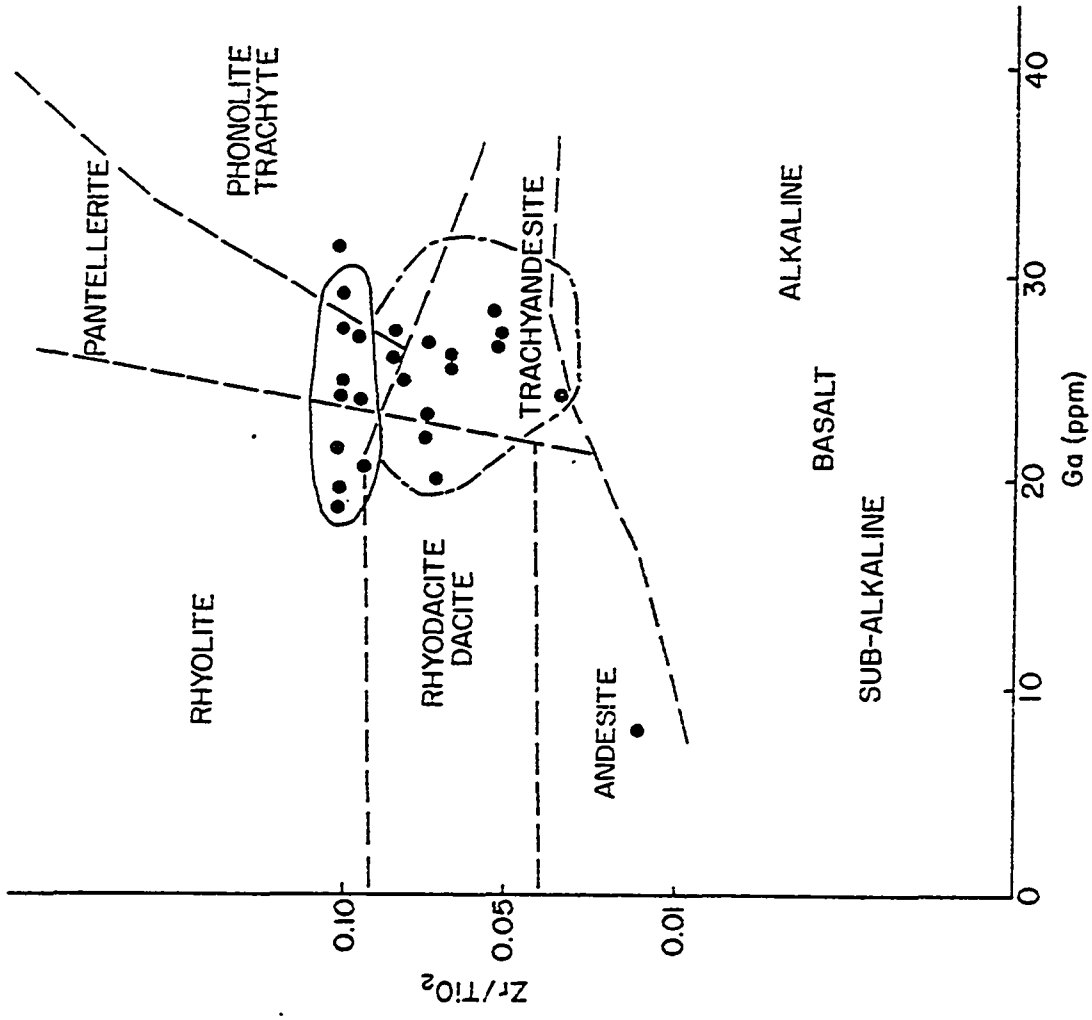

the Zr/TiO_2 ratio is a differentiation index (Winchester and Floyd, 1977). In this diagram rocks from Mt. Ararat are calc-alkaline, those from Dunedin volcano are alkaline and Eastern island rocks belong to a mildly alkaline suite. In general, K-bentonite bulk samples occupy the field of mildly alkaline rocks, namely trachyandesites and some have dacitic-to-rhyolitic composition in the calc-alkaline suite. Another feature of this plot is the suggestion of a possible differentiation of magma from intermediate (trachyandesite) to acid (rhyolite) compositions or presence of two different magma sources forming the K-bentonites under investigation, because the area encircled by the solid line is occupied by the samples from the two younger K-bentonite horizons and the area outlined by the dashed line covers data from the oldest K-bentonite layer studied. Resolution of this aspect will depend upon future regional studies involving a broader distribution of samples than those chosen for this study.

Figure 35 is a Zr/TiO_2 against Nb/Y discrimination diagram showing the fields of the most common volcanic rocks. Data obtained from the K-bentonite bulk samples cluster in the field of acid-intermediate volcanic rocks which have trachyandesitic to rhyolitic compositions. All the features shown by this diagram are similar to the previous plot, except the boundry lines between the different rock types give a better perspective to the compositions of the samples.

A similar pattern is found in the plot of Ga against Zr/TiO_2 ratio (Fig. 36). Based on this geochemical grid the original composition of the oldest K-bentonite horizon can be better distinguished from the two younger horizons. On this diagram the two major groups of samples do not show any marked change in Ga content, but their Zr/TiO_2 ratios do provide a better basis for differentiation.

These Figures demonstrate that five of the immobile elements or their ratios can identify the magma series and the original rock type of K-bentonites. They also suggest a progressive change in the differentiation index, Zr/TiO_2, towards a more acidic composition with a decrease in the age of K-bentonite horizons.

The Relationship Between K-Bentonites and Adjacent Limestones

In the study area there is a pronounced lithologic difference between K-bentonites and enclosing sublithographic Tyrone-equivalent limestone. For this reason, K-bentonites are easily recognized in the field, even when the surface weathering is intensive. A shallow, quiet water depositional environment is indicated by the dominant sublithographic character of the limestones (Cressman, 1973). Absence of shaly material in association with the K-bentonites shows that during the time of deposition fine terrigeneous material was not available from the adjacent land areas.

A number of samples just above and below the K-bentonites have been studied in thin-section to investigate their general petrography,

the effects of post-depositional alteration processes on limestones and the boundry characteristics among the two rock types in micro-scale. The petrology of the representative Middle Ordovician lithologies is described by Wilson (1971) and Ruppel and Walker (1977). During the present study, it was observed that the Tyrone Limestone is composed of micrite, sparry calcite, dolomite, silica, alkali-feldspars (sanidine and orthoclase), clay, biotite, opaques and fossils. Micrite is the most common calcite cement whereas sparry calcite generally occurs as void filling cement. The latter forms bird's eye texture which is very peculiar to the Tyrone Limestone in this region. Dolomite is a rare mineral. It is usually found as subhedral to euhedral rhombs and seems to replacing micrite in the samples. Cryptocrystalline varieties of quartz are observed in the thin-sections. They consist of chert and chalcedony, and chert is the most common variety. As observed in the field and reported by earlier workers cryptocrystalline quartz forms discontinuous beds mostly underlying thick K-bentonite horizons. Its microscopic examination suggests a chemical rather than a biogenic origin because no remains of organisms are detected. Chalcedony is rarely observed either as void fillings or as replacing the fossil shells. The amounts of alkali-feldspars, clay and biotite increases as K-bentonite beds are approached. Weaver (1953a) and Huff (1963a) also demonstrated this fact by examining the distribution of insoluble

residue in the Tyrone Limestone in detail. They showed that chert constitutes the majority of the insoluble residue adjacent to the beds, and volcanic heavy mineral and chlorite contents of limestone increase towards the K-bentonite beds whereas non-expanding dioctahedral 2:1 clay and non-volcanic minerals decrease in abundance. These observations show that volcanic ash is the major source of insoluble residue in enclosing Tyrone Limestone. Alkali-feldspars, biotite and opaque minerals are mostly fresh and form euhedral or subhedral crystals. The sparse fauna in the carbonates are represented mainly by ostracodes, bryozoans and brachiopods. Although fossil valves are separated, in general, they are neither broken or abraded, indicating little or no transportation.

Some effects of post-depositional alteration processes are observed in the Tyrone Limestone. They include recrystallization of micrite to form sparry calcite, dolomitization of micrite and silicification of the limestone. Recrystallization of micrite to form sparry calcite and dolomite occurred when the micrite that formed under the marine conditions was buried in the subsurface where saline waters came into contact with meteoric waters and salinity reduction occurred. In the absence of Mg-poisoning sparry calcite and dolomite could form as suggested by Folk (1974) and Folk and Land (1975). Origin of silica, on the other hand, has been discussed by various authors including Cooper and Prouty (1943),

Fox and Grant (1944) and Siever (1962) and has always been presumed that chert replacement of carbonate is a direct consequence of silica release during the devitrification of volcanic ash.

In some of the limestone samples and their thin-sections, intercalated laminae of carbonate and shaly material are present. It was previously discussed that the major source of non-carbonate minerals is bentonites, and intercalated laminae at the contact of K-bentonite beds with limestone indicate a slight reworking in the form of soft-sediment transportation during the beginning and towards the end of deposition of some bentonite beds.

RESULTS OF INVESTIGATION

PART II: CHEMICAL COMPOSITION AND CORRELATION

Introduction

Data regarding whole rock and trace element composition of Ordovician K-bentonites are sparse or lacking, and there has been no attempt to undertake a tephrochronological study based on the chemical variations in different K-bentonite horizons. Among earlier investigators, Nelson (1922b), Allen (1929, 1932) and Fox and Grant (1944) examined the major element chemistry of various K-bentonite samples and related their findings to the mineralogical pecularities of these beds. For example, Fox and Grant attributed the high content of Fe_2O_3 (4.39 percent) in B-6 (T-4 of Wilson, 1949) to biotite which is quite noticeable in the bentonite. He also concluded that the high CaO content (7.59 percent) of B-12 is due to secondary calcite. More recently, Smith, et al. (1971) published whole rock chemical analyses of nine K-bentonite samples from Alabama in search of information regarding the original composition of the volcanic ashes and accounting for the chemical variations noted between the bentonites and comparable rocks, such as shales. Unfortunately, none of the studies mentioned above have information on the trace element composition of these rocks.

As discussed previously (p. 12) the use of geochemical criteria as a tool to characterize individual tephra layers has proved to be

very useful with Cenozoic material. Important stratigraphic advances in terms of long distance correlation have been made by means of tephrochronologic studies based on these criteria. Yet, there has been no effort to extend similar studies to the stratigraphic correlation of Ordovician K-bentonites. Such an attempt will face certain difficulties because, for example, diagenetic alteration of K-bentonites precludes the use of glass shard composition, which seems to be one of the most useful characterization parameters among younger Cenozoic tephras. Thus, for older K-bentonites different techniques must be used and their usefulness tested for tephrochronological and correlation studies. Secondly, in a regional study such as this, scarcity of major and minor oxide analyses and an absence of trace element data from previous workers requires a substantial amount of data gathering before statistically reliable conclusions can be drawn. Furthermore, sample location must be founded on a basis of strong stratigraphic control and obtained from regionally widespread K-bentonite horizons to insure reliable results in their attempted correlation.

This chapter deals with the chemical composition and correlation of Ordovician K-bentonites. Chemical data presented here contribute to our general knowledge of major, minor and trace element composition of both bulk samples and their less than 2 μm clay fractions. It is anticipated that the synthesis of geochemical data will provide an understanding of how the mineralogic changes that

occurred during the post-depositional alteration of the original volcanic ash are accompanied by chemical changes in the bulk samples or in their clay size fractions. Consequently, the information gathered can be used to evaluate the chemical data for the geochronological study of the K-bentonite horizons. Finally, it is the ultimate objective of this chapter to show that the abundance and distribution of certain elements and elemental ratios which can differentiate between K-bentonite horizons can also be employed for long distance stratigraphic correlation.

Effects of Post-Depositional Alteration

In the previous chapter it has been shown that the original mineralogic composition of volcanic ash has undergone post-depositional alteration to secondary minerals composed mainly of interstratified illite-smectite. Alkali-feldspars and glass shards have suffered the most and the latter have completely devitrified. Under these circumstances one can expect that major and minor elemental composition of Ordovician K-bentonites will be different from that of the original rock, because possible gains or losses of mobile elements such as Ca, K and Na have occurred in what might be considered a semi-open geochemical system. During this study the nature of chemical changes in the composition of original volcanic ash is investigated by calculating the gains and losses using a method described by Krauskopf (1967, p. 100) and based on the assumption that alumina content did not change appreciably during

the post-depositional alteration. An average trachyandesite composition (Carmichael, et al., 1974, p. 396, 499 and 501) is used as a standard during these calculations. This decision is based on the discussions in the previous chapter that almost all of the K-bentonite samples originally had acid-to-intermediate compositions with the majority falling into the trachyandesite field (Figs. 34, 35 and 36). A consequence of this approach is a better understanding of the origin of K-bentonites, the gain, loss and redistribution of elements in both bulk samples and less than 2 μm clay fractions.

The data tabulated in Table I (App. F), concerning the major and minor element analyses of K-bentonite bulk samples are used for calculations and the results are shown as average values in Table 3. Columns 1 and 2 give composition in weight percents of average trachyandesite and of bulk samples, respectively. Column 3 shows the calculated weight in grams of each oxide in 91.58 g. of rock remaining from the alteration of 100 g. of fresh rock. Column 4 lists the gains and losses of each constituent in grams per 100 g. of fresh rock, and column 5 shows the same gains and losses in percentages of the original amounts. The last two columns suggest a decrease in the amounts of SiO_2, Fe_2O_3T, CaO, Na_2O and TiO_2 of the original rock, whereas its MgO and K_2O values have increased. Among these changes minimum silica loss and maximum potassium gain stand out at 5 percent and 92 percent, respectively. An important question one might ask at this point is whether these

TABLE 3. Calculation of gains and losses during post-depositional alteration processes based on the average of partial chemical analyses of 45 K-bentonite bulk samples.

Oxide	1	2	3	4	5
SiO_2	52.56	54.28	49.71	-2.85	- 5
Al_2O_3	18.39	20.08	18.39	0	0
Fe_2O_3T*	8.19	1.92	1.76	-6.43	-78
MgO	2.12	3.78	3.47	+1.35	+63
CaO	5.64	0.74	0.68	-4.96	-87
Na_2O	5.76	1.02	0.93	-4.82	-83
K_2O	3.91	8.22	7.53	+3.61	+92
TiO_2	1.73	0.37	0.34	-1.39	-80
MnO	0.14	0.03	0.02	-0.12	-86

* Total iron expressed as Fe_2O_3.

Explanation of column headings:

1. Average reference trachyandesite (weight percent)
2. Average of K-bentonite bulk samples (weight percent)
3. Recalculated weight of bulk sample after alteration (weight percent)
4. Difference of columns 1 and 3 (grams per 100 grams)
5. Difference in percentage of the original amount (%)

chemical changes as suggested by Table 3 account for what has been known as the chemical and mineralogical characteristics of K-bentonites and also demonstrate the effect of post-depositional alteration of volcanic ash on the adjacent limestones. More specifically, how for example, can the considerable gains or losses of magnesium, potassium, calcium and sodium play a role in formation of the present clay mineralogy of K-bentonites or, can an average of 5 percent loss of silica from the original volcanic ash be sufficient to account for what has always been presumed to be the origin of the discontinuous chert bands occurring mainly at the base of the thick K-bentonites. Here, the amount of silica loss seems to be insufficient to produce 1-2 inches thick chert layers, however, a more scientific answer to this question can be given by studying in the future both the petrography and chemistry of adjacent limestones and chert in detail and by including mass transfer calculations for both K-bentonite and limestone samples. Only preliminary data on these questions is considered in this study.

Table 4 gives a comparison of average oxide contents of K-bentonite bulk samples and their clay fractions. Columns 1 and 2 list the averages of calculated weight in grams of each oxide remaining from the alteration of 100 g. of fresh rock and the averages of oxide content in weight percent of the clay fractions, respectively. The differences between these two columns are

TABLE 4. Comparison of the average oxide contents of 21 K-bentonite bulk samples and their clay fractions.

Oxide	1	2	3	4	5	6
SiO_2	52.72	53.76	+1.04	60.69	60.13	-0.56
Al_2O_3	18.39	20.80	+2.41	21.17	23.27	+2.10
Fe_2O_3T*	1.80	1.48	-0.32	2.07	1.65	-1.41
MgO	3.49	4.48	+0.99	4.02	5.01	+0.99
CaO	0.89	0.43	-0.46	1.03	0.48	-0.55
Na_2O	1.04	1.25	+0.21	1.20	1.39	+0.19
K_2O	8.21	6.96	-1.25	9.45	7.79	-1.66
TiO_2	0.30	0.22	-0.08	0.35	0.25	-0.10
MnO	0.02	0.02	0.00	0.02	0.02	0.00
Total	86.86	89.40		100.00	100.00	
(+)Increase			+4.65			+3.28
(-)Decrease			-2.11			-3.28

*Total iron expressed as Fe_2O_3

Explanation of column headings:

1. Average of K-bentonite bulk samples recalculated after alteration (weight percent).
2. Average of clay fractions (weight percent).
3. Difference of columns 1 and 2.
4. Average of K-bentonite bulk samples recalculated (after column 1) to 100.
5. Average of clay fractions recalculated (after column 2) to 100.
6. Difference of columns 4 and 5.

tabulated in column 3, which indicates that clay fractions in general, have higher SiO_2, Al_2O_3, MgO and Na_2O but lower Fe_2O_3T, CaO, K_2O and TiO_2 values. The results of recalculations of the oxide values in columns 1 and 2 to 100 g. of rock is shown in columns 4 and 5, respectively, and column 6 tabulates the differences between them. The only significant difference between columns 3 and 6 is the opposite sign of SiO_2 although the rest of the constituents differ in the same direction.

A closer examination of Tables 3 and 4 reveal the relative intensity of gains and losses taking place during the alteration of volcanic ash and also shows the effects of non-clay minerals on the distribution pattern of differences in oxide values between the bulk samples and clay fractions. Silica content, the least affected constituent during alteration processes is slightly higher (0.56 g/ 100 g) in the bulk samples relative to clay fraction as a consequence of the presence of free quartz in bulk samples. It is the basic assumption that alumina remained constant during the post-depositional alteration. As shown in Table 4, the clay fraction contains more Al_2O_3 than the bulk sample does. This observation may also indicate that aluminum is increasingly incorporated into the clay mineral structure with increasing intensity of alteration of the original volcanic ash. Fe_2O_3T and TiO_2 values of the fresh rock are reduced considerably as a result of alteration, and as

demonstrated in Table 4, iron an titanium have remained mainly as the major components of the non-clay minerals such as Fe-Ti oxides. Magnesium has been added to the fresh rock so that 63 percent gain of MgO is observed in Table 3. This element is preferentially adsorbed by smectite clays rather than uniting with non-clay minerals as suggested by higher MgO contents of clay fractions than those of bulk samples, the difference averaging to 0.99 g. per 100 g. of sample. CaO and Na_2O are both lost during the post-depositional alteration of the volcanic ash. Comparison of bulk samples and clay fractions suggests that calcium remaining in the rock occurs as a non-clay mineral, namely calcite, whereas sodium is mainly incorporated into illite-smectite clays as they form. Finally, potassium, the element showing the highest degree of increase by the original rock, achieve high concentrations in clay fractions, although an average bulk sample contains more K_2O than an average clay sample. This suggests that potassium is mainly associated with clay minerals but potassium containing non-clay minerals such as alkali-feldspars and biotite which are common in K-bentonite samples contribute significantly to the K_2O content of the bulk samples. It is concluded that high K_2O content of the clay fraction reflects the formation of an interstratified mica-smectite phase as does the MgO and Al_2O_3 increase in the clay fraction.

So far the discussion of the effects of post-depositional alteration has been limited to gains or losses and to the comparison

of oxide contents of bulk samples and clay fractions. The results of investigation as tabulated as Table 3 and 4 can also be used in studying the origin of K-bentonites. The volcanic origin of K-bentonites has been demonstrated by optical methods (Ross, 1928; Allen, 1929, 1932) and on the basis of differential thermal analysis (Huff, 1963b; Mossler and Hayes, 1966). The results obtained from the chemical analyses during this study further support the same idea. As shown in Table 3 K-bentonite bulk samples are enriched in MgO, now averaging 3.78 percent. It is concluded that magnesium adsorption from sea water by smectite clay occurs during the devitrification of volcanic glass settled on the ocean floor. Weaver and Pollard (1973) compare MgO contents of illites formed in different environments and their findings are presented in Table 5. It is apparent that "marine" illite material formed from smectite during burial has a higher MgO content than illites resulting from the alteration of feldspars. Furthermore, low MgO illites and dioctahedral smectites in the same literature, all have lesser octahedral positions filled with magnesium when compared to those of calculated structural formulae of the interstratified illite/ smectite clays of K-bentonites. As discussed in the previous chapter magnesium replacement in the octahedral sheet is an essential mechanism in the origination of the latter clays.

The kinetics of illite formation from a number of glass compositions have been investigated by Eberl and Hower (1976) and

TABLE 5. Percent MgO in illites formed in different environments (Weaver and Pollard, 1973)

No.	Environment	%MgO	No.	Environment	%MgO
6	Weathered feldspar	1.09	2	Atchafalaya Bay mud	3.33
11	Weathered granite	1.37	3	Mississippi delta, marine mud	3.32
22	Veneer in shear planes	0.44	4	Gulf of Mexico, marine mud	2.90
27	Post-depositional		13	Slate from marine shale	3.56
	alteration of feldspar		14	Slate from marine shale	3.05
	in sandstone	1.49	23	Clay from marl	4.48

the application of the kinetic results have been discussed. The mechanism involves the chemical changes of smectite 2:1 layers before the formation of illite. During diagenesis the natural reaction might be,

$$Al^{+3} + K^{+} + \text{Smectite} \longrightarrow \text{Illite/Smectite} + SiO_2 \quad (4)$$

which involves the tetrahedral substitution of Al for Si. Electrical neutrality during the chemical changes is preserved by an accompanying increase in the adsorption of interlayer cations such as K^{+}. The possible sources of this ion may be decomposing feldspars (Heling, 1978), detrital illite (Perry and Hower, 1970) or an outside source such as the pore waters (Lawrence, et al., 1975). In the case of Ordovician K-bentonites only an outside source can account for the change in K_2O content of the original ash from 3.91 to 8.22 percent (Table 3) as a result of post-depositional alteration processes. However, the breakdown of minerals such as alkali-feldspars and biotite also provide an additional source for potassium incorporation into the interstratified illite-smectite clays. This is evidenced by the alteration of these minerals as observed under the optical microscope or supported by the x-ray studies of the 2-0.2 and 0.2-0.08 μm clay fractions which show that chlorite concentrates in the coarse fraction as a rare alteration by-product of biotite. The increase in the illite-smectite ratio of interstratified clays can occur as a result of the chemical changes discussed above either during the deep burial of the rock at 150°-166°C (Perry and Hower,

1970; Weaver and Beck, 1971; Weaver and Pollard, 1973) or during its long time exposure to K^{+} and Mg^{+2} etc. at lower temperatures and pressures. The latter seems to be more likely in the case of K-bentonites since they do not show any effects of deep burial within the study area.

Chemical Variation Within Individual K-Bentonite Beds

In considering the significance of any variation in bulk chemical composition between K-bentonite horizons, the possibility exists that within-bed variations in distribution and abundance of elements might be significant enough to conceal the variations which otherwise would fingerprint individual beds. Within-bed variation in the bulk chemical composition may arise from the lithologic features of the original tephra such as the concentration of crystals along certain horizons due to differential gravitational settling or sedimentary reworking of volcanogenic minerals. Naturally, any bulk sample from this particular horizon would not chemically represent the whole layer.

Data in Tables I and II (App. F) are plotted as Figure 37 in order to show within- and between-bed variations in the Al_2O_3, Fe_2O_3T, K_2O, TiO_2 and MgO contents of twenty nine bulk samples and their less than 2 μm clay fractions. Samples with similar numbers such as 7A through 7C or 19A through 19D indicate that they are from the same K-bentonite horizons, KB-7 and KB-19, respectively. Otherwise, the sequence of sample numbers from different horizons is arbitrary.

Only in two random cases horizontal lines are used to outline the distribution patterns of oxide contents in samples from two different horizons (KB-19 and KB-28) in order to illustrate within-bed variations more clearly.

Alumina curves reflect fluctuations ranging between 13.29-23.71 and 16.69-24.49 percents for bulk samples and clay fractions, respectively. As also shown in Figure 37, the variation of Al_2O_3 values in the bulk samples has wider range about a mean than that of the clay fraction. On the average, clays have slightly higher (0.95 percent) Al_2O_3 content than the bulk samples. It is observed that among most of the samples the two variation curves form an almost parallel pattern. Within- and between-bed variability are exemplified by samples from horizons KB-19 and KB-28. In both cases within-bed fluctuations are considerable, however, on the average the bulk samples from KB-19 have higher (19.53 percent) Al_2O_3 value than those of KB-28 (18.27 percent).

Fe_2O_3T contents of the bulk samples and clay fractions vary between 0.98-3.85 and 0.62-2.04 percents, respectively, indicating a wider range for the bulk samples. Figure 37 illustrates that the clays have lower Fe_2O_3T contents than bulk samples and the difference averages 0.4 percent for this particular set of samples. Both bulk and clay samples from the horizon KB-19 have higher Fe_2O_3T values than those of the horizon KB-28. For bulk compositions the difference equals to 0.16 percent on the average.

FIGURE 37. Distribution of Al_2O_3, Fe_2O_3T, K_2O, TiO_2 and MgO contents in 29 bulk samples and their clay fractions. Horizontal lines are drawn to indicate better the within-bed variations.

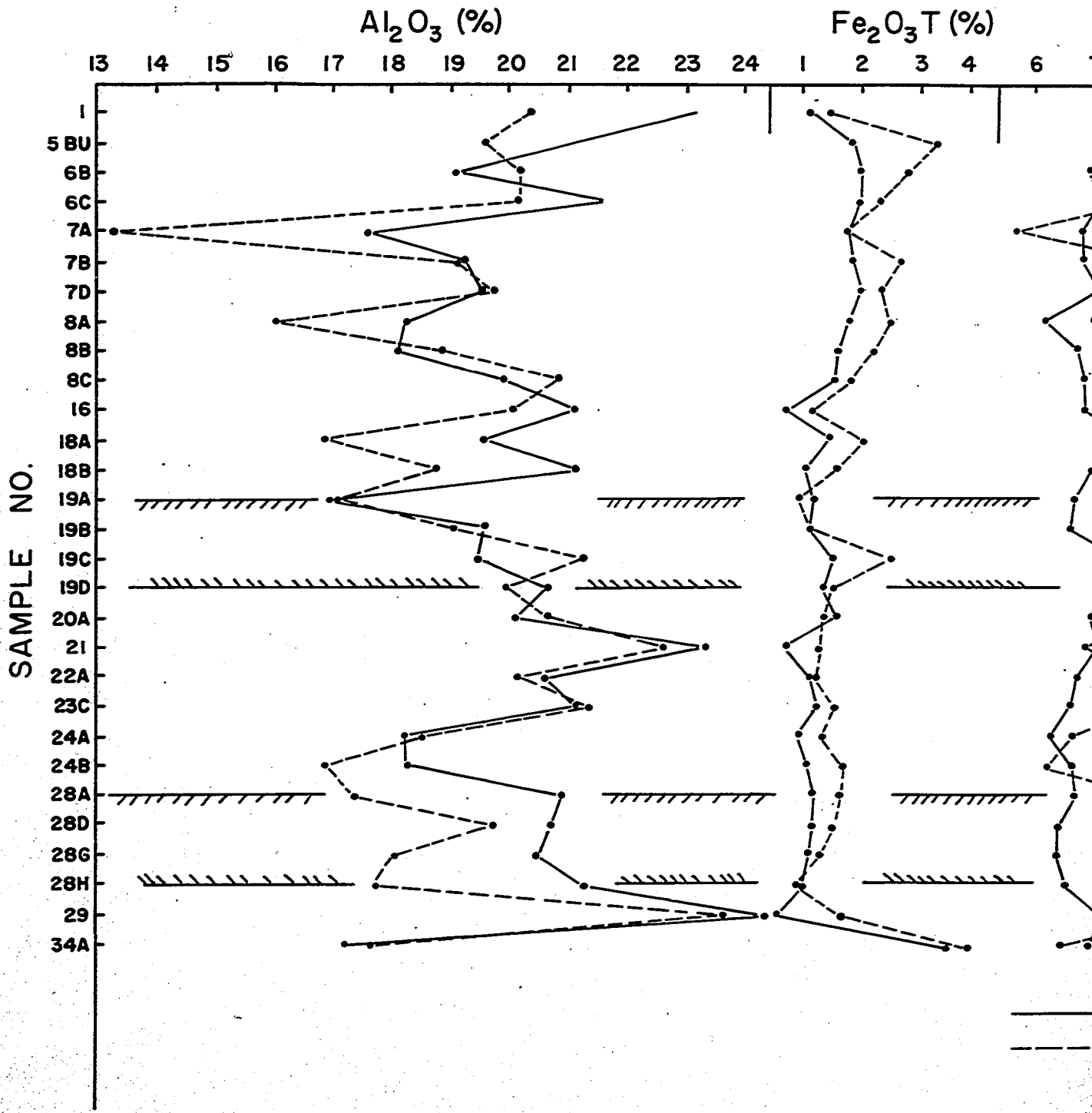

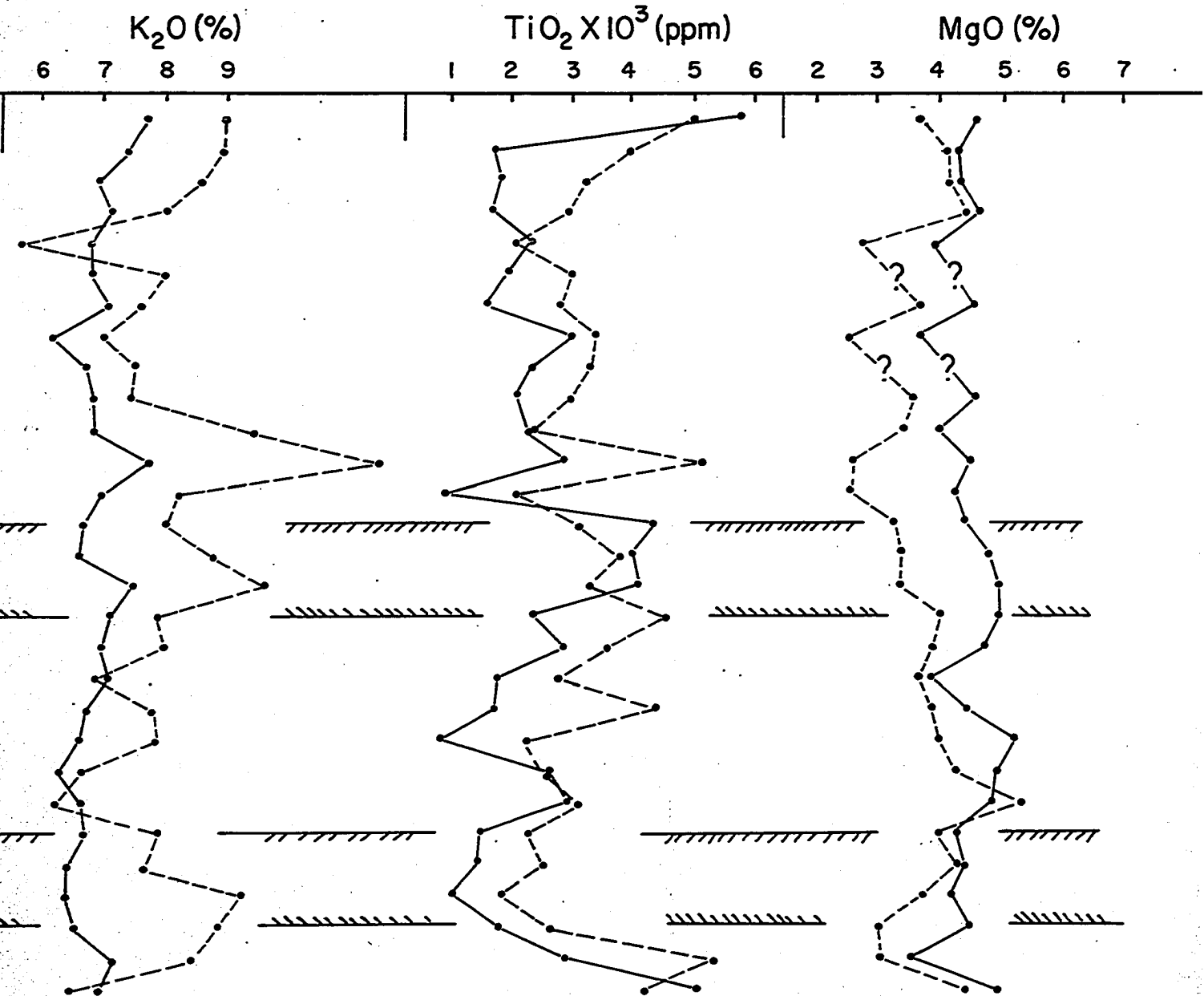

——— ∠2 m CLAY FRACTION
– – – – BULK SAMPLE

Variation curves of bulk samples and clay fractions are separated better when their K_2O contents are plotted in Figure 37. The bulk samples show wider fluctuations in the range of 5.71-11.54, averaging 8.06 percent, and the clays have more constant K_2O values varying between 6.20-7.75 with an average of 6.91. The extreme K_2O values of some bulk samples are due to the contributions of minerals such as biotite (18A) and calcite (7A) to the chemistry of bulk samples. Samples from the two K-bentonite horizons show within-bed variations, however, on the average, both the bulk samples and clay fractions from these horizons have very close K_2O values. In the case of bulk samples, for example, KB-19 and KB-28 have K_2O contents averaging at 8.59 and 8.47 percents, respectively. It appears that potassium content of K-bentonites are essentially the same even for different horizons. This conclusion is in accordance with the findings discussed in the previous chapter that the interstratified illite-smectite clays have a narrow range of potassium ion occuppancy in their structures.

TiO_2 contents of the bulk samples and clay fractions vary between 0.21-0.54, averaging 0.33 percent, and 0.09-0.59, averaging 0.25 percent, respectively. Figure illustrates considerable within-bed variations in TiO_2 values of the two horizons, though these fluctuations do not seem to mask between-bed variations, especially when the average values are considered. These values are 0.37 and 0.23 percents, respectively, in the bulk samples.

MgO variation curves are well separated in Figure 37. MgO values of the bulk samples ranges from 2.54 to 4.59, averaging 3.73 percent. The clay fractions fluctuate in the range of 3.65-5.35 with an average of 4.53 percent. Within-bed variations in both cases are restricted. In the case of bulk samples KB-19 and KB-28 have MgO values ranging between 3.31-4.09 with an average of 3.55, and 3.18-4.40, averaging 3.84 percents, respectively. Similar to K_2O, MgO values do not show a significant between-bed variability. Thus, MgO which is more concentrated in clay fraction, as also shown in Figure 37, has relatively constant values. A similar conclusion is arrived at during the compositional and structural investigations of the interstratified illite-smectite clays as discussed in the previous chapter.

Within-bed as well as between-bed variability of Ga, Y, Nb, Rb, Zn and Zr contents of fourty four bulk samples and their less than 2 μm clay fractions are similarly illustrated in Figure 38. The average gallium content for bulk samples and clay fractions are 22.75 ppm and 8.12 ppm, respectively. Variation ranges are rather small in both cases when between-bed differences are considered. For two K-bentonite horizons, KB-19 and KB-28, gallium values of the bulk samples range from 17.66 to 35.00, averaging 22.74 ppm, and from 25.44 to 31.37, with an average of 29.29 ppm, respectively. Averages of clay fractions from these horizons have almost equal values. KB-19 and KB-28 have correspondingly

FIGURE 38. Distribution of Ga, Y, Nb, Rb, Zn and Zr contents in the bulk samples and clay fractions. Horizontal lines are drawn to indicate better the within-bed variations.

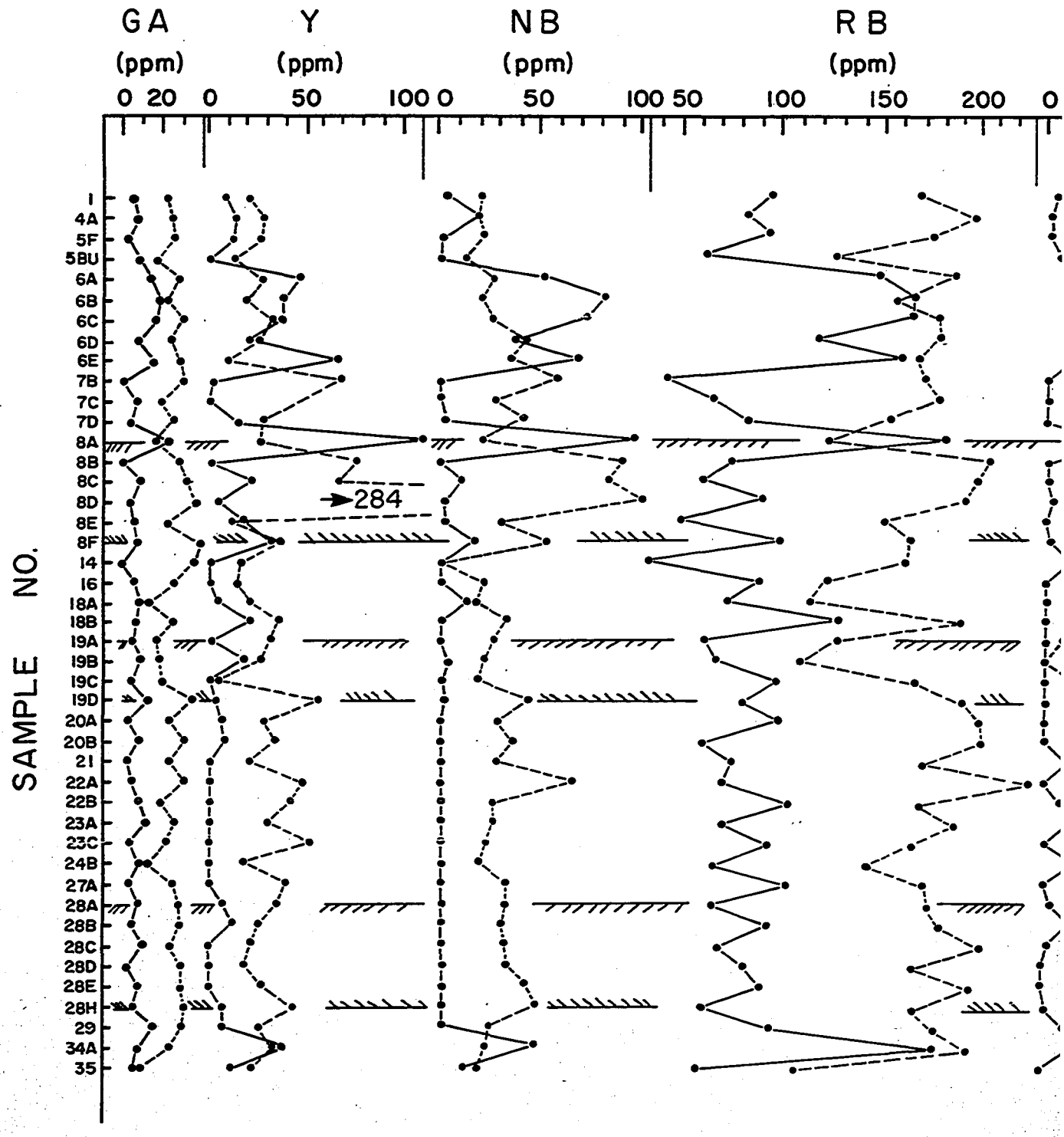

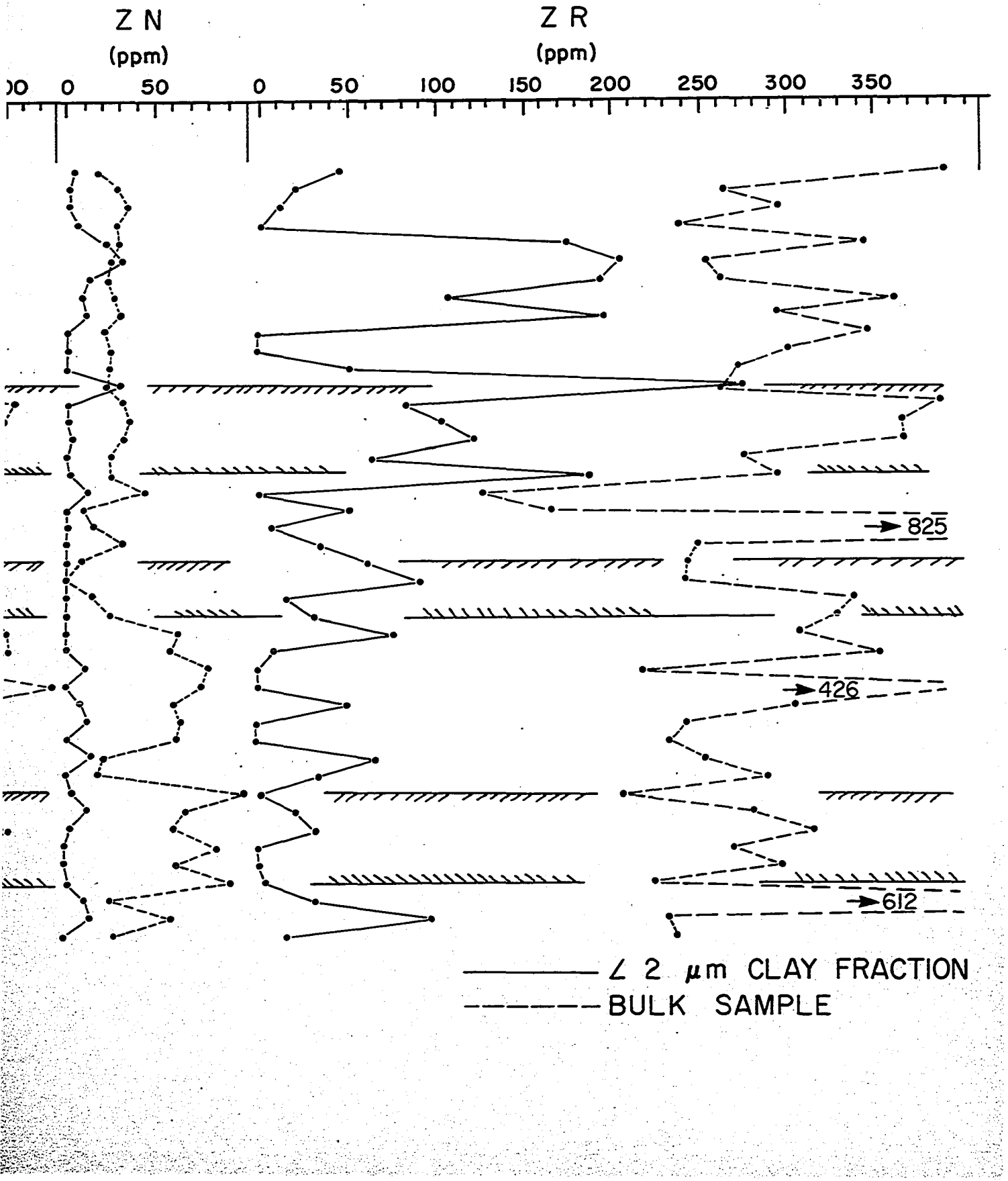

7.67 and 7.15 ppm gallium contents. Gallium is reported to show a close correspondence with aluminum and iron so that it enters into Al^{+3} and Fe^{+3} positions in mineral structures (Taylor, 1965; De Argollo and Schilling, 1978). Therefore, it is anticipated that the geochemical behavior of gallium in K-bentonite samples is influenced considerably by the abundance and distribution of aluminum and iron-rich minerals. As suggested by Taylor (1965) the large amount of aluminum, compared with ferric ion, is usually sufficient to mask the tendency of gallium to associate with the latter element. In the next section it is shown that gallium as well as aluminum is a poor discriminator between the individual K-bentonite horizons.

The average yttrium content of both bulk samples and clay fractions is 31.75 ppm and 13.95 ppm, respectively. The bulk samples from horizon KB-19 have yttrium values varying in the range of 2.97-56.66 ppm, and averaging 28.91. The yttrium content of bulk samples from horizon KB-28 ranges from 19.42 to 35.95 ppm, with an average of 29.19. Based on this comparison chemical fingerprinting of yttrium to distinguish between different K-bentonite horizons seems to be weak. In Figure 38 within-bed fluctuations are significant in another K-bentonite horizon (KB-8). Taylor (1965) indicates that Y^{+3} is closest in size to Ca^{+2}, and it concentrates in apatite and titanite during magmatic partitioning. Exotic fluctuation of the yttrium content of sample 8D can possibly

be due to the abundance of calcium rich minerals such as apatite and calcite in the sample.

The niobium content of both bulk samples and the clay fractions averages 30.81 ppm and 12.61 ppm, respectively. Figure 38 illustrates variability of the niobium content of bulk samples and their clay fractions. Niobium could not be detected in most of the clay fractions. Some bulk samples show within-bed variability as exhibited by the K-bentonite layers KB-8, KB-19 and KB-28. The last two have niobiom contents in the ranges of 21.46-43.85 ppm, averaging 27.60 and 30.14-48.13 ppm, with an average of 36.40, respectively. Nb^{+5} may substitute for Ti^{+4} and Zr^{+4} on the basis of ionic radii according to Taylor (1965) and it concentrates in the residual melts (Taylor, 1965; Gersimovskiy and Karpushina, 1977). Gersimovskiy and Karpushina, however, found that the geochemistry of niobium is governed mainly by alkalis (potassium). They could not detect any positive correlation between the contents of niobium and titanium in lavas of the basalt-andesite-rhyolite series, although there is a crystalochemical similarity between these two elements. In the light of these discussions, the fluctuations shown in Figure 38 may be related to the varying abundances of minerals which accumulate niobium in their crystal structures.

The bulk samples and clay fractions have rubidium contents averaging at 156.06 ppm and 93.78 ppm, respectively. For both kind of samples the graphs suggest within bed variability as

exemplified by KB-8, KB-19 and KB-28. The rubidium content of the bulk samples from horizon KB-19 varies between 109.80 and 193.80, with an average of 150.15 ppm. In the clay fractions the range is 62.19-99.55, averaging 77.75 ppm. The bulk samples and clay fractions from KB-28 have rubidium values ranging between 167.35-204.89 ppm, averaging at 180.99 ppm and 64.14-96.98 ppm, averaging at 79.57 ppm, respectively. Rubidium is very similar in size and chemical character to potassium, and in rocks these elements show a well known close association (Taylor, 1965). Rubidium is known to enter the potassium positions in feldspars and micas (Taylor, 1965; Higuchi and Nagasawa, 1969; Jensen, 1973), and as suggested by Randle, et al. (1971) this alkali metal can be concentrated in glass relative to coexisting crystalline phases as revealed by their study of Mazama ash. Under these considerations the limited fluctuation of the rubidium content of bulk samples can be expected in response to the varying concentrations of rubidium-carrying minerals. The distribution and abundance of rubidium in clay fractions suggest that during the post-depositional alteration of volcanic ash this element is adsorbed by the clay structure. Randle, et al. (1971) call attention to the possible significance of weathering on the rubidium contents of volcanic ashes. However, they conclude that abundances of this element in bulk samples can be used to support identification of an unknown ash sample. The value of rubidium in geochronologic studies and stratigraphic

correlations of K-bentonites will be discussed in the following sections.

The variations of zinc content in the bulk samples and clay fractions average at 35.18 and 5.19, respectively, and as illustrated in Figure 38, in most of the clay fractions zinc can not be detected. A group of bulk samples plotted at the lower half of the graph show higher zinc contents and wider within-bed fluctuations when compared to those samples plotted on the upper half of the graph. As an example, the bulk samples from horizons KB-19 and KB-28 have zinc content in the ranges of 0.00-24.21 ppm, averaging 11.56, and 61.58-102.70 with an average of 80.33 ppm. This feature of zinc distribution is in marked contrast to the other trace element distribution patterns. Zinc enters Fe^{+2} positions with increasing Zn^{+2}/Fe^{+2} ratio during fractionation in the silicate melts (Taylor, 1965), thus can originate as a primary constitunent of the igneous rocks. The resistance of zinc to the effects of sea water alteration of basalts is reported by Hart, et al. (1974). The value of zinc in distinguishing individual K-bentonite beds is discussed in the next sections.

Among the trace elements studied, zirconium has the widest range of abundance in the samples as shown in Figure 38. In bulk samples and clay fractions zirconium content averages 279.31 ppm and 60.78 ppm, respectively. Three of the bulk samples have very high zirconium content when compared to the average calculated

value. The bulk samples from KB-19 show a variation in the range of 330.05 to 244.43 ppm, averaging at 289.82. Average of zirconium content of the bulk samples from KB-28 is 268.93 ppm and the value of this element fluctuates from 209.81 to 319.72 ppm. Zirconium forms a separate phase, zircon, in igneous rocks, but Zr^{+4} may also substitute to some extent for Ti^{+4}, and hence accompany that element in substituting for Fe^{+3} (Taylor, 1965). The wide fluctuations shown in the Figure indicate inhomogeneous distribution of zircon crystals among the samples studied. In the clay fractions it is suspected that clay size zircon particles are present.

The variation curves prepared by plotting the raw chemical data obtained from the analyses of Al_2O_3, Fe_2O_3T, K_2O, TiO_2, MgO, Ga, Y, Nb, Rb, Zn and Zr of bulk samples and clay fractions exhibit significant within-bed variations for some elements such as potassium, yttrium and zirconium. Although the significance of these fluctuations in the geochronologic studies of K-bentonites based on the chemical composition can not be determined for sure from Figures 37 and 38, partly because of the limited number of samples used, it appears that in spite of these fluctuations between-bed variations exist for some elements such as iron, titanium, zinc and zirconium. In the next section it is shown that within-bed fluctuations in the contents of some elements do not mask the between-bed differences in the bulk samples. Further, when the average content rather than the individual values of

within-bed samples are used, the scattering of the data points can be reduced and a better between-bed separation can be obtained in the chemical discrimination diagrams. Another important feature of the graphs in Figure 38 is the lower values of the trace element contents of clay fractions with respect to those of the bulk samples. Figure suggests that Ga, Y and Rb contents of the clay fractions can be used in geochronological and correlation studies of K-bentonites.

Chemical Differentiation of Individual K-Bentonite Horizons

As pointed out earlier (p. 42) most of the bulk samples are collected from different K-bentonite horizons with well-established stratigraphic positions which can be correlated in the field. These serve as control samples whereas the rest of the samples are obtained from the horizons with doubtful stratigraphic settings. It is anticipated that once the geochemical identification of the known horizons is well-established, the stratigraphic relationships of doubtful horizons with them can be studied by chemical means.

Almost all of the bulk samples analyzed in this study have an acid-to-intermediate composition, and as shown in the Petrography section (p.88). The original ashes forming the younger horizons have a slightly more acidic character than the old ones. Can small differences in the chemical attributes of the bulk samples or clay fractions permit a subdivision into distinctive groups

which in turn represent individual K-bentonite horizons? And, if so, what are these chemical attributes? In this section the answers to these questions will be examined. To determine the reliability of these groups and the elements or elemental ratios that would be useful for their discrimination purposes, several multivariate analysis techniques are used as a tool for data interpretation. A short description of these techniques is presented here.

Data Processing

The results of the chemical analyses as listed in Tables I and II (App. F) were processed by an IBM System 370 computer, using a statistical program called BMDP (Biomedical Computer Program, P-Series). Chemical data were subjected to Q- and R-mode cluster analyses. Q-mode analysis was used to group bulk samples and their less than 2 μ m clay fractions. R-mode analysis was performed on the chemical data to identify as closely as possible statistically independent elements for binary and ternary plots. Cluster analysis is a non-parametric technique for the classification of large quantities of multivariate data, and as such, is easily applied in geochemical studies. Its use and application in geology are discussed by Miller and Kahn (1962), Parks (1966), Harbaugh and Merriam (1968), Bell (1976) and Smith and Nash (1976).

Q-mode cluster analysis seek natural groupings among the sixty one K-bentonite bulk samples and twenty six clay fractions using a

set of twelve (Al_2O_3, Fe_2O_3T, K_2O, TiO_2, Rb, Sr, Y, Zr, Zn, Nb, Ga and Ge) and eight (Al_2O_3, Fe_2O_3T, K_2O, TiO_2, Rb, Zr, Y and Ga) variables, respectively. The results of this sorting method for the bulk samples is illustrated in Figure 39, in the form of a dendogram. This arrangement shows similarity of association of clusters joined on a similarity coefficient scale ranging from 0.539 to 7.242, with those closest to 0.539 being most similar. The Figure also demonstrates that the majority of K-bentonite samples can be placed in one of three groups (groups 1-3) which are chemically distinct. These three chemical groups correspond to the three different K-bentonite horizons under the investigation, as will be discussed in future sections. Group 4 indicates the natural grouping of carbonate-rich samples collected from some outcrops and cores. These samples have CaO contents ranging from 15.00 to 62.30 percents, considerably above all other samples. The outcrop samples show the effects of extensive leaching on K-bentonite horizons. The core samples, on the other hand, are those with thin partings of limestone indicating slower settling of ash or some sea floor reworking permitting accumulation of interbedded calcareous ooze. Such samples are found to be less useful for geochronologic and correlation studies. According to the dendogram the two K-bentonite bulk samples from Marshal Co., Alabama (35 and 34A), bear no chemical similarity to any other groups. In the case of the clay fractions, only those belonging to the groups 1, 2 and 3 of bulk

FIGURE 39. Dendogram resulting from Q-mode cluster analysis of chemical data from K-bentonite bulk samples. Groups 1 through 4 are natural grouping of the samples. The first three, from youngest to oldest, correspond to the three different K-bentonite horizons under the investigation. Group 4 is composed of carbonate rich samples.

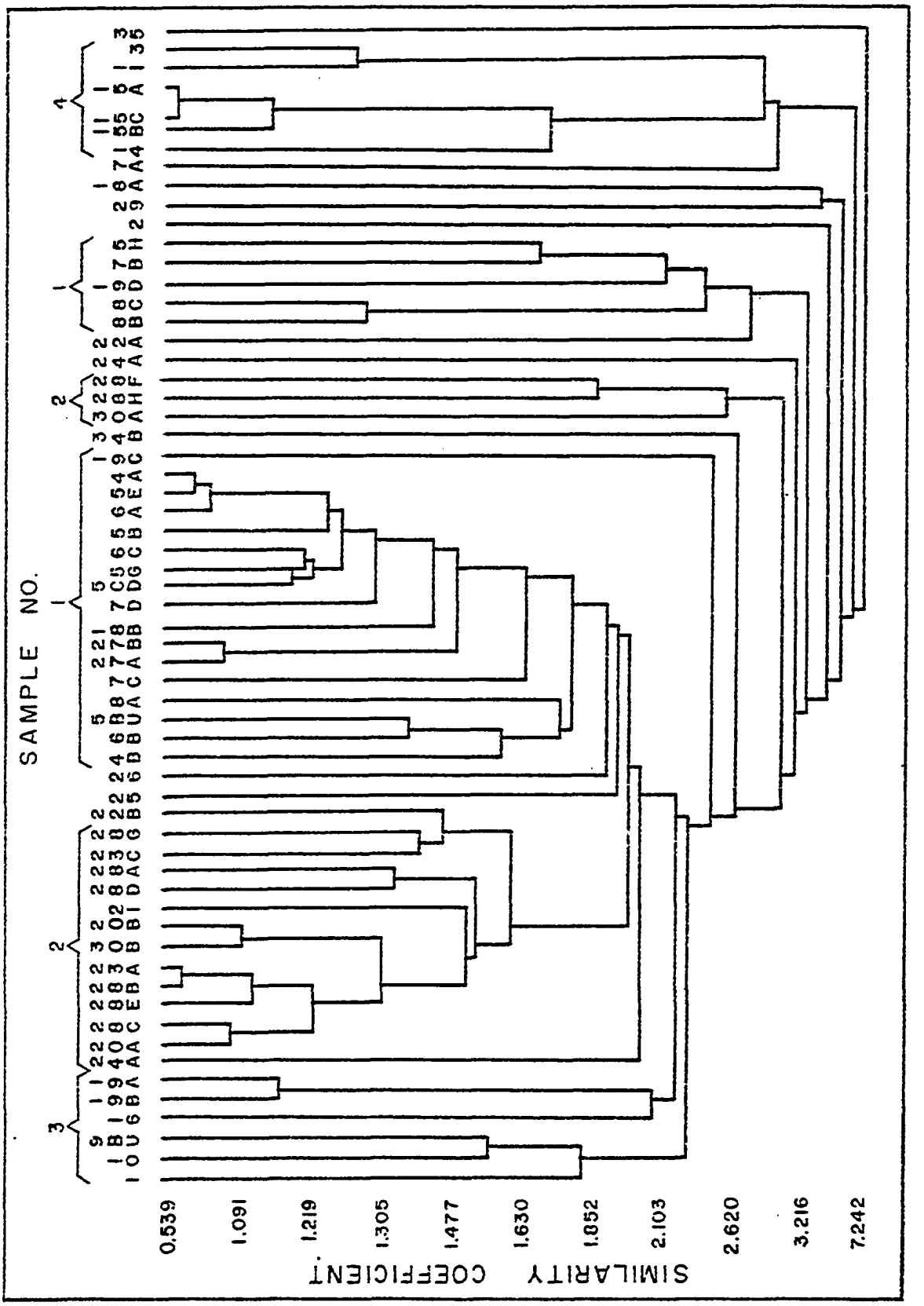

samples have been analyzed by Q-mode clustering technique, and these groups are poorly distinguished from each other.

R-mode cluster analysis is superior to an arbitrary selection of the elements which might be used in binary and ternary plots to discriminate between natural groupings of samples. Figure 40 shows the relationships among twelve bulk sample elements expressed as Al_2O_3, Fe_2O_3T, K_2O, TiO_2, Rb, Sr, Y, Zr, Zn, Nb, Ga and Ge. The linkage tree is printed over the correlation matrix in which the absolute values of the linear correlation coefficients times 100 are used.. As shown in the Figure, certain element pairs such as Al and Fe; Fe and Ti; Fe and Ge are weakly correlated as indicated by small correlation coefficients of 37, 27 and 3, respectively, and thus are found to be useful as characteristic parameters which can discriminate between different K-bentonite horizons. Application of R-mode cluster analysis to the clay fraction data indicates high values for correlation coefficients of Y, Rb and Ga, and investigations show that none of the elements studied can discriminate between the clay fractions of different K-bentonite horizons.

To summarize, cluster analyses are found to be very useful in developing a statistical method for comparing the chemical compositions of K-bentonite bulk samples from different stratigraphic settings and from various sampling locations. They also provide a basis for correlating the compositions of samples with uncertain stratigraphic positions to those of known positions. To determine

FIGURE 40. Linkage tree resulting from R-mode cluster analysis of chemical data from K-bentonite bulk samples.

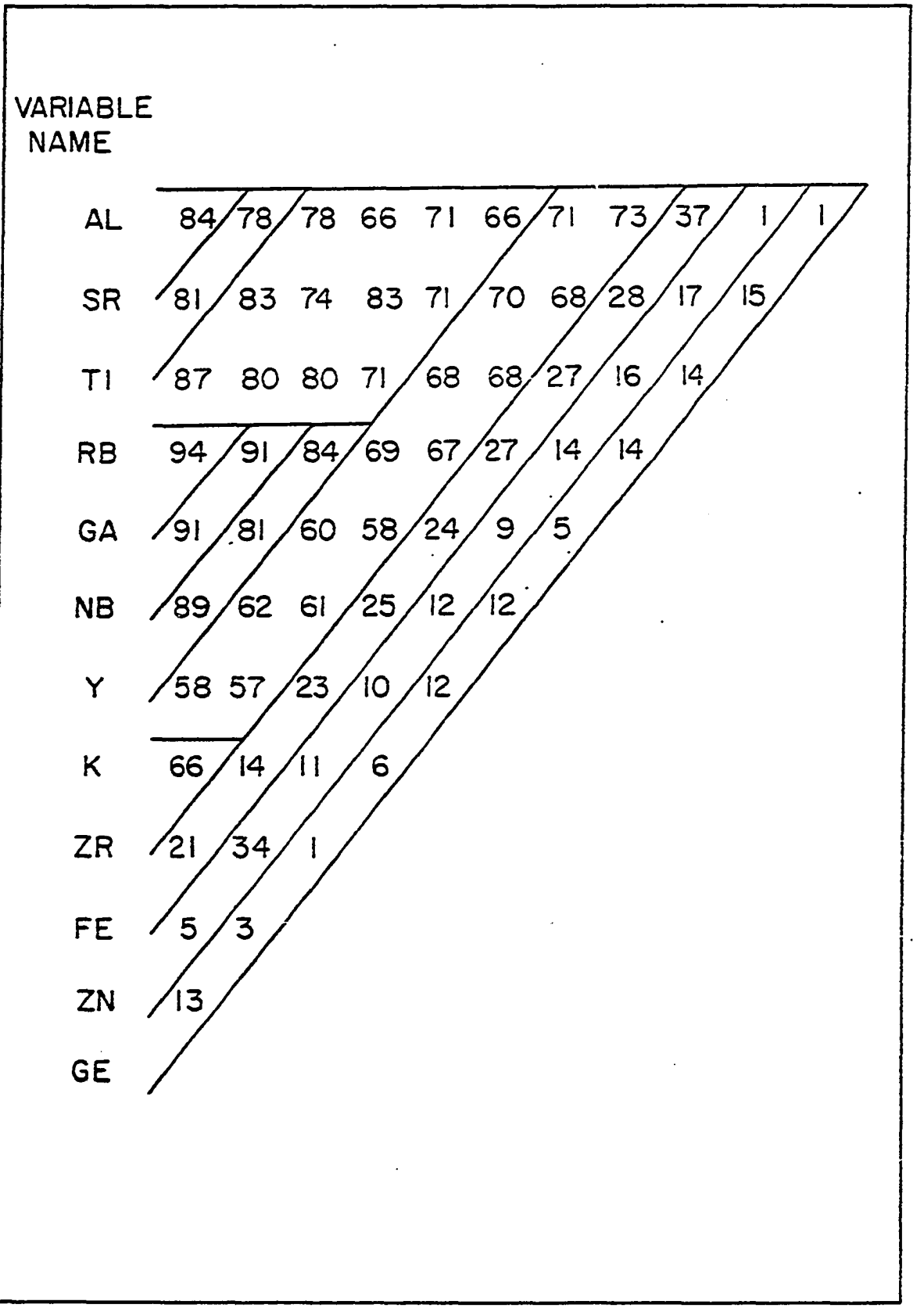

and chose among the elements or elemental ratios which might discriminate between the individual K-bentonite horizons, cluster analyses prove to be valuable tools both in selecting the most potential discriminators and also in reducing greatly the amount of time which otherwise might be spent for this purpose.

Binary Discrimination Diagrams

Compositional differences between the K-bentonite bulk samples are summarized in Figures 41 through 44 in the form of binary discrimination diagrams. Five elements, Fe, Ti, Al, Zr and Ge are sufficient to separate the samples into three chemically different groups (groups 1-3). In addition, the diagrams demonstrate the degree of discriminating power of the elements relative to each other.

Fe_2O_3T - Al_2O_3 Plot:

Figure 41 shows that the relative content of Al_2O_3 and Fe_2O_3T serves to distinguish group 1 samples distinctly, but the other two groups (2-3) are not separated from each other as well. Variability of Al_2O_3 contents between groups is not sufficient to yield a better clustering. Thus, Al_2O_3 is identified as poor discriminator between the K-bentonite horizons at discrete stratigraphic levels.

The data points on the left side of the diagram correspond to the carbonate rich samples. They form a different cluster on the low Al_2O_3 values side of the discrimination diagram.

The two Alabama samples plot outside the field of Figure because of their appreciably higher Fe_2O_3T contents.

FIGURE 41. Fe_2O_3T - Al_2O_3 plot showing the chemical grouping of K-bentonite bulk samples. Symbols are as follows: ● , Group 1; O, Group 2; ⌀ , Group 3; ◐ , Group 4 (carbonate rich samples).

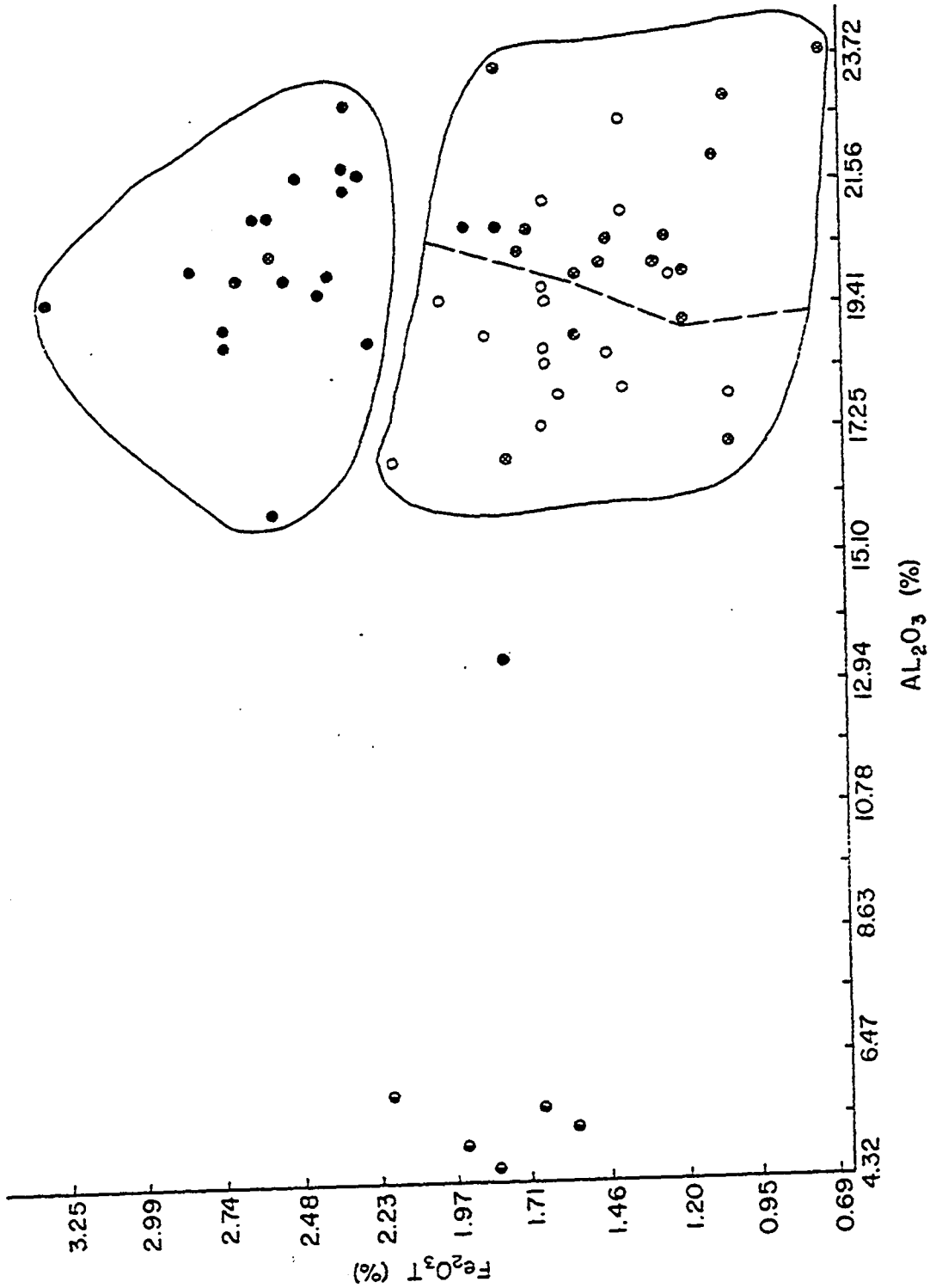

Fe_2O_3T - TiO_2 Plot:

A better discrimination of bulk samples is achieved by plotting TiO_2 against Fe_2O_3T (Fig. 42). More significant variation between the TiO_2 contents of samples belonging to the groups 2 and 3 causes a better separation between them. In this diagram carbonate rich group 4 samples plot in the fields of other groups. However, their erratic distribution in other diagrams prevents any correlation between these samples and any other of the chemical groups.

For the same reasons as given in the Fe_2O_3T - Al_2O_3 plot, Alabama samples are not shown on Figure 42.

Ge - Fe_2O_3T Plot:

Ge and Fe_2O_3T contents of bulk samples are likewise good discriminators (Fig. 43). The within group variability can also be observed from this Figure. The two Alabama samples are shown in the diagram indicating their very high Fe_2O_3T values relative to those of the rest of the samples. Carbonate rich samples are not shown, because of their very low Ge contents which are under the detection limit of the method used.

Ge - Zr Plot:

A plot of Ge against Zr is found to discriminate group 2 from groups 1 and 3 which are superimposed as shown in Figure 44. One of the Alabama samples (34A) which has higher Ge content than the other one (35), falls among the group 2 samples. Carbonate rich outcrop and core samples are not shown on the diagram because of the reason described during the explanation of the previous diagram.

FIGURE 42. $Fe_2O_3T - TiO_2$ plot showing the chemical grouping of K-bentonite bulk samples. Symbols as in Figure 41.

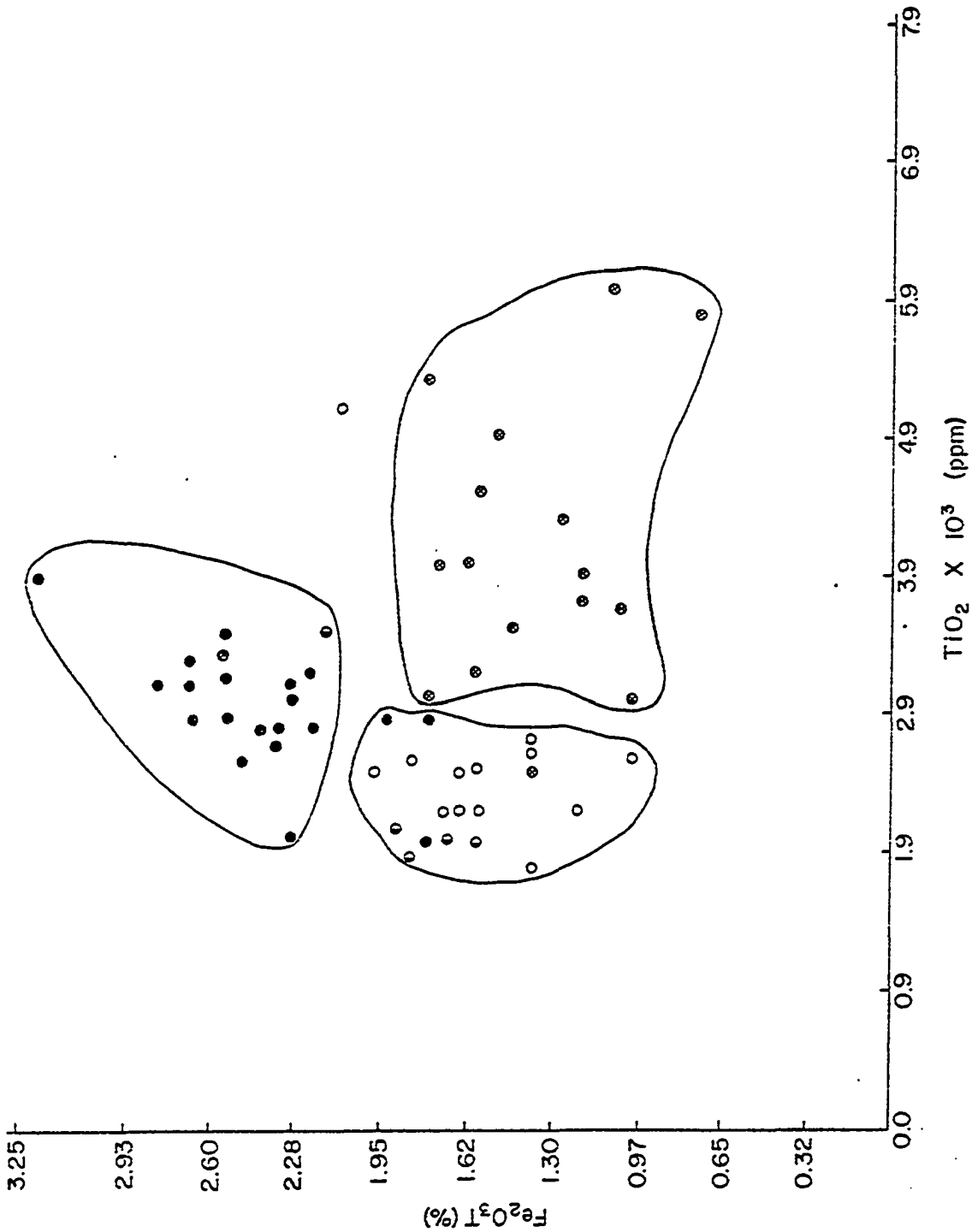

FIGURE 43. Ge - Fe_2O_3T plot illustrating the chemical grouping of K-bentonite bulk samples. Symbols as in Figure 41 and triangles indicate Alabama samples.

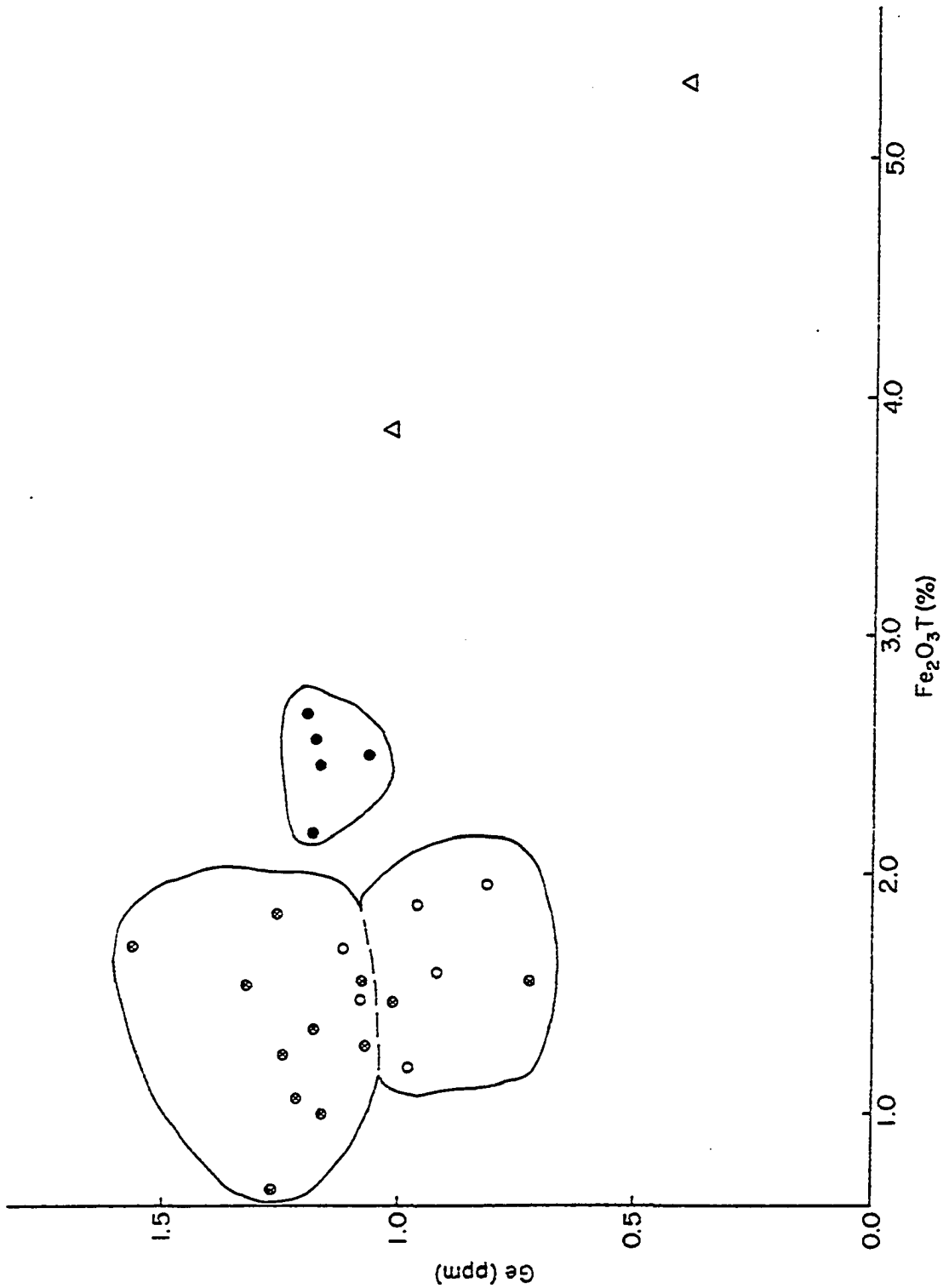

FIGURE 44. Plot of Ge against Zr showing the chemical grouping of K-bentonite bulk samples. Symbols as in Figure 43.

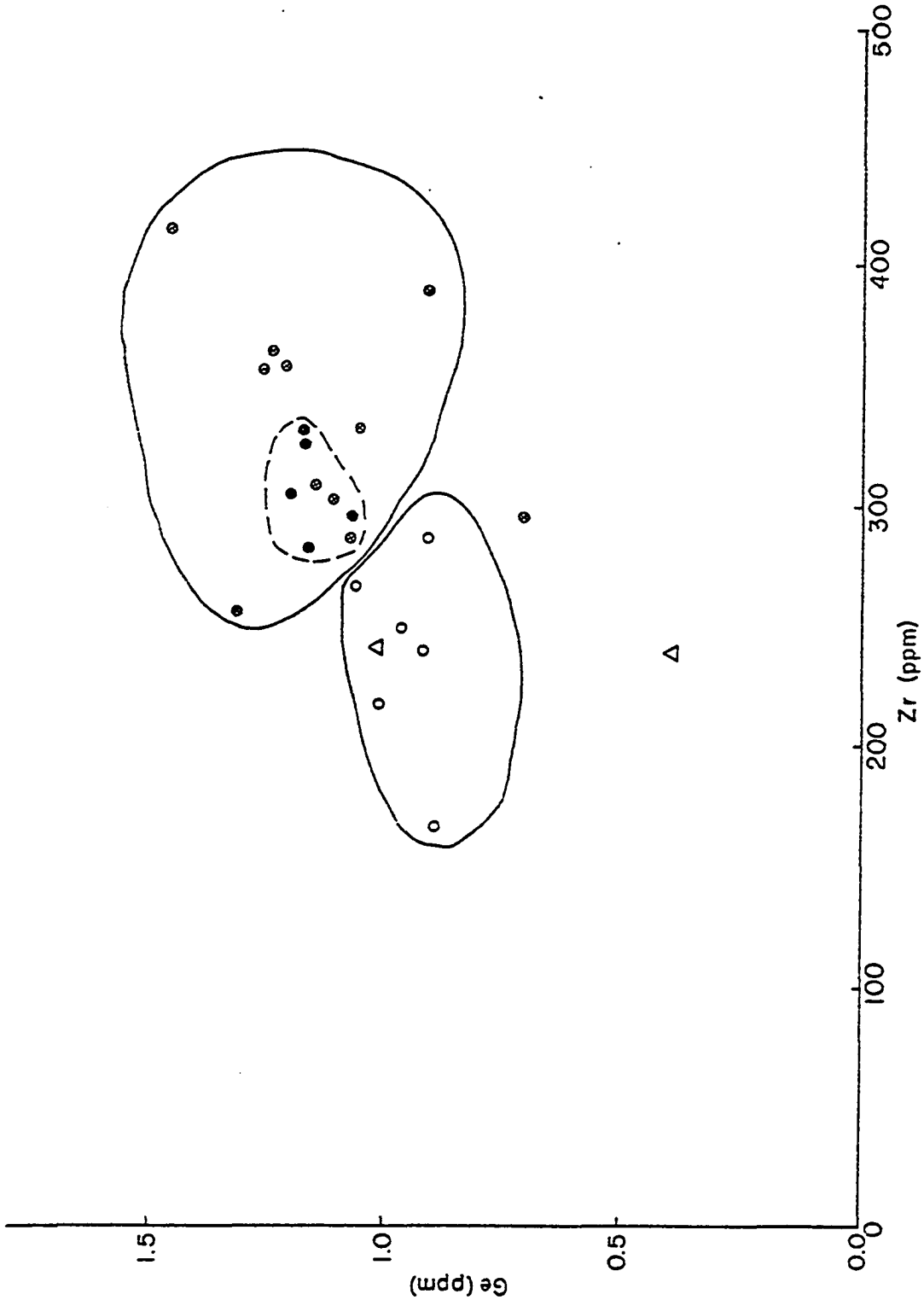

Binary discrimination diagrams reveal certain chemical features of the groups of samples. Group 3 occupies an area characterized by low Fe_2O_3T and high TiO_2, Ge and Zr values. Group 2, although having a similar Fe_2O_3T content to group 3, is distinguished from the latter by low TiO_2, Ge and Zr contents. Group 1 is discriminated from groups 2 and 3 by its much higher Fe_2O_3T value. This group has low TiO_2 content and is similar to group 2 in that respect. However, its composition is more similar to that of group 3 when its high Ge and Zr values are considered. All of the three groups have similar Al_2O_3 contents, in general, although group 2 is somewhat distinguished from group 3 by lower Al_2O_3 values.

The Alabama samples again have very different compositions than the three major groups of samples. They are characterized by higher Fe_2O_3T and TiO_2, and lower Ge and Zr contents.

Ternary Discrimination Diagrams

The major and trace element separation of K-bentonite bulk samples into chemical groups can also be investigated by means of ternary discrimination diagrams. The following diagrams yield similar clustering of samples to those described by the binary diagrams.

Fe - Zr - Ti Plot:

Ternary Fe-Zr-Ti plot (Fig. 45) classifies the bulk samples as previously designated groups. Most of the variation between the groups can be attributed to the variation of Zr and Fe, although

Ti shows an increase in group 3.

Fe - Zr - Ge Plot:

Compositional differences are shown in Figure 46 where relative abundances of Fe, Zr and Ge serve to distinguish between the three chemical groups. Group 3 has lowest Fe_2O_3T content when compared to the others, especially to group 1. Group 2 samples exhibit an intermediate chemical composition as also observed from the previous plot.

Ternary discrimination diagrams help to identify chemically different groups among K-bentonite bulk samples. Although in the diagrams presented, some data plot very close to the boundary lines between the groups, it is observed from Figures 45 and 46, and also from the other ternary plots studied, similar to these, the chemical variation of the samples belonging to each group is limited and the groups tend to form a chemical trend as exemplified by Figure 45, from iron-rich group 1 to zirconium-rich group 3.

It has been mentioned that each of the three chemical groups represents three different K-bentonite horizons. The next section will examine the stratigraphy of the control K-bentonite horizons and explore the extent to which it can be extended based on their chemical compositions. Correlation of the K-bentonites from poorly known stratigraphic settings will also be discussed.

FIGURE 45. Ternary plot of Fe-Zr-Ti showing the chemical groups of K-bentonite bulk samples. Symbols as in Figure 41.

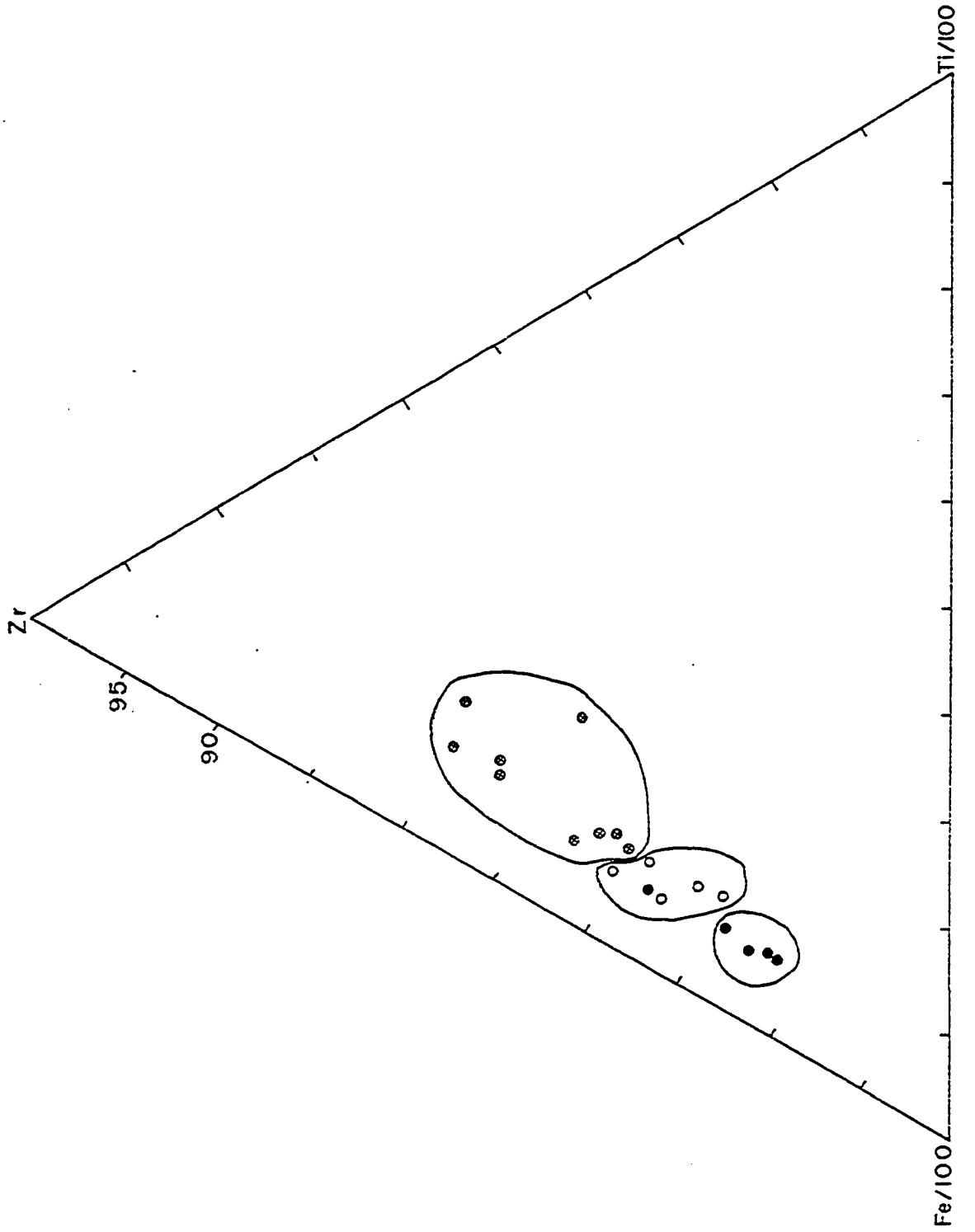

FIGURE 46. Fe-Zr-Ge plot showing the chemical groups of K-bentonite bulk samples. Symbols as in Figure 41.

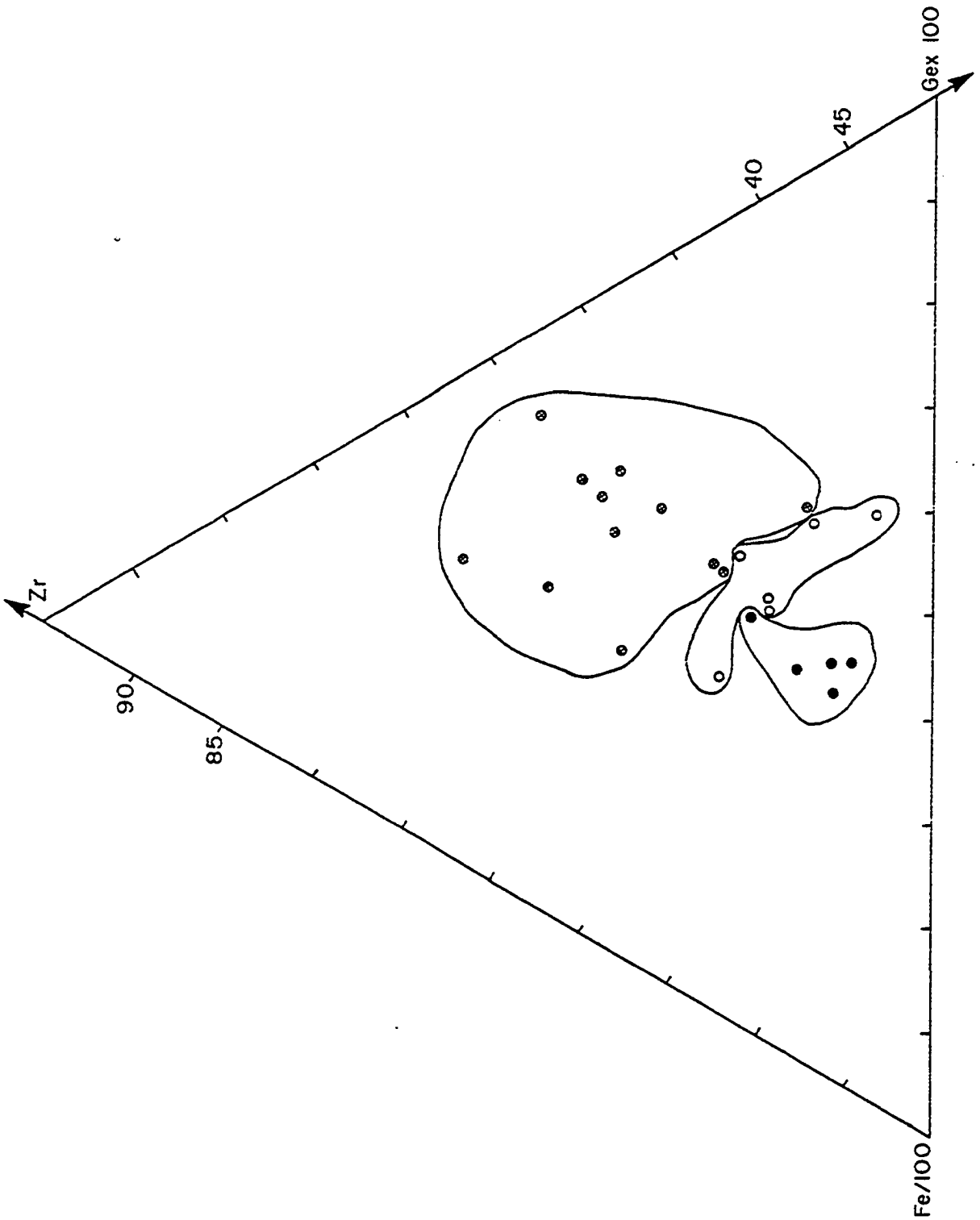

Correlation of K-Bentonite Beds

Probable correlations between various columnar sections of the Tyrone Limestone (Upper Carters of Wilson, 1949), oriented generally along north-south line between Smith County, Tennessee, and Lawrence County, Indiana, are shown in Figure 47. The section including the Alabama K-bentonites is not represented in the Figure because they do not bear any chemical relationship to the other K-Bentonite horizons studied, and their exact stratigraphic settings are not known. The distribution of the section localities within the study area is shown in the inset map. This correlation is based on unique chemical characteristics of K-bentonite samples as discussed previously in this chapter and supported by field evidence. K-bentonite horizons are marked as dark bands when their stratigraphic positions are known based on field evidence. Cross-hatching, on the other hand, indicates that precise information concerning the stratigraphic setting of these particular layers is lacking. Sample numbers are also written on the layers and more detailed information is available in Appendix A. The second column to the left is the generalized stratigraphic section for Chickamauga Dam and vicinity as reproduced from the 1944 paper of Fox and Grant. Dark beds referred to as B-2 to B-10 correspond to K-bentonite horizons among which B-8, B-6 and B-3 are the most widespread (Wilson, 1949) and the thickest ones as indicated (Fox and Grant, 1944; Wilson, 1949). These last three are the object of the present study.

FIGURE 47. Correlation diagram of K-bentonite horizons in the columnar sections of Tyrone Limestone between Smith County, Tennessee and Lawrence County, Indiana.

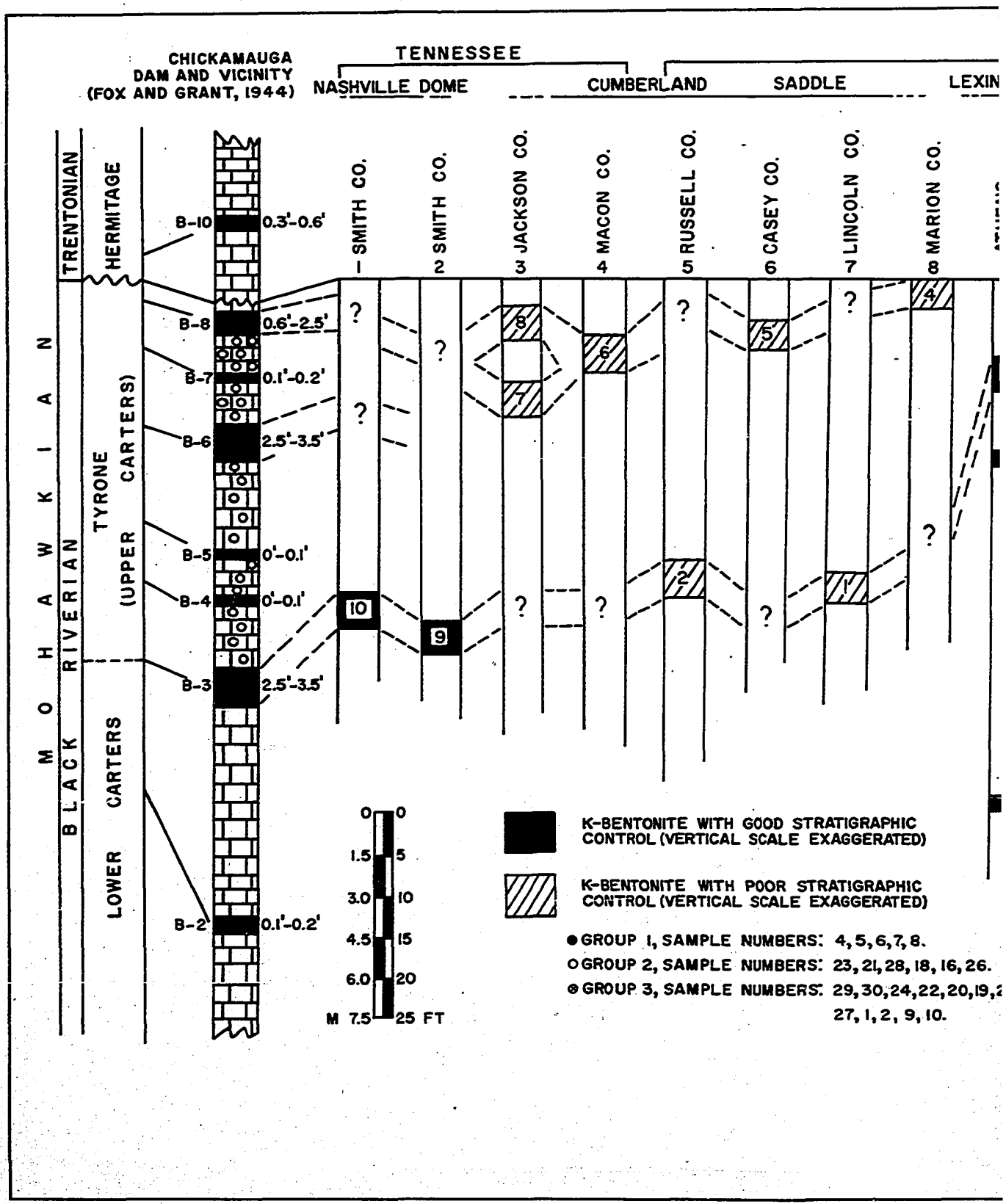

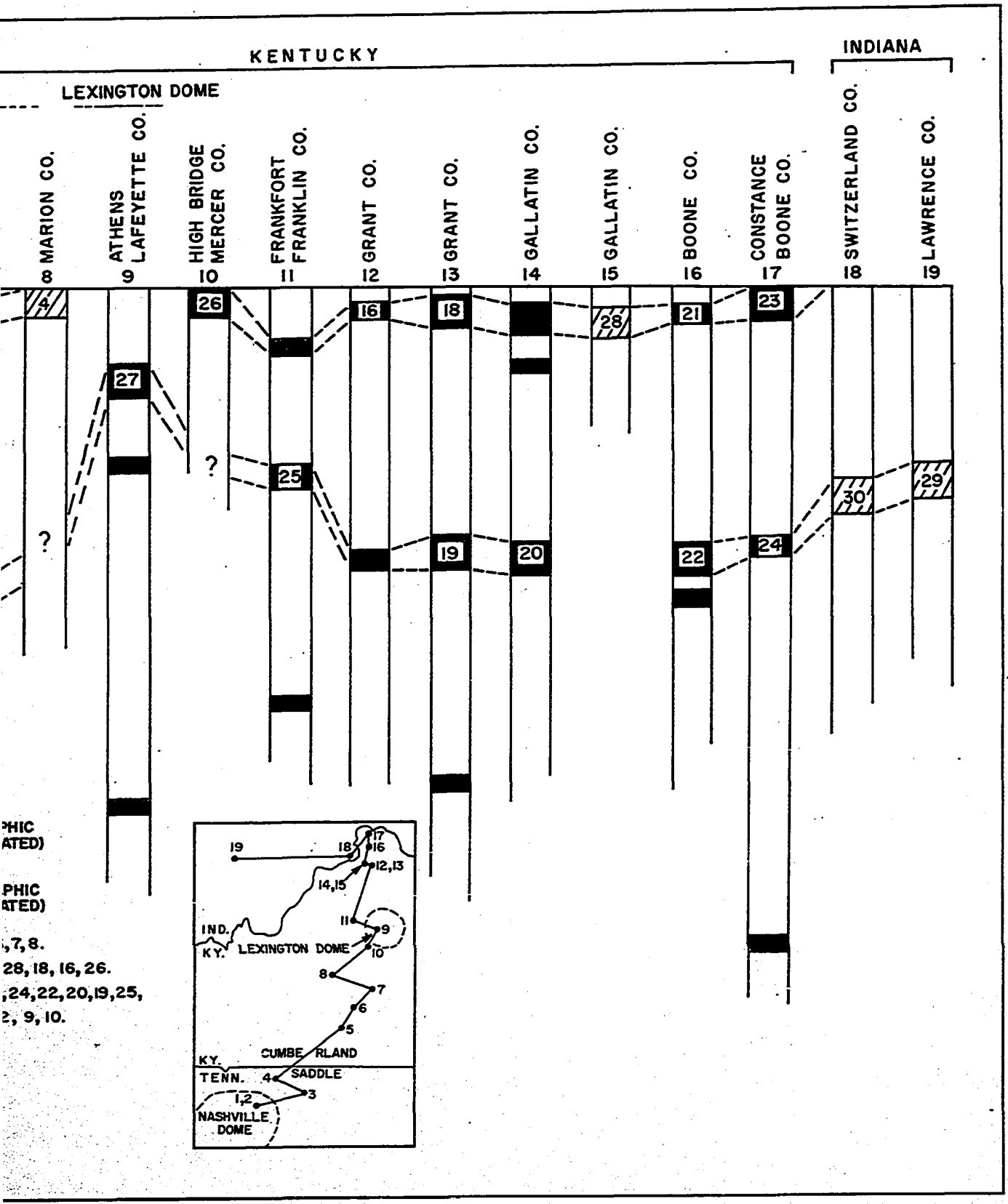

PHIC
ATED)

PHIC
ATED)

,7,8.
28,18,16,26.
,24,22,20,19,25,
2, 9, 10.

B-3 is Wilson's (1949) T-3 bed which separates Upper and Lower Carters Limestones in Tennessee. It is also known as the "pencil cave" of local usage in Kentucky. B-3 is underlain by a black, fossiliferous chert layer and characterized by almost complete absence of biotite. This K-bentonite horizon, as also shown in the Figure, is the most consistent and widespread among the three K-bentonite horizons under investigation. In Tennessee, the fresh exposures best occur east of Rome bridge over Round Lick Creek (Fig. 47), and in a section at South Carthage in a railroad cut (Wilson, 1941, Fig. 14, p. 74). In Kentucky and Indiana B-3 mostly occurs in the subsurface, although it is exposed in the Lambert Bros. Quarry, in Athens and at a subsurface quarry in Frankfort (Huff, 1963a).

B-6 is the "mud cave" of local usage in Kentucky, and is called T-4 by Wilson (1949). The interval between B-6 and B-3 is fairly constant in the study area averaging 25 feet (7.5 m) as reported by Cressman (1973). This K-bentonite horizon is easily distinguished from B-3 because it contains abundant biotite crystals forming biotite rich layers within the bed. B-6 is locally absent within the study area (Fig. 47). In Smith County, Rome, Tennessee (Sections 1 and 2 in Fig. 47) this bed is not exposed although farther east of Rome, at Carthage, Smith County, Wilson (1949) reported it to be present. According to the same investigator, B-6 is absent over the central and western parts of the central Basin in Tennessee

which occupy the Rutherford, Wilson, Davidson and Williamson Counties located on the Nashville dome as described in the second chapter of this study. It seems that in these areas B-6 is absent as a result of post-Carters erosion which eroded successively older beds of the Upper Carters Limestone. Again, as found by Wilson (1949, p. 63), eastward from the Nashville dome along the Sequatchie Valley in Bledsoe, Sequatchie and Marion Counties, Tennessee, B-6 occurs in the Upper Carters Limestone overlain by varying thicknesses (3-6 feet) of this cover rock. In central Kentucky (Fig. 47), B-6 occurs either at the top of the Tyrone Limestone, as it does near High Bridge, Mercer County (Section 10 in Fig. 47), or at a thin interval below the top of that Limestone. Close to the center of the Lexington dome, like section 9 (Fig. 47) at Athens, Lafeyette County, B-6 is missing due to the Hermitage-Tyrone disconformity. Cressman (1973) indicated that in the area east of Winchester and north of Lexington in Clark and Lafeyette Counties, respectively, about 10 feet (3 m) of uppermost Tyrone is removed, and B-6 is distributed towards south and west as shown in Figure 6 (p. 33). These observations and the discussions above suggest that B-6, although missing from the areas located towards the center of the Lexington dome, reappears away from the structurally higher geologic environments. In Indiana, detailed stratigraphic information is lacking in relation to the K-bentonite horizons studied during this investigation. However, an oral communication with J.B. Droste

(1978) of Indiana University, supports the conclusions based on the chemical classification of K-bentonites that they are the extensions of B-3 from Kentucky to southeastern Indiana.

B-8, as described by Fox and Grant (1944) is the uppermost K-bentonite horizon occurring in Tyrone Limestone section at Chickamauga Dam and vicinity. It is 10½ feet (3.15 m) above B-6 and similar in lithologic characteristics to B-6 and B-3 at this location. It appears to be absent throughout most of the study area (Fig. 47), and its distinction from the other two K-bentonite horizons studied is made by chemical means and field evidences as will follow. The B-8 horizon in Figure 47 covers a distance between section 9 at Athens, Lafeyette County and sections 1 and 2, at Smith County. Borella and Osborne (1978) described this area as the Cumberland Saddle which is a structural depression lying between the Lexington dome to the north and the Nashville dome to the south. Here, it is concluded that a volcanic ash which is now B-8 blanketed this structurally low area being protected from erosion and locally escaped the effects of the Hermitage-Tyrone erosion.

In conclusion, the correlation of the three K-bentonite horizons based on their chemical attributes has been demonstrated and the findings are in accordance with the available stratigraphic information. From oldest to youngest, B-3 is defined as chemical group 3. It is the most widespread K-bentonite horizon within the study area.

B-6, corresponds to chemical group 2, and is absent locally close to the centers of Nashville and Lexington domes and at southeastern Indiana. Finally, B-8, the uppermost K-bentonite horizon of the Tyrone Limestone in Figure 47, is only observed within the area occupied by the Cumberland Saddle, but otherwise is absent throughout most of the area investigated.

DISCUSSION

Discussion of the Methods

Mineralogic, petrographic and chemical investigation of K-bentonites were carried out by means of optical, x-ray powder diffraction, x-ray fluorescence and atomic absorbtion methods. Information was obtained on different practical and theoretical aspects of mineral assemblage, petrography and petrogenesis by the application of these various techniques.

Optical microscopy proved to be very useful for the study of non-clay minerals. Ordinarily, thin-section data of clayey rocks is, at best, merely supplementary to chemical analyses. However, in this study, a considerable amount of mineralogical and textural information was produced by them. In particular, the absence of terrigeneous material, the composition and fragmentation of minerals, and some surprisingly clear primary textural features all combine to reveal both original and secondary features of the ash.

X-ray powder diffraction is used to study the clay fractions of bulk samples. The method served both for the qualitative estimation of the clay minerals and for the determination of the ratio between expandable and nonexpandable layers of the interstratified clay structure. The diffraction patterns also provided additional information on the distribution of clay and non-clay minerals in the bulk samples. Absence of peaks belonging to non-clay minerals indicates the efficiency of procedure used for the separation

purpose, at least to the degree of the detection limit of the diffractometer used.

Chemical analyses are made using x-ray fluorescence and atomic absorption techniques. The precision, accuracy and within sample homogeneity which are presented in Appendices D and G for x-ray fluorescence and atomic absorbtion analysis, respectively, seem to be quite acceptable for all the elements except manganese. Very low concentration of this element in the samples causes difficulties in detecting its exact amount as reflected by a low precision value. For this reason manganese is not included in the discussions. The results of chemical analyses are integrated to draw conclusions about the origin of clay mineral suite, the original composition of volcanic ash, the effects of post-depositional alteration and the petrogenesis of K-bentonites in general. The geochronologic investigation and long-distance correlation of K-bentonite horizons are also based on the results of chemical analyses.

Among the statistical techniques, Q- and R-mode analyses are performed for data processing. The results obtained are very helpful in determining the natural grouping of K-bentonite bulk samples and in the identification of elements used to distinguish between different K-bentonite horizons.

Discussion of the Results

Origin of K-bentonites:

The data collected during this study in general support earlier

conclusions (Ross, 1928; Allen, 1929; Lounsbury and Melhorn, 1964; Mossler and Hayes, 1966) that K-bentonites are altered products of volcanic ash. These rocks consist mainly of biotite (Fig. 10), alkali-feldspars (Fig. 13), apatite (Fig. 15) and zircon (Fig. 16) crystals in varying proportions of a matrix composed of altered volcanic glass and very fine grained quartzofeldsphatic material (Figs. 18, 28, 30, 31, 33). The mineral association and relict textural features such as the crystal morphology (Fig. 32) and devitrified volcanic glass (Fig. 18, 19, 29) are clear evidences of a volcanic origin. The recognition of completely devitrified glass shards leads to the conclusion that interstratified illite-smectite clay originates as an alteration product of volcanic ash under marine conditions. Bonatti (1965) discusses the hydration and crystallization of volcanic glass in subaqueous conditions and mentions the formation of smectite group structures from glasses of intermediate and basic composition, provided that proper cations, particularly Mg^{+2} are present in the system. The latter, is not likely to be a limiting factor for devitrification on the ocean floor because the concentration and ionic activity of magnesium in sea water is high (Berner, 1971). Bonatti concludes that the rate of alteration of volcanic glass is conditioned by its hydration state and even at low temperatures (20°C) a volcanic glass with originally high water content can devitrify at much faster rates than an anhydrous glass. These observations fit suitably to the

interpretations of chemical compositions and structural formulae calculations during this study as summarized in Table 2 and in Figures 25, 26 and 27. The devitrification of volcanic glass and the consequent formation of smectite is indicated by magnesium content of the clay fraction and also by the high magnesium occupancy in the octahedral sheet. The octahedral charge resulting from the replacement of aluminum by magnesium is compensated for by the adsorption and fixation of interlayer cations, mainly potassium. This mechanism causes an increasing ratio of non-expandable to expandable layers in the interstratified clay and can explain their origin in K-bentonites in the course of time. This view is also supported by Weaver and Pollard (1973) who recognized the higher magnesium content of marine illites in comparison to those originating in other geologic environments (Table 5). Therefore it appears that smectite can form on the ocean floor in a relatively short span of time from volcanic glass in the original ash as suggested by Bonatti (1965). However, the formation of illite from smectite under the same conditions is questioned by Eberl and Hower (1976) who conclude that the reaction rate is too slow even though it is thermodynamically reasonable. A better understanding of this problem in explaining the origin of K-bentonites needs further research. Here, it is satisfactory to conclude that reaction (4),

$$Al^{+3} + K^{+} + \text{Smectite} \longrightarrow \text{Illite/Smectite} + SiO_2$$

(Eberl and Hower, 1976) explains the last step in the conversion of

volcanic glass to the interstratified clays found in the K-bentonites.

Structure and Composition of Interstratified Clays:

On the basis of x-ray diffraction studies it is concluded that the clay minerals are dioctahedral, regularly interstratified, allevardite-type (IM) with an illite to smectite ratio about 3:1 to 4:1. These data agree with the findings of Weaver (1953a, 1956), Huff (1963a) and Reynolds and Hower (1970). Chlorite occasionally is found as discrete packets, which were also detected by Weaver (1953a) and Coker (1962), instead of forming a separate interstratified illite-montmorillonite-chlorite phase (Coker, 1962).

The data obtained during this study reveal a reasonably homogeneous structure and composition as a distinctive feature of the clays. The x-ray diffraction patterns differ only slightly (Table 1, Figs. 22, 23) and the histograms showing the distribution of cations in various structural positions (Table 2, Figs. 25, 26, 27) lead to the conclusion that clays from a wide sample population can be defined by a definite and narrow composition range. The latter feature is exhibited further in Figures 37 and 38 as K_2O, MgO, Ga and Rb curves show a limited within-bed and between-bed variability in the clay fraction. These characteristics of the clays have been previously observed by Huff (1963a) who, based on cation exchange data, suggested a fairly stable structure and a narrow compositional range between those of end-member montmorillonite and illite.

The discussions above imply a relationship among the K-bentonites and physiochemical conditions existing within their geologic environment. It appears that an equilibrium condition has been achieved, at least between the clays and this environment. Furthermore, this equilibrium must have been achieved as a result of post-depositional alteration of the original ashes, because as shown in Figures 34, 35 and 36, different K-bentonite horizons had different compositions varying between acidic-to-intermediate, prior to their alteration. In other words, according to this study the possibility does not exist that all of the K-bentonite horizons had the same composition at the beginning, but as a result of post-depositional alteration processes their clay mineral composition and structure approached an equilibrium condition with their environment. However, small between-bed chemical differences provide a basis for distinguishing the different horizons and for their long-distance correlation when K-bentonite bulk samples are used for these purposes (Figs. 41 through 46).

Interpretation of the clay mineral structure and composition points out once again the importance of petrology of K-bentonites in studying their geologic environments as previously suggested by Weaver (1956) and Huff (1963a). The clays suggest an environment with a magnesium ion activity analogous to that of modern sea water. This appears to be valid according to a study by Cressman and Noger (1976) dealing with the carbonate environments in the High

Bridge Group of central Kentucky. They found that many features of the carbonate rocks including the Tyrone Limestone are similar to those of modern tidal-flat carbonates both of the Bahamas and Florida Bay. Thus, during Tyrone time, central Kentucky consisted of a complex of tidal-flats and intervening shallow marine lagoons to which normal marine waters had easy access. However, a very high potassium content of the clays and also the bulk samples is more difficult to explain. Even if Ordovician seas had high K^+ ion activity the transformation of smectite to illite/smectite clay (reaction 4) is too slow to take place on the ocean floor (Eberl and Hower, 1976). Similar studies to that of Velde (1977) proposing a phase diagram of clay minerals to determine relative grades of diagenesis are also required for K-bentonites so that such problems can be solved.

Composition of Original Ash and K-bentonite Bulk Sample:

Chemical separation of K-bentonite bulk samples using their immobile element concentrations leads to the conclusion that the majority of them are the alteration products of volcanic ashes with acid-to-intermediate composition (Figs. 34, 35, 36). As illustrated in the Figures, samples generally occupy trachyandesite fields although there are some others falling in the fields of more basic or acidic rocks. This distribution represents a mildly-alkaline and calc-alkaline suite for magmatic eruptions which also seem to be

characterized by a wider range of differentiation index (Zr/TiO_2) than an alkalinity index (Nb/Y). These findings furthermore, agree with the results of the optical studies indicating an acid-to-intermediate composition of original ash based on the non-clay mineral association of K-bentonite samples. Earlier studies by Weaver (1953a) and Smith, et al. (1971) also conclude that their K-bentonite samples compare with igneous rocks such as trachyte, latite, phonolite, trachyandesite and andesite.

Earlier studies have been concerned with the location of Middle Ordovician eruptive centers in the eastern United States, and predicted that K-bentonites originated from numerous local volcanoes located along Appalachia covering an area extending from Virginia to South Carolina (Whitecomb, 1932, 1934; Fox and Grant, 1944). Indeed, it is now well-established that the Carolina slate belt, which extends about 400 miles (645 km) from south central Virginia to central Georgia (Tectonic map of the United States, 1962) is a major metavolcanic tectonic province of the southern Appalachians (King, 1950, 1955; Hatcher, 1972). Detailed mapping of the area marks extensive volcanism which built the slate belt island arc system during early Paleozoic time (Whitney, et al., 1978) and most of the volcanism is reported to be probably submarine or subaerial from low volcanic islands during the early stages of island arc development. Much of the volcanic material appears to have been deposited within a marine environment as also indicated by

rocks in the Carolina slate belt. They are composed of both volcanic and sedimentary rocks including argillite, slate, phyllite, sandstone, conglomerate, greenstone and tuff (Butler, 1964).

During this study some stratigraphic, petrologic and chemical data have been obtained from the literature concerning the low-grade metavolcanic and intrusive rocks of the Carolina slate belt. The purpose is to establish a basis of comparison between the original composition of the K-bentonites under the investigation and the character of island arc volcanism occurring during the early Paleozoic and specifically during the Middle Ordovician. Whitney, et al. (1978) investigated the Little River Series of Cambrian age along the South Carolina-Georgia border which has a probable aggregate thickness in excess of 14,000 feet (4500 m). Their study area appears to be one of the principle centers of felsic volcanism as represented by the Lincolnton metadacite, and felsic pyroclastic rocks such as dacitic and quartz crystal tuffs. This petrogenetic suite is reported to be similar to that found in primitive island arc tholeiitic associations throughout the world. McCauley (1961) conducted a series of rock analyses from the northerly portion of the Carolina slate belt. He found that the average original bulk composition of the slate belt was andesitic. Further north, in North Carolina Conley and Bain (1965) studied the geology of the metavolcanic and metasedimentary rocks of the slate belt. The oldest rocks comprising the 20,000 feet (6000 m) thick Uwharrie

Formation are composed of subaerially deposited felsic pyroclastics with occasional interbedded felsic flows and mafic pyroclastics. Whitney, et al. (1978) recognized the lithologic similarities between the Uwharrie Formation and the Little River Series of North and South Carolinas, respectively. The Uwharrie Formation is overlain by a thick sequence of water-laid pyroclastics and sediments of the Efland Formation with a maximum thickness of 10,000 feet (3000 m). This formation consists of andesitic tuffs, with interbedded greenstones, conglomerates, graywackes and flows. Conley and Bain reported that the greenstones are mainly andesitic in composition, but also contain some material that might be classed as basaltic. The youngest formation within this sequence is called the Tater Top Group having an approximate thickness of 450 feet (135 m). From base to top the group is composed of basaltic tuffs and flows, overlain by rhyolitic flows. In addition to these pyroclastic and sedimentary rock sequences Conley and Bain mention the occurrences of plutonic rocks ranging in composition from granite to gabbro which are scattered throughout the slate belt. Butler (1964) analyzed a few volcanic rocks such as amygdaloidal greenstone and vitric crystal tuff from the Carolina slate belt in North Carolina. He suggested that volcanic rocks in the belt are probably calc-alkalic and range in composition from basaltic to rhyolitic.

Whitney, et al. (1978) suggest that within Carolinas volcanic series rocks younger than the Little River Series, such as the

Tater Top Group of Conley and Bain (1965), become more potassic and similar to volcanic rocks found in more developed volcanic arcs. Such a transition from early tholeiites to younger calc-alkaline series is typical of developing island arcs as reported by Jakes and White (1972) and as observed at Antilles (Donnelly, et al., 1971) and Japan (Kuno, 1966a, 1966b). When the findings of this study as illustrated in Figures 34, 35 and 36 are compared with the above data a similarity exists in the sense that the original mildly-alkaline composition of the K-bentonites (Fig. 34), occupies, logically a transitional stage in a developing island arc sequence similar to those between the calc-alkaline and alkaline rocks represented by Mt. Ararat and Dunedin, respectively. Yet, within this particular stage different K-bentonite horizons seem to have a variable original composition ranging from intermediate-to-acid character. It is suggested that these trachyandesitic to rhyolitic rocks agree both compositionally and in time and space with the volcanic rocks younger than the Little River Series and their equivalents. More specifically, the Efland Formation and Tater Top Group (Conley and Bain, 1965) or their equivalents in the slate belt can reasonably be assumed to be the products of the same episodes forming the K-bentonites.

Chemical analyses of volcanogenic rocks from the Carolina slate belt (McCauley, 1961; Butler, 1964; Whitney, et al., 1978), from the Ordovician Tetagouche Group of island arc system in New

Brunswick, Canada (Whitehead and Goodfellow, 1978), and from recent island arcs of tholeiitic, calc-alkaline and shoshonitic associations (Jakes and White, 1972; Bowles, et al., 1973; Masuda, et al., 1975; Keller, et al., 1978; Kohn and Topping, 1978) are compared with the possible trachyandesitic composition of the original volcanic ash and with the average composition of K-bentonite bulk samples in Table 6. In addition to the average trachyandesite composition (column 1) used as a standard during this study and the average composition of K-bentonite bulk samples (column 2) partial chemical analyses of some volcanogenic rocks from the Ordovician island arc sequence of North America are listed (columns 3-11). Although the island arc rocks show a considerable chemical variation, they differ significantly from K-bentonites in having consistently much lower K_2O content. Recent explosive volcanic activity in the Mediterranean region which produced the trachytic Campanian tephra deposits containing 6-8 percent K_2O has been reported by Keller, et al. (1978). However, the data such as those of Table 6 suggest that Ordovician volcanic activity when compared in time and space with K-bentonites, produced rocks with a significantly lower K_2O content. Therefore, it must be assumed that a considerable amount of K_2O was added to the volcanic ash during post-depositional alteration. In column 2, total iron and titanium appear to be depleted in K-bentonite samples during

* Total iron expressed as Fe_2O_3

** Not determined

Explanation of column headings:

1. Average trachyandesite composition used as a standard during this study (ref. Table 3).

2. Average composition of K-bentonite bulk samples (ref. Table 3).

3. Siliceous epidote-rich greenschist, originally was a basic tuffaceous material (McCauley, 1961, sample no. 48-N).

4. Hematitic schist, originally was a soda-rich tuffaceous material (McCauley, 1961, sample no. 262-N).

5. Amygdolaidal greenstone of basaltic composition (Butler, 1964, sample no. OC-28C.

6. Devitrified crystal-vitric tuff of rhyodacitic composition (Butler, 1964, sample no. OC-18A).

7. Volcanic breccia of rhyodacitic composition (Butler, 1964, sample no. OC-38).

8. Altered tuff (Whitney, et al., 1978, sample no. 8, Table 1).

9. Mafic dike (Whitney, et al., 1978, sample no. 1-13, Table 2).

10. Average composition of alkaline, mafic volcanic rocks from the Tetagouche Group, New Brunswick, Canada (Whitehead and Goodfellow, 1978, Table 2).

11. Average composition of felsic volcanic rocks (augen schist) from the Tetagouche Group, New Brunswick, Canada (Whitehead and Goodfellow, 1978, Table 2).

Columns 3-9 represent partial chemical analyses of Ordovician volcanogenic rocks from Carolina slate belt.

Columns 10-11 represent partial chemical analyses of Ordovician volcanogenic rocks from northern extention of Appalachian island arc system.

TABLE 6. Partial chemical analyses of some volcanogenic rocks from the Ordovician island arc sequence of North America.

Oxide	1	2	3	4	5	6	7	8	9	10	11
SiO_2	52.56	54.28	59.68	45.92	47.48	64.54	65.43	66.60	55.50	47.74	74.56
Al_2O_3	18.39	20.08	10.91	23.38	20.42	13.13	12.54	13.60	16.40	14.94	12.51
Fe_2O_3T*	8.19	1.29	10.85	18.78	10.41	7.81	7.24	5.90	7.10	12.34	1.93
MgO	2.12	3.78	3.66	0.31	4.53	1.18	1.35	3.70	2.64	6.26	0.76
CaO	5.64	0.74	9.25	1.24	10.52	2.81	4.08	0.43	9.75	8.28	0.41
Na_2O	5.76	1.02	0.13	3.13	2.00	4.18	4.14	0.72	1.72	2.93	2.68
K_2O	3.91	8.22	0.35	3.25	2.30	2.99	1.98	4.20	0.15	0.56	4.68
TiO_2	1.73	0.37	1.15	2.15	0.52	0.67	0.50	0.54	n.d**	2.63	0.26
MnO	0.14	0.03	0.12	0.01	0.22	0.13	0.16	0.17	0.13	0.16	0.29

alteration. However, here these differences are believed to be due to original variations within the same rock type rather than the effects of post-depositional alteration. For example, the four trachyandesite compositions published by Carmichael, et al. (1974, pp. 396, 499, 501) have total iron content ranging between 5.29 and 10.00 percents. Furthermore the iron and titanium content of K-bentonite bulk samples proved to be good between-bed stratigraphic discriminators as shown in the previous chapter (Figs. 41 through 47). Thus, an emprical conclusion is drawn that these elements appeared to be immobile during the post-depositional alteration of volcanic ash (also see Floyd and Winchester, 1975; Smith and Smith, 1976). However, more work needs to be done to properly understand this relationship. Calculations of gains or losses resulting from the alteration process (Table 3) are found to be reasonable âlso for silica, magnesium, calcium and sodium. However, earlier assumptions (Cooper and Prouty, 1943; Fox and Grant, 1944) that the chert layers adjacent to K-bentonite beds are due to silica release during the devitrification of volcanic ashes should be reinvestigated since about 10 percent average loss of silica may not account for these chert layers.

Geochronology and Correlation of K-Bentonite Horizons:

Chemical separation of the K-bentonite bulk samples into three major chemical groups is accomplished by using five elements, Fe, Ti, Al, Zr and Ge, as shown in the form of binary and ternary

diagrams (Figs. 41 through 46). The agreement between these groups and the K-bentonite horizons sampled during this study is investigated by means of available field information and published data. Throughout central Kentucky and northeastern central Tennessee, the distribution and correlation of B-3 and B-6 (Fig. 47) have been more extensively studied than elsewhere (Wilson, 1949; Cressman, 1973; Cressman and Noger, 1976), and it is widely accepted that the older B-3 horizon is the most widespread and continuous K-bentonite bed in the Tyrone Limestone. This feature of B-3 is also recognized during this study as shown in Figure 47. B-3 has been frequently employed as a datum plane for stratigraphic investigations of Middle Ordovician strata (Cressman and Noger, 1976), however, similar usage of younger bentonites, such as B-6, is more localized as a result of their rather discontinuous character.

The only information available on B-8 is the study of Fox and Grant (1944) in the vicinity of the Tennessee River in southeastern Tennessee. As discussed in the previous chapter it is not reported in central Kentucky and north central Tennessee. However, the chemical separation of K-bentonite bulk samples suggests the presence of this horizon between the Nashville and Lexington domes along the Cincinnati arch. The lithologic resemblance of B-8 and B-6 and the fact they are separated by only 10 feet (3 meters) of limestone (Fig. 47) most probably prevent the distinction of these two horizons in the field. Based on the results of this study, it

is concluded that correlation of the uppermost K-bentonite horizons (B-6 and B-8) in the Tyrone Limestone using only their lithologic characteristics or in reference to a datum plane, such as B-3, can cause erroneous results.

CONCLUSIONS AND SUGGESTIONS

Conclusions

The following conclusions are drawn from this study:

1. K-bentonites are the alteration products of volcanic tuff or ash. Their mineralogy consists mainly of non-clay minerals such as biotite, alkali-feldspars (sanidine and orthoclase), zircon, apatite, Fe-Ti oxides and rarely quartz in varying portions with a clay mineral matrix. Petrographycally, they are crystal, vitric-crystal and vitric tuffs exhibiting relict textures such as angular, euhedral to subhedral crystals which are sometimes embayed and/or corroded, and occasional glass shards.

2. The clay mineralogy consists of a dioctahedral, regularly interstratified allevardite-type (IM) layer silicate with an illite to smectite ratio between 3:1 and 4:1. Based on the chemical analyses and structural formulae calculations it is concluded that the clays have a fairly stable composition and structure. Structural variations are revealed by the values of octahedral Al and Mg, tetrahedral Si and Al occupancies as well as by the distribution of total octahedral cations and interlayer K. Apparently, these clays represent a definite structure between illite and smectite. Furthermore, the chemical data indicate a high octahedral substitution of Si by Al so that octahedral charge dominates in the total layer charge.

3. The interstratified clay originated from volcanic glass deposited on the ocean floor. The glass was devitrified to Mg-smectite in a relatively short span of time in a subaqueous environment with a high Mg ion activity similar to that of modern sea water. The high total charge produced as a result of high Mg for Al substitution in the octahedral sheet was compensated for by the adsorption of interlayer K and Na derived mainly from pore water. Undoubtedly, some portion of these interlayer cations were provided by decomposing feldspars and biotites as the effects of post-depositional alteration intensified. Fixation of K increased with time so that the proportion of 10Å layers in the interstratified structure eventually became dominant. The absence of diagenetic minerals characteristic of high temperature and pressure conditions suggests that the post-depositional alteration of volcanic ash took place at relatively low temperatures and pressures.

4. The chemical classification of K-bentonite bulk samples using Ti, Zr, Nb, Y and Ga reveals that the original volcanic ash had an acid-to-intermediate composition, very similar to that of trachyandesite. The magma series which produced the volcanic eruptions had a mildly alkaline character between calc-alkaline and alkaline magmas indicating an intermediate stage of development of an early Paleozoic island arc located along southeastern Appalachia. A comparison of the original composition of K-bentonites and of volcanic rocks which form thick sequences within

the early Paleozoic strata in the Carolina slate belt suggests that the Middle Ordovician eruptive centers were located along this belt.

5. Two possibilities exist for the explanation of the apparent difference between the original compositions of the oldest and the two younger K-bentonite horizons (Figs. 34, 35, 36). Either they were the eruptive products of the same magma source undergoing magmatic differentiation through intermediate-to-acidic compositions or these two groups of bentonite horizons were formed from two different mildly alkaline magma sources with slightly different compositions.

6. The interpretation of gain, loss and redistribution of major elements during the post-depositional alteration of K-bentonites accounts for their mineralogic characteristics. Based on the assumption that Al remained constant during alteration, losses of Si, Ca and Na can be compared to the gains of Mg and K. Fe and Ti emprically found to be unaffected by the alteration processes. High concentrations of Mg and K in the clay fraction and the redistribution of Al within decomposing ash towards higher concentrations in the clay fraction reflect the formation of an interstratified mica-smectite phase. The assumption of an external source for K is furthermore strengthened because of a high gain of K during alteration. The commonly held view that chert layers adjacent to K-bentonites resulted from the devitrification of volcanic ash is questioned

because not more than 10 percent silica loss is thought to be insufficient to account for the amount present.

7. Although within-bed variations are observed in Al, Fe, K, Ti, Mg, Ga, Ge, Y, Nb, Rb, Zn and Zr contents, they do not mask between bed variations when the Al, Fe, Ti, Ge, Zn and Zr contents of bulk samples are considered. Bulk samples show wider ranges in composition than the clay fractions, illustrating the effect of inhomogeneous distribution of non-clay minerals and also the narrow compositional range of the clay minerals. Close similarity of K_2O and MgO abundances of both bulk samples and clay fractions from different K-bentonite horizons indicates that a state of equilibrium has been reached at least between the interstratified clay and the geologic environment. This equilibrium must have resulted from the effects of post-depositional alteration on the original ash compositions since prior to alteration the ashes apparently had different compositions.

8. The geochronologic investigation of K-bentonite bulk samples based on chemical criteria distinguish between three chemical groups of samples which are correlated with three K-bentonite horizons namely, from oldest to youngest, B-3, B-6 and B-8 of Fox and Grant (1944). The elements: Fe, Ti, Zr, Ge, Zn and, to a lesser degree Al, have proved to be useful for discrimination purposes.

9. Long-distance stratigraphic correlation of K-bentonites along a generally north-south line from Lawrence County, Indiana to Smith County, Tennessee is accomplished on the basis of the data obtained during the geochronologic studies and on field evidence. Results show that B-3 is the most widespread and continuous of all three horizons whereas B-6 and B-8 occur only locally between Nashville and Lexington domes due to their removal by post-Tyrone erosional processes. Thus, the usage of the uppermost K-bentonite horizons within the study area for long-distance correlation purposes is limited when compared to that of B-3. Although they are among the thick K-bentonite horizons, their discontinuous nature and closeness of their stratigraphic positions impose difficulties during field correlations. These difficulties, however, can be overcome by using chemical criteria for their definition. While B-3 has proved to be useful for long-distance correlations, B-6 and B-8 can be employed for local correlations and for the investigations concerning with the extent of the post-Tyrone erosional processes.

Suggestions for Further Study

The following suggestions are made for further study of Middle Ordovician K-bentonites.

1. Further studies on the interstratified illite-smectite clay structure and composition are recommended to contribute more to our knowledge of clay mineralogy. Apparently, this clay mineral

is a species among the other clay minerals and hence, has a great potential as a geological environment indicator.

2. Chemical correlation of K-bentonite horizons should be extended over wider areas especially east and west from the Cincinnati arch. This will greatly improve our knowledge of using widespread K-bentonite horizons as reliable marker horizons and to solve stratigraphic problems, especially when they are interbedded with clastic sediments of miogeosynclinal strata in the west. K-bentonites also occur in Ordovician strata over wide areas in Europe. In the future, any successful attempt for a possible correlation between these and the North American K-bentonites will be challenging and can provide valuable information regarding plate tectonics.

3. The present study is the first attempt to establish long-distance stratigraphic correlation of K-bentonite horizons on the basis of their bulk chemical characteristics. It is recommended that future studies should develop other chemical methods, such as the analysis of non-clay minerals by electron microprobe techniques, for the sake of comparison of the efficiencies of different methods to be used for geochronologic and correlation works.

4. A detailed study of stratigraphy and immobile element chemistry of meta-volcanic and -plutonic rocks of the Carolina slate belt is recommended in order to find the exact location of the Middle Ordovician eruptive centers.

5. The role of K-bentonites in the formation of chert layers is a curious problem. It is thought that the solution of this problem rests on the detailed chemical and petrographic investigation of adjacent limestones with an overall consideration of the geologic environment of K-bentonites and their host carbonate rocks.

REFERENCES

REFERENCES

Abbey, S., 1973, Studies in "standard samples" of silicate rocks and minerals. Part 3: 1973 extension and revision of "useable" values: Geol. Survey of Canada, Paper 73-36, Dept. of Energy, Mines and Resources, 25 p.

_____ 1976, SY-2, SY-3 and MRG-1 report on the collaborative analysis of three Canadian rock samples for use as certified reference materials--Supplement 1: Geol. Survey of Canada, Canmet report, 76-36, 23 p.

_____ Gillieson, A. H., and Perrault, G., 1975, SY-2, SY-3 and MRG-1 report on the collaborative analysis of three Canadian rock samples for use as certified reference materials: Canada Centre for Mineral and Energy Technology Sciences Laboratories, MRP/MSL, 75-132 (TR), p. 56.

Adams, G. R., 1926, Crystalline rocks, in Geology of Alabama: Geol. Survey of Alabama Spec. Rept., no. 14, p. 25-40.

Adams, A. T., and Lester, S. G., 1957, Zonation of the Middle and Upper Ordovician strata in northwestern Georgia: Georgia Geol. Survey Bull., v. 66, 110 p.

Allen, V. T., 1929, Altered tuffs in the Ordovician of Minnesota: Jour. Geology, v. 37, p. 239-248.

_____ 1931, Ordovocian bentonite in Missouri (abs): Geol. Soc. America Bull., v. 42, p. 224.

_____ 1932, Ordovician altered volcanic material in Iowa, Wisconsin and Missouri: Jour. Geology, v. 40, p. 259-269.

Bayley, R. W., and Muehlberger, J. R., 1968, Basement rock map of the United States (exclusive of Alaska and Hawaii): Washington, U. S. Geol. Survey, 2 sheets, scale 1:2,500,000.

Bell, H., 3rd, 1976, Geochemical reconnaissance using heavy minerals from small streams in central South Carolina: U. S. Geol. Survey Bull., no. 1404, 23 p.

Bergström, S. M., and Nilsson, R., 1974, Age and correlation of the Middle Ordovician bentonites on Bernholm: Bull. Geol. Soc. Denmark, v. 23, p. 27-48.

_____ and Sweet, W. C., 1966, Conodonts from the Lexington Limestone (Middle Ordovician) of Kentucky and its lateral equivalents in Ohio and Indiana: Bull. Am. Paleontology, v. 50, no. 229, p. 271-441.

Berner, R. A., 1971, Principles of Chemical Sedimentology: McGraw-Hill Book Co., 240 p.

Berry, W. B. N., 1976, Aspects of correlation of North American shelly and graptolitic faunas, in Bassett, M. G., ed., The Ordovician Systems: Proceedings of a Palaeontological Association Symposium: Birmingham, University of Wales Press and National Museum of Wales, Cardiff, p. 153-169.

Black, D. F. B., Cressman, E. R., and MacQuown, W. C., Jr., 1965, The Lexington Limestone (Middle Ordovician) of central Kentucky: U. S. Geol. Survey Bull., no. 1224-C, 29 p.

Bodine, M. W., Jr., and Standaert, R. R., 1977, Chlorite and illite compositions from Upper Silurian rock salts, Retof, New York: Clays and Clay Mins., v. 25, p. 57-71.

Bonatti, E., 1965, Palagonite, hyaloclastite and alteration of volcanic glass in the ocean: Bull. Volcanologique, v. 28, p. 259-269.

Bonnie, C. A., and Honess, A. P., 1929, Bentonite in Pennsylvania: Pa. Acad. Sci. Proc., v. 3, p. 1-8.

Borchardt, G. A., and Harward, M. E., 1971, Trace element correlation of volcanic soils: Soil Sci. Soc. America Proc., v. 35, no. 4, p. 626-631.

_____ Harward, M. E., and Knox, E. G., 1971a, Trace element concentration in amorphous clays of volcanic ash soils in Oregon: Clays and Clay Mins., v. 19, p. 375-382.

_____ Harward, M. E., and Schmitt, R. A., 1971b, Correlation of volcanic ash deposits by activation analysis of glass separates: Quat. Research, v. 1, no. 2, p. 247-260.

_____ Norgren, J. A., and Harward, M. E., 1973, Correlation of ash layers in peat bogs of eastern Oregon: Geol. Soc. America Bull., v. 84, p. 3101-3108.

Borella, P. E., and Osborne, R. H., 1978, Late Middle and early Late Ordovician history of the Cincinnati arch province, central Kentucky to central Tennessee: Geol. Soc. America Bull., v. 89, p. 1559-1573.

Bowen, R. L., 1967, Volcanic events in the Middle Ordovician in eastern North America (abs.): Am. Geophys. Union Trans., v. 48, no. 1, p. 226.

Bowles, F. A., Jack, R. N., and Carmichael, I. S. E., 1973, Investigation of deep-sea volcanic ash layers from equatorial Pacific cores: Geol. Soc. America Bull., v. 84, p. 2371-2388.

Bradley, W. F., 1945, Diagnostic criteria for clay minerals: Am. Mineralogist, v. 30, p. 704-713.

Brindley, G. W., 1961, Chlorite minerals, in Brown, G., ed., X-ray identification and crystal structures of clay minerals: Mineralogical Society, p. 242-296.

Burst, J. F., Jr., 1969, Diagenesis of Gulf Coast clayey sediments and its possible relation to petroleum migration: Bull. Am. Assoc. Petrol. Geologists, v. 53, p. 73-93.

Butler, J. R., 1964, Chemical analyses of rocks of the Carolina slate belt: Southeastern Geol., v. 5, p. 101-112.

Butts, C., 1926, Paleozoic rocks, in Geology of Alabama: Geol. Survey of Alabama Spec. Rept., no. 14, p. 41-230.

Byström, A. M., 1954, "Mixed-layer" minerals from the Ordovician bentonite beds at Kineekulle, Sweden: Nature, v. 173, nc. 4408, p. 783-874.

_____ 1956, Mineralogy of the Ordovician bentonite bed at Kinnekulle, Sweden: Sueriges Geologiska Undersökning, Årsbok, v. 48, no. 5, 62 p.

Byström-Asklund, A. M., Baadsgoard, H., and Folinsbee, R. L., 1961, K/Ar age of biotite, sanidine and illite from Middle Ordovician bentonites at Kinnekulle, Sweden: Geol. Fören. Stockh. Förh., v. 83, p. 92-96.

Cann, J. R., 1970, Rb, Sr, Y and Nb in some ocean floor basaltic rocks: Earth and Planet. Sci. Letters, v. 10, p. 7-11.

Carmichael, I. S. E., Turner, F. J., and Verhoogen, J., 1974, Igneous Petrology: McGraw-Hill Book Co., 739 p.

Coker, A. E., 1962, A mineralogical study of an Ordovician metabentonite near Clinton, Anderson County, Tennessee (M. S. Thesis): University of Tennessee, 49 p.

Collinson, D. W., and Runcorn, S. K., 1960, Polar wandering and continental drift, evidence from paleomagnetic observations in the United States: Geol. Soc. America Bull., v. 71, p. 915-958.

Conley, C. F., and Bain, G. L., 1965, Geology of the Carolina slate belt west of the Deep River-Wadesboro Triassic Basin, North Carolina: Southeastern Geol., v. 6, p. 117-138.

Cook, E. F., 1965, Stratigraphy of Tertiary volcanic rocks in eastern Nevada: Nevada Bureau of Mines Rept. no. 11, 66 p.

Cooper, G. A., 1956, Chazyan and related brachiopods: Smithsonian Misc. Colln., v. 127, part 1, 1025 p.

Cooper, N. B., and Prouty, C. E., 1943, Stratigraphy of the lower Middle Ordovician of Tazewell County, Virginia: Geol. Soc. America Bull., v. 54, no. 6, p. 846-847.

Cressman, E. R., 1973, Lithostratigraphy and depositional environments of the Lexington Limestone (Ordovician) of central Kentucky: U. S. Geol. Survey Prof. Paper, no. 768, 59 p.

_____ and Noger, M. C., 1976, Tidal-flat carbonate environments in the High Bridge Group (Middle Ordovician) of central Kentucky: Kentucky Geol. Survey, Rept. of Invesigations, no. 18, Series X, 15 p.

Czamanske, G. K., and Porter, S. C., 1965, Titanium dioxide in pyroclastic layers from volcanoes in the Cascade Range: Science, v. 150, p. 1022-1025.

Davis, J. C., 1973, Statistics and Data Analysis in Geology: New York, John Wiley and Sons, Inc., 550 p.

De Argollo, R., and Schilling, J. G., 1978, Ge-Si and Ga-Al fractionation in Hawaiian volcanic rocks: Geochim. et Cosmochim. Acta, v. 42, p. 623-630.

De Long, S. E., and McCullough, D., 1973, Compton--scattered tungsten x-rays as a measure of mass-absorption coefficients in rocks: Am. Mineralogist, v. 58, p. 1073-1075.

Donnelly, T. W., Rodgers, J. J. W., Pushkar, P., and Armstrong, R. L., 1971, Chemical evaluation of the igneous rocks of the eastern West Indies: an investigation of thorium, uranium and potassium distributions, and lead and strontium isotopic ratios; in Donnelly, R. W., ed., Caribbean geophysical tectonic and petrologic studies: Geol. Soc. America Mem., no. 130, p. 181-224.

Drahovzal, J. A., and Neathery, T. L., 1971, Middle and Upper Ordovician stratigraphy of the Alabama Appalachians, in Drahovzal, J. A., and Neathery, T. L., eds., Middle and Upper Ordovician of the Alabama Appalachians: Guidebook for the 9th Annual Field Trip, Alabama Geol. Soc., p. 1-62.

Dunoyer de Segonzac, G., 1965, Les argilles du Cretace superieur dans le bassin de Douala (Cameron). Problemes de diagenese: Bull. Serv. Carte. Geol. Als. Low., t. 17, fasc. 4, p. 287-310.

_____ Ferrero, G., and Kubler, B., 1968, Sur la cristallinité de l'illite dans la diagenese et l'anchimétamorphisme: Sedimentologie, v. 10, p. 137-143.

Eberl, D., 1978, The reaction of montmorillonite to mixed-layer clay: the effect of interlayer alkali and alkaline earth cations: Beochim. et Cosmochim. Acta, v. 42, p. 1-7.

_____ and Hower, J., 1976, Kinetics of illite formation: Geol. Soc. America Bull., v. 87, p. 1324-1330.

Elsheimer, H. N., and Fabbi, B. P., 1977, Application of an automatic fusion technique to minor and trace element XRF analysis of silicate rocks (abs.): 26th Annual Conference on Application of X-ray Analysis, University of Denver, p. 31-33.

Fabbi, B. P., 1970, A die for pelletizing samples for x-ray fluorescence analysis: U. S. Geol. Survey Prof. Paper, No. 700-B, p. B187-B189.

Fenneman, N. M., 1938, Physiography of eastern United States: New York, McGraw-Hill Book Co., Inc., 714 p.

Fettke, C. R., 1948, Subsurface Trenton and Sub-Trenton rocks in Ohio, New York, Pennsylvania and West Virginia: Pa. Topog. and Geol. Survey Bull., no. G-21, p. 1457-1492.

Fetzer, J. A., 1973, Biostratigraphic evaluation of some Middle Ordovician bentonite complexes in eastern North America (M. S. Thesis): Ohio State University, 160 p.

Field, D., and Elliott, R. B., 1974, The chemistry of gabbro/amphibolite transitions in south Norway: Contrib. Mineral. Petrol., v. 47, p. 63-76.

Flanagan, F. J., 1969, U. S. Geological Survey standards II. First compilation of data for the new U. S. G. S. rocks: Geochim. et Cosmochim. Acta, v. 33, p. 81-120.

_____ 1976, Descriptions and analyses of eight new U. S. G. S. rock standards: U. S. Geol. Survey Prof. Paper, no. 840, 192 p.

Floyd, P. A., and Winchester, J. A., 1975, Magma type and tectonic setting discrimination using immobile elements: Earth and Planet. Sci. Letters, v. 27, p. 211-218.

_____ and Winchester, J. A., 1978, Identification and discrimination of altered and metamorphosed volcanic rocks using immobile elements: Chemical Geol., v. 21, p. 291-306.

Folk, R. L., 1974, The natural history of crystalline calcium carbonate: effect of magnesium content and salinity: Jour. Sed. Petrology, v. 44, p. 40-53.

_____ and Land, L. S., 1975, Mg/Ca ratio and salinity: two controls over crystallization of dolomite: Bull. Am. Assoc. Petrol. Geologists, v. 59, p. 60-68.

Foster, M. D., 1960, Interpretation of the composition of trioctahedral micas: U. S. Geol. Survey Prof. Paper, no. 354-B, 48 p.

Fox, P. P., and Grant, C. F., 1944, Ordovician bentonites in Tennessee and adjacent states: Jour. Geology, v. 52, p. 319-341.

Gersimovskiy, V. I., and Karpsuhina, V. A., 1977, Zirconium and niobium in Icelandic rocks: Trans. from Geokhimiya, no. 3, p. 373-381.

Grim, R. E., 1968, Clay Mineralogy: New York, McGraw-Hill Book Co., Inc., 596 p.

_____ and Güven, N., 1978, Bentonites, Geology, Mineralogy, Properties and Uses: New York, Elsevier Scientific Publ. Co., 256 p.

Gutstadt, A. M., 1958, Cambrian and Ordovician stratigraphy and oil and gas possibilities in Indiana: Indiana Geol. Survey Bull., 103 p.

Hagemann, F., and Spjeldnoes, N., 1955, The Middle Ordovician of the Oslo region, Norway. Part 6, notes on bentonites (K-bentonites) from Oslo-Osker district Norsk: Geol. Tidssk. bd. 35, p. 29-51.

Harbaugh, J. W., and Merriam, D. F., 1968, Computer Applications in Strati-Graphic Analysis: New York, John Wiley and Sons, Inc., 282 p.

Harris, L. D., and Milici, R. C., 1977, Characteristics of thin-skinned style of deformation in the southern Appalachians and potential hydrocarbon traps: U. S. Geol. Survey Prof. Paper, no. 1018, 40 p.

Hart, S. R., Erlank, A. J., and Kable, E. J. D., 1974, Sea floor basalt alteration: Some chemical and Sr isotopic effects: Contrib. Mineral. Petrol., v. 44, p. 219-230.

Hatcher, R. D., Jr., 1972, Developmental model for the southern Appalachians: Geol. Soc. America Bull., v. 83, p. 2735-2760.

Hazel, J. E., 1970 Binary coefficients and clustering in biostratigraphy: Geol. Soc. America Bull., v. 81, p. 3237-3252.

Hein, J. R., and Scholl, D. W., 1978, Diagenesis and distribution of late Cenozoic volcanic sediment in the southern Bering Sea: Geol. Soc. America Bull., v. 89, p. 197-210.

Heling, D., 1978, Diagenesis of illite in argillaceous sediments of the Rhinegraben: Clay Minerals, v. 13, p. 211-219.

Higuchi, H., and Nagasawa, H., 1969, Partitioning of trace elements between rock-forming minerals and the host volcanic rocks: Earth and Planet. Sci. Letters, v. 7, p. 281-287.

Hower, J., 1959, Matrix corrections in x-ray spectrographic trace element analysis of rocks and minerals: Am. Mineralogist, v. 44, p. 19-32.

_____ and Mowatt, T. C., 1966, The mineralogy of illites and mixed-layer illite/montmorillonites: Am. Mineralogist, v. 51, p. 825-854.

Huff, W. D., 1963a, A study of Middle Ordovician K-bentonites in Kentucky and southern Ohio (Ph.D. Thesis): University of Cincinnati, 115 p.

_____ 1963b, Mineralogy of Ordovician K-bentonites in Kentucky: Clays and Clay Mins., v. 11, p. 200-209.

_____ 1972, Morphologic effects on illite as a result of potassium depletion: Clays and Clay Mins., v. 20, p. 295-301.

Hutchison, C. S., 1974, Laboratory Handbook of Petrographic Techniques: New York, Wiley-Interscience Publ. Co., 527 p.

Jack, R. N., and Carmichael, I. S. E., 1969, The chemical "fingerprinting" of acid volcanic rocks: California Division, Mines and Geology Spec. Rept., no. 100, p. 17-32.

_____ Lajoie, K. R., and Carmichael, I. S. E., 1967, "Fingerprinting" of obsidian and pumice from western United States (abs.): Geol. Soc. America Prog. Annual Meeting, p. 107.

Jakes, P., and White, A. J. R., 1972, Major and trace element abundances in volcanic rocks of orogenic areas: Geol. Soc. America Bull., v. 83, p. 29-40.

Jenkins, R., and De Vries, J. L., 1967, Practical X-ray Spectrometry: New York, Springer-Verlag Inc., 182 p.

Jensen, B. B., 1973, Patterns of trace element partitioning: Geochim. et Cosmochim. Acta, v. 37, p. 2227-2242.

Kay, M. G., 1931a, Hounsfield metabentonite (abs.): Geol. Soc. America Bull., v. 42, p. 225.

_____ 1931b, Stratigraphy of the Ordovician Hounsfield metabentonite: Jour. Geology, v. 39, p. 361-370.

_____ 1935, Distribution of Ordovician altered volcanic materials and related clays: Geol. Soc. America Bull., v. 46, p. 225-244.

Keller, J., Ryan, W. B. F., Ninkovich, D., and Altherr, R., 1978, Explosive volcanic activity in the Mediterranean over past 200,000 years as recorded in deep-sea sediments: Geol. Soc. America Bull., v. 89, p. 591-604.

Kerr, P. F., and Kulp, J. L., 1949, Reference clay localities--United States: American Petrol. Inst. Project no. 49, clay mineral standards, p. 81-83.

Kidd, J. T., and Copeland, C. W., 1971, Review of Ordovician subsurface stratigraphy of north Alabama, in Drahovzal, J. A., and Neathery, T. L., eds., Middle and Upper Ordovician of the Alabama Appalachians: Guidebook for the 9th annual field trip, Alabama Geol. Soc., p. 137-152.

King, P. B., 1950, Tectonic framework of southeastern United States: Bull. Am. Assoc. Petrol. Geologists, v. 34, p. 635-671.

_____ 1955, A geologic section across the southern Appalachians: an outline of the geology in the segment in Tennessee, North Carolina and South Carolina, in Russell, R. I., ed., Guides to southeastern geology: Geol. Soc. America, Boulder, Colorado, p. 332-373.

_____ 1964, Further thoughts on tectonic framework of southeastern United States, in Lowry, W. D., ed., Tectonics of the southern Appalachians: VPI Department of Geological Sciences, Mem. no. 1, p. 5-31.

Kittleman, L. R., 1973, Mineralogy, correlation and grain size distribution of Mazama tephra and other postglacial layers, Pacific northwest: Geol. Soc. America Bull., v. 84, p. 2957-2980.

Knight, W. C., 1898, Bentonite (Wyoming): Eng. and Min. Journal, v. 66, p. 491.

Kohn, B. P., and Topping, W. W., 1978, Time-space relationships between Late Quaternary rhyolitic and andesitic volcanism in the southern Taupo volcanic zone, New Zealand: Geol. Soc. America Bull., v. 89, p. 1265-1271.

Kraus, I., 1978, Distribution of minor elements in clays in relation to their genesis (abs.): 6th International Clay Conference, University of Oxford, England, p. 313.

Krauskopf, K. B., 1967, Introduction to Geochemistry: New York, McGraw-Hill Book Co., Inc., 721 p.

Kuno, H., 1966a, Lateral variation of basalt magma type across continental margins and island arcs: Bull. Volcanologique, v. 29, p. 195-222.

_____ 1966b, Lateral variation of basaltic magma across continental margins and island arcs, in Poole, W. H., ed., Continental margins and island arcs: Geol. Survey of Canada, Paper 66-15, p. 317-336.

Larsen, L. H., and Poldervaardt, A., 1957, Measurement and distribution of zircons in some granitic rocks of magmatic origin: Min. Mag., v. 31, p. 544-564.

Lawrence, J. R., Grieskes, J. M., and Broecker, W. S., 1975, Oxygen isotope and cation composition of DSDP pore waters and the alteration of layer II basalts: Earth and Planet. Sci. Letters, v. 27, p. 1-10.

Lerbekmo, J. F., and Campbell, F. A., 1969, Distribution, composition and source of the White River Ash, Yukon Territory: Canadian Jour. Earth Sci., v. 6, p. 109-116.

Lounsbury, R. W., and Melhorn, W. N., 1964, Clay mineralogy of Paleozoic K-bentonites of the eastern United States (Part I): Clays and Clay Mins., v. 12, p. 557-565.

MacQuown, W. C., Jr., 1967, Factors controlling porosity and permeability in the Curdsville Member of the Lexington Limestone: Kentucky University Water Resources Inst. Research Rept., no. 7, 80 p.

Martin, R., Litz, P. E., and Huff, W. D., 1979, A new technique for making thin sections of clayey sediments: Jour. Sed. Petrology, v. 49 (in press).

Masuda, Y., Nishimura, S., Ikeda, T., and Katsui, Y., 1975, Rare-earth and trace elements in the Quaternary volcanic rocks of Hokkaido, Japan: Chemical Geol., v. 15, p. 251-271.

McCauley, J. F., 1961, Rock analyses in the Carolina slate belt and the Charlotte belt of Newberry County, South Carolina: Southeastern Geol., v. 3, p. 1-20.

McFarlan, A. C., 1943, Geology of Kentucky: Waverly Press Inc., 531 p.

McGuire, W. H., and Howell, P., 1963, Oil and gas possibilities of the Cambrian and Lower Ordovician in Kentucky: Lexington, Ky., Spindletop Research Center, 216 p.

McLaughlin, R. J. W., 1967, Atomic absorption spectroscope, in Zussman, J., ed., Physical Methods in Determinative Mineralogy: Academic Press, p. 475-486.

Medlin, J. H., Suhr, N. H., and Bodkin, J. B., 1969, Atomic absorption analysis of silicates employing $LiBO_2$ fusion: Atomic Absorption Newsletter, v. 8, no. 2, p. 25-29.

Milici, R. C., 1969, Middle Ordovician stratigraphy in central Sequatchie Valley, Tennessee: Southeastern Geol., v. 11, no. 2, p. 111-127.

_____ and Smith, J. W., 1969, Stratigraphy of the Chickamauga Supergroup in its type localtiy: Georgia Geol. Survey Bull., v. 80, p. 5-35.

Miller, A. M., 1919, The geology of Kentucky: Dept. of Geology and Forestry of Kentucky, Ser. 5, Bull. 2, p. 16-30.

Miller, R. L., and Kahn, J. S., 1962, Statistical Analysis in the Geological Sciences: New York, John Wiley and Sons Inc., 483 p.

_____ and Fuller, J. D., 1954, Geology and oil resources of Rose Hill district--the fenster area of the Cumberland overthrust, Block-Lee County, Virginia: Virginia Geol. Survey Bull., v. 71, 383 p.

Moore, N. K., 1977, Distribution of the benthic algal flora in Middle Ordovician carbonate environmental units of the southern Appalachians, in Ruppel, S. C., and Walker, K. R., eds., The echostratigraphy of the Middle Ordovician of the southern Appalachians (Kentucky, Tennessee and Virginia), U. S. A.: a field excursion: University of Tennessee, Studies in Geol., no. 77-1, p. 18-29.

Mossler, J. H., and Hayes, J. B., 1966, Ordovician potassium bentonites of Iowa: Jour. Sed. Petrology, v. 36, no. 2, p. 414-427.

Muddox, D. G., 1930, Bentonite in the Ordovician near Collingwood, Ontario: Science, v. 72, p. 630.

Muir, I. D., 1967, Microscopy: transmitted light, in Zussman, J., ed., Physical Methods in Determinative Mineralogy: Academic Press, p. 31-102.

Nelson, W. A., 1921, Notes on a volcanic ash bed in the Ordovician of middle Tennessee: Tennessee State Geol. Survey Bull., v. 25, p. 46-48.

_____ 1922a, Mid-Ordovician volcanic ash in Tennessee: Pan-Am. Geologists, v. 27, no. 3, p. 251-252.

_____ 1922b, Volcanic ash beds in the Ordovician of Tennessee, Kentucky and Alabama: Geol. Soc. America Bull., v. 33, p. 605-615.

_____ 1925, Two new volcanic ash horizons in the Stones River Group of the Ordovician of Tennessee (abs.): Geol. Soc. America Bull., v. 36, p. 159.

Neuman, R. B., 1976, Ordovician of the eastern United States, in Bassett, M. G., ed., The Ordovician System: Proceedings of a Paleontological Association symposium: Birmingham, University of Wales Press and National Museum of Wales, Cardiff, p. 195-207.

Norrish, K., and Chappel, B. W., 1967, X-ray fluorescence spectrography, in Zussman, J., ed., Physical Methods in Determinative Mineralogy: Academic Press, p. 161-214.

_____ and Hutton, J. T., 1969, An accurate x-ray spectrographic method for the analysis of a wide range of geological samples: Geochim. et Cosmochim. Acta, v. 33, p. 431-453.

Parks, J. M., 1966, Cluster analysis applied to multivariate geologic problems: Jour. Geology, v. 74, no. 5, p. 703-715.

Pearce, J. A., and Cann, J. R., 1971, Ophiolite origin investigated by discriminant analysis using Ti, Zr, Y: Earth and Planet. Sci. Letters, v. 12, p. 339-349.

Perry, E., and Hower, J., 1970, Burial diagenesis in Gulf Coast pelitic sediments: Clays and Clay Min., v. 18, p. 165-177.

Powers, M. C., 1959, Adjustments of clays to chemical change and concept of the equivalence level: Clays and Clay Min., v. 6, p. 309-326.

Randle, K., Goles, G. G., and Kittleman, L. R., 1971, Geochemical and petrological characterization of ash samples from Cascade Range volcanoes: Quat. Research, v. 1, p. 261-282.

Read, J. F., and Tillman, C. G., 1977, Field trip guide to lower Middle Ordovician platform and basin facies rocks, southwestern Virginia, in Ruppel, S. C., and Walker, K. R., eds., The ecostratigraphy of the Middle Ordovician of the southern Appalachians (Kentucky, Tennessee and Virginia), of Tennessee, Studies in Geol., no. 77-1, p. 141-146.

Reynolds, R. C., Jr., 1963, Matrix corrections in trace element analysis by x-ray fluorescence: estimation of the mass-absorption by Compton scattering: Am. Mineralogist, v. 48, p. 1133-1143.

_____ and Hower, J., 1970, The nature of interlayering in mixed-layer illite-montmorillonites: Clays and Clay Min., v. 18, p. 25-36.

Rimsaite, J., 1975, Natural alteration of mica and reactions between released ions in mineral deposits: Clays and Clay Min., v. 23, p. 247-255.

Rodgers, J., 1953, Geologic map of east Tennessee with explanatory text: Tenn. Dept. Conserv. Div. Geology Bull., v. 58, pt. II, 168 p.

Ross, C. S., 1928, Altered Paleozoic volcanic materials and their recognition: Bull., Am. Assoc. Petrol. Geologists, v. 12, p. 143-161.

_____ 1955, Provenance of pyroclastic materials: Geol. Soc. America Bull., v. 66, p. 427-434.

_____ and Kerr, P. F., 1931, The clay minerals and their identity: Jour. Sed. Petrology, v. 1, p. 59-63.

_____ and Kerr, P. F., 1934, Bentonite and related clays (abs.): Geol. Soc. America Proc. no. 1934, p. 380.

_____ and Shannon, E. V., 1926, The minerals of bentonite and related clays and their physical properties: Jour. Amer. Ceramic Soc., v. 9, p. 72-96.

Ruppel, S. C., 1977, The Chickamauga Limestone--a complex mosaic of supratidal to subtidal carbonate shelf environments, in Ruppel, S. C., and Walker, K. R., eds., The echnostratigraphy of the Middle Ordovician of the southern Appalachians (Kentucky, Tennessee and Virginia), U. S. A.: a field excursion: University of Tennessee, Studies in Geology, no. 77-1, 171 p.

_____ and Walker, K. R., 1977, The echostratigraphy of the Middle Ordovician of southern Appalachians (Kentucky, Tennessee and Virginia), U. S. A.: a field excursion: University of Tennessee, Studies in Geology, no. 77-1, 171 p.

Sardeson, F. W., 1924, Volcanic ash in Ordovician rocks of Minnesota: Pan-Am. Geologist, v. 42, p. 45-52.

_____ 1933, Ordovicic bentonite zones: Pan-Am. Geologist, v. 61, no. 1, p. 19-28.

Shearrow, G. G., 1959, Correlation of the Sandhill, Wood County, West Virginia deep well with the aid of insoluble residues: a symposium on the Sandhill deep well, Wood County, West Virginia: West Virginia Geol. Survey, Rept. of Investigations, no. 18, p. 29-97.

Siever, R., 1962, Silica solubility, 0° - 200°C, and the diagenesis of siliceous sediments: Jour. Geology, v. 70, p. 127-149.

Slaughter, M., and Early, J. M., 1965, Mineralogy and geologic significance of the Mowry bentonites: Geol. Soc. America Spec. Paper, no. 83, 116 p.

Smith, D. G. W., and Westgate, J. A., 1969, Electron probe technique for characterizing pyroclastic deposits: Earth and Planet. Sci. Letters, v. 5, no. 5, p. 313-319.

Smith, E. W., Neathery, T. L., and Drahovzal, J. A., 1971, Ordovician K-bentonites in Alabama, in Drahovzal, J. A., and Neathery, T. L., eds., The Middle and Upper Ordovician of the Alabama Appalachians: Guidebook for the 9th annual field trip, Alabama Geol. Soc., p. 125-135.

Smith, R. E., and Smith, S. E., 1976, Comments on the use of Ti, Zr, Y, Sr, K, P and Nb in classification of basaltic magmas: Earth and Planet. Sci. Letters, v. 32, p. 114-120.

Smith R. P., and Nash, W. P., 1976, Chemical correlation of volcanic ash deposits in the Salt Lake Group, Utah, Idaho and Nevada: Jour. Sed. Petrology, v. 46, no. 4, p. 930-934.

Smith, R. W., 1931, Shales and brick clays of Georgia: Georgia Geol. Survey Bull., v. 45, 348 p.

Snäll, S., 1977, Silurian and Ordovician bentonites of Gotland (Sweden): Acta Universitatis Stockholmiensis, Stockholm Contrib. in Geology, v. 31: 1, 99 p.

Stose, G. W., and Jonas, A. I., 1927, Ordovician shale and associated lava in southeastern Pennsylvania: Geol. Soc. America Bull., v. 38, no. 3, p. 505-536.

Suchecki, R. K., Perry, E. A., and Hubert, J. F., 1977, Clay petrology of Cambro-Ordovician continental margin, Cow Head klippe, western Newfoundland: Clays and Clay Min., v. 25, p. 163-170.

Sweet, W. C., and Bergström, S. M., 1976, Conodont biostratigraphy of the Middle and Upper Ordovician of the United States midcontinent, in Bassett, M. G., ed., The Ordovician System: proceedings of a Palaentological Association symposium: Birmingham, University of Wales Press and National Museum of Wales, Cardiff, p. 121-151.

Taylor, S. R., 1965, The application of trace element data to problems in petrology, in Ahrens, L. H., et al., eds., Physics and Chemistry of the Earth: New York, Pergamon Press, v. 6, p. 133-213.

Theisen, A. A., Borchardt, G. A., Harward, M. E., and Schmitt, R. A., 1968, Neutron activation for distinguishing Cascade Range pyroclastics: Science, v. 161, p. 1009-1011.

Twehhofel, W. H., Bridge, J., Cloud, P. E., Jr., Cooper, B. N., Cooper, G. A., Cumings, E. R., Cullison, J. S., Dunbar, C. O., Kay, M., Liberty, B. A., McFarlan, A. C., Rodgers, J., Whittington, H. B., Wilson, A. E., and Wilson, C. W., Jr., 1954, Correlation of the Ordovician formations of North America: Geol. Soc. America Bull., v. 65, p. 247-298.

Ulrich, E. O., 1888, A correlation of the Lower Silurian horizons of Tennessee and of the Ohio and Mississippi Valleys with those of New York and Canada: Am. Geologist, v. 1, p. 100-110; 179-190; 305-315, v. 2, p. 39-40.

Van Eysinga, F. W. B., 1975, Geologic Time Table, 3rd edition: Elsevier Scientific Publ. Co., Amsterdam.

Velde, B., 1977, A proposed phase diagram for illite, expanding chlorite, corrensite and illite-montmorillonite mixed-layer minerals: Clays and Clay Min., v. 25, p. 264-270.

_____ and Brusewitz, A. M., 1978, Evidence for metasomatic diagenesis and non-metasomatic metamorphism of Ordovician metabentonites in Sweden (abs.): 6th International Caly Conference, University of Oxford, England, p. 306.

Walker, K. R., 1974, Community patterns: Middle Ordovician of Tennessee, in Ziegler, A. M., et al., eds., Principles of benthic community analysis: Comp. Sed. Lab., University of Miami, Sedimenta, v. 4, p. 9.1-9.5.

Weaver, C. E., 1953a, Mineralogy and petrology of some Ordovician K-bentonites and related limestones: Geol. Soc. America Bull., v. 64, p. 921-943.

_____ 1953b, A lath-shaped non-expanded dioctahedral 2:1 clay mineral: Am. Mineralogist, v. 38, p. 279-289.

_____ 1956, The distribution and identification of mixed-layer clays in sedimentary rocks: Am. Mineralogist, v. 41, p. 202-221.

_____ 1960, Possible uses of minerals in search for oil: Bull. Am. Assoc. Petrol. Geologists, v. 44, p. 1505-1518.

_____ 1965, Potassium content of illite: Science, v. 147, p. 603-605.

_____ and Beck, K. C., 1971, Clay water diagenesis during burial: how mud becomes gneiss: Geol. Soc. America Spec. Paper no. 134, 96 p.

_____ and Pollard, L. D., 1973, The Chemistry of Clay Minerals: Elsevier, New York, 213 p.

Webb, E. J., 1969, Geologic history of the Cambrian System in the Appalachian basin: Kentucky Geol. Survey, Series X, Spec. Publ. no. 18, p. 71-15.

Westgate, J. A., 1977, Identification and significance of Late Holocene tephra from Otter Creek, southern British Columbia, and localities in west-central Alberta: Canadian Jour. Earth Sci., v. 14, no. 11, p. 2593-2600.

_____ and Dreimanis, A., 1967, Volcanic ash layers of Recent age at Banff National Park, Alberta, Canada: Canadian Jour. Earth Sci., v. 4, p. 155-161.

_____ Christiansen, E. A., and Boellstorff, J. D., 1977, Wascana Creek Ash (Middle Pleistocene) in southern Saskatchewan: characterization, source, fission track age, paleomagnetism and stratigraphic significance: Canadian Jour. Earth Sci., v. 14, no. 3, p. 357-374.

_____ and Fulton, R. J., 1975, Tephra-stratigraphy of Olympia interglacial sediments in south-central British Columbia, Canada: Canadian Jour. Earth Sci., v. 12, p. 489-502.

_____ and Smith, D. G. W., and Tomlinson, M., 1970, Late Quaternary tephra layers in southwestern Canada: Proc. 2nd annual Paleo-environmental workshop of the University of Calgary Archaeological Assoc., v. 12, p. 13-34.

Whitecomb, L., 1932, Correlation by Ordovician bentonite: Jour. Geology. v. 40, p. 522-534.

_____ 1934, Possible volcanic sources of the Ordovician bentonite (abs.): Geol. Soc. America Proc. no. 1933, p. 382.

Whitehead, R. E. S., and Goodfellow, W. D., 1978, Geochemistry of volcanic rocks from the Tetagouche Group, Bathurst, New Brunswick, Canada: Canadian Jour. Earth Sci., v. 15, p. 207-219.

Whitney, J. A., Paris, T. A., Carpenter, R. H., and Hartley, M. E., 3rd, 1978, Volcanic evolution of the southern slate belt of Georgia and South Carolina: a primitive oceanic island arc: Jour. Geology, v. 86, p. 173-192.

Wilson, A. O., 1971, Petrology of parts of the Black River age strata of the Chickamauga Limestone, Etowah and Dekalb Counties, Alabama, in Drahovzal, J. A., and Neathery, T. L., eds., Middle and Upper Ordovician of the Alabama Appalachians: a guidebook for the 9th annual field trip, Alabama Geol. Soc., p. 79-100.

Wilson, C. W., Jr., 1949, Pre-Chattanooga stratigraphy in central Tennessee: Tennessee Dept. Conserv. Div. Geol. Bull., v. 56, 407 p.

_____ 1958, Guidebook to geology along Tennessee highways: Tennessee Div. Geol. nos. 1-10, Rept. Investigations no. 5, p. 30-33; 90-95.

_____ 1962, Stratigraphy and geologic history of Middle Ordovician rocks of central Tennessee: Geol. Soc. America Bull., v. 73, p. 481-504.

Winchester, J. A., and Floyd, P. A., 1977, Geochemical discrimination of different magma series and their differentiation products using immobile elements: Chemical Geol., v. 20, p. 325-343.

Wolcott, D. E., Cressman, E. R., and Connor, J. J., 1972, Trend-surface analysis of the thickness of the High Bridge Group (Middle Ordovician) of central Kentucky and its bearing on the nature of the post-Knox unconformity: U. S. Geol. Survey Prof. Paper no. 800-B, p. B25-B33.

Wood, S. H., 1977, Distribution, correlation and radiocarbon dating of Late Holocene tephra, Mono and Inyo Craters, eastern California: Geol. Soc. America Bull., v. 88, p. 89-95.

Woodward, H. P., 1961, Preliminary subsurface study of southeastern Appalachian interior plateau: Bull. Am. Assoc. Petrol. Geologists, v. 45, p. 1634-1655.

Yoder, H. S., and Eugster, H. P., 1955, Synthetic and natural muscovites: Geochim et Cosmochim. Acta, v. 8, p. 225-280.

Young, D. M., 1940, Bentonite clay horizons and associated chert layers of central Kentucky: University of Kentucky Research Club Bull., v. 6, p. 27-31.

Zussman, J., 1967, Physical Methods in Determinative Mineralogy: Academic Press, p. 261-334.

APPENDICES

APPENDIX A

SUMMARY OF DATA ON MIDDLE ORDOVICIAN K-BENTONITE AND ADJACENT LIMESTONE SAMPLES

K-bentonite: KB-1 (C-115)*; core sample; Stanford Quad., Lincoln Co., Kentucky; depth: 508 feet; color is grayish-green; fissile; few biotite crystals visible to naked eye.

Limestone: LS-1A (C-115); Tyrone Limestone; just above KB-1. Color is light gray; sublithographic with very small white specks; undulated shaly laminae intercalated with calcerous material.

Limestone: LS-1B (C-115); Tyrone Limestone; 10 inches below KB-1. Color is light gray; sublithographic with coarse crystalline bird's eye calcite.

K-bentonite: KB-2 (C-211)*; core sample; Eli Quad., Russell Co., Kentucky; depth: 1118-1118.5 feet. Color is gray; fissile; few biotite crystals.

Limestone: LS-2A (C-211); Tyrone Limestone; just above KB-2. Color is light gray; sublithographic with shaly laminae close to K-bentonite.

Limestone: LS-2B (C-211); Tyrone Limestone; just below KB-2. Color is brownish-gray; sublithographic with bird's eye calcite; very hard.

K-bentonite: KB-4A (C-114)*; core sample; Gravel Switch Quad., Marion Co., Kentucky; depth: 314 feet. 10 inches thick bentonite. Top K-bentonite sample: color is light green; fissile; fresh biotite crystals are visible to naked eye. 2 inches thick chert layer overlies KB-4A.

K-bentonite: KB-4B (C-114); bottom K-bentonite sample. Color is light green; fine grained; fissile; a discontinuous chert layer underlies K-bentonite KB-4B.

Limestone: LS-4A (C-114); Tyrone Limestone; just above KB-4A. Color is gray; sublithographic; few undulated shaly laminae are present close to K-bentonite layer.

Limestone: LS-4B (C-114); Tyrone Limestone; just below KB-4B. Color is dark gray; sublithographic; cherty; abundant pyritic inclusions.

K-bentonite: KB-5A (C-205)*; core sample; Dunville Quad., Casey Co., Kentucky. From top of 13 inches thick K-bentonite. Color is green; fissile; few biotite crvstals; fresh.

K-bentonite: KB-5C (C-205); 2 inches below KB-5A. Color is green; fissile; abundant biotite crystals; fresh.

K-bentonite: KB-5CD (C-205); 3 inches below KB-5A; core and lithologic description is similar to KB-5A.

K-bentonite: KB-5D (C-205); 4 inches below KB-5A. Color is green; fissile; relatively coarse grained; abundant biotite crystals.

K-bentonite: KB-5E (C-205); 6 inches below KB-5A. Color is green; fissile; less abundant biotite crystals with respect to KB-5D; fresh.

K-bentonite: KB-5F (C-205); 8 inches below KB-5A. Lithologic description is same as KB-5E.

K-bentonite: KB-5G (C-205); 10 inches below KB-5A. Color is gray with green patches; fissile; very fine grained biotite crystals; fresh; hard.

K-bentonite: KB-5H (C-205); 12 inches below KB-5A. Color is gray; fissile; very few biotite crystals; fresh.

K-bentonite: KB-5B (C-205); 13 inches below KB-5A. Lithologic description is same as KB-5H.

K-bentonite: KB-5BU (C-205); Random sample from KB-5 horizon. Color is green; fissile; coarse grained with abundant biotite crystals.

Limestone: LS-5A (C-205); Tyrone Limestone; just above KB-5A. Color is light gray; coarse crystalline.

Limestone: LS-5B (C-205); Tyrone Limestone; just below KB-5B. Color is dark gray; sublithographic.

K-bentonite: KB-6A (CA-8)**; core sample; Macon Co., Tennessee; depth: 365.5 feet, top sample of 18 inches thick K-bentonite. Color is light green; fine crystalline; fissile; abundant fresh biotite crystals; fresh; sharp contact with limestone at top.

K-bentonite: KB-6D (CA-8); 2 inches below KB-6A. Lithologic characteristics are same as KB-6A.

K-bentonite: KB-6B (CA-8); 6 inches below KB-6A. Lithologically very similar to KB-6A, only more coarsly crystalline.

K-bentonite: KB-6E (CA-8); 12 inches below KB-6A. Lithologically similar to KB-6A.

K-bentonite: KB-6C (CA-8); 16 inches below KB-6A. Lithologically similar to KB-6A.

Limestone: LS-6A (CA-8); Tyrone Limestone; depth: 365.5 feet. Color is dark gray; sublithographic with bird's eye calcite; inclusions of small size calcerous fragments; hard.

Limestone: LS-6B (CA-8); Tyrone Limestone; depth. 367 feet. Color is greenish-gray; sublithographic with bird's eye calcite; few shaly laminae close to the bottom of K-bentonite layer.

K-bentonite: KB-8A (CA-125)**; core sample; Whitleyville, Sec. 16, 46E 1S; Jackson Co., Tennessee; depth: 317 feet; sample is from the top of 24 inches thick K-bentonite layer. Color is dark gray; very fine crystalline; biotite crystals are abundant but hardly visible; hard; few fossil shells close to limestone; sharp contact with limestone at top.

K-bentonite: KB-8E (CA-125); 4.4 inches below KB-8A. Lithologically similar to KB-8A.

K-bentonite: KB-8B (CA-125); depth: 318.6 feet. Color is dark gray; very fine crystalline; fissile; fresh; hard; biotite crystals are hardly visible to naked eye.

K-bentonite: KB-8F (CA-125); 13.6 inches below KB-8A. Lithologically similar to KB-8B.

K-bentonite: KB-8C (CA-125); 18 inches below KB-8A. Lithologically similar to KB-8B.

K-bentonite: KB-8D (CA-125); 22 inches below KB-8A. Color is light green; very fine crystalline with rare biotite crystals; massive; conchoidal fracture, hard.

Limestone: LS-8A (CA-125); Tyrone Limestone; depth: 317 feet. Color is dark gray; sublithographic with occasional fossil shells.

Limestone: LS-8B (CA-125); Tyrone Limestone; depth: 319.4 feet. Color is gray; sublithographic limestone in gradational contact with overlying K-bentonite; fossils are replaced by calcite; indications of wave-bottom action.

K-bentonite: KB-7A (CA-125); depth 324.4 feet. 2 inches thick bentonite. Color is gray; fissile; fine crystalline; abundant fresh biotite crystals; fresh; calcerous.

K-bentonite: KB-7B (CA-125); depth: 324.9 feet; top sample of 12 inches thick K-bentonite horizon. Color is greenish-gray; fissile; fine crystalline; fine grained biotite is very abundant; fresh.

K-bentonite: KB-7C (CA-125); 5 inches below KB-7B. Color is green; fissile; fine crystalline with abundant biotite crystals; fresh.

K-bentonite: KB-7D (CA-125); 11.5 inches below KB-7B. Color is grayish-green; coarse to fine crystalline; fissile; very abundant and fresh biotite crystals; fresh.

K-bentonite: KB-9A; outcrop sample; T-3 K-bentonite at Round Lick Creek on U.S. Highway 70 N from Cookeville to Nashville; Rome; Tennessee (ref: Wilson, 1958, Log. no. 30B, p. 92, 76.4-78.2 miles); K-bentonite is exposed at 500 feet north of the bridge on top of the hill; sample is from the top of almost 16-20 inches thick K-bentonite layer. Color is white and yellowish brown; fine crystalline; highly weathered.

K-bentonite: KB-9C; 8 inches below KB-9A; color is white to yellowish-brown when weathered and light green when fresh; fine crystalline; biotite crystals hardly visible; moderately weathered.

K-bentonite: KB-9D; 10 inches below KB-9A; lithologically similar to KB-9C.

K-bentonite: KB-9B; 18 inches below KB-9A; lithologically similar to KB-9C.

K-bentonite: KB-9BU; random sample from T-3 K-bentonite at Round Lick Creek. Lithologically similar to KB-9C.

Limestone: LS-9A; Carters Limestone; just above KB-9A. Color is light gray; sublithographic; no chert is observed but silicified fossils are present.

Limestone: LS-9B; Carters Limestone; just below KB-9B. Lithologically similar to LS-9A. Below T-3 there is a chert layer, but it is not always in contact with K-bentonite.

Limestone: LS-9C; Carters Limestone. Color is light gray; sublithographic with bird's eye calcite; massive.

Chert: LS-9D; In Carters Limestone at Round Lick Creek; below T-3.

K-bentonite: KB-10; Quarry sample; Round Lick Creek, Rome, Tennessee. Color is light green; sandy appearance; weathered.

K-bentonite: KB-11; Quarry sample; T-2 (?). K-bentonite in Carters Limestone; nearly 60 feet below the top of quarry at south of U.S. Highway 231 from Murfreesboro to Lebanon (ref: Wilson, 1958, Log. no. 10A, p. 32, 27.3 miles); a continuous bed of almost 8 inches thick. Color is light gray; fine crystalline; calcerous.

K-bentonite: KB-12; quarry sample; T-3 horizon in Carters Limestone; same locality as KB-11; thickness of the bentonite layer is almost 28 inches. Color is mostly white with brownish and light green patches; sandy appearance; highly weathered.

K-bentonite: KB-13; outcrop sample; T-3 horizon in Carters Limestone; on U.S. Highway 231, almost 4 miles south of Lebanon (ref: Wilson, 1958, Log. no. 10A, p. 32, 26.3-26.5 miles); almost 16 inches thick K-bentonite layer. Color is yellowish brown with light green patches; sandy appearance; highly weathered.

Limestone: LS-13A; Carters Limestone; overlying T-3 sample KB-13. Color is gray; sublithographic; massive.

Limestone: LS-13B; Carters Limestone; underlying T-3 sample KB-13. Color is gray; sublithographic; massive; cherty.

K-bentonite: KB-14; outcrop sample; High Bridge, Kentucky; on U.S. Highway 68 from Wilmore to Harrodsburg; in Tyrone Limestone K-bentonite B-6 is exposed at southwest of railroad (ref: Kerr and Kulp, 1949); 8 inch thick layer. Color is light-gray when fresh and brownish-yellow when weathered; fine crystalline; massive; weathered.

Limestone: LS-14A; Tyrone Limestone; just above KB-14. Color is gray; sublithographic with bird's eye calcite; massive.

Limestone: LS-14B; Tyrone Limestone; just below KB-14. Lithologically similar to LS-14A.

K-bentonite: KB-15A; quarry sample; High Bridge, Kentucky; on U.S. Highway 68 from Wilmore to Harrodsburg; in Tyrone Limestone K-bentonite B-3 is exposed in the quarry (ref: Kerr and Kulp, 1949); thickness is almost 2 feet; sample is from the top of K-bentonite layer. Color is light gray; fine crystalline; massive; highly weathered.

K-bentonite: KB-15C; 12 inches below KB-15A. Lithologically similar to KB-15A.

K-bentonite: KB-15B; 22 inches below KB-15A. Lithologically similar to KB-15A.

Limestone: LS-15A; Tyrone Limestone; at almost 80 feet below the top of quarry and above B-3. Color is gray; sublithographic with bird's eye calcite; massive.

Limestone: LS-15B; Tyrone Limestone; below T-3. Lithologically similar to LS-15A.

K-bentonite: KB-16 (KB-1G)***; core sample; Cincinnati Gas and Elec. Co., hole 4, box 49; Grant Co., Kentucky. 10 inches thick K-bentonite. Color is light greenish-gray; fissile; fine crystalline with few biotite crystals visible to naked eye; slightly calcerous.

K-bentonite: KB-17 (KB-2G); core sample; Cincinnati Gas and Elec. Co., hole 4, box 51; Grant Co., Kentucky; depth: 525 feet; 3 inches thick K-bentonite. Color is light gray; fine crystalline with barely visible biotite flakes; massive; slightly calcerous.

K-bentonite: KB-18A (KB-1F)***; core sample; Cincinnati Gas and Elec. Co., hole 3, box 26; Grant Co., Kentucky; depth: 267 feet, 4 inches; 20 inches thick K-bentonite. Color is light green; fissile; fine crystalline with fairly abundant and fresh biotite crystals.

K-bentonite: KB-18B (KB-1F); core description is same as KB-18A; but is at lower part of the K-bentonite layer. Lithologically similar to KB-18A.

K-bentonite: KB-19A (KB-2F); core sample; Cincinnati Gas and Elec. Co., hole 3, box 28; Grant Co., Kentucky. 25 inches thick K-bentonite. Color is greenish gray; fine crystalline; very few biotite crystals; conchoidal fracture; massive.

K-bentonite: KB-19B (KB-2F); core description is same as KB-19A, but it is at lower part of the bentonite layer. Lithologic description is similar to KB-19A.

K-bentonite: KB-19C (KB-2F); core description is same as KB-19A; sample from the bottom of K-bentonite layer. Color is green; fine crystalline; very few biotite crystals; fresh.

K-bentonite: KB-19D (KB-2F); core and lithologic descriptions are the same as KB-19C. Only core includes a sharp contact between a green, very fine grained lithology and a light green coarser grained lithology.

K-bentonite: KB-20A (KB-3E)***; core sample; Cincinnati Gas and Elec. Co., hole 2, box 26; Gallatin Co., Kentucky; 20 inches thick K-bentonite. Color is green with dark green patches; very fine crystalline; very few biotite crystals; massive; fresh.

K-bentonite: KB-20B (KB-3E); core description is same as KB-20A. Color is green with dark green patches; fissile; fine to coarse crystalline; fairly abundant biotite crystals.

K-bentonite: KB-21 (KB-1D)***; core sample; Cincinnati Gas and Elec. Co., hole 1, box 24; Big Boone, Boone Co., Kentucky; top of Tyrone: 244.83 feet. Depth: 248.08 feet. 9 inches thick K-bentonite. Color is light gray; fissile; very fine crystalline with very few biotite crystals; slightly calcerous.

K-bentonite: KB-22A (KB-2D); core sample; Cincinnati Gas and Elec. Co., hole 2, box 26; Boone Co., Kentucky; depth: 281 feet 6 inches; 22 inches thick K-bentonite layer. Color is green with dark green patches; very fine crystalline with few biotite crystals visible to naked eye; fresh; massive.

K-bentonite: KB-22B (KB-2D); core and lithologic descriptions are similar to KB-22A.

K-bentonite: KB-23A (KB-1C)***; core sample; Cincinnati Gas and Elec. Co., hole 1, box 34, Constance, Kentucky; depth: 348 feet; 24 inches thick bentonite. Color is light gray; fissile; fine to coarse crystalline with abundant biotite flakes.

K-bentonite: KB-23C (KB-1C); core and lithologic descriptions are same as KB-23A.

K-bentonite: KB-24A (KB-2CA)***; core sample; Cincinnati Gas and Elec. Co., hole 1, box 23, Constance, Kentucky; depth: 481 feet; 12 inches thick bentonite; color is light gray; very fine crystalline; massive.

K-bentonite: KB-24B (KB-2CB); core description is same as KB-24A; depth: 487 feet; 7 inches thick bentonite. Lithologically similar to KB-24A.

K-bentonite: KB-25 (KR-14); quarry sample; Frankfort, Kentucky; on Kentucky route 1211; depth: 15 feet below top of Tyrone Limestone; 8 inches thick bentonite; obtained from Dr. Launsbery, Purdue University.

K-bentonite: KB-26 (KR-9); quarry sample; High Bridge, Kentucky; at top of Tyrone Limestone (ref: Kerr and Kulp, 1949). Color is gray when fresh, brown when weathered; fine crystalline; massive.

K-bentonite: KB-27A (KR-4); quarry sample; Athens, Kentucky; in Tyrone Limestone. Color is gray; very fine crystalline; few biotite crystals; fresh; massive.

K-bentonite: KB-27B (KR-4); quarry sample; Athens, Kentucky; 6 feet below the top of Tyrone Limestone; from new quarry. Lithologic description is similar to KB-27A.

K-bentonite: KB-28A (C-2); core sample; Glencoe Quad., Gallatin Co., Kentucky; 20 inches thick bentonite; in Tyrone Limestone. Color is gray; fissile; fine to coarse crystalline with abundant biotite crystals; fresh.

K-bentonite: KB-28B (C-2); 4.5 inches below KB-28A. Lithologic description is same as KB-28A.

K-bentonite: KB-28C (C-2); 6.4 inches below KB-28A. Color is light green; fine crystalline with abundant biotite crystals; fissile; fresh.

K-bentonite: KB-28D (C-2); 8 inches below KB-28A. Lithologic description is same as KB-28C.

K-bentonite: KB-28E (C-2); 10.4 inches below KB-28A. Lithologically similar to KB-28C.

K-bentonite: KB-28F (C-2); 15.2 inches below KB-28A. Color is light green; fine to coarse crystalline with abundant coarse biotite crystals; fissile.

K-bentonite: KB-28G (C-2); 17 inches below KB-28A. Lithologic description is same as KB-28F.

K-bentonite: KB-28H (C-2); 19 inches below KB-28A. Color is green with dark green patches; fine crystalline with fairly abundant biotite crystals; fresh; massive.

K-bentonite: KB-29; core sample; Lawrence Co., Indiana; Twp. 5N, Rge. 2E, Sec. 27, SE NE NE; K-bentonite at top of Black River Formation; depth: 1706 feet; obtained from Indiana Geological Survey, Bloomington, Indiana. Color is greenish-gray; very fine crystalline; massive.

K-bentonite: KB-30A; core sample; Switzerland Co., Indiana; Twp. 2N, Rge. 1W, Sec. 1, NW SE SE; K-bentonite at top of Black River Formation; depth 335 feet; 10 inches thick bentonite; sample is from the top of K-bentonite layer; obtained from Indiana Geological Survey, Bloomington, Indiana. Lithologic description is similar to KB-29.

K-bentonite: KB-30B; 4 inches below KB-30A. Lithologically similar to KB-30A.

K-bentonite: KB-30C; 9.5 inches below KB-30A. Lithologically similar to KB-30A.

K-bentonite: KB-34A; core sample; Columbus City Quad., Marshal Co., Alabama; Murphy Hill bentonite samples, box 6, hole AH-40; obtained from Tennessee Valley Authority, Knoxville, Tennessee; from undivided Ordovician Chickamauga Formation. Color is green; coarse crystalline with very abundant biotite crystals; fissile; fresh.

K-bentonite: KB-34B; 4.8 inches below KB-34A. Core and lithologic descriptions are same as KB-34A.

K-bentonite: KB-35; core sample; Columbus City Quad., Marshall Co., Alabama; Murphy Hill bentonite sample, box 7, hole AH-40; obtained from Tennessee Valley Authority, Knoxville, Tennessee; from undivided Ordovician Chickamauga Formation. Color is dark green; fine crystalline; few biotite crystals fairly visible to naked eye; massive; fresh.

Numbers in parenthesis refer to old call numbers:

* University of Kentucky, U.S.G.S. Log Store House call number

** Tennessee K-bentonite core samples. Courtesy of Cominco American Co., Cookeville, Tennessee.

*** Ref: Huff, 1963 a, p. 12.

APPENDIX B

SAMPLE PREPARATION FOR THE STUDY TECHNIQUES

Preparation of Fused Borate Glass Pellets for X-Ray Fluorescence Analysis:

The fusion mixture is prepared as follows:

1 q preignited rock powder (minus 100 mesh)

6 q anhydrous lithium tetraborate ($Li_2B_2O_7$)

1.5q lithium nitrate ($LiNO_3$)

After complete mixing, the mixture is transferred into a platinum crucible and 4 drops of HBr solution are added to the flux to reduce stress cracking and also to serve as a nonwetting agent.

The mixture is heated in a covered platinum crucible on a gas-air Meeker burner at 1100°C for 15 minutes. After the first 10 minutes of heating, the melt is stirred in order to insure homogenization. Meanwhile a graphite mold and an aluminum plunger are kept on a hot plate about 220°C. After 15 minutes the melt is quickly poured into the graphite mold and the plunger is immediately brought down gently to mold and quench the melt. After 1 minute the plunger is then withdrawn and the glass pellet is put between two clean asbestos mats on the hot plate. After the preparation of the other glass pellets, the hot plate is turned off and the pellets allowed to cool slowly to room temperature. The pellets are then ready for analysis. However, surfaces to be irradiated should be cleaned with acetone before each analysis.

Preparation of Thin-Sections from K-Bentonite Bulk Samples:

This method is described by Martin, Litz and Huff (1979) and is primarily used to prepare thin-sections of clayey sediments and other friable materials.

First, the rock is sawed flat and trimmed into a small wafer in the required orientation without using any coolant. Ideally, the rock slab is a rectangular prism, its larger surface (approximately 24 x 34 mm) fitting the glass slide on which it will be mounted, and having a thickness of approximately 1/2 inch. Then, one face of the wafer is temporarily mounted on a glass slide with Lakeside 70 and the opposite face is ground dry until flat. This new surface is impregnated with an epoxy (100 parts of resin, Epon 815 and 11 parts of hardener, diethylenetriamine-DTA, supplied by Miller-Stephenson Chemical Co., Inc., Danbury, Connecticut, 06810) at +200°F for 5 minutes. A second slide is attached to the impregnated surface and is allowed to cure.

In the next step the second glass slide mounted with epoxy is ground off with a thin-section cut-off saw, leaving 0.020 inch of slab attached to the slide. Then, by using a coolant, the surface of the rock slab is ground until a thickness of rock totally impregnated by the epoxy is reached. On this new surface a third, frosted glass slide is attached using Hillquist thin-section epoxy, and it is allowed to cure at +200°F.

The last step involves the grinding off the second slide attached by the epoxy and the reducing the thickness of the rock slab to 30 m (0.03 mm). Final grinding is done by hand and excellent control over final thickness with standard birefrengence colors are provided. The slide is covered by a cover glass following the standard methods of thin-section preparation.

APPENDIX C

OPERATING CONDITIONS FOR X-RAY FLOURESCENCE SPECTROMETRY

TABLE I - X-Ray spectrograph operating conditions

Element	Target	Crystal	Peak 2	Line	Detector	Path	DCK	mA	KVP
Al	Cr	PET	144.67	K	Flow	Vacuum	1800	50	55
Fe	Cr	LiF-4.08Å	57.52	K	Flow	Air	1800	30	45
K	Cr	LiF-4.08Å	136.68	K	Flow	Air	1800	50	55
Ti	Cr	LiF-4.08Å	86.13	K	Flow	Air	1800	30	45
Rb	W	LiF-4.08Å	26.62	K	Flow	Air	1800	30	55
Sr	W	LiF-4.08Å	25.15	K	Flow	Air	1800	30	55
Y	W	LiF-4.08Å	23.80	K	Flow	Air	1800	40	60
Zr	W	LiF-4.08Å	22.55	K	Flow	Air	1800	30	55
Zn	Cr	LiF-4.08Å	41.80	K	Flow	Air	1800	40	60
Nb	W	LiF-4.08Å	21.40	K	Flow	Air	1800	40	60
Ga	Cr	LiF-4.08Å	38.92	K	Flow	Air	1800	40	60
Ge	Cr	LiF-4.08Å	36.33	K	Flow	Air	1800	40	60

APPENDIX D

PRECISION, ACCURACY AND WITHIN SAMPLE HOMOGENEITY OF X-RAY FLUORESCENCE TECHNIQUE

TABLE I - The precision of X-Ray fluorescence technique.

(Means for Al_2O_3, Fe_2O_3T, K_2O in weight percent; for TiO_2, Rb, Sr, Y, Zr, Zn, Nb, Ga, Ge in parts per million.)

Oxide or Element	No. of Observations	Standard Used	Mean	Variance	Std. Dev. (±)	Coeff. of Variation
Al_2O_3	12	AGV-1	17.44	0.180	0.43	0.024
Fe_2O_3T	12	AGV-1	6.77	0.002	0.05	0.007
K_2O	12	AGV-1	2.82	0.008	0.09	0.032
TiO_2	12	AGV-1	10522	12566	112.00	0.010
Rb	12	G-2	168.13	84.26	9.17	0.054
Sr	12	G-2	429.13	470.43	21.68	0.050
Y	10	G-2	20.84	50.12	7.07	0.339
Zr	12	G-2	346.07	215.01	14.66	0.042
Zn	12	G-2	84.69	11.00	3.31	0.039
Nb	12	G-2	25.12	8.31	2.88	0.114
Ga	12	G-2	19.07	5.87	2.42	0.127
Ge	12	G-2	0.688	0.022	0.149	0.216

TABLE II - The accuracy of X-Ray fluorescence technique (Standard concentrations after Abbey (1973), only the contents of Al_2O_3, Fe_2O_3T, K_2O and TiO_2 recalculated considering ignition. Al_2O_3, Fe_2O_3T and K_2O in weight percent; TiO_2, Rb, Sr, Y, Zr, Zn, Nb, Ga and Ge in parts per million.)

Oxide or Element	No. of Observations	Standard Used	Concentration in Standard (std)	Mean ($\bar{x}$)	Accuracy (std-$\bar{x}$)
Al_2O_3	12	AGV-1	17.39	17.44	0.05
Fe_2O_3T	12	AGV-1	6.90	6.77	0.13
K_2O	12	AGV-1	2.95	2.82	0.13
TiO_2	12	AGV-1	10600.00	10522.00	78.00
Rb	12	G-2	170.00	168.13	1.87
Sr	12	G-2	480.00	429.00	50.14
Y	12	G-2	12.00	20.84	8.84
Zr	12	G-2	300.00	346.07	46.07
Zn	12	G-2	85.00	84.69	0.31
Nb	12	G-2	14.00	25.12	11.12
Ga	12	G-2	23.00	19.07	3.93
Ge	12	G-2	0.71	0.7179	0.0079

TABLE III - Within sample homogeneity for K-bentonite bulk samples 28C and 28D during the X-Ray fluorescence analyses.
(Means for Al_2O_3, Fe_2O_3T and K_2O in weight percent; for TiO_2, Rb, Sr, Y, Zr, Zn, Nb, Ga and Ge in parts per million.)

Oxide or Element	No. of Observations	Sample Used	Mean	Variance	Std. Dev. (±)	Coeff. of Variation
Al_2O_3	8	28C	20.15	0.430	0.650	0.032
Fe_2O_3T	8	28C	1.36	0.0004	0.021	0.015
K_2O	8	28C	7.92	0.033	0.182	0.023
TiO_2	8	28C	2651.00	4113.00	64.00	0.024
Rb	8	28D	185.51	261.72	16.17	0.087
Sr	8	28D	102.45	298.73	17.28	0.168
Y	8	28D	32.55	129.58	11.38	0.349
Zr	8	28D	292.20	803.83	28.35	0.097
Zn	8	28D	93.64	49.83	7.05	0.075
Nb	8	28D	37.34	81.91	9.05	0.242
Ga	8	28D	23.94	48.71	6.97	0.291
Ge	8	28D	1.064	0.1343	0.366	0.344

APPENDIX E

CALIBRATION CURVE FOR MASS-ABSORBTION COEFFICIENT DETERMINATIONS

TABLE I - Calculated values of $\mu_{1.5\text{Å}, \text{std}}$ and measured X-Ray fluorescent intensities of 17 standards.

Standard	$\mu_{1.5\text{Å}, \text{std}}$	$IWL\alpha_c$
Na_2CO_3	16.79	0.618
$MgCO_3$	16.83	0.538
85% $MgCO_3$ + 15% SY-2	22.31	0.726
Al_2O_3	28.33	0.974
50% $MgCO_3$ + 50% SY-2	35.12	1.102
RGM-1 (Rhyolite)*	39.26	1.242
G-2 (Granite)**	42.15	1.310
SCo-1 (Cody Shale)*	43.75	1.283
QLO-1 (Quartz Latite)*	44.75	1.433
GSP-1 (Granodiorite)**	45.89	1.362
MAG-1 (Marine Mud)*	47.51	1.469
SDO-1 (Ohio Black Shale)***	50.01	1.428
AGV-1 (Andesite)**	50.26	1.463
SY-2 (Syenite)****	53.42	1.602
80% $CaCO_3$ + 20% $MgCO_3$	59.23	1.599
BCR-1 (Basalt)**	63.87	1.811
$CaCO_3$	69.84	1.826

* Chemical analyses from Flanagan (1976).
** Chemical analyses from Flanagan (1969).
*** Chemical analyses are obtained from J.B. Maynard, Dept. of Geology, University of Cincinnati.
**** Chemical analyses from Abbey et. al. (1975).

FIGURE E. I. Relation between the intensities of Compton-scattered x-rays and calculated mass-absorbtion coefficients from materials of known composition.

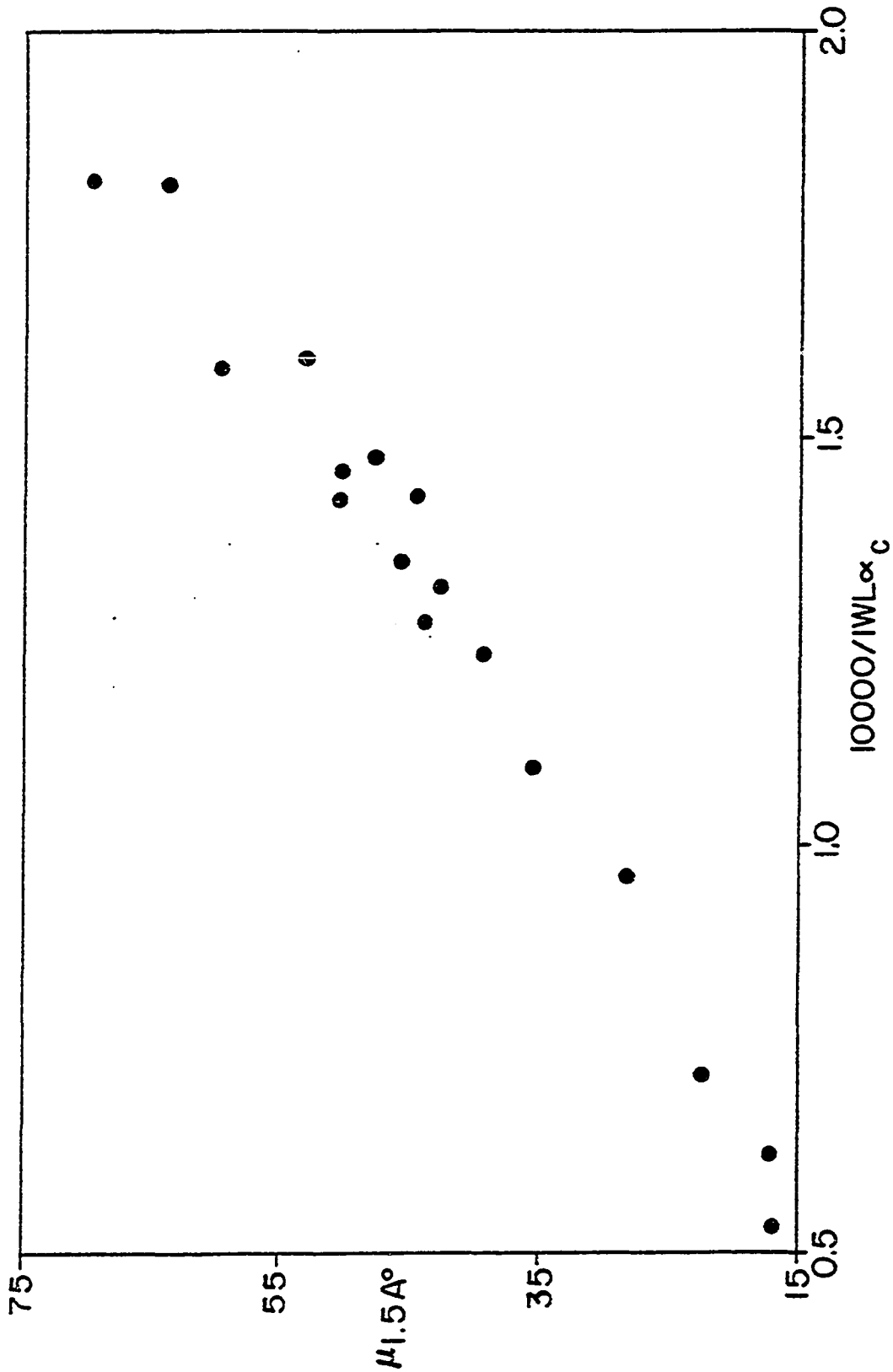

Statistical Information on Figure E.1.

Scatter diagram is obtained by using the computer program SPSS (Statistical Package for the Social Sciences).

Correlation (R)	:	0.98623
Std. Err. of Est.	:	2.61560
R Squared	:	0.97264
Intercept	:	-7.82756
Significance	:	0.00001
Slope (B)	:	39.58454

APPENDIX F

PARTIAL CHEMICAL ANALYSES OF K-BENTONITE BULK SAMPLES AND LESS THAN 2 μm CLAY FRACTIONS

TABLE I - Chemical analyses of K-bentonite bulk samples. (SiO_2, Al_2O_3, Fe_2O_3T, MgO, CaO, Na_2O, K_2O, TiO_2, MnO in weight percent; Rb, Sr, Y, Zr, Zn, Nb, Ga and Ge in parts per million).

Sample No.	1	2	3	4A	4B	5A	5B
SiO_2	54.60	56.50	22.90	55.80	53.80	n.d	53.70
Al_2O_3	20.37	20.80	5.87	19.99	20.56	n.d	21.73
Fe_2O_3T	1.48	1.71	2.16	2.64	2.53	n.d	2.21
MgO	3.71	3.24	4.16	4.50	3.83	n.d	3.76
CaO	0.80	0.55	39.97	0.39	0.38	n.d	0.58
Na_2O	0.99	1.05	0.41	1.22	1.36	n.d	1.31
K_2O	8.93	9.93	2.37	8.26	8.16	n.d	8.12
TiO_2	0.50	0.99	0.35	0.33	0.36	n.d	0.29
MnO	0.04	0.05	0.10	0.03	0.08	n.d	0.05
Rb	168.50	134.88	7.69	187.55	165.75	191.82	189.58
Sr	90.12	88.74	194.14	81.19	77.46	102.81	111.04
Y	20.33	36.65	---	28.47	21.01	35.51	19.45
Zr	390.94	418.31	38.18	264.93	392.66	288.80	293.21
Zn	17.72	18.39	---	29.90	24.62	5.60	31.46
Nb	20.61	29.20	---	19.14	10.98	25.27	33.78
Ga	22.10	24.55	---	24.46	17.52	27.21	30.46
Ge	0.913	1.567	---	1.405	0.958	1.739	1.422

TABLE I - Chemical analysis of K-bentonite bulk samples - Continued

Sample No.	5CD	5D	5E	5F	5G	5H	5Bu
SiO_2	n.d	n.d	60.05	49.00	51.20	53.40	59.50
Al_2O_3	21.91	n.d	n.d	19.97	22.98	21.63	19.61
Fe_2O_3T	2.28	n.d	n.d	2.46	2.30	2.30	3.25
MgO	n.d	n.d	3.74	3.71	4.00	3.44	4.16
CaO	n.d	n.d	0.48	0.20	---	---	0.03
Na_2O	n.d	n.d	1.21	1.18	1.14	1.33	1.49
K_2O	7.77	n.d	n.d	7.34	7.66	8.04	8.92
TiO_2	0.21	n.d	n.d	0.27	0.32	0.31	0.39
MnO	n.d	n.d	---	0.02	0.04	0.03	0.04
Rb	187.41	173.07	185.45	175.53	187.61	199.86	125.94
Sr	116.27	101.94	112.42	98.73	100.98	122.51	54.86
Y	21.68	25.66	12.27	26.53	23.23	49.94	13.50
Zr	244.81	306.31	302.54	297.26	279.47	345.45	239.54
Zn	24.57	34.74	25.09	34.11	27.48	37.19	28.57
Nb	38.06	45.27	30.98	20.89	25.28	52.76	13.25
Ga	23.74	25.67	24.20	25.99	21.78	25.86	17.64
Ge	1.025	1.334	0.970	1.329	0.824	1.213	1.241

TABLE I - Chemical analysis of K-bentonite bulk samples - Continued

Sample No.	6A	6B	6C	6D	6E	7A	7B
SiO_2	54.20	54.60	54.3	51.60	60.60	39.30	n.d
Al_2O_3	21.16	20.19	20.16	n.d	n.d	13.29	19.14
Fe_2O_3T	2.51	2.80	2.32	n.d	n.d	1.76	2.69
MgO	4.18	4.20	4.49	3.83	3.19	2.82	n.d
CaO	0.30	0.13	0.76	0.44	0.37	15.00	n.d
Na_2O	0.80	0.93	1.25	1.07	0.83	0.85	n.d
K_2O	7.47	8.54	8.02	n.d	n.d	5.71	8.06
TiO_2	0.29	0.32	0.29	n.d	n.d	0.21	0.29
MnO	0.04	0.02	0.07	0.04	0.07	0.06	n.d
Rb	187.31	158.77	177.57	179.32	169.10	58.59	171.58
Sr	84.34	61.16	104.50	80.33	86.77	116.71	141.33
Y	27.98	19.63	33.34	24.32	8.57	0.61	68.50
Zr	345.65	254.67	262.01	362.88	294.71	101.47	347.29
Zn	27.16	26.13	22.40	27.07	29.08	1.61	20.84
Nb	28.97	20.16	27.97	42.41	35.68	---	59.33
Ga	28.58	22.76	30.54	24.50	0.846	1.305	30.47
Ge	1.224	1.001	0.956	28.98	0.999	0.088	1.33

TABLE I - Chemical analysis of K-bentonite bulk samples - Continued

Sample No.	7C	7D	8A	8B	8C	8D	8E
SiO_2	54.10	59.30	61.30	n.d	49.10	n.d	62.20
Al_2O_3	18.96	19.75	16.00	18.87	20.88	20.98	21.86
Fe_2O_3T	2.68	2.36	2.51	2.22	1.86	1.75	2.43
MgO	3.97	3.77	2.54	n.d	3.64	n.d	2.42
CaO	0.51	0.58	2.93	n.d	0.70	n.d	2.47
Na_2O	1.17	1.30	1.03	n.d	1.02	n.d	1.05
K_2O	7.90	7.60	7.00	7.52	7.40	7.31	7.92
TiO_2	0.32	0.28	0.34	0.33	0.30	0.3	0.29
MnO	0.04	0.02	---	n.d	0.07	n.d	0.01
Rb	189.42	155.62	124.32	206.16	200.19	194.18	152.10
Sr	98.41	75.59	101.55	175.88	150.32	152.65	119.88
Y	47.83	27.22	25.98	76.64	65.47	284.30	12.93
Zr	301.82	273.80	262.56	389.21	365.56	369.45	276.74
Zn	23.13	24.56	22.05	32.63	35.29	32.00	24.97
Nb	27.01	42.60	20.96	90.06	83.92	100.87	30.08
Ga	19.13	25.80	18.45	27.56	31.50	37.81	21.77
Ge	0.941	1.353	1.016	1.151	1.212	1.587	0.978

TABLE I - Chemical analysis of K-bentonite bulk samples - Continued

Sample No.	8F	9Bu	10	11	14	15A	15B
SiO_2	56.70	50.80	58.60	16.20	14.30	14.90	16.00
Al_2O_3	n.d	23.72	22.01	5.56	2.16	4.63	5.21
Fe_2O_3T	n.d	0.69	1.06	1.63	0.91	1.82	1.57
MgO	3.55	3.15	3.41	2.82	1.18	6.22	6.50
CaO	0.48	0.40	0.89	41.00	62.30	38.81	40.31
Na_2O	1.90	0.16	0.09	0.33	0.20	0.23	0.29
K_2O	n.d	8.70	9.04	1.66	1.24	1.70	2.12
TiO_2	n.d	0.58	0.61	0.21	0.07	0.19	0.21
MnO	0.04	0.01	---	0.02	0.06	0.04	0.06
Rb	165.23	162.08	157.33	---	---	---	---
Sr	106.04	98.29	69.64	205.13	79.98	113.06	79.57
Y	34.94	20.19	27.84	---	---	---	---
Zr	299.26	356.53	356.98	---	---	---	---
Zn	25.63	21.36	41.94	---	---	---	---
Nb	53.76	42.97	26.84	---	---	---	---
Ga	39.41	28.59	26.47	---	---	---	---
Ge	1.316	1.261	1.212	---	---	---	---

TABLE I - Chemical analysis of K-bentonite bulk samples - Continued

Sample No.	15C	16	17	18A	18B	19A	19B
SiO_2	14.90	57.20	n.d	60.00	56.40	41.40	45.20
Al_2O_3	4.96	20.11	n.d	16.88	18.78	17.10	19.13
Fe_2O_3T	1.91	1.20	n.d	2.11	1.63	1.00	1.16
MgO	6.91	3.42	n.d	2.68	2.62	3.31	3.39
CaO	25.01	3.20	n.d	2.07	2.53	9.66	6.90
Na_2O	0.26	0.96	n.d	0.66	0.79	0.89	0.95
K_2O	2.24	9.48	n.d	11.54	8.20	8.03	8.81
TiO_2	0.22	0.23	n.d	0.52	0.21	0.31	0.38
MnO	0.08	0.06	n.d	---	0.07	---	0.01
Rb	3.87	123.02	136.48	114.31	190.57	129.50	109.80
Sr	128.47	67.26	92.92	220.13	89.05	129.87	102.68
Y	---	14.22	8.71	20.31	35.01	30.23	25.78
Zr	15.03	169.08	268.57	825.88	250.73	244.43	243.52
Zn	2.50	9.01	4.97	15.51	32.02	7.62	---
Nb	---	20.57	20.67	16.76	33.94	26.53	21.46
Ga	---	25.71	14.05	12.79	26.69	17.66	18.45
Ge	---	0.995	0.780	0.882	1.057	0.914	0.910

TABLE I - Chemical analysis of K-bentonite bulk samples - Continued

Sample No.	19C	19D	20A	20B	21	22A	22B
SiO_2	44.00	52.00	55.80	55.00	54.80	54.70	54.20
Al_2O_3	21.23	19.99	20.69	19.99	22.67	20.21	20.70
Fe_2O_3T	2.56	1.53	1.42	1.16	1.36	1.24	1.20
MgO	3.42	4.09	3.97	3.62	3.74	3.98	4.00
CaO	5.69	0.53	0.65	0.51	0.86	0.40	---
Na_2O	0.97	1.56	1.41	1.10	1.18	1.07	0.96
K_2O	9.66	7.85	8.06	8.17	6.91	7.85	8.11
TiO_2	0.33	0.46	0.36	0.39	0.28	0.44	0.39
MnO	0.01	0.03	0.02	0.07	0.02	0.02	0.02
Rb	167.52	193.80	201.29	204.88	171.87	230.81	170.76
Sr	119.08	116.10	133.36	108.43	121.45	155.57	88.32
Y	2.97	56.66	28.82	34.79	20.91	49.04	41.14
Zr	341.31	330.05	309.51	355.59	219.33	425.83	307.21
Zn	14.41	24.21	63.85	59.87	80.75	78.58	61.14
Nb	18.59	43.85	29.20	36.82	28.19	65.01	26.44
Ga	19.85	35.00	23.46	31.40	23.34	32.58	19.45
Ge	0.844	1.633	0.987	1.136	1.108	1.672	0.817

TABLE I - Chemical analysis of K-bentonite bulk samples - Continued

Sample No.	23A	23C	24A	24B	25	26	27A
SiO_2	47.70	57.40	47.50	43.20	53.20	52.10	n.d
Al_2O_3	19.69	21.39	18.56	16.89	18.91	19.65	20.56
Fe_2O_3T	1.63	1.59	1.39	1.74	1.53	1.96	1.71
MgO	4.08	4.09	4.35	5.41	3.31	4.09	n.d
CaO	1.60	0.56	9.39	16.50	0.10	---	n.d
Na_2O	0.90	1.21	1.01	0.62	0.94	0.10	n.d
K_2O	7.99	7.89	6.71	6.33	10.10	7.78	7.86
TiO_2	0.23	0.23	0.26	0.31	0.32	0.26	0.41
MnO	0.05	0.02	0.03	0.02	0.06	0.05	n.d
Rb	190.58	167.65	184.02	144.80	155.74	168.18	173.82
Sr	101.20	72.54	141.27	141.48	82.25	53.80	99.76
Y	30.97	52.61	31.82	17.73	25.81	47.74	40.12
Zr	244.76	235.44	342.61	255.31	259.60	286.82	292.03
Zn	66.14	63.50	26.05	22.76	10.73	19.78	19.87
Nb	26.20	22.35	41.91	19.01	42.87	22.28	33.63
Ga	26.36	22.27	25.47	12.02	26.85	21.56	25.77
Ge	0.953	0.873	0.903	0.535	1.323	0.809	1.156

TABLE I - Chemical analysis of K-bentonite bulk samples - Continued

Sample No.	27B	28A	28B	28C	28D	28E	28F
SiO_2	60.30	54.70	54.80	n.d	49.40	56.40	57.10
Al_2O_3	20.85	17.41	19.00	21.10	19.77	18.61	17.91
Fe_2O_3T	1.65	1.68	1.81	1.35	1.60	1.61	1.56
MgO	4.47	4.05	4.07	n.d	4.40	4.13	3.95
CaO	0.86	0.30	0.69	n.d	0.40	0.13	0.52
Na_2O	0.18	1.10	1.64	n.d	1.07	1.03	1.09
K_2O	8.26	7.95	7.78	7.96	7.72	8.20	7.81
TiO_2	0.41	0.23	0.27	0.27	0.26	0.23	0.26
MnO	0.02	0.04	0.01	n.d	---	---	0.05
Rb	179.28	175.22	181.16	204.89	167.35	189.52	178.83
Sr	132.64	96.61	110.44	132.54	86.84	116.77	100.48
Y	35.69	35.95	26.82	22.10	19.42	27.73	38.26
Zr	308.75	209.81	284.77	319.72	272.15	300.08	272.86
Zn	15.31	102.70	69.63	61.58	89.97	63.14	118.57
Nb	29.53	32.99	30.14	32.01	33.93	41.22	39.09
Ga	25.87	28.70	29.66	25.44	30.23	30.37	37.39
Ge	1.083	0.931	0.986	0.689	1.054	1.199	1.571

TABLE I - Chemical analysis of K-bentonite bulk samples - Continued

Sample No.	28G	28H	29	30A	30B	30C	34A
SiO_2	57.80	57.20	51.60	35.70	46.50	n.d	56.50
Al_2O_3	18.12	17.80	23.71	23.09	18.80	n.d	17.72
Fe_2O_3T	1.37	0.98	1.73	1.03	0.98	n.d	3.85
MgO	3.81	3.12	3.19	4.19	4.03	n.d	4.59
CaO	0.20	0.18	0.40	0.40	0.10	n.d	0.90
Na_2O	1.03	1.54	0.84	1.09	0.96	n.d	0.92
K_2O	9.33	8.91	8.50	7.53	7.72	n.d	6.53
TiO_2	0.19	0.27	0.54	0.37	0.36	n.d	0.42
MnO	0.03	0.09	0.01	---	0.04	n.d	0.02
Rb	170.58	167.84	179.45	172.73	199.38	181.71	199.57
Sr	94.20	107.27	252.89	91.21	125.35	111.83	122.04
Y	42.76	43.16	26.17	66.22	31.38	46.89	27.66
Zr	263.99	227.09	612.78	281.44	323.27	324.45	249.36
Zn	55.12	95.10	25.52	94.03	47.13	71.01	62.93
Nb	21.94	48.13	24.09	45.25	32.01	59.62	26.59
Ga	23.53	31.37	30.86	24.05	26.72	31.65	29.95
Ge	1.035	1.155	1.251	0.985	1.318	1.327	1.249

TABLE I - Chemical analysis of K-bentonite bulk samples - Continued

Sample No.	34B	35	14 carbonates destructed
SiO_2	n.d	48.20	52.20
Al_2O_3	n.d	18.96	n.d
Fe_2O_3T	n.d	5.30	n.d
MgO	n.d	4.71	2.33
CaO	n.d	2.87	5.64
Na_2O	n.d	0.78	2.64
K_2O	n.d	9.01	n.d
TiO_2	n.d	1.15	n.d
MnO	n.d	---	0.05
Rb	148.94	110.80	163.03
Sr	79.76	54.93	109.31
Y	34.02	22.25	15.80
Zr	236.04	240.66	135.99
Zn	62.40	29.09	44.92
Nb	22.24	18.32	17.24
Ga	24.72	8.05	35.59
Ge	0.811	0.40	1.227

n.d : not determined
--- : not detected

TABLE II - Chemical analyses of clay fraction (<2μm) of K-bentonite samples. (SiO_2, Al_2O_3, Fe_2O_3T, MgO, CaO, Na_2O, K_2O, TiO_2, MnO in weight percent; Rb, Sr, Y, Zr, Zn, Nb, Ga and Ge in parts per million).

Sample No.	1	4A	5F	5Bu	6A	6B	6C
SiO_2	53.30	n.d	n.d	56.70	n.d	56.50	38.00
Al_2O_3	23.70	n.d	n.d	21.16	n.d	19.11	21.71
Fe_2O_3T	1.18	n.d	n.d	1.87	n.d	2.00	2.04
MgO	4.60	n.d	n.d	4.34	n.d	4.35	4.68
CaO	0.40	n.d	n.d	0.70	n.d	0.10	0.40
Na_2O	1.84	n.d	n.d	1.60	n.d	1.16	1.44
K_2O	7.71	n.d	n.d	7.41	n.d	6.93	7.15
TiO_2	0.54	n.d	n.d	0.17	n.d	0.18	0.17
MnO	0.03	n.d	n.d	0.03	n.d	0.06	---
Rb	95.17	83.00	93.67	62.15	148.27	165.71	165.66
Sr	---	---	6.24	---	84.76	136.72	120.90
Y	8.73	14.22	12.44	---	46.13	37.80	36.84
Zr	46.50	20.62	11.80	---	176.90	206.64	194.04
Zn	3.61	---	---	5.20	22.15	30.03	11.53
Nb	3.58	19.22	---	---	50.77	83.14	73.22
Ga	6.06	8.85	3.81	9.58	14.67	18.35	16.39
Ge	---	---	---	---	0.106	0.345	0.108

TABLE II - Chemical analyses of clay fraction (<2μm) of K-bentonite samples - Continued

Sample No.	6D	6E	7A	7B	7C	7D	8A
SiO_2	n.d	n.d	55.50	57.30	n.d	57.10	58.50
Al_2O_3	n.d	n.d	17.60	19.25	n.d	19.64	18.24
Fe_2O_3T	n.d	n.d	1.81	1.86	n.d	2.00	1.78
MgO	n.d	n.d	3.96	4.54	n.d	4.62	3.74
CaO	n.d	n.d	7.20	0.80	n.d	0.60	0.60
Na_2O	n.d	n.d	1.27	1.32	n.d	1.28	1.32
K_2O	n.d	n.d	6.81	6.82	n.d	7.11	6.20
TiO_2	n.d	n.d	0.24	0.20	n.d	0.16	0.30
MnO	n.d	n.d	0.03	0.02	n.d	0.02	0.01
Rb	118.13	160.59	n.d	44.12	67.25	84.18	181.46
Sr	67.74	106.71	n.d	---	---	19.69	150.47
Y	22.58	65.06	n.d	2.21	---	15.74	108.30
Zr	108.78	187.55	n.d	---	---	51.56	276.58
Zn	8.49	13.98	n.d	---	---	---	29.46
Nb	39.22	69.94	n.d	---	---	2.78	97.47
Ga	9.34	15.60	n.d	---	7.31	4.34	23.63
Ge	---	0.149	n.d	---	---	---	0.613

TABLE II - Chemical analyses of clay fraction (<2μm) of K-bentonite samples - Continued

Sample No.	8B	8C	8D	8E	8F	14	16
SiO_2	59.60	53.50	n.d	n.d	n.d	n.d	60.00
Al_2O_3	18.13	19.94	n.d	n.d	n.d	7.5	21.12
Fe_2O_3T	1.65	1.60	n.d	n.d	n.d	3.69	0.76
MgO	4.43	4.63	n.d	n.d	n.d	n.d	4.05
CaO	0.60	0.20	n.d	n.d	n.d	n.d	0.70
Na_2O	1.65	1.29	n.d	n.d	n.d	n.d	1.15
K_2O	6.72	6.86	n.d	n.d	n.d	3.93	6.84
TiO_2	0.23	0.21	n.d	n.d	n.d	0.32	0.23
MnO	0.01	0.03	n.d	n.d	n.d	n.d	0.03
Rb	76.10	61.55	92.75	50.09	101.42	n.d	90.09
Sr	---	---	---	---	12.30	n.d	---
Y	---	22.31	4.19	19.82	32.75	n.d	---
Zr	83.63	103.87	123.19	64.80	190.25	n.d	53.92
Zn	---	---	1.53	---	1.67	n.d	---
Nb	---	10.18	1.17	0.71	17.84	n.d	---
Ga	---	9.57	4.04	5.99	7.21	n.d	6.83
Ge	---	---	---	---	---	n.d	---

TABLE II - Chemical analyses of clay fraction (<2μm) of K-bentonite samples - Continued

Sample No.	18A	18B	19A	19B	19C	19D	20A
SiO_2	52.30	52.40	50.00	43.70	47.50	55.10	55.40
Al_2O_3	19.58	21.15	16.96	19.59	19.52	20.69	20.19
Fe_2O_3T	1.49	1.13	1.26	1.20	1.58	1.43	1.65
MgO	4.53	4.34	4.50	4.84	5.01	5.05	4.82
CaO	0.40	0.10	7.60	2.00	0.40	0.10	---
Na_2O	0.92	1.18	1.67	1.67	1.15	1.06	1.72
K_2O	7.75	7.00	6.72	6.60	7.50	7.15	7.06
TiO_2	0.28	0.09	0.44	0.40	0.41	0.24	0.29
MnO	0.01	---	0.06	0.02	0.01	0.01	0.07
Rb	73.14	130.82	62.19	68.00	99.55	81.29	100.83
Sr	---	5.85	---	7.56	---	---	31.05
Y	4.33	20.56	---	18.89	---	3.18	6.32
Zr	9.09	37.54	63.33	93.02	15.15	30.91	78.37
Zn	---	---	---	---	---	---	---
Nb	13.00	---	---	2.90	---	1.13	---
Ga	9.61	7.13	4.91	9.46	4.88	11.43	2.81
Ge	0.114	---	---	---	---	---	---

TABLE II - Chemical analyses of clay fraction (<2μm) of K-bentonite samples - Continued

Sample No.	20B	21	22A	22B	23A	23C	24A
SiO_2	n.d	57.80	51.80	n.d	n.d	53.70	48.90
Al_2O_3	n.d	23.41	20.64	n.d	n.d	21.26	18.28
Fe_2O_3T	n.d	0.78	1.22	n.d	n.d	1.29	0.95
MgO	n.d	3.98	4.58	n.d	n.d	5.35	5.03
CaO	n.d	0.50	0.50	n.d	n.d	1.10	3.90
Na_2O	n.d	1.31	1.18	n.d	n.d	1.11	1.23
K_2O	n.d	7.11	6.75	n.d	n.d	6.66	6.35
TiO_2	n.d	0.18	0.17	n.d	n.d	0.09	0.26
MnO	n.d	0.01	0.02	n.d	n.d	0.01	0.03
Rb	61.32	77.54	71.77	105.86	73.82	95.22	n.d
Sr	---	---	---	---	---	---	n.d
Y	7.90	---	---	1.30	---	---	n.d
Zr	8.53	---	---	50.94	---	---	n.d
Zn	---	10.27	---	7.31	12.57	---	n.d
Nb	----	---	---	---	---	---	n.d
Ga	8.80	3.00	4.54	9.75	11.94	4.26	n.d
Ge	---	---	---	---	---	---	n.d

TABLE II - Chemical analyses of clay fraction (<2μm) of K-bentonite samples - Continued

Sample No.	24B	27A	28A	28B	28C	28D	28E
SiO_2	53.80	n.d	53.70	n.d	n.d	51.90	n.d
Al_2O_3	18.30	n.d	20.95	n.d	n.d	20.74	n.d
Fe_2O_3T	1.14	n.d	1.26	n.d	n.d	1.26	n.d
MgO	4.89	n.d	4.37	n.d	n.d	4.49	n.d
CaO	3.10	n.d	---	n.d	n.d	0.50	n.d
Na_2O	1.30	n.d	1.44	n.d	n.d	1.49	n.d
K_2O	6.69	n.d	6.74	n.d	n.d	6.50	n.d
TiO_2	0.29	n.d	0.15	n.d	n.d	0.15	n.d
MnO	0.02	n.d	0.01	n.d	n.d	0.04	n.d
Rb	69.09	105.36	68.57	96.98	71.03	84.58	92.14
Sr	---	6.37	---	1.80	---	---	---
Y	---	---	7.11	13.17	---	---	---
Zr	69.97	35.31	1.88	23.17	34.84	---	1.28
Zn	15.24	---	3.99	13.27	3.03	---	---
Nb	---	---	---	---	---	---	---
Ga	7.49	3.99	9.92	5.22	10.89	3.00	8.59
Ge	---	---	---	---	---	---	---

TABLE II - Chemical analyses of clay fraction (<2μm) of K-bentonite samples - Continued

Sample No.	28G	28H	29	34A	35	14 carbonates destructed
SiO_2	56.60	55.60	50.90	48.30	57.60	46.00
Al_2O_3	20.55	21.35	24.47	17.29	19.70	18.20
Fe_2O_3T	1.19	1.07	0.62	3.52	n.d	n.d
MgO	4.28	4.62	3.65	5.05	5.80	2.90
CaO	0.60	0.40	0.50	0.80	0.80	13.00
Na_2O	1.08	1.27	1.07	0.46	0.99	1.33
K_2O	6.43	6.59	7.26	7.01	n.d	n.d
TiO_2	0.11	0.18	0.29	0.51	n.d	n.d
MnO	0.04	0.02	0.02	---	0.01	0.04
Rb	n.d	64.14	99.03	178.81	60.22	35.58
Sr	n.d	---	109.17	47.71	---	---
Y	n.d	7.92	7.53	39.65	12.19	---
Zr	n.d	5.81	34.34	100.19	19.65	---
Zn	n.d	2.71	12.33	15.06	---	12.00
Nb	n.d	---	---	45.90	10.08	---
Ga	n.d	5.29	15.29	9.46	6.35	---
Ge	n.d	---	0.027	---	---	---

APPENDIX G

PRECISION, ACCURACY AND WITHIN SAMPLE HOMOGENEITY OF ATOMIC ABSORBTION TECHNIQUE

TABLE I - The precision of atomic absorbtion technique

(Means in weight per cent)

Oxide	No. of Observations	Standard Used	Mean	Variance	Std. dev. (±)	Coeff. of Variation
SiO_2	12	G-2	67.40	3.71	1.92	0.028
MgO	12	G-2	0.99	0.042	0.204	0.202
CaO	12	G-2	1.58	0.091	0.302	0.191
Na_2O	12	GSP-1	2.92	0.019	0.139	0.047
MnO	12	GSP-1	0.03	0.0005	0.022	0.758

TABLE II - The accuracy of atomic absorbtion technique. (Standard concentrations after Abbey (1973), but recalculated considering ignition. Concentrations of all the oxides are in weight percent).

Oxide	No. of Observations	Standard Used	Concentration in standard (std)	Mean ($\bar{x}$)	Accuracy (std-x)
SiO_2	12	G-2	69.58	67.40	2.18
MgO	12	G-2	0.77	0.99	0.22
CaO	12	G-2	1.99	1.58	0.41
Na_2O	12	GSP-1	2.82	2.92	0.10
MnO	12	GSP-1	0.04	0.03	0.01

TABLE III - Within sample homogeneity for the Geological Survey of Canada standard rock sample SY-2 (Abbey, 1976). (Means are in weight percent).

Oxide	No. of Observations	Mean	Variance	Std. Dev. (±)	Coeff. of Variation
SiO_2	8	59.43	6.33	2.51	0.042
MgO	8	2.78	0.012	0.113	0.040
CaO	8	8.91	0.113	0.336	0.037
Na_2O	8	4.18	0.084	0.290	0.069
MnO	8	0.36	0.0009	0.031	0.087

APPENDIX H

OPERATING CONDITIONS FOR X-RAY POWDER DIFFRACTION EQUIPMENT

X-ray tube	:	Copper target, Cu K_{α} radiation 40 KV 16 mA Ni Filter
Goniometer	:	Speeds: 2°, 0.4° 2θ - angle per minute
Power Supply	:	About 9.5 D.C. Kilovolts
Rate meter	:	Range: c.p.s. 200 Time constant: 2.0 Range: 70
Gain	:	Fine: 80 Coarse: 8 Window: EL = 1.65 EU = 1.80
Chart speed	:	2° 2θ - angle per minute